Biochemical investigation of catalysis by lytic polysaccharide monooxygenases

Biokjemiske undersøkelser av katalyse i lytiske polysakkarid-monooksygenaser

Philosophiae Doctor (PhD) Thesis

Jennifer Sarah Maria Loose

Department of Chemistry, Biotechnology and Food Science
Faculty of Veterinary Medicine and Bioscience
Norwegian University of Life Sciences

Ås 2016

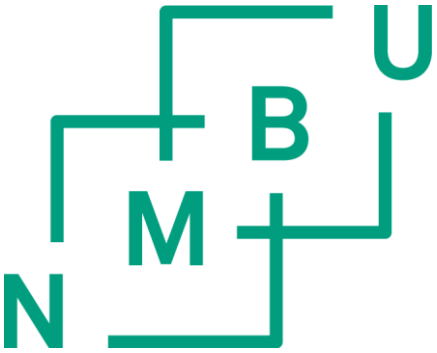

Thesis number 2016:69
ISSN 1894-6402
ISBN 978-82-575-1977-3

Table of contents

Acknowledgements

The work presented in this thesis was carried out in the Protein Engineering and Proteomics (PEP) group at the Department of Chemistry, Biotechnology and Food Science at the Norwegian University of Life Sciences (NMBU) in the period 2012-2016. The work was funded in part by the Research Council of Norway through the project "Mechanism, function and diversity of a novel family of biomass degrading enzymes".

First of all, I would like to thank **Gustav Vaaje-Kolstad** for accepting me as a PhD student here in Norway and introducing me to this exciting topic. Thank you so much for all the support, help, patience and for always having some advice. I really appreciate that is so easy talking to you and that you always took the time for a short talk. It is incredible how you can always be so positive and motivating. And thank you for trying to calm me down when the control-freak in me took over. It has been a pleasure working and discussing with you!

I would also like to thank **Vincent Eijsink**. Thank you for the great ideas, inspiration, motivation and your honest criticism. I am really grateful that you always found some time for me in your very full schedule.

A special thanks to **Morten Sørlie** and **Åsmund Røhr**. It was fun working with you! Thank you so much for your support and for explaining and explaining and explaining…

Furthermore, I would like to thank **Roland Ludwig** and **Daniel Kracher**. Thank you so much for all your input, the interesting discussions and especially for making the time I spent in Vienna a lot of fun!

A huge thank you to all members of the PEP group. You made work fun! Especially **Zarah "B" Forsberg**, thanks for your friendship. Zarah, **Bastien "Basse B" Bissaro** and **Gerdt Müller**, it is good to have a family here. **Ben Kunath**, thanks for all the little breaks and all the cookies! It is great that you are always motivated and also that you keep "fika" alive. **Adrian Naas**, it has been fun sharing the office with you.

My family… What can I say, but you are the BEST! My parents, brother, uncles, aunts and cousins, thank you for believing in me and supporting me. I am lucky to have you. All of you!

Last but not least, **Philipp Gröschler**, thank you so much for being there for me and supporting me, especially during the most challenging period of this work. I am so happy that you moved to Norway. I know that I can always rely on you. Thanks for making me happy and showing me that life is not all about work.

Jennifer Loose

Ås, August 2016

Summary

Lytic polysaccharide monooxygenases (LPMOs) are copper-dependent enzymes that catalyze the oxidative cleavage of glycosidic bonds in the presence of dioxygen and an external electron donor. Currently, these enzymes are classified in families 9, 10, 11 and 13 of the auxiliary activities (AAs) in the CAZy database. LPMOs are able to degrade insoluble polysaccharides such as crystalline cellulose and chitin and some variants also depolymerize non-crystalline or soluble substrates such as starch, xyloglucan, xylan and beta-glucans. LPMOs are important in biomass conversion because they act in synergy with glycoside hydrolases, thereby enhancing overall polysaccharide conversion efficiency. Even though these enzymes have been intensely investigated since their discovery in 2010, several aspects of their catalytic mechanism and their mode of action remain unclear. LPMOs are abundant and show high sequence diversity, which suggests functional roles beyond biomass degradation. Interestingly, some family AA10 LPMOs have been identified as virulence factors. The experimental work described in this thesis was aimed at creating increased understanding of LPMO functionality.

Paper I describes an assay designed to quantitatively assess the activity of chitin-active LPMOs in a fast and convenient way. By application of post-reaction treatment with a chitinolytic enzyme cocktail, the complex product mixtures generated by the LPMO were reduced to a single product (chitobionic acid) that represented LPMO activity. In addition, the generation of a standard allowed quantification of the product. As part of this study, a putative LPMO that is part of GbpA, a virulence factor from *V. cholerae*, was shown to be catalytically active on chitin.

Paper II shows that a fungal cellobiose dehydrogenase (CDH) from *Myriococcum thermophilum* can act as an electron donor for bacterial AA10s, a role that at the time only had been suggested for CDH and fungal AA9s. Using this protein as electron donor allowed a more controlled supply of electrons compared to when using small electron donors, and stable reaction kinetics were obtained. The data also provided experimental evidence for the notion that one LPMO reaction consumes two externally delivered electrons. Further studies of the influence of the electron donor on the catalytic rate of a chitin-active AA10 from *Serratia marcescens* (CBP21) showed that the rates of chitin-oxidation are dependent on the concentration of reducing agent, an important fact that has so far not been considered when

studying LPMO activity. Combining this observation with the notion that the initial one-electron reduction of the LPMO is not rate-limiting, leads to the suggestion that delivery of the second electron needed for catalysis may be a crucial step.

Paper III describes an in-depth study of the enzymatic properties of CBP21. The importance of 13 conserved residues located in the substrate-binding surface or in the active site was investigated by analyzing the effects of mutations on enzyme activity, substrate binding, the electron transfer from CDH to the LPMO, and the character of the copper-binding site (by electron paramagnetic resonance spectroscopy). The activity data unexpectedly showed that most mutations did not influence the rate of the enzyme, but rather the enzyme stability and, hence, product yield. Most mutations that reduced product yields had a negative impact on substrate binding, indicating a link between enzyme lifetime and adhesion to chitin. The reduction of the CBP21 variants by CDH in solution was highly influenced by several of the mutations. However, the altered electron transfer could not be correlated to the activity and apparent stability of the mutants. The observation that most mutants displayed electron transfer rates that were much higher than the rate of LPMO catalysis indicated that initial one-electron reduction of the LPMO is not rate limiting for the reaction. EPR spectroscopy showed that the catalytic copper site was affected by several, both near and distant from the copper ion. It is conceivable that changes in the copper site, i.e. the site where redox-active oxygen species are generated, affect catalytic efficiency, either directly or by changes in the generation of damaging oxidative compounds or the sensitivity for such compounds.

Taken together the present data provide new insights into how catalytic activity of LMPOs may be assessed and into possible pitfalls when doing so. The mutant collection described in Paper III forms a valuable resource for further studies on unraveling the structural basis of LPMO activity and may contribute to, eventually, unravelling how LPMO performance could be improved, either by engineering the enzyme or by optimizing process conditions

Sammendrag

Lytisk polysakkarid-monooksygenaser (LPMO) er kobberavhengige enzymer som katalyserer oksidativt brudd av glykoksidbindinger i nærvær av molekylært oksygen og en ekstern elektrondonor. Enzymene er klassifisert som hjelpeenzymer (auxiliary activities, AA) i familier (henholdsvis 9, 10, 11 og 13) i CAZy databasen. Disse redoksaktive enzymene er i stand til å degradere uløselige polysakkarider som krystallinsk cellulose og kitin. Visse typer depolymeriserer også løselige substrater slik som xyloglukan, xylan og betaglukaner. Den viktige rollen til LPMOer i biomassekonvertering reflekteres i deres evne til å oppnå synergi med glykoksidhydrolaser og med det øke polysakkaridnedbrytningseffektiviteten. Selv om disse enzymene er nøye studert siden deres oppdagelse i 2010, er det fortsatt flere uklarheter vedrørende deres katalytiske mekanisme og virkemåte. LPMOer er tallrike og viser høy sekvensdiversitet hvilket antyder funksjonelle roller utenom biomassenedbrytning. En interessant oppdagelse er at noen familie AA10 LPMOer er blitt identifisert som virulensfaktorer i bakterier, selv om deres rolle i sykdomsutvikling er dårlig forstått.

Artikkel I beskriver et hurtig og praktisk assay for kvantitativ LPMO aktivitet mot kitin. Den komplekse produktprofilen etter LPMO katalyse ble forenklet til et enkelt produkt ved anvendelse av en ”post-reaksjon” enzymbehandling. Fremstilling av en standard ga i tillegg mulighet for kvantifisering av produktet. Videre ble det påvist enzymatisk aktivitet for en LPMO som tidligere har blitt vist å være en virulensfaktor, GbpA, fra *V. cholerae*.

Artikkel II viser at en fungal CDH fra *Myriococcum thermophilum* kan virke som elektrondonor for bakterielle AA10. Tidligere var denne rollen foreslått kun for fungale AA9. En slik elektrondonor gir mer kontrollert tilførsel av elektroner og stabil reaksjonskinetikk enn vanlig benyttede små elektrondonorer. Videre ble effekten elektrondonorer har på den katalytiske hastigheten til den kitinaktive CBP21 (AA10) fra *Serratia marcescens* studert. Hastighetene for kitinoksidasjon var avhengig av konsentrasjonen til den reduserende agent hvilket tidligere ikke har blitt tatt hensyn til når man har studert LPMO aktivitet.

Artikkel III er en dyptgående studie av de enzymatiske egenskapene til CBP21. Viktigheten av 13 høyt konserverte residuer på substratbindingsoverflaten eller i det aktive setet ble undersøkt med hensyn på enzymaktivitet, substratbinding, elektronoverføringsegenskaper (fra CDH til LPMOen) og kobberbindingsegenskaper (ved hjelp av elektron paramagnetisk resonans, EPR). Aktivitetsdataene viste overraskende nok at mutasjonene ikke påvirket

enzymhastigheten. I stedet var det tidslengden for aktivitet som ble berørt. De fleste mutasjonene resulterte i redusert substratbinding hvilket indikerer en kobling mellom enzymlivstid og adhesjon til kitin. Reduksjon av CBP21-variantene ved hjelp av CHD var kraftig påvirket av mutasjonene. De fleste mutanter viste en meget høy (per sekund) elektronoverføringshastighet hvilket antyder at dette ikke er det hastighetsbestemmende trinn for reaksjonen. Til slutt viste EPR-spektroskopiresultatene at det kobber-aktive setet er berørt av mange aminosyrer i CBP21, både nært og fjernt i avstand fra kobberionet.

Alt i alt har studiene gikk ny innsikt i hvordan aktiviteten til LPMOer kan analyseres og hvilke praktiske utfordringer man må ta hensyn til når man jobber med denne typen enzymer. Samlingen av mutanter beskrevet i artikkel III utgjøre en verdifull ressurs for fremtidige studier som ønsker å komme til bunns i hvordan LPMOer fungerer. Samlingen vil også være av betydning for fremtidig forskning på hvordan disse enzymene kan endres på for å skape varianter bedre egnet for industrielle betingelser.

Abbreviations

AA	Auxiliary activity
Ao	*Aspergillus oryzae*
CAZy	Carbohydrate-active enzymes
CBM	Carbohydrate-binding module
CBP	Chitin-binding protein
CDH	Cellobiose dehydrogenase
CE	Carbohydrate esterase
Cj	*Cellvibrio japonicus*
CYT	Cytochrome
DD	Degree of deacetylation
DH	Dehydrogenase
EPR	Electron paramagnetic resonance
ET	Electron transfer
Ef	*Enterococcus faecalis*
GH	Glycoside hydrolase
GlcNAc	*N*-acetylglucosamine (N-Acetyl-D-Glucosamine)
GMC	Glucose-methanol-choline
GT	Glycosyltransferase
HILIC	Hydrophilic interaction chromatography
IET	Interdomain electron transfer
ITC	Isothermal titration calorimetry
K_d	Dissociation constant
Lm	*Listeria monocytogenes*
LPMO	Lytic polysaccharide monooxygenase
MD	Molecular dynamics
Mt	*Myriococcum thermophilum*
Nc	*Neurospora crassa*

NMR	Nuclear magnetic resonance
PMO	Polysaccharide monooxygenase
PUL	Polysaccharide utilization locus
Sm	*Serratia marcescens*
Ta	*Thermoascus aurantiacus*
UPLC	Ultra-performance liquid chromatography

List of papers

Paper I

A rapid quantitative activity assay shows that the *Vibrio cholerae* colonization factor GbpA is an active lytic polysaccharide monooxygenase

Jennifer S.M. Loose, Zarah Forsberg, Marco W. Fraaije, Vincent G.H. Eijsink, Gustav Vaaje-Kolstad, 2014, *FEBS Lett.,* 588**,** 3435-3440.

Paper II

Activation of bacterial lytic polysaccharide monooxygenases with cellobiose dehydrogenase

Jennifer S.M. Loose, Zarah Forsberg, Daniel Kracher, Stefan Scheiblbrandner, Roland Ludwig, Vincent G.H. Eijsink, Gustav Vaaje-Kolstad, 2016

Manuscript submitted to *Biochemistry*, under revision

Paper III

Insights into catalysis by lytic polysaccharide monooxygenases through site-directed mutagenesis of CBP21 from *Serratia marcescens*

Jennifer S.M. Loose, Åsmund K. Røhr, Bastien Bissaro, Daniel Kracher, Roland Ludwig, Morten Sørlie, Vincent G.H. Eijsink, Gustav Vaaje-Kolstad, 2016

Manuscript in preparation

Other publications by the author

***Listeria monocytogenes* has a functional chitinolytic system and an active lytic polysaccharide monooxygenase.** Dafni K. Paspaliari*, Jennifer S.M. Loose*, Marianne H. Larsen, Gustav Vaaje-Kolstad, 2015, *FEBS J,* 282**,** 921-936.

A small lytic polysaccharide monooxygenase from *Streptomyces griseus* targeting alpha- and beta-chitin. Yuko S. Nakagawa, Madoka Kudo, Jennifer S.M. Loose, Takahiro Ishikawa, Kazuhide Totani, Vincent G.H. Eijsink, Gustav Vaaje-Kolstad, 2015, *FEBS J,* 282**,** 1065-1079.

Structural and Functional Analysis of a Lytic Polysaccharide Monooxygenase Important for Efficient Utilization of Chitin in *Cellvibrio japonicus.* Zarah Forsberg, Cassandra E. Nelson, Bjørn Dalhus, Sophanit Mekasha, Jennifer S.M. Loose, Lucy I. Crouch, Åsmund K. Røhr, Jeffrey G. Gardner, Vincent G.H. Eijsink, Gustav Vaaje-Kolstad, 2016, *J Biol Chem,* 291**,** 7300-7312.

*the authors contributed equally to this work.

1. Introduction

Life on earth is an ancient mystery. Some of the earliest potential evidence for life are as old as 3400-3800 million years (Awramik, 1992, Mojzsis et al., 1996, Tice and Lowe, 2006), but due to recent findings, an even earlier origin of life starting approximately 4100 million years ago has been suggested (Bell et al., 2015). Through evolution, microorganisms have developed a variety of metabolic pathways for the sake of obtaining energy. One of these pathways allowed microorganisms to use solar energy to reduce carbon dioxide and convert it to biomass. This process is called photosynthesis and revolutionized life on earth by yielding molecular oxygen as a metabolic byproduct (Nowicka and Kruk, 2016). The oxygenation of the biosphere by marine cyanobacteria promoted the development of high-energy aerobic metabolisms and more complex forms of life (Grula, 2005). The later appearance of terrestrial life and evolution of land plants mainly depended on photosynthesis as well. Different plant morphologies arose from simple plant bodies and more complex structures and organs diverged. When plants started to grow vertically, competition for light began, evoking the need to develop structural tissue that would give support when facing physical strains such as wind and gravitational force. At this point cell wall associated crystalline cellulose fibrils evolved to meet this challenge, allowing vertical growth of the plant tissue (Duchesne and Larson, 1989). Later, several major groups of trees further evolved the cell wall matrix by incorporating the hydrophobic, polyphenolic compound lignin into the cellulose structure. This resulted in the enormous production of lignified wood (Kenrick and Crane, 1997), an organic material with great decay-resistance that lead to the abundant hydrocarbon depositions utilized for energy by modern society. Lignin provides not only the mechanical support for growth but also protection. In parallel, soluble polysaccharides known as hemicellulose were integrated in the cell wall structure for its adhesive and elastic properties, eventually yielding the complex composite structure found in the plants and trees of today. Roughly, the amount of cellulose, hemicellulose and lignin in trees and plants are in the order of 40-50, 20-40 and 20-30%, respectively (Corrêa et al., 2016).

In parallel to the development of cellulose in plants, the animal-kingdom developed a similar substance for the purpose of structural integrity, mechanical strength and protection, namely the nitrogen containing polysaccharide chitin. Currently, the oldest fossil chitin found is 505 million years old (Ehrlich et al., 2013). It is hypothesized that chitin is only utilized as a

structural polymer by organisms that have access to an abundance of reduced nitrogen, e.g. in marine environments, and that plants therefore were "forced" to utilize cellulose (Duchesne and Larson, 1989). An estimated $10^{10} – 10^{11}$ tons of chitin is produced annually (Gooday, 1990), making it the second most abundant biopolymer after cellulose that has an estimated annual production of approximately 1.5×10^{12} tons (Klemm et al., 2005). Both cellulose and chitin are thermally and chemically stable structures that are thermodynamically challenging to degrade. The glycosidic bond is thought to represent the most stable biomolecular bond on earth, having a half-life of approximately 22 million years (Wolfenden et al., 1998). Two-thirds of the carbon in the biosphere exist as carbohydrates (Sinnott, 1990), however clearly, there is little accumulation of cellulose/chitin in the biosphere. The reason for this is primarily the efficient decomposing systems developed by microorganisms and fungi to recycle the carbon and in the case of chitin also nitrogen, stored in organic matter and reintroduce them into the carbon- and nitrogen cycles respectively. The greatness of these enzymes is reflected in the enormous rate-enhancement they achieve in cleavage of the glycoside bond, peaking at 10^{17} when compared to the uncatalyzed reaction (Wolfenden et al., 1998). In modern society, where hydrocarbon reservoirs are slowly being depleted and greenhouse gas emissions are rising, the interest in using renewable materials for the production of fuel, energy, materials and chemicals is rising. Thus, there is a substantial interest in enzymes that efficiently depolymerize the abundant recalcitrant materials such as cellulose and chitin.

1.1 Carbohydrates

In the beginning of the 19th century, J. L. Gay-Lussac and L.J. Thénard improved the methods for compositional elementary analyses of organic compounds and found that the empirical formula CH_2O described many vegetable materials including starch and sugar (Hon, 1994). Due to this finding, these substances were named "hydrate de carbone" which is French for "hydrate of carbon" (i.e. carbohydrate). Even though we know that carbohydrates are polyhydroxy aldehydes and ketones mainly appearing as acetals or hemiacetals, or substances that can be hydrolyzed to such, the historical name has been kept. Carbohydrates are single sugars or several monosaccharides that are linked via α- or β-glycosidic bonds and appear as di-, tri-, oligo- or polysaccharides. The heterogeneity of monosaccharides in combination with different glycosidic linkages and several modifications yield an enormous amount of variation.

1.1.1 Chitin

Chitin was first discovered by H. Braconnot (published in 1811), when he isolated a substance from mushrooms that contained nitrogen and acetyl moieties (Muzzarelli et al., 2012). Chitin is a linear polymer composed of β-1,4 linked *N*-acetylglucosamine (GlcNAc) moieties that each are rotated 180° relative to each other (Figure 1), making the disaccharide chitobiose the repeating subunit. In its native form it is crystalline and occurs in two major allomorphs, α- and β-chitin (Rinaudo, 2006). In the α-form the chains are arranged in an anti-parallel fashion, where extensive intermolecular hydrogen-bonds result in a densely packed, rigid material (Minke and Blackwell, 1978). The β-allomorph of chitin is formed by a parallel orientation of the chains. Due to fewer intramolecular hydrogen-bonds between the chains, this crystalline structure is less densely packed compared to α-chitin. The β-chitin crystal structure can accommodate water molecules, which makes β-chitin particles swell substantially when exposed to an aqueous solvent (Saito et al., 2000, Rinaudo, 2006, Gardner and Blackwell, 1975). Some studies also report the existence of a third allomorph, γ-chitin, where the crystalline structure is formed by the repetitive combination of two parallel chitin chains and one anti-parallel chain. However, the existence of this chitin allomorph is controversial (Rinaudo, 2006).

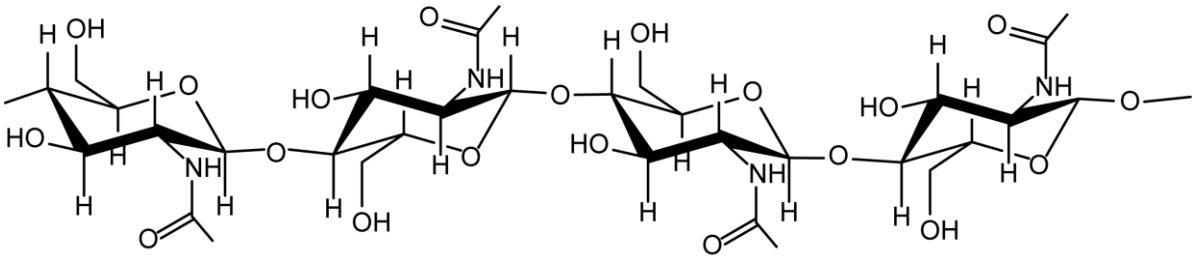

Figure 1. Chemical structure of chitin

In Nature, chitin is mostly found as a crystalline structure (Rinaudo, 2006) that occurs in combination with protein, minerals and/or other polyphenolic compounds. *N*-deacetylations are possibly involved in the interactions of chitin with protein (Blackwell, 1988). Low amounts of deacetylations are usually found in chitin, however α- and β-chitin remain insoluble (Rinaudo, 2006). Higher degrees of deacetylation yield a soluble derivative called chitosan which consists of *N*-acetylglucosamine and D-glucosamine residues. By treating chitin (usually from crustaceans) with sodium hydroxide, random deacetylation of the chitin chains is achieved. At a degree of deacetylation (DD) of approximately 50% the polysaccharide becomes soluble in water (Kurita, 2006, Rinaudo, 2006). The DD varies substantially depending on the production method and chitin source used. Normally, a DD of 60-70% is reached, but up to 100% has been reported (Croisier and Jérôme, 2013, Kumar, 2000, Kurita, 2006). The degree of acetylation of naturally occurring chitin is typically close to 90%, but studies have reported that some fungi contain chitosan, presumably resulting from the action of chitin deacetylases (Kurita, 2006). Since chitosan production in fungi is largely related to growth conditions, chitosan with reproducible chemical properties can be isolated from fungal mycelia (Croisier and Jérôme, 2013).

1.1.1.1 Occurrence of chitin and its economic importance

Due to its rigidity, it is not surprising that chitin is used by a variety of organisms as structural component or in protective exoskeletons. In marine environments chitin is abundantly found in the exoskeleton of crustaceans (e.g. shrimp, crab, lobster), the protective housing of zooplankton (e.g. copepods and krill), the cell walls of diatoms and some algae (usually as silica-chitin composite), the central internal “pen”/”bone” and beak of squids/cuttlefish, the nacre of bivalve shells, the tube housing of deep sea animals such as the vestimentiferan tube

worms, and in the cell walls of fungi (Gooday, 1990, Rinaudo, 2006, Gaill et al., 1992, Levi-Kalisman et al., 2001). Most chitin found in marine organisms exists as a composite composed of α-chitin, $CaCO_3$ and protein (Kurita, 2006). The β-chitin allomorph is rarer than α-chitin and is predominantly found in squid "pens" and in the flotation spines of some diatoms. In terrestrial and limnic environments chitin is most commonly found in the cell walls of fungi (both hyphae and fruiting bodies), the exoskeleton, gut lining and pupal housing of arthropods and arachnids, and in the eggshells of nematodes. In contrast to marine chitin, the chitin found on land or in fresh water is not embedded in a $CaCO_3$ matrix, but rather associated with polysaccharides such as beta-glucans and/or mannans, proteins (fungal cell walls) or catechol-crosslinked proteins (insect exoskeletons).

Chitin is readily available as a waste product from the seafood industry, mainly as shrimp and crab shells. Next to approximately 15-40% chitin, the shells also contain 20-40% protein and 20-50% $CaCO_3$ (Kurita, 2006). To obtain pure chitin the shells are treated with hydrochloric acid for decalcification followed by sodium hydroxide to remove the proteins. Due to that treatment the degree of *N*-acetylation of commercially available α-chitin is approximately 90-95% for β-chitin approximately 90% (Kurita, 2006).

Since chitin and chitosan are biocompatible, biodegradable, almost non-toxic and possess a molecular structure that can be modified, they can be used for various applications. Chitin-based materials can be used in waste water treatment for example, where they efficiently remove heavy metals (Gerente et al., 2007, Muzzarelli et al., 1989, Kumar, 2000). Chitosan is used in agriculture due to its antifungal, crop protecting and antimicrobial properties (Tharanathan and Kittur, 2003, Muzzarelli et al., 2012) and in the food industry to remove polyphenolic compounds or as flocculent (Muzzarelli et al., 2012). In the medical sector chitin and chitosan are used amongst others for tissue engineering (Croisier and Jérôme, 2013), wound dressing (Jayakumar et al., 2011, Kurita, 2006) and controlled drug release (Rinaudo, 2006, Kumar, 2000). Moreover, chitin-based materials are utilized to produce food packaging (Muzzarelli et al., 2012, Tharanathan and Kittur, 2003), cosmetics and other materials (Tharanathan and Kittur, 2003, Kumar, 2000) that are exploited in various branches of industry. These examples show that chitin is a valuable biomaterial, which, however, is still "underused" and whose full potential is yet to be discovered.

1.1.2 Cellulose and the plant cell wall

In 1839, “cellulose” was first mentioned in a report of the French academy on the work of Anselme Payen. This French chemist had described a resistant fibrous solid that could be extracted from various plant tissues and determined the molecular formula to be $C_6H_{10}O_5$ (Klemm et al., 2005). Cellulose is a linear homo-polymer consisting of D-glucopyranose subunits that are connected via β-1,4 glycosidic bonds. Comparable to chitin, the repeating unit is the disaccharide, cellobiose, since the single glucose units are rotated 180° relative to each other (Cocinero et al., 2009). The structure of cellulose (Figure 2) resembles chitin (Figure 1). The latter has an acetamido group at C2, whereas cellulose possesses a hydroxyl group at this position. The cellulose strands form micro fibrils that are stabilized by intra- and intermolecular hydrogen bonds and van der Waals forces.

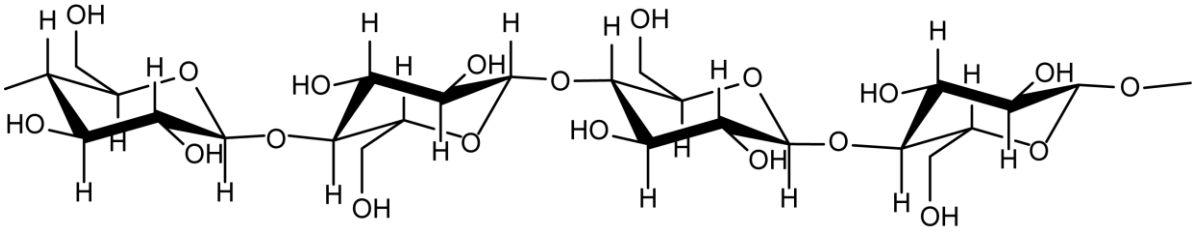

Figure 2. Chemical structure of cellulose

There are seven polymorphs of cellulose with cellulose I being considered the native form. Cellulose I can be divided into cellulose I_α and I_β which are found alongside each other (Klemm et al., 2005, O'Sullivan, 1997). The ratio of these types of cellulose I depends on the origin (Klemm et al., 2005).

Cellulose is the main component of the plant cell wall, where it is associated with other polysaccharides (hemicelluloses), hemicellulose and polyphenolic lignin making, the plant cell wall a very complex substrate for enzymes. Depending on the origin, the amounts of these components differ. The plant cell wall provides not only mechanical strength and protection, but serves also for physiological processes like signaling.

1.1.3 Microbial degradation of chitin and cellulose

The chemical, structural and functional similarity between cellulose and chitin has resulted in similar degradative machineries being evolved for these carbohydrates, although lignocellulosic material seems to require a larger array of complementary enzyme activities. Strategies for enzymatic depolymerization of both chitin and cellulose will be described below, but with emphasis on chitin since bacterial chitinolytic enzymes represent the main focus of this thesis.

The use of chitin as a carbon and nitrogen source is widespread among microbes. Since the ocean is especially rich in chitinous biomass, a substantial amount of the chitin-degrading animals and microbes are found in this biotope. The activity of chitinoclastic bacteria is thought to be high since little chitinous material accumulates in marine sediments (Zobell and Rittenberg, 1938, Keyhani and Roseman, 1999, Gooday, 1990). Systematic studies enriching for chitin-degrading bacteria from marine sediments have revealed a plethora of species capable of utilizing chitin as a nutrient source (Campbell and Williams, 1951, Zobell and Rittenberg, 1938). These bacteria primarily perform aerobic mineralization of chitin (Gooday, 1990, Campbell and Williams, 1951), but other reports have also identified anaerobic chitin degraders (Reguera and Leschine, 2001). The most common heterotrophic chitin degrading genera are represented by *Aeromonas*, *Actinomycetes*, *Enterobacter*, *Serratia*, *Bacillus*, *Erwinia* and *Vibrio* (Brzezinska et al., 2014, Gooday, 1990). Of the marine chitinoclastic bacteria, the *Vibrio* genus has been most thoroughly characterized by a comprehensive effort made by the Roseman lab from 1989 to 2007, that published more than 20 articles on chitin catabolism by this genus (several are cited in the following key review; (Keyhani and Roseman, 1999)). Key findings from these studies include determination of the chitinolytic cascade (Li and Roseman, 2004) and mechanisms for chitooligosaccharide uptake and processing (Park et al., 2000, Keyhani et al., 2000).

Most chitinoclastic activity on land is found in soil where especially insect remnants, fungal hyphae and fruiting bodies represent a large source of chitin. Studies enriching for bacteria in soil with the ability to utilize chitin as a nutrient source have identified multiple genuses, several of which are also found in marine environments (Monreal and Reese, 1969, Carroad and Tom, 1978). Both studies identified the *Serratia* genus (more specifically the *Serratia marcescens* strain) as a potent chitin degrader. This discovery led to a substantial research effort on deciphering the molecular mechanisms of chitinolysis by this bacterium, making it

the best understood microbial system for chitin degradation in soil (see (Vaaje-Kolstad et al., 2013) for an in-depth review). The chitinolytic system of *S. marcescens* will be described in more detail in section 1.2.2. It is beyond doubt that *S. marcescens* is an efficient chitin degrader, but recent data on the soil bacterium *Cellvibrio japonicus*, which is mostly known for its ability to degrade plant cell wall polysaccharides, indicate that this bacterium has a chitinolytic system that is at least as efficient as the one of *S. marcescens* (Tuveng et al., 2016). Another genus that is important for chitin depolymerization in soil, and especially in the rhizosphere, are the Actinomycetes (Gooday, 1990). *Steptomyces* species utilize chitin as a source of carbon and nitrogen and are highly chitinolytic. Their chitinolytic system is able to degrade a variety of chitinous substrates including the mycelia of fungi (Schrempf, 2001). Finally, it is important to realize that most of the data on microbial degradation of chitin was derived from traditional microbiological work using culturable organisms. The current metagenomics era has given possibilities to investigate how bacterial communities, with many unculturable members, interact. Some studies have reported data for chitinoclastic communities that showed an enrichment of *Actinobacteria*, γ-*proteobacteria* and β-*proteobacteria* (some completely novel) in a soil community supplemented with chitin (Jacquiod et al., 2013).

It should of course be noted that chitin degradation is not limited to bacteria. Chitin-degrading enzymes have also been detected in, fungi, archaea, algae, rotifers, the digestive tracts of higher animal, and even in carnivorous plants (Beier and Bertilsson, 2013).

As already noted, cellulose constitutes the largest source of organic carbon on the planet and represents an energy source for many bacteria, fungi and protozoa. Since plant derived cellulose is embedded in a highly complex matrix of hemicellulose and lignin, microorganisms display likewise complex enzymatic machineries to get access to the cellulose micro fibrils. The strategy used by the microorganisms to carry out this acquisition of nutrients seems to depend on the availability of dioxygen. Bacteria and fungi growing in aerobic environments commonly display secretion of free enzymes that degrade the substrate, whereas anaerobic organisms tend to keep their enzyme apparatus attached to the outside of the cell wall. A more detailed description of these enzyme systems is given in section 1.2.1.

Aerobic microbial decomposition of plant cell wall derived cellulose has been a subject for intense research since the 1950ies. The fungal *Trichoderma* species are of special interest, due to their ability to degrade cellulose containing fabrics that relies on the secretion of various cellulolytic enzymes (Bischof et al., 2016). *Trichoderma reseei* possesses a

remarkably efficient protein secretion machinery. Its cellulolytic system has been studied intensely over the last decades and now, serves as a model system for lignocellulose degradation (Martinez et al., 2008) and is exploited industrially in biorefineries for the saccharification of lignocellulosic material (Bischof et al., 2016). In nature, *Trichoderma* spp. colonize all kinds of cellulosic material like the rhizosphere of plants or decaying plant material (Schuster and Schmoll, 2010). Some of the best studied bacteria are the thermotolerant *Thermobifida fusca* and the soil bacterium *Cellvibrio japonicus.* Another important microbial player in cellulose degradation is the genus *Streptomyces*. *Streptomyces* are abundant in soil and produce antimicrobial metabolites to reduce competition and are considered to be significant contributors to the deconstruction of cellulosic biomass (Book et al., 2016). Interestingly, the ability of *Streptomyces* to degrade cellulose is often associated with symbiotic strains of insects feeding on plant biomass (Book et al., 2016, Takasuka et al., 2013).

More recently, metagenomics methods have also been used to characterize aerobic cellulolytic systems, expanding the understanding of how microbial communities collaborate and/or compete in the acquisition of cellulose as an energy source.

The digestive tract of plant eating animals represents an anaerobic niche that hosts an abundance of cellulolytic bacteria. It has been estimated that 10% of the bacteria in the rumen are cellulolytic, but the habitat also accommodates cellulose-degrading fungi and protozoa (Russell et al., 2009, Wilson, 2011). Evidence for microbiomes that are able to degrade cellulose have also been found in other herbivores like the giant panda (Zhu et al., 2011), reindeer (Pope et al., 2012) and insects (Warnecke et al., 2007, Burnum et al., 2011).

1.2 Carbohydrate active enzymes

The theoretically possible amount of linear and branched isomers of one single reducing hexameric oligosaccharide yields 10^{12} unique structures (Laine, 1994). Combined with the large diversity of monosaccharides, the multiple types of intersugar linkages and the fact that almost all organic macromolecules can be glycosylated results in an enormous amount of carbohydrate structures and conjugates. Furthermore, since all such carbohydrates must both be synthesized and broken down, the amount and especially the complexity of enzymes performing such activities is enormous. Enzymes that are involved in the synthesis,

modification or breakdown of glycoconjugates or complex polysaccharides are collectively called Carbohydrate-Active enZymes or short, CAZymes (Cantarel et al., 2009). A huge effort has been done and is still ongoing to classify and group these enzymes in a central database called the CAZy database [www.cazy.org]. The CAZy classification groups the proteins in families according to amino acid sequence similarity and was introduced to obtain a classification regime that was more appropriate than the EC system, which is based on the reaction mechanism only (Henrissat, 1991, Lombard et al., 2014, Levasseur et al., 2013). Due to the modular structure of many CAZymes, for example when a carbohydrate-binding module is attached to a glycoside hydrolase, it is possible to find one protein in several families (Lombard et al., 2014).

In 2008, the CAZy database covered approximately 300 protein families divided into five classes: glycoside hydrolases, glycosyl transferasers, polysaccharide lyases, carbohydrate esterases and non-catalytic carbohydrate-binding modules. This database grows progressively and is constantly updated with new sequence information, 3D structures and biochemical characterizations (Lombard et al., 2014). In 2013, a novel enzyme class was introduced, covering redox-enzymes that work in concert with CAZymes, which have been named Auxiliary Activities (Levasseur et al., 2013, Lombard et al., 2014). Currently, the CAZy database holds more than 350 protein families divided into six classes and provides a consistent nomenclature for CAZymes.

Glycosyltransferases (GTs) are responsible for the enzymatic formation of glycosidic bonds using an activated donor sugar substrate with a phosphate leaving group. Other sugars or lipids, proteins nucleic acids and small molecules can act as the acceptor substrate (Lairson et al., 2008). According to the stereochemistry of the substrates and the products, these enzymes can be either retaining or inverting (Sinnott, 1990, Coutinho et al., 2003). GTs show great diversity in donor, acceptor and product specificity and can potentially generate an infinite number of glucoconjugates, oligo- and polysaccharides (Coutinho et al., 2003). At present, the class of glycosyltransferases contains almost 100 protein families.

Carbohydrate esterases (CEs) are a class of CAZymes that remove ester-based modifications by de-*O* or de-*N* acylation of a substituted saccharide in a hydrolytic manner.

Polysaccharide lyases (PLs) use β-elimination instead of a hydrolytic mechanism to cleave uronic acid containing polysaccharides. The resulting products are an unsaturated hexenuronic acid residue and a reducing end where the cleavage was carried out. PLs form a

complimentary strategy to the degradation of C-6 carboxylated polysaccharides by glycoside hydrolases (Lombard et al., 2010).

Glycoside hydrolases (GHs) form the enzyme class with most families, comprising more than 130 at present. These enzymes are responsible for the hydrolysis of glycosidic bonds between two carbohydrate moieties or one carbohydrate and one non-carbohydrate moiety. The variation of activities in the GH family is large, including enzymes that predominantly target insoluble substrates, soluble oligosaccharides of variable or strictly defined chain length and branch points of branched polysaccharides. This large variation is reflected in the extreme variation in carbohydrate structures that exist. GH activity on polysaccharides can be endo- or exo-, referring to their ability to cleave the polysaccharide chain randomly or from the chain end. Exo-acting enzymes may prefer either the reducing or the non-reducing end and usually show processive properties, i.e. are able to perform several hydrolytic events before dissociating from the substrate chain (Davies and Henrissat, 1995). Common to all GHs is that the catalytic mechanism that leads to either inversion or to retention of the anomeric configuration (Koshland, 1953, Rye and Withers, 2000).

As already mentioned, auxiliary activities (AAs) are the latest addition to the CAZy database. AAs involve proteins that are potentially able to aid other CAZymes in degrading a complex substrate. Hence they comprise a wide array of enzymes that are active on polysaccharides and non-polysaccharides like lignin, which, without exception is found in combination with polysaccharides in the plant cell wall (Levasseur et al., 2013). This class of enzymes includes laccases, cellobiose dehydrogenases (CDHs), copper radical oxidases and other enzymes that utilize a redox mechanism. Lytic polysaccharide monooxygenases (LPMOs) are enzymes that were previously classified as family 61 of the GHs and family 33 of the carbohydrate binding modules. The finding that these proteins were oxidative enzymes acting on chitin (Vaaje-Kolstad et al., 2010) or cellulose (Forsberg et al., 2011, Quinlan et al., 2011, Phillips et al., 2011a) was one major reason for extending the CAZy database in order to reclassify these proteins. Currently, the CAZy database holds four AA families that are comprised of LPMOs, AA9, AA10, AA11 and AA13 (Levasseur et al., 2013). These enzymes work in synergy with many GHs and stimulate their activity by increasing the accessibility to the substrate (Horn et al., 2012). LPMOs will be discussed in more detail in section 1.3 of this thesis.

The only non-catalytic class of proteins found in the CAZy database are the carbohydrate binding modules (CBMs). CBMs are connected with other CAZymes in multimodular structures and promote association with the substrate. By recognizing and binding the target

structure, the catalytic domain is brought in close proximity to the substrate which may potentiate catalysis (Bolam et al., 1998, Boraston et al., 2004). The beneficial effect of CBMs on systems with low substrate concentrations has been shown recently (Várnai et al., 2013). The same study also shows that CBMs are less important in systems with high substrate concentrations. CBMs recognize their target structure within their natural context e.g. the plant cell wall (Boraston et al., 2004). Interestingly, binding to non-substrate polysaccharides in an intact plant cell wall, potentiates degradation of the substrate as well by means of the proximity effect (Herve et al., 2010).

1.2.1 Cellulolytic enzyme systems

In contrast to the relatively simple enzymatic systems for chitin degradation (see 1.2.2), microbial strategies for cellulose depolymerization are substantially more complex, most likely due to the high complexity of the plant cell wall.

In order to enable utilization of insoluble cellulose as such, multiple enzymatic activities are required: endoglucanases that randomly hydrolyse the β-1,4 glycosidic bonds in amorphous regions, exoglucanases that produce glucose or cellobiose from either end of the cellulose chain in a processive manner, and β-glucosidases that produce glucose from cello-oligomers (Hasunuma et al., 2013). For efficient depolymerization of cellulose in the plant cell wall hemicellulases such as pectinases, xylanases, mannanases, xyloglucanases also play an important role in exposing hemicellulose covered cellulose fibrils for the cellulases (Martinez et al., 2008, Dekker and Richards, 1976, Shallom and Shoham, 2003). Next to the interplay between the already mentioned enzymes several AAs, such as lignin modifying enzymes and the LPMOs (see chapter 1.3) also play a role. In contrast to cellulases, LPMOs carry out an oxidative cleavage of the crystalline parts of the cellulose to make is more accessible for the glycoside hydrolases (Horn et al., 2012).

Aerobic bacteria and fungi secrete a variety of cellulolytic enzymes into the surroundings once the organism is triggered by cellulose as a carbon source. The free enzymes need to diffuse to and bind their substrate in order to initiate depolymerization and release of soluble sugars and their concomitant uptake (Cragg et al., 2015). A proposed downside of this strategy is the putative consumption of dissolved sugars by other competing organisms.

The “free enzyme” strategy is not common for anaerobic bacteria and fungi. It seems that anaerobic conditions and the environments where such conditions are found have forced the development of alternative strategies. One such strategy utilized by anaerobic bacteria entails organization of cellulases, hemicellulases, pectinases and other proteins on a molecular scaffold to build a large multi-enzyme complex (Fontes and Gilbert, 2010, Shoham et al., 1999).

In cellulsomes, the catalytic modules bind to the protein scaffold in a “plug-and-socket” way via cohesin-dockerin interactions (Bayer et al., 2004). In addition, these protein assemblies feature a CBM3a which is specific in cellulose binding (Fontes and Gilbert, 2010). The organization of cellulosomes is illustrated in Figure 3. In contrast to the free enzyme systems, cellulosomes arrange carbohydrate-active enzymes on a scaffold to enhance synergistic activity and bring the enzyme consortium in close proximity to the substrate via CBMs.

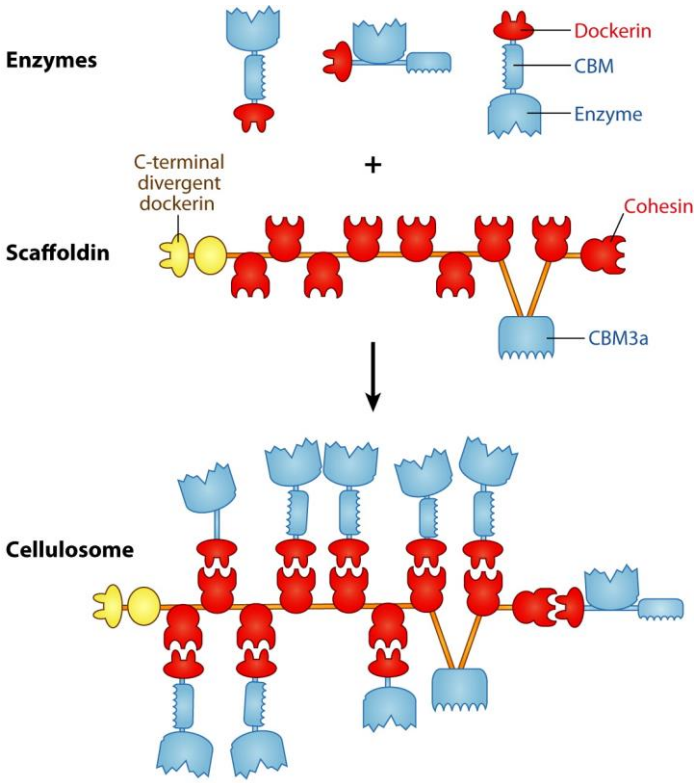

Figure 3. Modular composition of cellulosomes. Cellulases and hemicellulases have appended CBMs and dockerins. The enzymatic modules assemble on a non-catalytic scaffoldin via dockerin-cohesin interactions. The CBMs bind to plant cell walls whereas the C-terminal divergent dockerin targets the cellulosome to the bacterium. The figure was taken from (Fontes and Gilbert, 2010); Copyright © 2010, Annual Reviews.

Additionally, the cellulosomes are tethered to the bacterial surface (Fontes and Gilbert, 2010, Bayer et al., 2004, Gilbert, 2007). This promotes the uptake of produced mono- and oligosaccharides by the host organism. Moreover, a study has shown that cellulose degradation by cellulosomes bound to the cell surface of *Clostridium thermocellum* is higher than when the complex was unbound, probably reflecting product inhibition when the sugars are less efficiently absorbed by the organism (Lu et al., 2006, Fontes and Gilbert, 2010).

A second distinct strategy utilized by several anaerobic bacteria (residing predominantly in rumen/gut environments) involves the arrangement of large polysaccharide degrading protein complexes on the outer membrane. The genes encoding these proteins are localized in one large operon, referred to as a polysaccharide utilization locus (PUL). PULs are clusters of co-regulated genes (Figure 4A) that encode a machinery for glycan degrading and importing proteins (Martens et al., 2009).

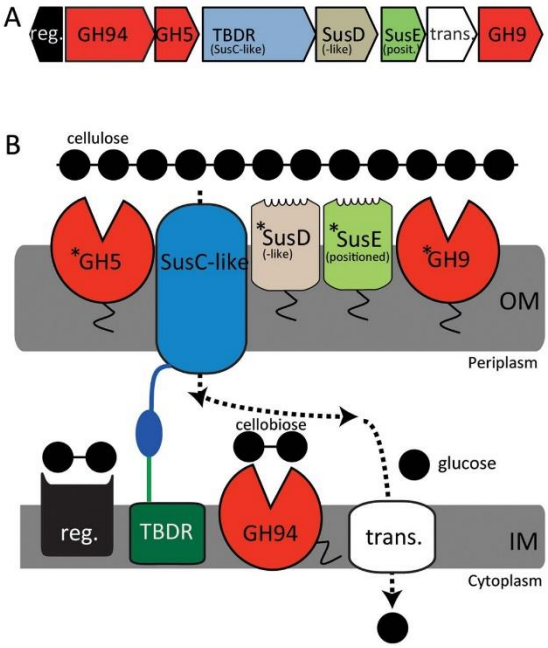

Figure 4. Hypothetical PUL from uncultivated bacteria found in cow rumen. (A) Gene organization encoding various proteins needed in PULs. (B) Hypothetical model of a cellulose-degrading PUL that consists of membrane-bound GHs, transporters and regulators. Cellulose is degraded by GHs to cellobiose, which is then transported to the periplasm where a further degradation to glucose takes place. The monomeric sugar is subsequently translocated to the cytoplasm via a transporter in the inner membrane. The figure was taken from (Naas et al., 2014).

They differ in polysaccharide specificity, so one organism can possess a number of PULs, in the case of *B. thetaiotaomicron* this number is 88 (Martens et al., 2008). The most well studied PUL is the starch utilization system (Sus) from *B. thetaiotaomicron* that encodes eight proteins transcribed from two divergent promoters (Foley et al., 2016). PULs responsible for the specific degradation of complex hemicelluloes such as xyloglucan (Larsbrink et al., 2014) and mannan (Cuskin et al., 2015), have been described and recently, Naas et al. (2014) reported characterization of several enzymes from a seemingly functional cellulose degrading PUL (Figure 4B).

1.2.2 Chitinolytic enzyme systems

To use chitin as a nutrient source, a chitinolytic machinery is needed that produces short, soluble sugars that can be taken up by the organism. Chitinolytic systems and the interaction of the enzymes within these systems has been described for bacteria such as *Enterococcus faecalis* (Vaaje-Kolstad et al., 2012), *Streptomyces griseus* (Nakagawa et al., 2015), *Listeria monocytogenes* (Paspaliari et al., 2015) and *S. marcescens* (Vaaje-Kolstad et al., 2013). The main enzymatic components of chitinolytic machineries are chitinases, which convert the chitin chains into soluble chitooligosaccharides, β-*N*-acetylhexosaminidases that convert chitooligosaccharides to GlcNAc and the chitin-targeting lytic polysaccharide monooxygenases that cleave chitin chains in their crystalline context using an oxidative mechanism. The complementing activities of the chitinolytic enzymes yield a synergism that enables efficient solubilization of insoluble, crystalline chitin (Suzuki et al., 2002, Vaaje-Kolstad et al., 2005a, Nakagawa et al., 2013). An overview of the common activites of a chitinolytic system is illustrated in Figure 5 which shows the well-studied chitinolytic system of *S. marcescens*.

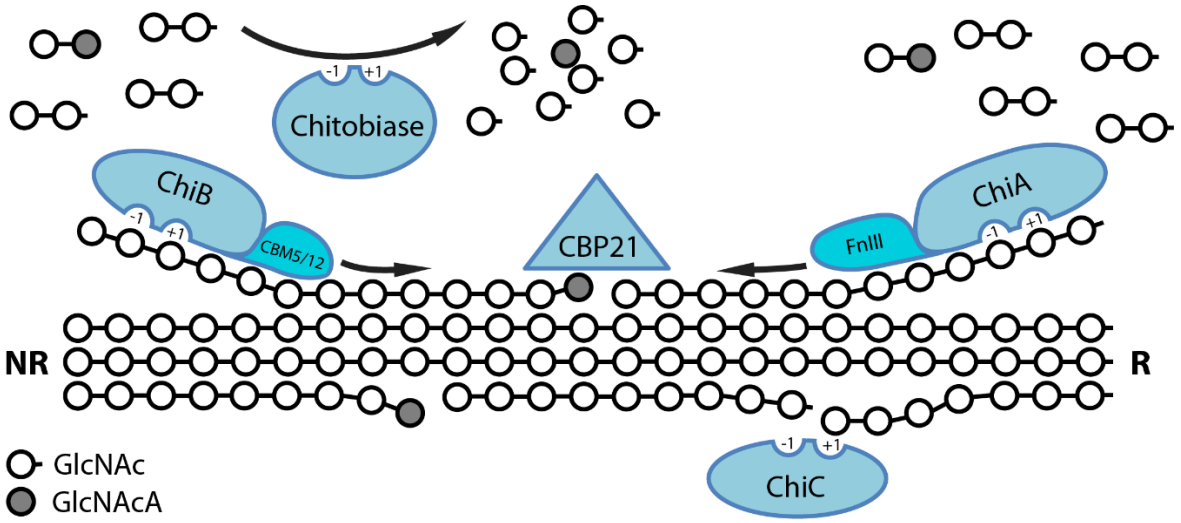

Figure 5. Chitin degradation by the chitinolytic system of *S. marcescens*. The *N*-acetylglucosamine (GlcNAc) subunits of chitin are shown as open circles. The two exo-processive enzymes ChiA and ChiB degrade the substrate from the reducing end (labelled R) and the non-reducing end (labelled NR) respectively producing mainly chitobiose. ChiC is an endo-active enzyme and produces random cuts in more amorphous areas of the chitin, enabling the exo-active chitinases to act in these regions. ChiC has a CBM whose position is unknown due to lacking structural data. CBP21 (chitin-binding protein 21 kDa, (Suzuki et al., 1998)) is an LPMO that disrupts the crystalline areas of the substrate in an oxidative manner producing aldonic acids (GlcNAcA, filled circles). CBP21 activity increases ChiA and ChiB activity by producing new chain ends. Chitobiose and other soluble sugars are degraded to GlcNAc by a β-*N*-acetylhexosaminidase called chitobiase. This figure was adapted from (Vaaje-Kolstad et al., 2013). © 2013 The Authors Journal compilation © 2013 FEBS. Reprinted with permission.

1.2.2.1 Chitinases

Hydrolytic enzymes responsible for releasing soluble oligomeric sugars from chitin are called chitinases. In general, chitinases can be grouped into two families according to their mode of action and their structure. In the CAZy database, chitinases are found in families GH18 and GH19. The GH18 family contains representatives from all domains of life and is the enzyme family that is associated with chitin degradation for metabolic purposes. The GH19 family was earlier thought to be restricted to plants, where the function was related to detecting and combating pathogens (Dixon et al., 1996). However, the genomic era has identified several thousand GH19 genes in bacteria, but the importance of these enzymes for chitin degradation is still not well explored. The fold of the catalytic domain of GH18s shows a $(\beta/\alpha)_8$ TIM-barrel whereas the fold of GH19s shows a high content of α-helices (Figure 6) and exhibits structural similarities with chitosanases and lysozyme (Hoell et al., 2006, Monzingo et al., 1996). Both,

GH18 and GH19 chitinases are often multi-modular where one or more chitin binding domains can be found attached to the catalytic domain.

A fundamental difference between GH18 and GH19 chitinases is found in the reaction mechanism. GH18 chitinases perform chitin hydrolysis by a double displacement substrate assisted catalysis, which gives retention of the anomeric configuration of the product containing the reducing end [(van Aalten et al., 2001, Tews et al., 1997, Brameld and Goddard, 1998b); Figure 7]. The GH19 chitinases, on the other hand, perform catalysis that yields inversion of the configuration of the anomeric carbon, most likely through a single displacement mechanism for inverting enzymes as suggested by Brameld and Goddard (1998a).

The topology of the chitinase binding clefts give information about their mode of action. The deep binding cleft in the *S. marcescens* GH18 chitinases ChiA (Figure 6A) and ChiB is a signature property of processive exo-acting enzymes. In contrast, the shallow binding cleft in the *S. marcescens* GH18 chitinase ChiC (Figure 6B) demonstrates the common topological property of a non-processive endo-acting enzyme. For efficient chitin degradation the interplay between these enzyme types is crucial. As illustrated in Figure 5 and experimentally demonstrated by Hult *et al*. (2005), ChiA degrades the substrate from the reducing end and ChiB from the non-reducing end. Newly formed chain ends from either an LPMO or an endo-acting enzyme provide new sites for productive attachment of ChiA or ChiB (Figure 5).

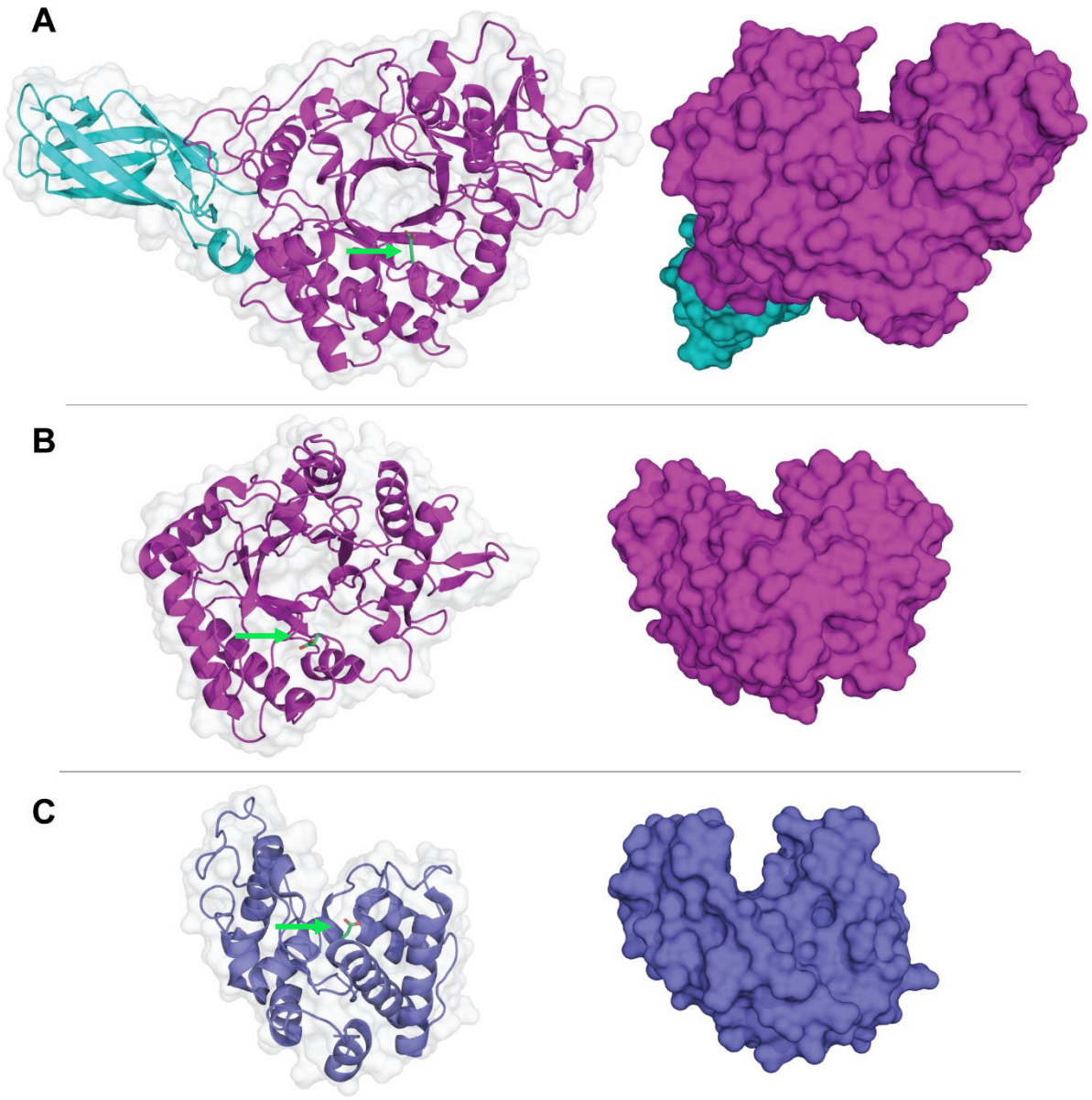

Figure 6. Structural overview of GH18 (magenta) and GH19 (blue) chitinases. The left figures show the crystal structures with the catalytic acids in green (also indicated by green arrows). The figures on the right in each panel illustrate the binding cleft of the enzymes. (A) The exo-processive ChiA from *S. marcescens* (PDB ID 1CTN) possesses an N-terminal fibronectin III-like chitin binding domain (cyan) and a catalytic domain with the $(\beta/\alpha)_8$ TIM-barrel fold that is typical for GH18s, with a deep substrate binding cleft. The catalytic acid is Glu315. (B) The endo-non-processive catalytic domain of ChiC (PDB ID 4AXN) from *S. marcescens* exhibits a $(\beta/\alpha)_8$ TIM-barrel fold and a shallow binding cleft. The catalytic acid is Glu141. Due to lacking structural data, the C-terminal fibronectin III module and CBM12 of ChiC are not shown. (C) ChiG from *Streptomyces coelicolor* (PDB ID 2CJL) shows a high content of α-helices and a deep binding cleft. The catalytic acid is Glu68. The figures were made with PyMol (DeLano and Lam, 2005).

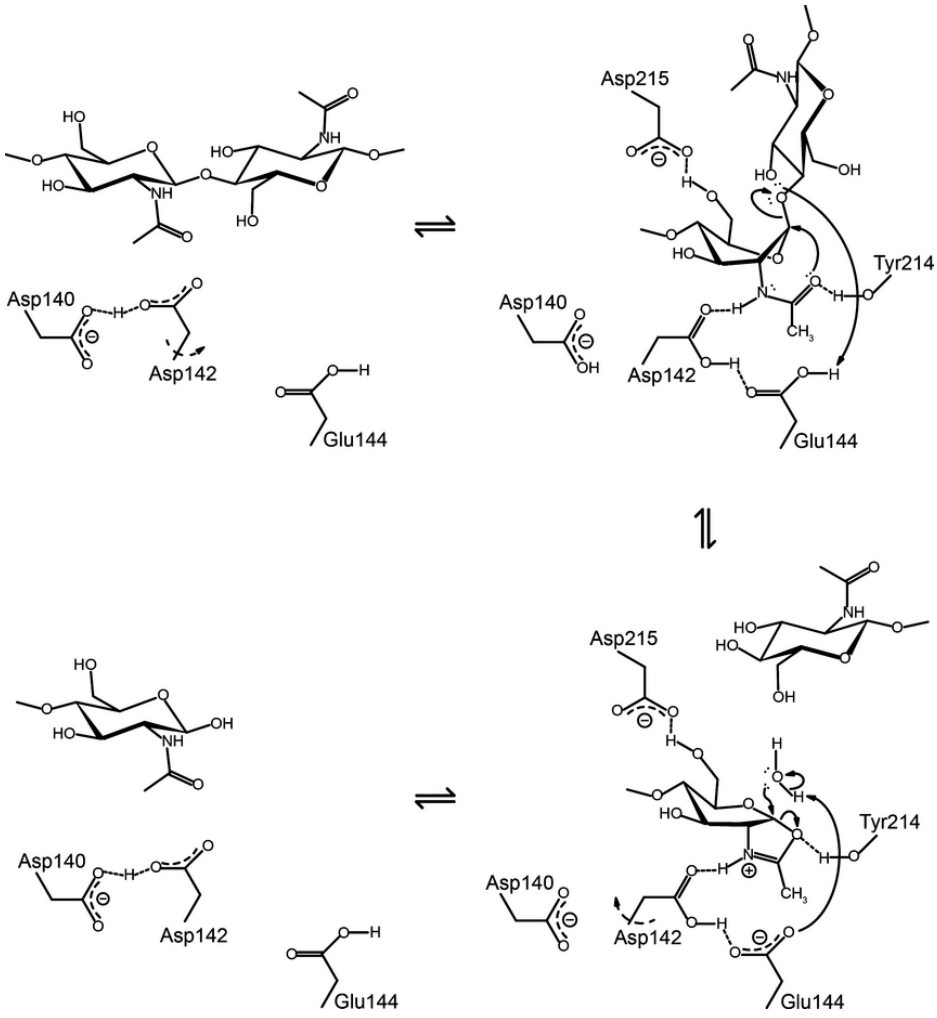

Figure 7. Schematic overview of the substrate assisted mechanism used by GH18 chitinases. Amino acid numbering is based on the sequence of *S. marcescens* ChiB. The catalytic cycle is initiated by binding of the substrate, which mediates distortion of the pyranose ring to a skewed boat conformation. At the same time Asp142 rotates towards the catalytic glutamate, thereby hydrogen bonding this residue as well as the acetamido group of the substrate. Acting as a general acid, Glu144 protonates the glycosidic oxygen, cleaving the glycosidic bond as the acetamido group concomitantly performs a nucleophilic attack on the anomeric carbon, forming an oxazolinium ion intermediate. At this point in catalysis, Asp144 abstracts a proton from an incoming water molecule that hydrolyses the oxazolinium ion. The product is displaced from the active site and Asp142 rotates back to its original conformation. The products resulting from catalysis show retention of the configuration at the anomeric carbon, meaning that the substrate's original conformation is preserved. The figure was adapted from (Vaaje-Kolstad et al., 2013).

1.2.2.2 β-hexosaminidases

The product of chitin hydrolysis by chitinases is mainly chitobiose. Most chitinolytic bacteria utilize family GH20 β-hexosaminidases to convert chitobiose and short chito-oligosaccharides into the monomer N-acetylglucosamine. A β-hexosaminidase produced by *S. marcescens* chitobiase, is a large four-domain protein (Tews et al., 1996). It is the largest protein in the chitinolytic machinery of *S. marcescens* and has its catalytic site in domain III (Figure 8). Similar to GH18s, the catalytic domain comprises a $(\beta/\alpha)_8$ barrel fold. Toratani *et al*. (2008) have shown the physiological importance of this enzyme by growing a chitobiase deficient *S. marcescens* mutant on GlcNAc or $(GlcNAc)_2$. While growth was wildtype-like with GlcNAc, it was severely retarded with $(GlcNAc)_2$ (Toratani et al., 2008). Notably, a study on the marine organism *Vibrio furnissii* has revealed another protein, a cytoplasmic phosphorylase that is able to convert $(GlcNAc)_2$ to GlcNAc and GlcNAc-α-1-P by phosphorolysis, that microbes may use to metabolize chitobiose (Park et al., 2000).

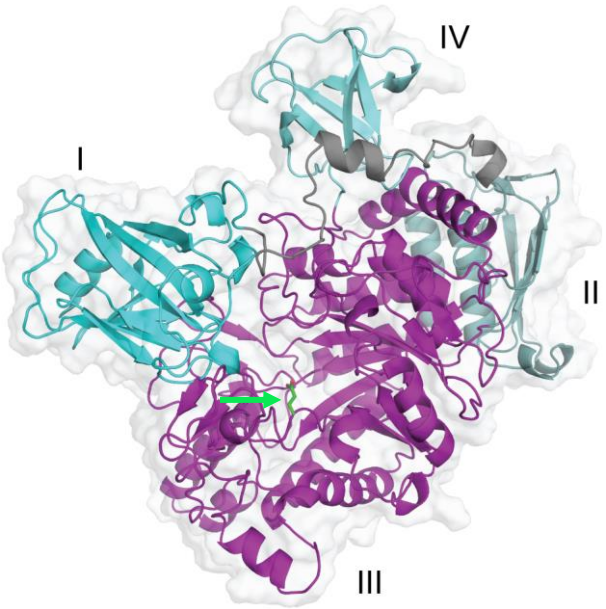

Figure 8. Structure of the complete four-domain β-hexosaminidase (chitobiase) from *S. marcescens* (PDB ID 1QBA). The domains are numbered I-IV and the catalytic acid, Glu540 in domain III is shown in green (also indicated by green arrow). The figure was made with PyMol (DeLano and Lam, 2005).

1.2.2.3 Chitin-active lytic polysaccharide monooxygenases

Proteins boosting the activity of GHs were first detected in 2005 (CBP21; (Vaaje-Kolstad et al., 2005a) and in 2010 these proteins were shown to be enzymes (Vaaje-Kolstad et al., 2010) that today are known as lytic polysaccharide monooxygenases (Horn et al., 2012). Before the enzymatic activity was discovered, it was already known that LPMOs are crucial for efficient chitin degradation (Vaaje-Kolstad et al., 2005a). When the enzymatic activity of CBP21, the LPMO from *S. marcescens* was uncovered, the synergistic effect was shown to be even more dramatic (Vaaje-Kolstad et al., 2010). This synergistic effect has also been shown for other chitinolytic systems (see chapter 1.2.2). Since LPMOs are the main focus of this thesis, these enzymes will be described in more detail in the next chapter.

1.3 Lytic polysaccharide monooxygenases (LPMOs)

1.3.1 History of LPMOs

In 1950, Reese and co-workers published a study in which they discussed whether there was a difference between the enzymatic conversion of cellulose derivatives and native cellulose. They carried out a series of experiments using cellulolytic and non-cellulolytic organisms and showed that many organisms, even non-cellulolytic ones are able to degrade soluble cellulose derivatives. In contrast, the ability to use native cellulose as a substrate was more restricted. Based on these results they postulated that the process of converting native cellulose into soluble molecules is carried out by at least two enzyme systems; C_1 and C_x.

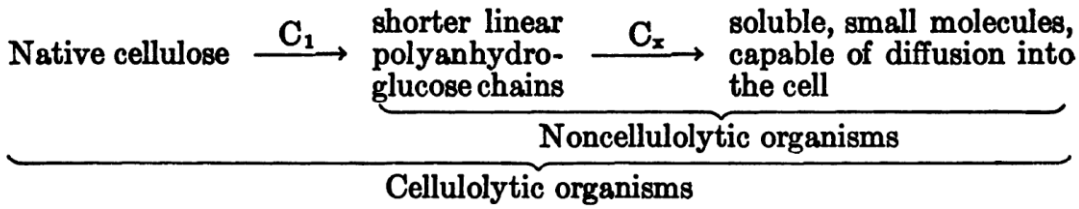

Figure 9. The C_1C_x hypothesis proposed by Reese *et al*. for the degradation of cellulose. The figure was taken from (Reese et al., 1950); Copyright © 1950, American Society for Microbiology.

In this postulated model (Figure 9), the C_1 process converts the native cellulose into smaller cellulose fragments that are then accessible for C_x that further degrade the substrate into oligomeric and monomeric sugars that can diffuse into the cell (Reese et al., 1950). For the first time, it was thus hypothesized that crystalline polysaccharides needed a form of enzymatic pretreatment, in order to allow solubilization.

Later, in 1974 Eriksson and co-workers compared an unfractionated culture solution of the fungus *Sporotrichum pulverulentum* with an artificial one that contained the same amounts of the five endo-1,4-β-glucanases and the one exo-1,4-β-glucanase that had previously been purified and characterized. They observed that the unfractionated culture solution was able to degrade 52.1% of the substrate, dewaxed cotton, whereas the artificial enzyme mixture managed to degrade only 20%. They showed that this was due to the oxidizing character of an additional enzyme by doing the same experiment in the presence of nitrogen instead of air. In the absence of oxygen, the unfractionated culture solution degraded 21.5% of the substrate.

In addition, Eriksson *et al*. (1974) were able to show oxygen consumption upon addition of powdered cellulose, cellobiose, lactose and other substrates to a cell-free culture solution. Indeed, efficient decomposition of cellulose seemed to be dependent on a form of oxidative activity.

Since these two interesting studies were published, not much progress was made on these enigmatic activities (i.e. a C_1-type activity and/or an oxidative activity). On the other hand, a substantial amount of work was carried out on proteins that were binding to carbohydrates, and believed to have no or only low depolymerizing activity. These proteins were categorized as CBM33s. In the beginning of the 1990s, studies using DNA libraries showed that secreted enzymes of unknown activity were potentially linked to cellulose degradation (reviewed by (Beeson et al., 2015)). Due to a minor hydrolytic activity detected in purified protein preparations, other enzymes were thought to have hydrolytic activity and were hence annotated as family 61 of the glycoside hydrolases. Later, a GH61 gene from *Trichoderma reesei* was found to be co-regulated with cellulase genes in this organism. This gene was cloned and expressed and the protein, Cel61A (formerly EG IV), was shown to have endoglucanase activity (Saloheimo et al., 1997). A closer investigation of this enzyme in another study revealed that its activity on different cellulose substrates is several orders of magnitudes lower compared to another cellulase produced by the same organism, whereas a wide screen on a large number of other oligo- and polysaccharides revealed no activity (Karlsson et al., 2001). In the same publication, the authors discussed whether the low activity could be due to contaminations as for other proteins, but could exclude this with high probability.

In the same time period, Hildgund Schrempf and co-workers identified and isolated several bacterial proteins that were found to bind to chitin and therefore were called chitin-binding proteins (CBPs/CHBs) (Schnellmann et al., 1994, Kolbe et al., 1998, Saito et al., 2001, Schrempf, 2001, Chu et al., 2001). A set of conserved aromatic residues was suggested to be responsible for the chitin binding properties (Zeltins and Schrempf, 1997), based on the known hydrophobic binding surfaces of other carbohydrate binding modules. Another chitin-binding protein was found in the culture supernatant of *Serratia marcescens*, when grown on chitin and was called CBP21 due to the size of the protein (Suzuki et al., 1998). This protein had probably been observed previously, as an approximately 21 kDa heavy protein purified from a *Serratia marcescens* culture supernatant (Fuchs et al., 1986). These CBPs/CHBs were later classified as family 33 of the carbohydrate-binding modules (CBMs) since one such

module was found attached to a GH5 mannanase, thus indicating the role of a CBM (Sunna et al., 2000).

How these GH61s and CBM33s are connected was first uncovered by structural and later functional analyses. In 2005, the first crystal structure of a CBM33 protein, CBP21, revealed that most of the tryptophans with a suggested role in chitin-binding were buried in the core of the protein, participating in the formation of a β-sheet sandwich. Instead, a flat patch of highly conserved polar residues was found on the protein surface. The role of a subset of these residues in chitin-binding was investigated and all single point mutations influenced the binding properties negatively (Vaaje-Kolstad et al., 2005b). The first structure of the GH61 protein Cel61B (formerly EGVII) from *Hypocrea jecorina* (anamorph *Trichoderma reesei*) was published in 2008. It showed a β-sheet sandwich and a flat surface with no obvious candidates for a canonical oligosaccharide-binding tunnel, cleft or pocket and the structure being most similar at that time was that of CBP21 (Karkehabadi et al., 2008).

In a breakthrough discovery in 2005, CBP21 was found to promote the degradation of chitin by chitinases (Vaaje-Kolstad et al., 2005a). Since the protein had no structural features of an enzyme, CBP21 was believed to be a non-catalytic protein that by an unknown mechanism, possibly involving substrate disruption promoted the degradation of chitin by chitinases. The mechanism of CBP21 was demonstrated as it was shown to increase the product formation by GH18 chitinases from *Serratia marcescens* and, to an even larger extent by a GH19 chitinase from *Streptomyces coelicolor* (Vaaje-Kolstad et al., 2005a). In 2010, Harris *et al.* reported similar effects for a GH61 protein from *Thielavia terrestris* in the depolymerisation of cellulose. The protein had no measurable catalytic activity, still it significantly enhanced cellulase activity in the presence of divalent metal ions such as Zn^{2+} and Ni^{2+} (Harris et al., 2010). In the same year, Vaaje-Kolstad *et al*. (2010) published their findings that CBP21 is in fact an enzyme that cleaves glycosidic bonds by an oxidative mechanism. The authors reported chitin degradation in the presence of a chemical reductant and molecular oxygen and also indicated dependency on a divalent metal ion (Vaaje-Kolstad et al., 2010). Indeed, the reductant proved to be the missing piece of the puzzle that had prevented the identification of this enzyme family at an earlier time point. In the following year, oxidative, catalytic activity on cellulose was shown for another CBM33 (Forsberg et al., 2011) and several GH61s (Quinlan et al., 2011, Phillips et al., 2011a, Langston et al., 2011). Collectively, the two enzyme families were named lytic polysaccharide monooxygenases (LPMOs) (Medie et al.,

2012, Horn et al., 2012), although some groups in the field also use the term PMO (i.e. lacking the word “lytic”).

Due to the fact that these proteins actually are enzymes and not carbohydrate binding modules, they were re-classified and belong now to family 10 of the auxiliary activities (AA10). Enzymes that were previously known as GH61 were re-classified to family 9 of the auxiliary activities (AA9) (Levasseur et al., 2013). Since then two new LPMO families have been assigned, namely AA11 (Hemsworth et al., 2014) and AA13 (Vu et al., 2014b, Lo Leggio et al., 2015).

Revisiting the two key publications from 1950 and 1974 with this more recent research in mind, there are striking similarities. With the C_1/C_x hypothesis, Reese et al. postulated that the degradation of crystalline cellulose depends on at least two systems, one that enhances substrate accessibility, a role that has been suggested for LPMOs, and one that degrades accessible fibers to smaller sugars, the task of glycoside hydrolases. The importance of oxidizing enzymes in biomass degradation reinforce the findings of Eriksson *et al*. (1974). In a recent study, Müller *et al*. (2015) compared the degradation of cellulosic biomass using commercial enzyme cocktails containing LPMOs in the presence and absence of air (i.e. oxygen). When carrying out the degradation of steam exploded birch wood in air, significantly higher saccharification yields were achieved compared to the degradation in anaerobic conditions. These findings show a striking resemblance with the cotton degradation experiments reported in 1974. The role of LPMOs in biomass conversion does indeed seem important.

1.3.2 Occurrence of lytic polysaccharide monooxygenases

LPMOs have been identified in a myriad of organisms, but mainly in bacteria and fungi. They are currently categorized as families 9, 10, 11 and 13 of the auxiliary activities (Levasseur et al., 2013). Family AA9 contains only fungal enzymes that were previously referred to as GH61s. Family AA10 proteins (previously CBM33) are found in all domains of life, namely archaea, bacteria and eukaryota. They have even been identified in several viruses. Most structural and functional data on LPMOs have been obtained by studying these two families. Family AA11 has mainly fungal members, but one LPMO11 has been detected in an uncultured bacterium. The latest addition to the auxiliary activities is family AA13, which, as

family AA9, exclusively comprises fungal LPMOs. At the time this thesis was written (July 2016) the CAZy database [www.cazy.org] had one entry for an archaeal LPMO, 125 entries for viral LPMOs, 418 entries for eukaryotic LPMOs (mainly fungal), and 1874 entries for bacterial LPMOs and 6 LPMOs of unknown origin.

This universal occurrence of LPMOs indicates biologically important roles that may include tasks beyond breaking down cellulosic and chitinous materials. Genomes of biomass degrading fungi usually encode several LPMO genes with numbers up to over 40. The transcription and expression of fungal LPMOs are influenced by the growth conditions of the organism and seem to be upregulated in the presence of biomass (Wymelenberg et al., 2010, Yakovlev et al., 2012, Phillips et al., 2011b, Eastwood et al., 2011, Berka et al., 2011). Bacterial LPMOs are secreted upon growth on biomass as well (Suzuki et al., 1998, Takasuka et al., 2013, Tuveng et al., 2016). Interestingly, AA10s also occur in pathogenic bacteria and viruses, suggesting a different role than enhancing the depolymerization of recalcitrant biomass. Some of these LPMOs are putative virulence factors and will be described in more detail later in this thesis (see chapter 1.3.8).

1.3.3 Tertiary structure of LPMOs

Even though the LPMOs families share little sequence identity, their overall fold is similar. They possess an immunoglobin-like core consisting of β-strands organized in a β-sandwich. The strands are connected by series of loops featuring a varying amount of short α-helices (Vaaje-Kolstad et al., 2005b, Karkehabadi et al., 2008, Harris et al., 2010, Li et al., 2012, Vaaje-Kolstad et al., 2012, Wu et al., 2013, Hemsworth et al., 2014, Lo Leggio et al., 2015). Some of these loops are involved in forming the relatively flat binding surface of the protein that, in contrast to many glycoside hydrolases, does not display a deep binding groove or tunnel. This flat binding surface, which accommodates a type-2 copper center (Quinlan et al., 2011), likely enables the protein to be active on the flat crystalline surface of the substrate (Horn et al., 2012, Vaaje-Kolstad et al., 2010). As an exception, the family AA13 LPMO *Ao*AA13, was recently shown to possess a shallow groove leading through the copper active site, which probably can accommodate a polysaccharide chain (Lo Leggio et al., 2015).

Since the structure of CBP21 was solved in 2005, 23 additional unique LPMO structures have been solved. The structural relationship between these LPMO structures was investigated by

clustering these LPMO structures based purely on structural similarity using the DALI protein structure comparison database (Figure 10). The LPMOs cluster in nine different groups that obviously differ in structure, but also seem to differ in substrate preference. LPMOs have been shown to have different substrate specificities (see details in section 1.3.5). It is also clear from this analysis that the central β-sandwich core is the common core of the LPMOs.

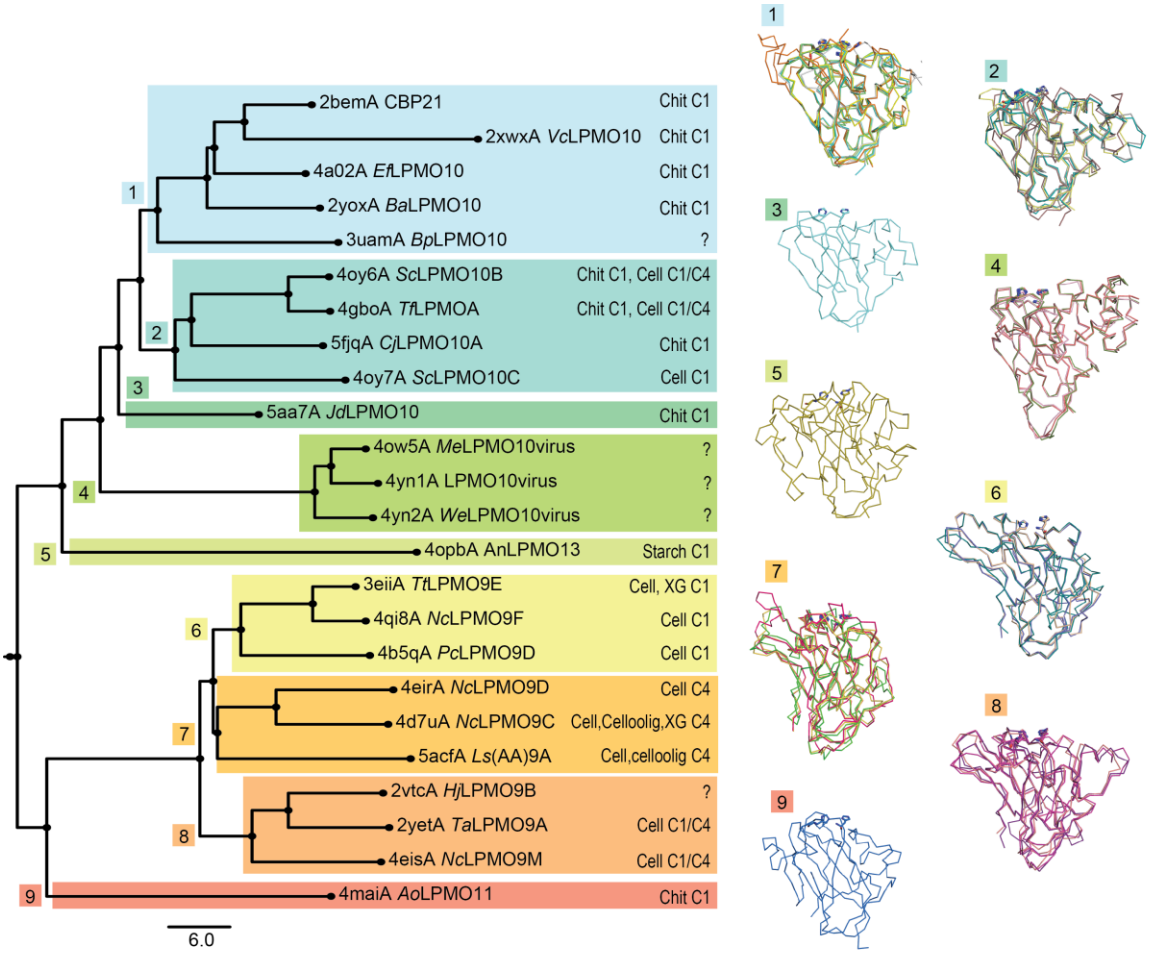

Figure 10. Structural clustering of LPMOs. The dendrogram on the left shows the structural clustering of the 24 currently available unique LPMO structures. The scale indicates the DALI Z-score. All representatives of each cluster are shown structurally aligned on the right hand side of the dendrogram. Structural alignment was performed using the "align" function of the PyMol software suite. Structural clustering was performed using the DALI structural comparison server (Holm and Rosenstrom, 2010), using the "all against all" option.

Most of the variability of the LPMO structures is located in the region located between β-strand 1 and 3, also called "loop 2" abbreviated "L2" (Li et al., 2012, Wu et al., 2013, Forsberg et al., 2014a). This region consists of both loops and short helices and is believed to determine substrate recognition and specificity as it constitutes large parts of the substrate binding surface (Li et al., 2012, Wu et al., 2013, Book et al., 2014, Forsberg et al., 2014a, Vu et al., 2014a, Borisova et al., 2015). Figure 11 illustrates one representative of each LPMO cluster from the DALI analysis (Figure 10).

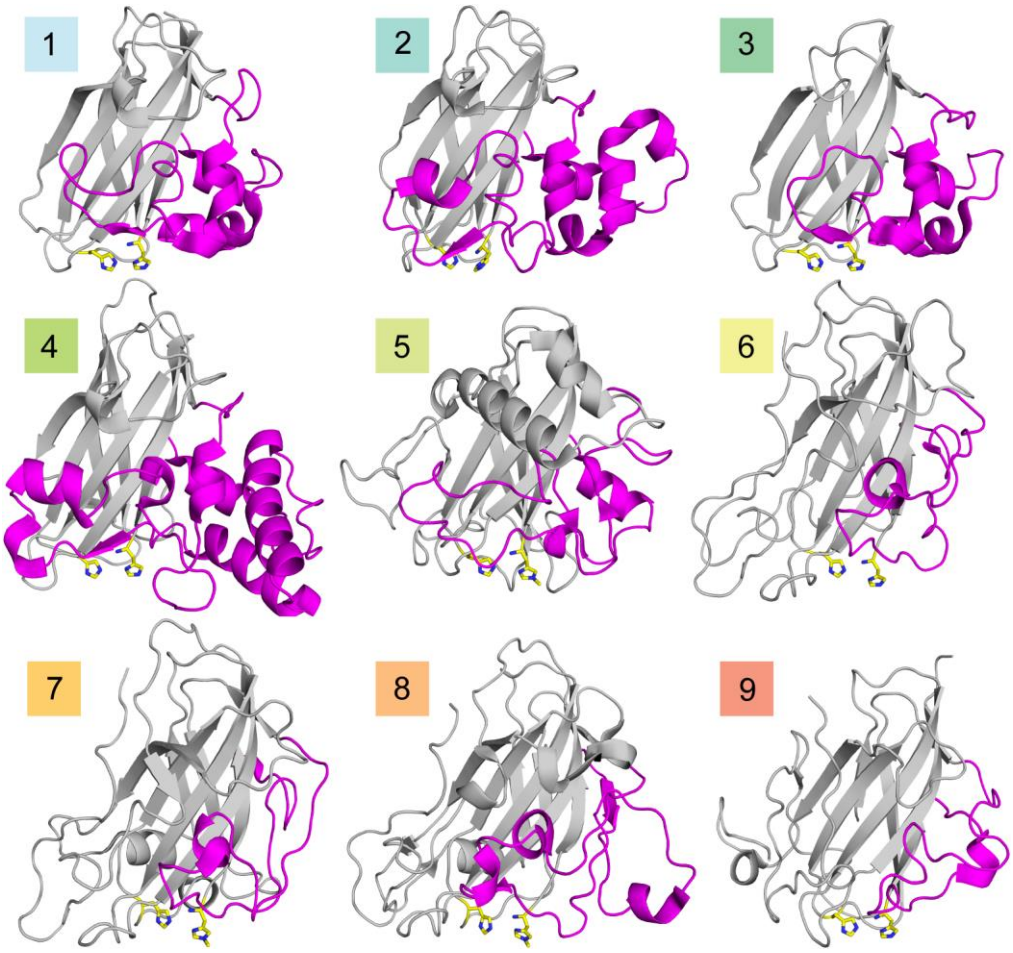

Figure 11. Cartoon representation of LPMOs showing the variability in the so-called "loop 2" area and corresponding regions. Regions between the first β-strand and the last β-strand before the β-sandwich are shown in magenta. The colors and numbers correspond to the structural clustering of LPMOs in Figure 10. Each cluster is represented by one protein. The PDB IDs are given in parenthesis after the protein name. (1) CBP21 (2BEM), (2) *Sc*LPMO10B (4oy6), (3) *Jd*LPMO10 (5AA7), (4) *Me*LPMO10 (4ow5), (5) *Ao*LPMO13 (4OPB), (6) *Tt*LPMO9E (3EII), (7) *Nc*LPMO9D (4EIR), (8) *Ta*LPMO9A (2YET), (9) *Ao*LPMO11 (4MAI). Note that fungal LPMOs have an additional loop area at the distal site of loop 2.

1.3.4 The copper active site

The copper active site is the key to LPMO reactivity and highly conserved in all LPMO families. The first crystal structure of an LPMO in which the metal binding site was identified was from Cel61B from *H. jecorina* (*T. reseei*). Karkehabadi and colleagues identified a solvent exposed nickel binding site, where the metal ion was bound in a hexacoordination sphere (i.e. an octahedral geometry; Figure 12). The cation was coordinated by the δ-nitrogen and the amino group of the N-terminal histidine, the ε-nitrogen of another highly conserved histidine, the hydroxyl group of a tyrosine in addition to two water molecules (Karkehabadi et al., 2008).

Before copper was shown to be the correct metal of the active site, the importance of divalent metal ions for protein activity was probed in two studies in which Ca^{2+}, Ni^{2+}, Mn^{2+}, Co^{2+}, Mg^{2+} and Zn^{2+} were included in reactions mixtures (Harris et al., 2010, Vaaje-Kolstad et al., 2010). Interestingly, these metals yielded LPMO activity and the inhibition of enzymatic activity by EDTA confirmed the pivotal role of a divalent metal ion (Harris et al., 2010, Vaaje-Kolstad et al., 2010). In retrospect, it is likely that contaminating copper ions in the metal solution used in these studies may have been responsible for the LPMO activity observed. The first solid proof that this metal binding site is a type 2 copper site was given by Quinlan and co-workers who could not detect significant binding of the previously used metals, but very tight binding of Cu^{2+} in isothermal titration calorimetry (ITC) experiments. By means of EPR experiments the type 2 copper site was identified and crystallography confirmed coordination of the metal ion by three nitrogen atoms, provided by two histidines in a so-called “histidine brace”. The hydroxyl group of the axial tyrosine contributed to shaping the binding site. In the same publication the authors report methylation of the ε-nitrogen in the N-terminal histidine which could have an impact on activity (Quinlan et al., 2011). Shortly after the Quinlan study was published, the Marletta group reported equally convincing data on the topic of the active site metal, showing that only copper gave LPMO activity in enzymes reconstituted with various metals and that LPMO-Cu(II) stoichiometry measured by ICP-AES on purified LPMOs was 1:1 (Phillips et al., 2011a). Since then, the structure and binding affinity of the copper binding site has been studied in different LPMOs, confirming the key observations by Quinlan *et al*. and Phillips *et al*. but also revealing variation, especially between the different LPMO families.

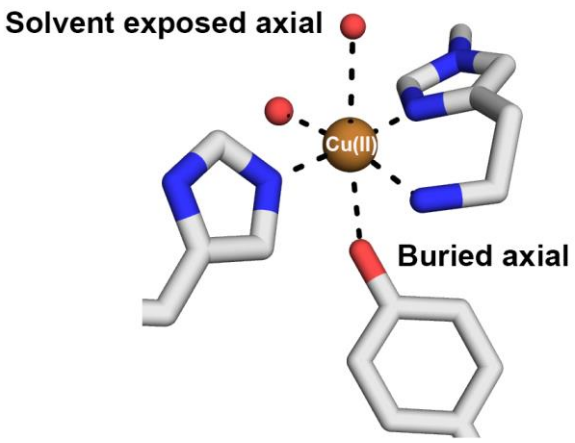

Figure 12. Detailed view of copper coordination of a AA9 LPMO (*Ls*AA9A) from *Lentinus similis*; PDB ID 5ACG) where copper is present in its Cu(II) form. Red spheres represent water molecules. Amino acid side chains are shown in stick representation. The axial positions of the copper coordination sphere are indicated. The equatorial positions are inhabited by the three nitrogen ligands and the second water molecule. The figure was made with PyMol (DeLano and Lam, 2005).

Copper-binding to LPMOs has been observed to be extremely tight. By means of ITC various dissociation constants (K_d) have been determined. A K_d of less than 1 nM at pH 5 has been estimated for *Ta*LPMO9A and Cu(II) (Quinlan et al., 2011). For CBP21 the K_d for Cu(II) was measured to be 55 nM at pH 6.5 (Aachmann et al., 2012). In the same study it was also reported that binding of Cu(I) was tighter compared to Cu(II) and that the K_d for CBP21-Cu(I) was calculated to be 1 nM (Aachmann et al., 2012). In other studies authors have reported a dissociation constant ranging from 6 nM at pH 5 to 80 nM at pH 7 for *Ba*AA10A from *B. amyloliquefaciens* (Hemsworth et al., 2013b) and a K_d <1 nM for *Ao*AA11 at pH 5 (Hemsworth et al., 2014). In a recent study, divergent copper-binding exhibiting two different K_ds was observed, one with nanomolar and one with micromolar value. Based on their findings the authors suggest flexibility in the apo copper-binding site and that correct coordination of the copper may be steered by delivery of the copper to the LPMO by specific copper-chaperones (Chaplin et al., 2016).

A unique property of fungal LPMOs is the presence of a methyl group on the ε-nitrogen of the N-terminal histidine of LPMOs expressed in fungal hosts (Quinlan et al., 2011, Li et al., 2012, Lo Leggio et al., 2015). The role of this post-translational modification is unknown, but it has been suggested to influence catalysis by modification of the histidine pK_a or alteration of the active site electronic properties (Aachmann et al., 2012, Hemsworth et al., 2013a, Beeson et al., 2015). Kim *et al*. (2014) used a theoretical approach i.e. quantum mechanical

calculations and suggested based on their results, that this posttranslational modification has only very minor or no influence on the LPMO catalytic activity. Fungal LPMOs expressed in *P. pastoris* or *E. coli* do not show this modification, but still show activity (Kittl et al., 2012, Wu et al., 2013, Hemsworth et al., 2014, Borisova et al., 2015).

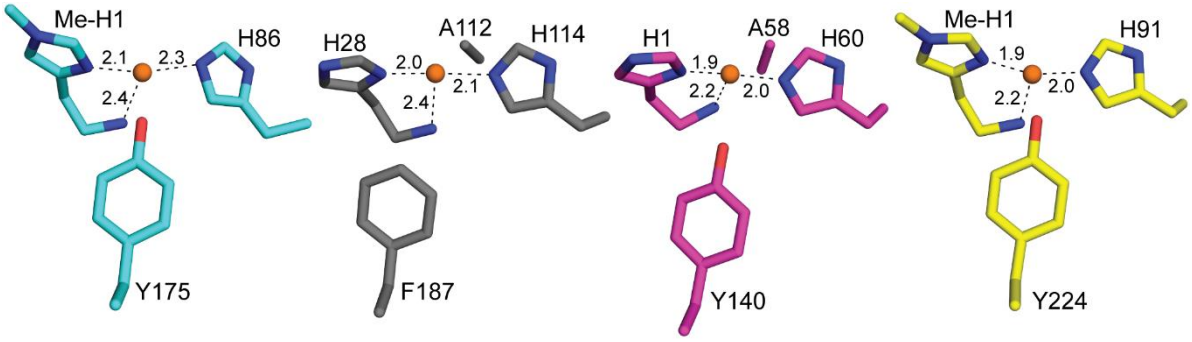

Figure 13. Stick representations of the T-shaped coordination of the copper active sites of LPMOs highlighting conserved residues close to the copper (orange sphere). Non-protein ligands are not shown. The figure shows an AA9 (cyan, *Ta*AA9A, PDB ID 2YET), AA10 (gray, CBP21, PDB ID 2BEM), AA11 (magenta, *Ao*LOMO11, PDB ID 4MAI) and an AA13 (yellow, *Ao*AA13, PDB ID 4OPB). The distances between the atoms in the histidine brace are given in Å. It should be noted that all enzymes except CBP21 were crystallized in the presence of copper. The figure was made with PyMol (DeLano and Lam, 2005).

Even though there is some variation in the non-protein ligands of LPMOs with a Cu(II) bound, the T-shaped histidine brace formed by the copper and its nitrogen ligands is conserved in all LPMO families when the copper is in the reduced state. However, the surroundings of both axial positions show some variation (Figure 13). In the buried axial position, the hydroxyl group of the conserved axial ligand tyrosine, which is present in AA9s, AA11s and AA13s, contributes to the octahedral coordination of the Cu(II) ion (Quinlan et al., 2011, Harris et al., 2010, Wu et al., 2013). In AA10s, a phenylalanine usually takes this position although some AA10s have a tyrosine, similar to the fungal LPMOs. In the solvent exposed axial position, most AA10s have a highly conserved alanine, which restricts access and may prevent binding of dioxygen at this position as pointed out by Hemsworth *et al.* (2013b). Notably, a C1/C4 oxidizing AA10 shows a displacement of the conserved alanine possibly allowing ligand binding at the solvent exposed axial position (Forsberg et al., 2014a). Similar to AA10s, a restricted access to the solvent exposed axial position also occurs in some AA9s. Borisova *et al*. (2015) and Forsberg *et al.* (2014), both carried out structural comparisons showing that a

hydroxyl group of a conserved tyrosine restricts access to the solvent exposed axial position in strict C1 oxidizing AA9s. In strictly C4 oxidizing AA9s this axial position appears to be unrestricted and C1/C4 oxidizing AA9s exhibit an intermediate architecture (Borisova et al., 2015). AA11s possess features from both, AA9s and AA10s. Next to the axial tyrosine as present in AA9s they also feature the axial alanine like in AA10s (Figure 13; (Hemsworth et al., 2014)).

The photoreduction of Cu(II) to Cu(I) is a common event in crystallography and has been observed several times (Hemsworth et al., 2013b, Hemsworth et al., 2014, Lo Leggio et al., 2015). The structural changes that accompany this reduction have been investigated by Gudmundsson and colleagues. A continuous shift from a trigonal bipyramidal copper coordination to a T-shaped copper coordination i.e. no copper-bound water molecules, was observed with increasing doses of X-ray radiation in studies of *Ef*CBM33A, the only AA10 from *E. faecalis* (Gudmundsson et al., 2014). Other structures of AA10s (e.g. *Ba*AA10A (Hemsworth et al., 2013b) and *Jd*LPMO10A (Mekasha et al., 2016)) show no other ligands bound to the copper than the three nitrogens, indicating that the copper ion is in Cu(I) state, resulting from X-ray photoreduction.

As already mentioned, EPR analyses of the cellulose-active *Ta*AA9A loaded with Cu(II) clearly identified the type 2 copper center (Quinlan et al., 2011). In a later study of an AA10, also loaded with Cu(II), a copper coordination geometry was observed that lies between type 1 and type 2 in the Peisach-Blumberg classification [(Peisach and Blumberg, 1974)] (Hemsworth et al., 2013b). In 2014, Forsberg and colleagues compared the structures and EPR spectra of chitin- and cellulose-active AA10s and showed that the cellulose-active proteins possess a type 2 copper center whereas the chitin-active LPMOs fall between the Peisach-Blumberg type 1 and type 2 classifications (Figure 14) (Forsberg et al., 2014b). However, a general prediction of substrate specificity by EPR is not possible, since two chitin-active LPMOs, *Ao*LPMO11 and *Cj*LPMO10A, both display a type 2 copper site (Hemsworth et al., 2014, Forsberg et al., 2016).

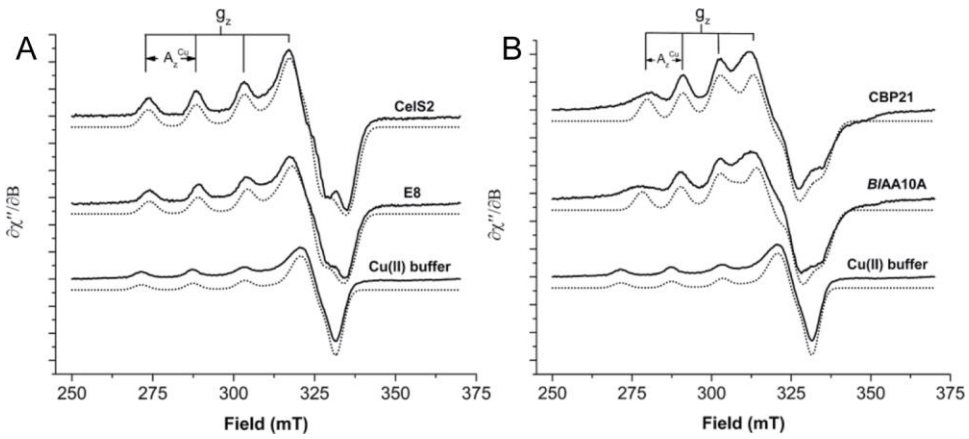

Figure 14. Typical LPMO EPR signatures. A: Type-2 copper B: mixed. Adapted with permission from [Forsberg, Z. 2014. Comparative study of two chitin-active and two cellulose-active AA10-type lytic polysaccharide monooxygenases. Biochemistry, 53, 1647-1656]. Copyright (2014) American Chemical Society.

1.3.5 Substrates and substrate binding

The first LPMO activity discovered was the oxidative cleavage of crystalline β-chitin by CBP21 (Vaaje-Kolstad et al., 2010). Another study on this enzyme revealed activity on crystalline α-chitin, yet to a lower extent, and that synergy with *S. marcescens* chitinases decreased with decreasing degree of crystallinity of the substrate (Nakagawa et al., 2013). Further studies uncovered activity of an AA10 from *Streptomyces coelicolor* and an array of AA9s on cellulose (Forsberg et al., 2011, Quinlan et al., 2011, Langston et al., 2011, Phillips et al., 2011a). In subsequent studies, LPMO activity on additional substrates has been revealed. For example, *Nc*LPMO9C (NCU02916) from *Neurospora crassa*, exhibits not only activity on crystalline cellulose, but also on soluble cello-oligomers (Isaksen et al., 2014). The same LPMO was found to cleave β-1,4 glucan bonds in hemicelluloses, in particular xyloglucan, showing its ability to accept substitutions in various positions in the β-glucan backbone (Agger et al., 2014). Later, it was shown that an AA9 from *Myceliophtora thermophila* (*Mt*LPMO9A) is active on xylan-coated cellulose and cleaves the β-1,4 xylosyl bonds in xylan as well as the β-1,4 glucosyl bonds in cellulose (Frommhagen et al., 2015). All these substrates show a common feature, namely the β-1,4 linkages connecting the single sugar moieties in the backbone. Vu and co-workers discovered that LPMOs were not only restricted to cleave β-1,4 linkages by showing activity of a *N. crassa* family AA13 LPMO

towards starch (i.e. α-1,4 bonds; (Vu et al., 2014b)). Later, a starch active LPMO was also identified from the fungus *A. nidulans* (Lo Leggio et al., 2015). Thus, LPMO substrates are indeed more diverse than initially assumed.

The interactions between LPMOs and their substrates have been addressed in several studies. Many LPMOs do not possess a CBM that could help directing substrate binding by the protein. Binding to cellulose is probably driven at least in part aromatic-carbohydrate π interactions (Beeson et al., 2015). Structural analyses have shown that solvent exposed aromatic residues, mainly tyrosines, form a rather planar surface that seems suited to bind to crystalline cellulose similar to a CBM1 (Harris et al., 2010). Li and colleagues have modelled the interactions of these subsets of surface-aromatic residues from a CBM1 and three different AA9s with the hydrophobic face of crystalline cellulose. Their results showed that the distance and position of these residues corresponds to those of the pyranose units (Li et al., 2012). Additional MD simulations have shown that other, mainly polar residues are also involved in binding to cellulose (Wu et al., 2013). Structural investigations of *Ls*AA9A, an AA9 from *Lentinus similis,* with bound cello-oligomers have indeed shown that a network of hydrogen bonds between the cello-oligomer and polar surface residues contributes to binding of the soluble substrate [(Figure 15); (Frandsen et al., 2016)]. This study also revealed an aromatic stacking interaction between a prominent (conserved) tyrosine, Tyr203 for *Ls*AA9A, and the substrate.

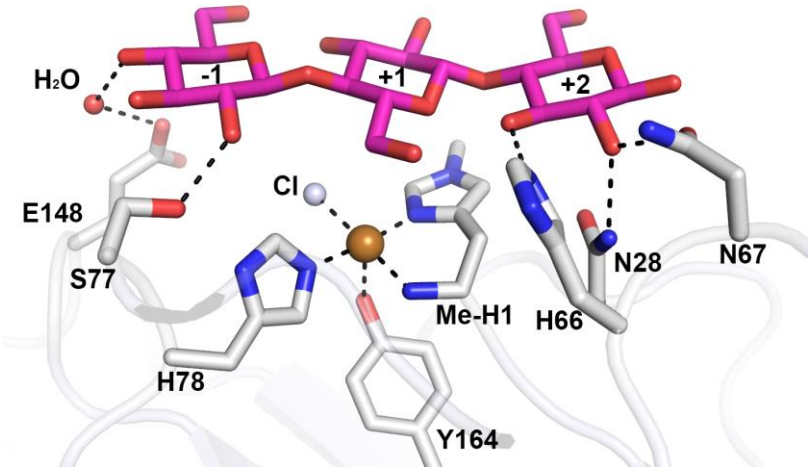

Figure 15. Structure of *Ls*AA9A with a bound cellotriose. The principle contacts between the protein and the substrate are indicated. A chloride ion (light blue) is coordinated in the equatorial position of the Cu(I) (golden sphere). Subsites are indicated in the pyranose rings of the substrate. The figure is made in PyMol (DeLano and Lam, 2005) and based on [(Frandsen et al., 2016); Figure 3d].

The recent study by Frandsen *et al.* (2016) also provides insight into how the enzyme-ligand interaction affects the conformations of the interaction partners. Whereas the substrate seemed to adopt a native structure with virtually no distortion, substrate binding led to clear changes in the copper coordination sphere (Frandsen et al., 2016). Changes in the copper active site upon substrate binding had previously been shown for *Nc*LPMO9C where altered g-values and copper hyperfine splittings were observed by EPR (Borisova et al., 2015). Frandsen *et al.* (2016) report similar EPR data and their structural data reveal that, indeed, minor structural rearrangement of the copper site takes place.

Further insight into LPMO-substrate interactions have been obtained from NMR studies (Aachmann et al., 2012; Courtade et al., 2016). In the most recent work, broad-specificity *Nc*LPMO9C was used to identify residues interacting with cellohexaose, oligomeric xyloglucan and polymeric xyloglucan. Binding of the ligands was found to primarily affect the copper site and nearby regions of the rather flat surface of the LPMO. The amino acids most affected by substrate binding were the two residues that form the histidine brace, a nearby additional surface-histidine and an alanine close to the solvent exposed axial copper coordination sphere [(Figure 16); (Courtade et al., 2016)]. The highly conserved tyrosine close to the active site (Tyr204 in *Nc*LPMO9C and Tyr 203 in *Ls*AA(9A)), indicated to contribute to cellulose binding by the Frandsen *et al.* (2016) study, was not affected by binding of the hexasaccharide, but was clearly affected by binding of the xyloglucan substrates (Courtade et al., 2016). Courtade and colleagues also reported that the strength of the ligand binding is not affected by the copper, but increases when cyanide is added to the copper-loaded enzyme. Cyanide is a known LPMO inhibitor and it is conceivable that CN^- mimics O_2^- (see below for a further discussion of the mechanism). This finding is compatible with the data shown by Frandsen *et al.* (2016), where binding of chloride (also an ion with superoxide-like properties) in the LPMO active site, result in a substantial increase in substrate binding.

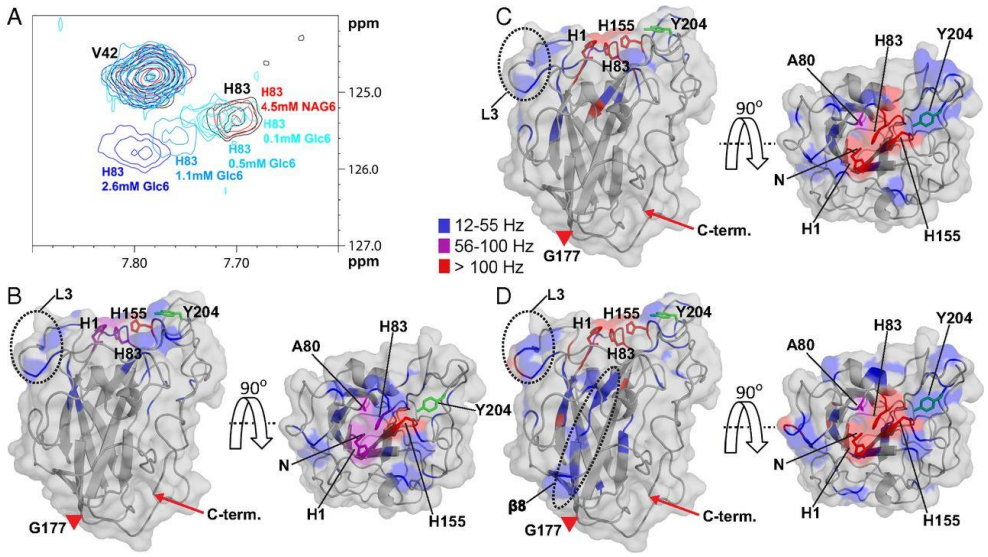

Figure 16. Apo-*Nc*LPMO9C interactions with different substrates. Overlaid area of interest of ^{15}N-HSQC spectra of *Nc*AA9C in the presence of $GlcNAc_6$ (NAG6) or increasing Glc_6 concentrations (A). (B)-(D) Cartoon and surface representation of *Nc*AA9C in a side and top view. Compound change in chemical shifts caused by binding of cellohexaose (B), xyloglucan 14-mer (C) and polymeric xyloglucan (D) are mapped on the protein structure. The compound change is indicated by a coloring scheme in which grey represents no change. The figure was taken from [Courtade, G. et al. 2016. Interactions of a fungal lytic polysaccharide monooxygenase with beta-glucan substrates and cellobiose dehydrogenase. *Proc Natl Acad Sci U S A,* 113**,** 5922-5927].

Chitin-active LPMOs exhibit a variety of conserved hydrophilic residues that are thought to be involved in chitin-binding via hydrogen bonding and usually a single solvent exposed aromatic amino acid that is presumed to interact with the substrate through π-stacking (Vaaje-Kolstad et al., 2005a, Vaaje-Kolstad et al., 2005b, Beeson et al., 2015). Binding of AA10s to chitin has been investigated for CBP21. Before it was known that CBP21 was an LPMO, a site-directed mutagenesis study of conserved amino acids was carried out to identify residues important for adsorption of the protein to chitin. CBP21 possesses only one aromatic residue on its flat active-site-containing surface. Binding experiments identified this tyrosine and four hydrophilic amino acids (two glutamates, one asparagine and one aspartate) as important for chitin binding. These data suggest that, in addition to hydrophobic interactions, specific hydrogen bonding networks between the substrate and conserved hydrophilic residues are involved in chitin binding (Vaaje-Kolstad et al., 2005b). An NMR study carried out on the same protein detected that mainly polar residues are involved in substrate binding in addition to the copper site and the single solvent-exposed tyrosine (Figure 17 panels A&B).

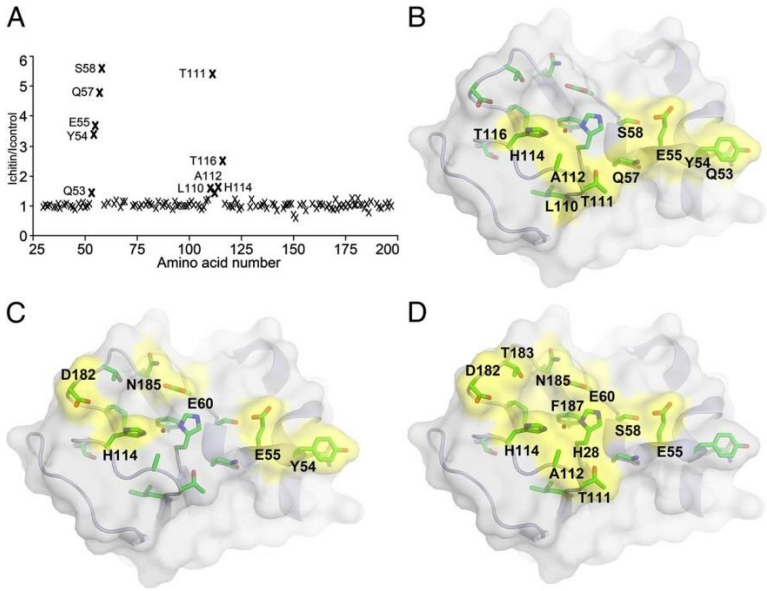

Figure 17. Chitin-binding surface of CBP21. (A) Residues involved in chitin binding by CBP21 determined by NMR in a chitin binding experiment. Residues shielded by chitin binding show a number higher than 1. (B) Residues identified in (A) plotted on the CBP21 surface and colored by yellow surface. (C) Residues involved in chitin binding identified from site-directed mutagenesis experiments; labeled and colored by yellow surface (Vaaje-Kolstad et al., 2005b). (D) Highly conserved residues on the substrate binding surface of CBP21; labeled and colored by yellow surface. The figure was taken from [Aachmann, F. L. *et al*. 2012. NMR structure of a lytic polysaccharide monooxygenase provides insight into copper binding, protein dynamics, and substrate interactions. *Proc. Natl. Acad. Sci. U.S.A.,* 109**,** 18779-18784].

Notably, the combined results of both studies clearly show that the primary interactions between substrate and enzyme happen in close proximity to the copper-site (Aachmann et al., 2012).

As described in detail in the next section (chapter 1.3.6), oxidative cleavage of the β-1,4 glycosidic bond by an LPMO leads to oxidation of the C1 or C4 carbon of the substrate. Some LPMOs display mixed activities, meaning that both C1- and C4-oxidized products are generated. The mode of substrate binding has been suggested to be important for the oxidative regioselectivity of LPMOs. In the C1/C4 oxidizing AA9s *Nc*LPMO9M and *Ta*LPMO9A, a short α-helix extension in loop L2 that is positioned parallel to the active site has been suggested to be important for C4-oxidation (Vu et al., 2014a). Vu *et al*. also suggests that a conserved small additional helix forming sequence motif on the substrate binding surface of NCU01050, possibly interacts with the cellulose substrate directly and leads to C4-oxidation (Vu et al., 2014a). The capability to perform C4-oxidation has also been suggested to be related to the accessibility of the distant (solvent exposed) axial position, which is blocked by a conserved alanine in strict C1 oxidizing AA10s (Forsberg et al., 2014a). Similar

observations were made for AA9s where the axial position is restrained by the hydroxyl group of a conserved tyrosine (Borisova et al., 2015). So far, C4-oxidation has only been observed for cellulolytic LPMOs.

It should be noted that the data described above are insufficient to conclude if and how the mode of substrate-binding affects the oxidative regioselectivity. However, the observations made show interesting correlations that could be explored further in future structure-function studies.

1.3.6 Reaction mechanism

The first evidence for LPMO activity was discovered for a chitin-active enzyme (CBP21), which was shown to produce C1-oxidized chito-oligosaccharides (chito-oligosaccharides oxidized at the reducing end; aldonic acids) in the presence of a reducing agent and dissolved dioxygen. Isotope labelling experiments using $H_2{}^{18}O$ and ${}^{18}O_2$ provided information about the source of the incorporated oxygen atoms and showed clearly that one is derived from water and the other one from molecular oxygen (Figure 18). The initial work on CBP21 was done using ascorbic acid as reductant. In the past few years a plethora of reducing agents that can activate LPMOs has been identified. More information about these reducing agents will be given in the next chapter (1.3.7).

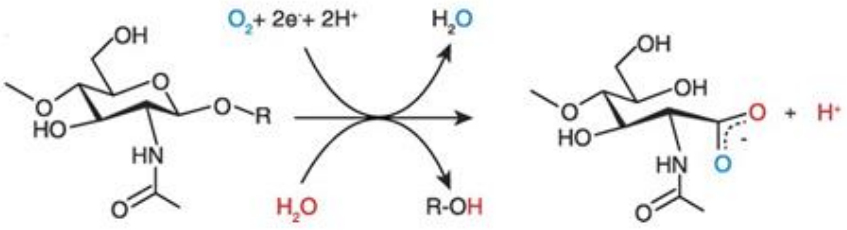

Figure 18. Oxidative chitin cleavage catalyzed by CBP21. The final oxidized product is an aldonic acid that contains one oxygen atom from water (red) and one from molecular oxygen (blue). From [Vaaje-Kolstad, *et al*. 2010. An oxidative enzyme boosting the enzymatic conversion of recalcitrant polysaccharides. *Science,* 330**,** 219-222]. Reprinted with permission from AAAS.

Subsequent to the study on CBP21, oxidative cleavage of cellulose leading to C1-oxidation was shown for an AA10 (Forsberg et al., 2011) and for several AA9s (Quinlan et al., 2011, Phillips et al., 2011a, Beeson et al., 2012, Wu et al., 2013, Westereng et al., 2011). Degradation of phosphoric acid swollen cellulose by *Ta*LPMO9A (Quinlan et al., 2011) yielded a relatively complex product profile which was further investigated by permethylation of the LPMO products followed by MS analysis to determine the position of the oxidized carbon. The generated mass shifts indicated that, similar to what Vaaje-Kolstad *et al.* (2010) showed, the oxidation occurred at the C1 carbon. Based on their results Quinlan *et al.* (2011) also suggested an additional C6 oxidation mode, but today it seems generally accepted in the field that C6 oxidation does not occur and that the additional oxidation mode observed by Quinlan *et al.* (2011) most likely is C4-oxidation. In parallel to the Quinlan *et al.* (2011) study, the activity of three different AA9s from *Neurospora crassa* was reported by Phillips *et al.* (2011), revealing a complex spectrum of products. Next to aldonic acids already reported by Vaaje-Kolstad *et al.* (2010) and Quinlan *et al.* (2011) further oxidized species were found whose masses were consistent with a gemdiol, the hydrated product of a C4 oxidized sugar (Phillips et al., 2011a), i.e. an oligosaccharide oxidized at the non-reducing end. The generation of C4 oxidized products has later been confirmed by several studies (Beeson et al., 2012, Isaksen et al., 2014, Vu et al., 2014a, Forsberg et al., 2014a). Notably, particularly strong biochemical evidence for C4 oxidation is provided in Beeson *et al.* (2012) and Isaksen *et al.* (2014), using a chemical approach and NMR analysis of the product, respectively. Today it is well established that discrimination between C1 and C4 oxidized products is conveniently achieved by HPLC and even MS, despite having some overlapping masses with aldonic acids, as described in (Forsberg et al., 2014b) and (Westereng et al., 2016a, Westereng et al., 2016b).

The products initially formed by C1 and C4 oxidation are δ-1,5-lactones and 4-ketoaldoses respectively. In an aqueous solution, the lactone spontaneously forms an aldonic acid and hydration of the ketoaldose leads to the formation of a geminal diol (Figure 19). Both these events are pH dependent, where increasing pH drives the equilibrium towards the hydrated variants. LPMO products oxidized at both the reducing and non-reducing ends (also called "double oxidized" products) have been observed with LPMOs that exhibit mixed C1/C4 activity; such products can emerge if the same polysaccharide chain is cleaved twice, once by C1 oxidation and once by C4 oxidation (Forsberg et al., 2014a).

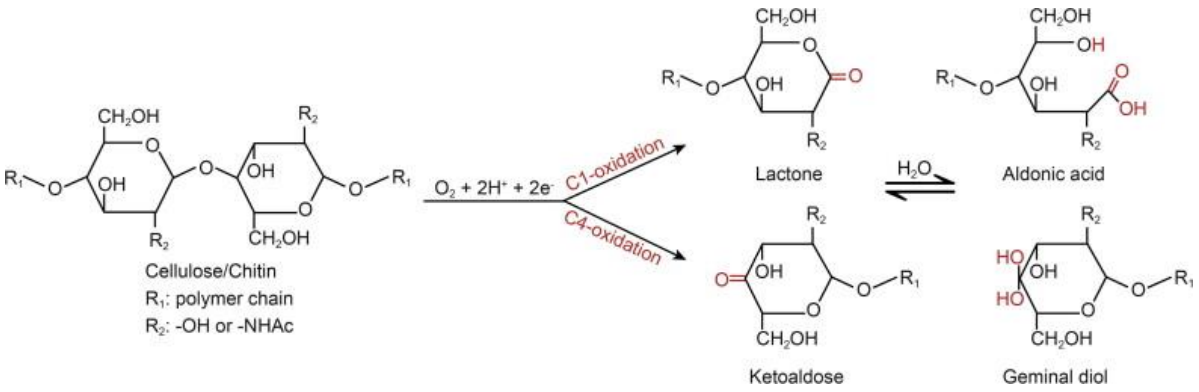

Figure 19. Oxidized products formed by LPMOs. C1 oxidation yields a lactone whereas C4 oxidation leads to the formation of a ketoaldose. Both products are in a pH-dependent equilibrium with their corresponding hydrated forms, the aldonic acid and the geminal diol respectively. The figure was taken from (Loose et al., 2014). © 2014 Federation of European Biochemical Societies. Reprinted with permission.

Vu *et al.* carried out a phylogenetic investigation of fungal LPMOs and could divide them into four groups: PMO1 with C1 activity, PMO2 with C4 activity, PMO3 exhibiting mixed activity, and PMO3*, containing members with sequences similar to PMO3s but with C1 activity (Vu et al., 2014a). Indeed, there seem to be detectable correlations between sequence/structural features of LPMOs and oxidative regioselectivity, as alluded to above, but further work is needed to unravel the precise nature of these correlations. Notably, Vu and colleagues use the term PMO, rather than the much more commonly used term LPMO, because they claim that the lytic character of LPMOs (reflected in the L) has not been sufficiently demonstrated (Beeson et al., 2015).

The putative reaction mechanism has been addressed in several publications and is predominantly based on studies on other similar enzyme systems, combined with some computational and experimental data on LPMOs [see (Beeson et al., 2015) and (Walton and Davies, 2016) for excellent, detailed reviews]. The first steps towards explaining the reaction mechanism were made by the Marletta group, where Phillips *et al.* and Beeson *et al.* suggested the pathway S1 (brown) as indicated in Figure 20. The starting point is the reduction of a resting state LPMO-Cu(II) to LPMO-Cu(I) and the subsequent formation of a Cu(II)-superoxo intermediate [Cu(II)-$O_2^{\bullet-}$] via activation of oxygen by the reduced LPMO-Cu(I). The superoxo intermediate subsequently abstracts a hydrogen from the substrate to produce a substrate radical and a Cu(II)-hydroperoxo species that is further converted to a Cu(II)-oxyl radical [Cu(II)-$O^{\bullet}$] (i.e. a second electron is needed). The two formed radicals (substrate$^{\bullet}$ and

LPMO-Cu(II)-O•) react with each other to yield the product anion and the protein returns to the Cu(II) resting state (Phillips et al., 2011a, Beeson et al., 2012).

A second suggested pathway S2 ((pink); Figure 20) displays an alternative pathway to S1 and is similar to that proposed for peptidylglycine α-hydroxylating monooxygenase [(Chen and Solomon, 2004) reviewed by (Beeson et al., 2015)]. In this pathway, hydroxylation of the substrate occurs via reaction of the substrate-radical with the hydroperoxo-species and cleavage of the glycosidic bond takes place via an elimination reaction. The resulting oxyl radical is then reduced and the enzyme returns to the resting state and can enter the next reaction cycle (Kim et al., 2014, Beeson et al., 2015).

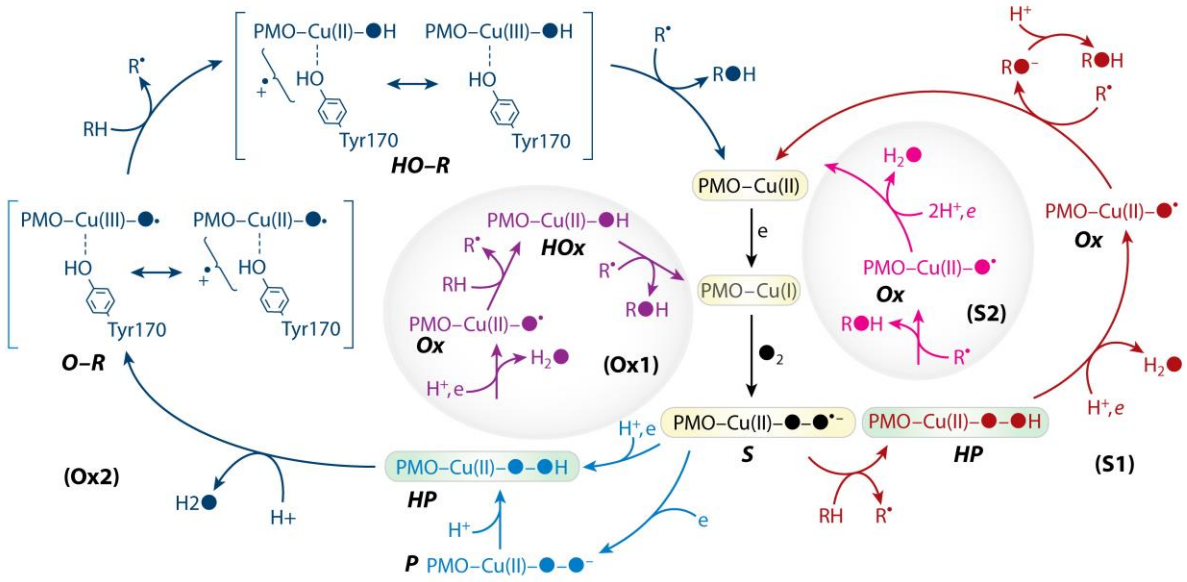

Figure 20. Overview of the suggested single turnover mechanisms by LPMOs (called PMOs in this figure). Pathways S1 and S2 use a Cu(II)-superoxo intermediate for hydrogen abstraction from the substrate whereas pathways Ox1 and Ox2 utilize a more reactive intermediate, a Cu(II)-oxyl radical. All pathways start with the reduction of the LPMO-Cu(II) to LPMO-Cu(I) which then activates oxygen and forms a superoxo species. See text for a more detailed description. The figure has been adapted from (Beeson et al., 2015); Copyright © (2015) Annual Reviews.

Other suggested reaction mechanisms involve an oxyl radical for initial hydrogen abstraction from the substrate instead of a superoxo intermediate. Kim *et al*. (2014) proposed one of these pathways, Ox1 (purple) in Figure 20, based on DFT calculations. They suggested direct reduction of the superoxo intermediate to form a species with stronger oxidative properties, namely an LPMO-Cu(II) oxyl radical (i.e. a three-electron reduction overall). This ROS then

abstracts a hydrogen from the substrate resulting in an LPMO-Cu(II)-OH complex and a substrate radical. Next, the hydroxyl group from the LPMO-Cu(II)-OH is transferred to the substrate radical via an oxygen rebound mechanism that leaves an LPMO-Cu(I) which can restart a catalytic cycle (Kim et al., 2014). Note that this reaction mechanism consumes three electrons in the first catalytic cycle. Since the LPMO leaves the cycle as a Cu(I) species, every subsequent catalytic cycle consumes two electrons.

Pathway Ox2 (dark blue in Figure 20) involves the conserved tyrosine located at the buried axial copper coordination site. After heterolytic bond cleavage of the hydroperoxo complex (cleavage of the O-O bond, resulting in the formation of a radical), a Cu(III)-O$^{\bullet}$ is formed. The Cu(III)-O$^{\bullet}$ is most likely very unstable and may thus be stabilized by oxidation of the active site tyrosine, shown as a Cu(III)-O$^{\bullet}$ and a Cu(II)-oxyl-ligand cation radical in Figure 20 (named "O-R"). After abstraction of a hydrogen from the substrate a Cu(III)-OH and the corresponding cation radical that involves tyrosine as ligand are formed. After hydroxylation of the formed substrate radical, the LPMO returns into the resting state possessing a Cu(II) (Beeson et al., 2015).

Two pathways (depicted as S2 and Ox1 in Figure 20) were subject to density functional theory calculations by Kim *et al*. (2014). These authors used an AA9 active site model based on the structure of C1/C4 oxidizing *Ta*LPMO9A (i.e. the same enzyme as used by Kjaergaard et al., 2014). Their calculations revealed overall activation barriers of 39.9 – 43.0 kcal/mol for the mechanism with a Cu(II)-superoxo intermediate as reactive species and 18.8 – 24.0 kcal/mol for the mechanism using a Cu(II)-oxyl radical as the reactive species, leading to the conclusion that a Cu(II)-oxyl radical is the catalyst in LPMO reactions (Kim et al., 2014).

The binding position of dioxygen upon activation by Cu(I) has so far not been identified experimentally, but studies of LPMO structures and computational experiments have provided some hypotheses. As described in section 1.3.4, many AA10s display a solvent exposed axial position that is occupied by a highly conserved alanine that most likely prevents binding of dioxygen at this position (Hemsworth et al., 2013b). A similar "blockage" has been seen in C1-oxidizing AA9s where the hydroxyl group of a conserved tyrosine restricts access to the axial position (Borisova et al., 2015). Hence, the non-protein occupied equatorial position may represent the position for dioxygen binding in these enzymes. The recent study by Frandsen *et al.* (2016) shows the presence of a chloride (superoxide mimic) in the available equatorial position, even though the enzyme has an "open" solvent exposed axial position. It should be noted that the latter position was occupied by the substrate in the study, thereby

preventing dioxygen binding there. In contrast to the Frandsen *et al.* (2016) data, the computational simulation performed by Kim *et al*. (2014), positioned the dioxygen molecule in the solvent exposed axial position for their studies. It is clear that more experimental data are needed to determine the binding position of dioxygen to copper in LPMOs.

As already mentioned, the proposed mechanisms for the LPMOs are primarily based on existing studies of similar systems of copper-active enzymes. However, some experimental data exist. Kjaergaard *et al.* (2014) observed that reoxidation of the Cu(I) in an AA9, by molecular oxygen, takes place within seconds and showed that the cycling between the oxidized and the reduced form of the copper ion occurs with only little reorganization of the protein, thereby facilitating the thermodynamically difficult one electron reduction of O_2 (Kjaergaard et al., 2014). Following this line of thought, the same authors argued that the binding of the superoxide to the Cu(II) is what drives O_2 activation (i.e. one electron reduction). Indeed, LPMOs have been observed to produce H_2O_2 in the absence of substrate [(Kittl et al., 2012, Isaksen et al., 2014) paper II of this thesis], indicating release of superoxide from the enzyme. In solution, superoxide rapidly disproportionates to H_2O_2 (pH dependent reaction). The observation of a putative superoxide molecule in an X-ray crystallographic structure of an LPMO (Li et al., 2012) also supports the ability of LPMOs to activate O_2 by one electron reduction.

In their recent review, based in part on the recent structural data for an enzyme-substrate complex (Frandsen et al., 2016), Walton and Davies (2016) suggest an interesting scenario in which O_2 activation is enabled by substrate binding, indicating that the production of highly reactive ROS is more or less prevented by free enzymes in solution. The hypothesis would also allow processive LPMO activity (i.e. the LPMO could slide over the substrate in between catalytic cycles), but depends on the premise that electrons, protons and oxygen can enter the active site via channels (Walton and Davies, 2016). Even though electron transfer pathways through the protein have been proposed for AA9s and AA11s (Hemsworth et al., 2014, Li et al., 2012, Walton and Davies, 2016), LPMO activation by cellobiose dehydrogenases (further discussed in chapter 1.3.7) suggests that LPMOs need to dissociate from the substrate in order to be reduced (Courtade et al., 2016).

1.3.7 Electron supply

The enzymatic oxidation of polysaccharides by LPMOs depends on the external supply of electrons. Several sources of electrons have been shown to activate these enzymes since their discovery. LPMO activity was observed in the presence of small molecule reductants such as ascorbic acid, reduced glutathione (Vaaje-Kolstad et al., 2010) and gallic acid (Quinlan et al., 2011). A plethora of other reducing agents was found to be able to stimulate LPMOs in subsequent studies, amongst others cysteine, pyrogallol (Lo Leggio et al., 2015), resveratrol, catechin, caffeic acid and synaptic acid (Westereng et al., 2015).

Harris and colleagues observed that an AA9 (then known as GH61) from *T. terrestris* promoted degradation of lignocellulosic biomass, but not purified cellulose, by cellulases. They did so prior to the discovery of the redox enzyme character of LPMOs (Harris et al., 2010). This observation was later confirmed and explained by other authors who showed that the respective LPMOs can be activated by lignin (Cannella et al., 2012, Dimarogona et al., 2012), a compound abundantly available in lignocellulosic biomass. The electron supply by lignin has been suggested to take place via long-range electron transfer where soluble low molecular weight lignin compounds shuttle electrons from high molecular weight lignin to the LPMO (Westereng et al., 2015).

Interestingly, other groups of redox-active enzymes are able to act as a reductant for LPMOs. Cellobiose dehydrogenases (CDH; Figure 21) are flavocytochromes that can be found in fungal secretomes (Henriksson et al., 2000, Phillips et al., 2011b, Kracher et al., 2016). CDH contains two prosthetic groups, a flavin containing two electrons and a haem containing one electron when the enzyme is fully reduced (Igarashi et al., 2002). The flavin domain, also referred to as the dehydrogenase (DH) domain, belongs to the glucose-methanol-choline (GMC) oxidoreductases and is classified as an AA3, whereas the haem *b*-binding cytochrome (CYT) domain belongs to family AA8 as classified in the CAZy database (Levasseur et al., 2013).

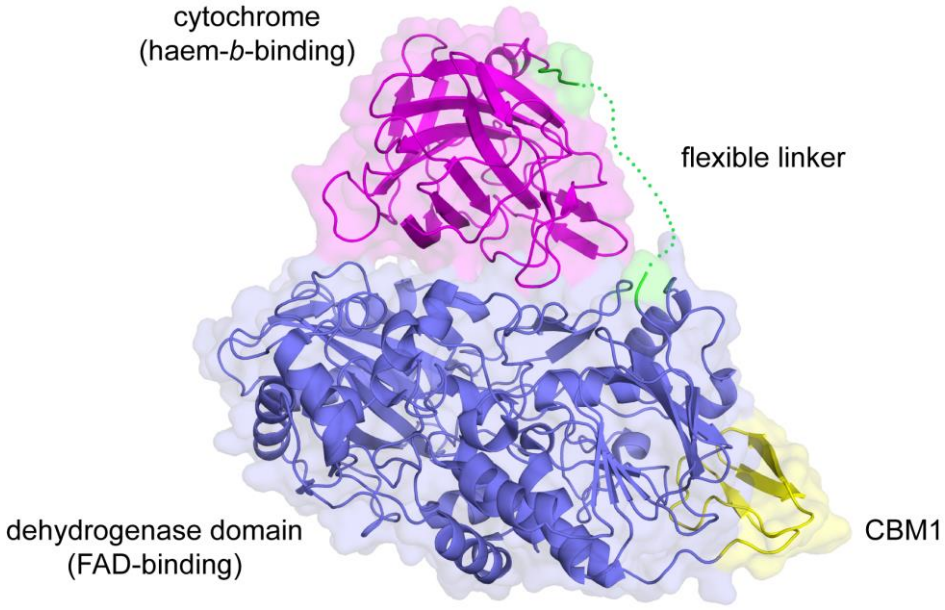

Figure 21. Structure of *Mt*CDH (PDB ID 4QI6) in the 'closed' state that allows IET between the cytochrome domain (magenta) and the dehydrogenase domain (blue). The CBM1 domain is shown in yellow and the flexible linker that did not crystallize, is shown as green dotted line. The figure was made with PyMol (DeLano and Lam, 2005).

The oxidation of cellobiose (and other substrates) to 1-5-δ-lactones is catalyzed by the DH domain. The CYT domain acquires electrons via interdomain electron transfer (IET) from the reduced DH domain to the haem (Tan et al., 2015). Tan *et al*. observed that CDH is present in two conformations in solution, in the 'closed' and the 'open' state. The interaction between the CYT domain and the DH domain in the 'closed' state is important for efficient IET whereas the open state allows ET to an external electron acceptor like an LPMO (Tan et al., 2015). Figure 21 shows the closed conformation of *Mt*CDH. A reduced CYT domain is able to reduce a wide range of substrates like metal ions, quinones or oxygen (Phillips et al., 2011a). In a knockout study, Phillips *et al*. (2011a) showed the importance of CDH for cellulose degradation by *N. crassa*. The culture supernatant of the knockout strain was significantly less efficient in the degradation of Avicel, but reached wildtype activity when external CDH was added. The same study also reported that CDH was able to serve as an electron donor for three different LPMOs from *N. crassa* (Phillips et al., 2011a) and suggested that this was likely to be the biologically relevant role of CDH. Thus, AA9-type LPMOs are not only activated by small molecule reductants, but also by CDHs (Phillips et al., 2011a, Langston et al., 2011, Beeson et al., 2012). Figure 22 illustrates the activation of LPMOs by CDH. The interaction between CDH and fungal LPMOs has been suggested to occur via a conserved surface patches co-evolved on both enzymes (Li et al., 2012). The same authors

suggested that ET takes place through long distance electron transfer via a conserved hydrogen bond network or conserved aromatic residues (Li et al., 2012). In contrast, the authors of a recent NMR study showed that interaction between a CDH and an LPMO occurs directly at the copper active site (Courtade et al., 2016), thus indicating the absence of a conserved site for ET on the LPMO. So far, CDHs and related proteins have only been found in fungi. Bacteria do not seem to encode a protein analogous to CDH. However, a large multimodular protein with predicted cytochrome domains (i.e. redox activities) identified in *Cellvibrio japonicus* was indeed able to activate an LPMO (Gardner et al., 2014). It is thus possible that bacteria produce proteins that are able to provide electrons to secreted LPMOs.

Fungal CDHs are not the only redox active proteins that contribute to LPMO activation. Kracher *et al.* (2016) recently showed that a variety of plant-derived or fungal diphenols can efficiently reduce an AA9 from *Neurospora crassa,* but that they are irreversibly depleted in the process. However, regeneration of these reductants could be achieved by addition of GMC oxidoreductases, implying that the phenolic compounds can act as a redox mediators between GMC oxidoreductases and LPMOs. In another very recent study, Garajova *et al*. (2016) observed that flavoenzymes of family AA3 are also able to directly interact with AA9s, extending the array of LPMO stimulating protein based reductants.

Other researchers have used quite different approaches to reduce LPMOs. By using the energy of light Cannella and co-workers were able to activate an AA9-type LPMO in the presence of a pigment, either thylakoids or chlorophyllin, and an electron source such as ascorbate and lignin. By using this system the authors claim an up to two orders of magnitude increase in catalytic activity compared to previously reported values (Cannella et al., 2016). In another study Bissaro *et al*. (2016) report that vanadium-doped TiO_2 can be used to activate AA10s. The photocatalyst catalyzes the light-driven oxidation of water, thereby providing electrons to the LPMO. Notably, these two light-driven scenarios are quite different. The first yields much higher LPMO activity, but relies on externally added reducing equivalents. In contrast, the second relies on light and catalyst only, but gives low activity.

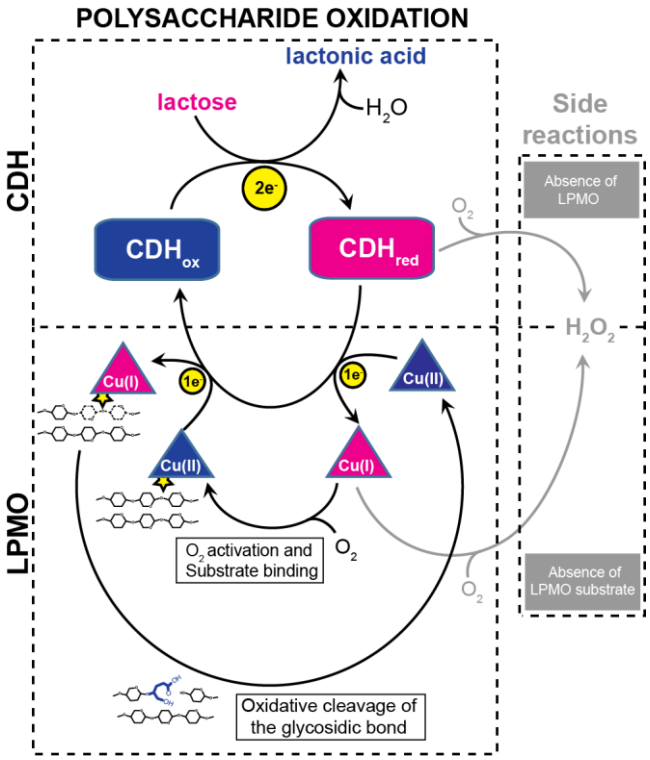

Figure 22. Lytic polysaccharide oxidation by the CDH-LPMO system. An oxidized CDH (square) acquires electrons from a substrate (here: lactose). The reduced CDH then transfers the electrons to an oxidized Cu(II)-LPMO (triangle) and thereby, gets re-oxidized. The reduced LPMO activates dioxygen and then oxidatively cleaves a substrate thus, it gets re-oxidized. In the absence of an intact LPMO or an LPMO substrate, CDH or the LPMO respectively transfer electrons to dissolved O_2 which results in the formation of hydrogen peroxide. Enzymes are colored blue in their oxidized form and pink in their reduced form. The figure was taken from [paper II in this thesis (Loose *et al*., submitted)].

1.3.8 LPMOs as virulence factors

Many pathogens, opportunistic pathogens and viruses that have no obvious role in biomass degradation, encode an AA10-type LPMO. Some of these LPMOs have already been identified as virulence factors, for example GbpA from *Vibrio cholerae* (Kirn et al., 2005) and *Lm*LPMO10A (Lmo2467) from *Listeria monocytogenes* (Chaudhuri et al., 2010). These reports suggest that there is more to LPMOs than their role in turnover of recalcitrant biomass, but these aspects of LPMOs have so far not received much attention.

Two examples of LPMOs acting as virulence factors by mediating degradation of host chitin can be found in a bacterium and a virus that target insects. In a recent study, an AA10 was identified as key virulence factor in a honey bee disease called American foulbrood, which is

caused by *Paenibacillus larvae*. Garcia-Gonzalez and colleagues used *P. larvae* mutants lacking expression of the AA10 (*Pl*CBP49) and observed that the absence of the enzyme clearly reduced the degradation of the chitin-rich peritrophic matrix of bees, and that the mutant had almost lost its virulence (Garcia-Gonzalez et al., 2014). Another insect pathogen targeting moth larvae, namely the nuclear polyhedrosis viruses, also encode AA10 LPMOs in the genomes (called fusolins or GP39). The importance of the N-terminal AA10 LPMO of a viral fusolin was discovered before it was known that these domains actually were enzymes. Takemoto and colleagues observed that this domain, which judged by sequence is an LPMO, was essential for the enhancement of peroral infections (Takemoto et al., 2008). Indeed, the function of these domains have been related to disintegration of the chitin rich peritrophic matrix of the insect larvae gut lining (Mitsuhashi et al., 2007), indicating a chitin degrading role of the virus LPMO. Recent investigations have confirmed that fusolins are indeed structurally related to AA10s and include the characteristic histidine brace (Chiu et al., 2015).

Bacteria that invade and infect hosts that do not contain chitin (e.g. mammals) have also been reported to display LPMOs as virulence factors. For example, the only AA10 from the opportunistic pathogen *Enterococcus faecalis* may play a role other than in chitin depolymerization as it is observed to be up-regulated when the bacterium is exposed to urine and serum (Vebø et al., 2009, Vebø et al., 2010). However, there are no data that clearly proof a role of this protein in virulence, and biochemical characterization of the protein revealed that it is a chitin-active LPMO (Vaaje-Kolstad et al., 2012), possibly part of a minimal chitinolytic system.

The opportunistic pathogen *Serratia marcescens* possesses a well characterized chitinolytic machinery with an active LPMO, as discussed above (chapter 1.2.2). CBP21 knockout strains of *S. marcescens* show significantly decreased adherence to colonic epithelial cells which could be restored by complementation (i.e. plasmid-driven overexpression of CBP21) (Kawada et al., 2008). Interestingly, Kawada *et al*. (2008) reported a similar result for CBP21-overexpressing *E. coli* cells; overexpression of CBP21 increased adhesion of non-pathogenic *E. coli* to colonic epithelial cells but had no effect on the rate of invasion.

Another LPMO likely involved in virulence is *Lm*LPMO10A from *L. monocytogenes*. Experiments using mouse model systems have shown that this protein and two chitinases contribute to virulence during bloodstream infection using *L. monocytogenes* deletion mutants and the wildtype (Chaudhuri et al., 2010). In contrast, no effect could be observed in tissue cultures. Intracellular growth and cell-to-cell spread in infected Caco2-cell monolayers did

not show any changes compared to the wildtype, when a deletion mutant was used (Chaudhuri et al., 2010). The experiments by Chaudhuri *et al*. were conducted before it became evident that LPMOs are enzymes and need a reducing agent for activity. Adding a reductant to tissue culture experiments might change the outcome of the experiment. Notably, Paspaliari et al. (2015) have shown that *Lm*LPMO10A indeed is an active LPMO. Interestingly, *Lm*LPMO10A is not co-regulated with the chitinases upon exposure of the bacterium to chitin, possibly indicating a role other than in chitin degradation.

Kirn and colleagues have shown that a multi-modular protein called GbpA (GlcNAc-binding protein A) promotes binding of *V. cholerae* to epithelial cells, chitin, GlcNAc and zooplankton. A GbpA deficient *V. cholerae* strain showed an approximately tenfold deficiency for colonization compared to the wildtype strain using a murine system. Moreover, the survival of mice infected with wildtype *V. cholerae* was significantly enhanced when the inoculum was mixed with a hyperimmune serum from GbpA-immunized rabbits (Kirn et al., 2005). GbpA interacts not only with chitin and chito-oligosaccharides but also with mucins (Bhowmick et al., 2008, Wong et al., 2012), strengthening the notion that this protein is important for virulence.

GbpA is a four-domain protein (Figure 23) whose structure was solved by Wong *et al*. (2012). The protein contains an N-terminal LPMO-domain (domain 1) and a C-terminal chitin-binding domain CBM5/12 (domain 4). The structures of the two middle domains are distantly related to bacterial surface proteins. Domain 2 resembles a domain of a bacterial flagellin that supposedly interacts with the bacterial surface and domain 3 is similar to a chaperone that is involved in folding components of *E. coli* surface pili and transporting them.

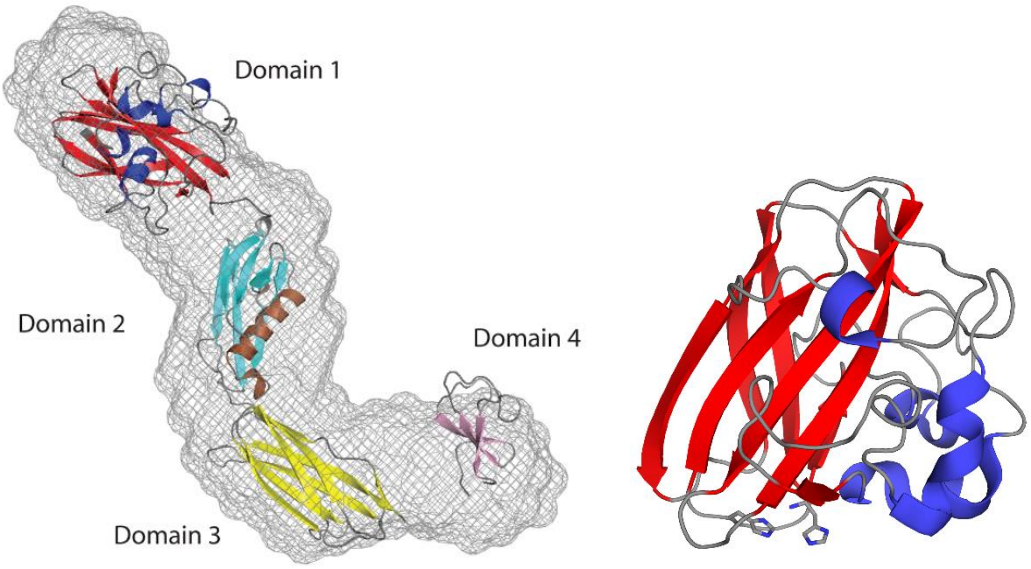

Figure 23. Structure of GbpA. The structure on the left side shows a GbpA full-length SAXS model superimposed onto the GbpA (domains 1-3) crystal structure and the modelled structure of domain 4. The figure was taken from (Wong et al., 2012). The structure on the right side shows the LPMO domain of GbpA. The figure was made with PyMol (DeLano and Lam, 2005).

What it takes a pathogen to be successful, is initial survival in the hostile gastro-intestinal tract or other environments and the colonization of these environments. Overall, it appears from currently available data that LPMOs are important in host-microbe interactions, facilitating the colonization of the host. Since many of the organisms that possess potentially virulent LPMOs have adapted to an opportunistic pathogenic lifestyle it is conceivable that these proteins have more than one purpose. They may be involved in gaining nutrients by degrading chitin, contribute to survival in the environment and colonization of the host (Kirn et al., 2005).

2. Outline and purpose of the thesis

LPMOs occur in all three domains of life. Their presence in biomass-degrading organisms and pathogens has been enigmatic for a long time, in part because they originally appeared to be non-catalytic binding proteins. Their enzymatic activity was discovered in 2010 and since then, several studies have shown their activity in the context of biomass degradation and their application in industrial cellulose degradation. Even though a lot of work has been done on LPMOs, experimental data on the mode of action are scarce. Furthermore, the role of LPMOs in pathogenesis remains unknown.

Insight into the function and catalysis of LPMOs is particularly important in order to apply them in an efficient way in industrial catalysis and to understand their role as a virulence factor. A major objective of the work presented in this thesis was to investigate and optimize LPMO reaction conditions to allow quantitative analysis of product formation and thus overcome some of the major challenges related to LPMO research. Another major objective was to use fundamental work on assay development to eventually learn more about how LPMOs really work.

The first paper describes a fast quantitative assay that allows determination of the initial product formation rate of chitin-active LPMOs. Reducing the complexity of the product profile and developing an in-house made oxidized standard was the main focus of this work. Additionally, this paper describes that a protein whose natural function relates to virulence contains an active LPMO domain.

In paper II the advances described in paper I were used and taken further. This study compares the use of a small molecule reductant and an enzymatic electron donor. The results demonstrate, for the first time, that bacterial AA10s can be reduced by a fungal CDH and that controlling electron supply is beneficial for LPMO activity. We also show that both the catalytic rate and duration of activity (i.e. stability of the catalytic system) are strongly influenced by the amount of reductant and that a well-balanced system does not perform futile cycling (i.e. no measurable amounts of hydrogen peroxide are produced).

The purpose of the study described in paper III was to investigate the roles of conserved amino acids in AA10 LPMOs by site-directed mutagenesis. Fifteen mutants of the chitin-active LPMO from *S. marcescens* known as CBP21 were characterized with respect to substrate

binding, apparent catalytic rate, electron transfer and properties of the copper-binding active site. A major finding of the study arising from the co-interpretation of the binding and apparent rate data, is that substrate binding seems to protect the LPMO from inactivation. This finding has major implications for future studies of LPMOs as well as for their application as industrial catalysts. The comparison of a small molecule reductant and an enzymatic reductant revealed differences in activity and allowed identification of residues that are crucial for accepting electrons from different sources. Further, electron transfer from CDH to CBP21 in solution was found to be very fast and does not seem rate limiting for catalysis. Finally, the effect of the mutations on the copper active site were investigated by EPR, revealing that this site is influenced by many of the surrounding amino acids.

3. Main results and discussion

Paper I

The oxidative action of LPMOs in the presence of a reducing agent and molecular oxygen has been known since 2010 (Vaaje-Kolstad et al., 2010). These enzymes work in concert with canonical glycoside hydrolases (Vaaje-Kolstad et al., 2005a, Harris et al., 2010, Nakagawa et al., 2013) and all hitherto characterized LPMOs yield complex product profiles that display oxidized oligosaccharides of various lengths and properties (Vaaje-Kolstad et al., 2010, Forsberg et al., 2011, Quinlan et al., 2011, Phillips et al., 2011a). This implies that the determination of LPMO activity can either be done directly by quantifying various oxidized products or indirectly by measuring the activity of other hydrolytic enzymes LPMOs work in synergy with.

The first goal of this thesis was to develop a kinetic assay that allows quantitative estimation of chitin-active LPMOs. For this task, a protein with no obvious role in biomass degradation that had been shown to be a colonization factor of *V. cholerae* (Kirn et al., 2005, Bhowmick et al., 2008) was selected. GbpA is a four-domain protein with an N-terminal LPMO domain, two domains that potentially bind bacterial surface proteins and a chitin binding domain (CBM5/12) at the C-terminus (Wong et al., 2012), as described in the introduction (Figure 23). For further understanding the role of the virulence factor, it was of importance to investigate whether the LPMO module was capable of catalyzing the oxidation of glycosidic bonds.

Special attention was paid to the copper loading of the protein. This had been neglected in previous rate estimations, where the LPMO was used “as is” (Vaaje-Kolstad et al., 2010, Agger et al., 2014), thereby risking a situation where not all enzymes contain copper in the active site. The fact that several published structures of family AA10 LPMOs do not contain copper in the active site (e.g. CBP21, PDB ID 2BEM; EfCBM33A, PDB ID 4A02; GbpA, PDB ID 2XWX; all crystallized “as is”) was a strong motivation for this attention. On the other hand, the high affinity of LPMOs for copper (Quinlan et al., 2011, Aachmann et al., 2012, Hemsworth et al., 2013b) implies that these enzymes would be able to scavenge copper ions from the surroundings, as pointed out by Quinlan *et al*. (2011). Indeed, experiments using LPMOs in their apo-form, suggest that the enzymes are able to pick up copper ions from the

surroundings, most likely the substrate (Quinlan et al., 2011). Nevertheless, making sure every LPMO batch is completely copper saturated is good practice and essential when conducting kinetic analysis of these enzymes. In paper I, GbpA was copper-saturated and carefully desalted to avoid carry-over of excess copper. The desalting step was thought to be critical, since catalytic amounts of free copper in solution may catalyze the auto-oxidation of small molecule-type reducing agents that are used in LPMO assays. It is well known that the most popular reducing agent used for probing LPMO activity, ascorbic acid, is prone to auto-oxidation catalyzed by free copper (Peterson and Walton, 1943, Weissberger et al., 1943).

One of the main challenges when conducting enzyme assays with insoluble substrates is particle heterogeneity. For example, the chitin particles used in this study form a non-uniform suspension that is difficult to pipette when taking samples from reaction mixtures. To overcome this particle heterogeneity issue we took advantage of a unique property of β-chitin. When exposed to ultrasonication in an acidic solution, the chitin-nanofibrils dissociate and form a gel-like substance (Fan et al., 2008). By using a diluted solution of chitin nano-fibers, pipetting issues could be avoided and the reproducibility of the activity assay became excellent. Using the β-chitin nano-fibers as a substrate for GbpA yielded linear initial rates and a linear dose- response curve when varying the amount of protein. Interestingly, when using a truncated version of GbpA, i.e. the LPMO domain only, a linear dose-response curve was not observed (results not shown in paper I). Possible explanations for this puzzling observation could relate to the way products were quantified, the substrate itself and/or the altered binding properties of the truncated variant. The product analysis method used in the study reflects solubilized products only, not products remaining attached to the insoluble chitin nano-fibers. Whether all products formed were solubilized is unknown, but it was shown for another chitin-active LPMO, *Cj*LPMO10A, that the full length protein, including a CBM5, solubilized all formed products. In contrast, the truncated version, i.e. the LPMO domain lacking the CBM5, showed solubilization of less than 50% of the total products (Forsberg et al., 2016). Thus, it may be that increasing the concentration of truncated GbpA increased product formation more than observed with the assay used. This question could easily have been resolved by fully degrading the insoluble chitin fraction before analysis (such an approach was used in assays described in paper III).

The next hurdle to overcome in the quantitative assay was the relatively complex product profile. The technique used to stop the LPMO reaction was merely to separate the chitin nanofibers from the protein by filtration. The filtrate would contain the soluble oxidized

products and the enzyme, but no insoluble chitin that could be further degraded by the LPMO. An important issue to address was the potential of GbpA to oxidize soluble chito-oligosaccharides. At the time paper I was published, oxidative degradation of soluble substrates by LPMOs had been described for one AA9 (Isaksen et al., 2014), so such an activity could also be envisioned for GbpA. However, overnight reactions of GbpA incubated with GlcNAc, $GlcNAc_2$, $GlcNAc_4$ and $GlcNAc_6$ revealed that the protein was not active on soluble chito-oligosaccharides (unpublished observations). Hence, the filtrate could be stored and analyzed without further treatment.

The large variation in product DP made quantification laborious and challenging. This problem was solved by adding an "overdose" of chitinases to the filtrate followed by incubation to promote chitinase activity. This procedure led to decreased complexity of the product profile but still, more than one oxidized chito-oligomer was left, rendering this approach sub-optimal. The solution was adding a β-hexosaminidase instead of one or more of the chitinases. Chitobiase from *S. marcescens*, a family GH20 β-hexosaminidase, cleaves off single GlcNAc units from chito-oligosaccharides until GlcNAc is the single product. In paper I, we show that chitobionic acid is the sole oxidized product upon incubation of chitobiase with C1-oxidized chito-oligosaccharides. Thus, when using this enzyme to treat the LPMO reaction filtrate, a simple product profile containing only GlcNAc and chitobionic acid is obtained, both of which can easily be quantified, if standards are available.

Chitobionic acid is not available commercially, thus potentially making it difficult to quantify the products of chitin-active LPMOs. Conveniently, Heuts *et al*. (2008) observed that an enzyme from *Fusarium graminearum*, ChitO, oxidizes the reducing end of chito-oligosaccharides to an aldonic acid. We made use of this enzyme and detected very efficient oxidation of chito-oligosaccharides of various lengths. By incubating a known amount of native chitobiose, we were able to produce a standard of known concentration that we employed in our assay.

Reaction products were analyzed by means of UPLC, run in HILIC mode. This system allowed separation of all soluble products and to easily distinguish between native and oxidized chito-oligosaccharides. Under these chromatographic conditions the α- and β-anomer of the native sugars are partially separated and elute in close proximity to each other. Aldonic acids elute as a single peak. The drawback of quantifying LPMO products with the UPLC-HILIC based method is the time consumption. The analytical methods for base line separation of chito-oligosaccharides with various lengths take approximately 15-25 min per

run. Due to the reduced complexity of the product profile, the standard chromatographic method could be adjusted, now allowing much shorter analysis times. A new analytical method was developed that is specific for quantification of chitobionic acid. Even though a 4-5 min isocratic method would suffice to quantify the product, a short gradient was employed in order to have control over the degradation of the longer chito-oligosaccharides (i.e. to verify that all products had been completely degraded by chitobiase). In the end, the method was shortened to 7 min, decreasing the analytical time and the consumption of organic solvent. Application of the gained knowledge in a single assay, yielded linear initial rates for GbpA that could be quantified using the in-house made standard.

Even though the novel assay described in Paper I is easy to apply, it is important to note its limitations. The nano-fiber substrate gets more difficult to produce with increasing chitin concentrations, limiting the amount of chitin that can be used in an assay. For example, it may be difficult to obtain reaction conditions where the substrate concentration is saturating. Depending on the source and pretreatment of the β-chitin used, also the concentration of acetic acid and the sonication time must be adjusted. The fact that production of chitin nanofibers only can be achieved in acidic conditions (optimal dissociation is usually obtained in 20-200 mM acetic acid, 1.8 mM in our assay), creates another issue. The pH of the substrate is lowered, implicating that a quite high buffer concentration is needed to control the pH. Moreover, acetate is present in the reactions, which may interact with the copper and interfere with the activity. Nevertheless, the assay resulting from the work described in Paper I is fast and relatively easy, giving reproducible results.

Until paper I was published, it was not clear whether GbpA had enzymatic activity. As discussed in the introduction, the protein had been shown to be a virulence factor in *V. cholerae*. Since its activity was still undetected, its function was ascribed to the adherence to host tissue. Adhesion of *V. cholerae* to chitin substrates and the mammalian intestine is a complex process that involves several adhesins, including a mannose-sensitive haemagglutinin (Pruzzo et al., 2008) and GbpA. Using attachment assays, Kirn *et al*. (2005) showed that GbpA is important for adhesion of *V. cholerae* cells to GlcNAc or chitin. Bhowmick and co-workers provided data that demonstrated the importance of GbpA in binding of *V. cholerae* to murine intestine (Bhowmick et al., 2008). In a study conducted by Wong and colleagues, domains 1 and 4 of the protein (the LPMO domain and the CBM 5/12 chitin binding module respectively) were identified as important for binding to chito-oligosaccharides, whereas the LPMO domain itself was required for mucin binding.

Furthermore, experiments on a mouse model system showed that domains 1-3 were needed for intestinal colonization (Wong et al., 2012). All experiments conducted on GbpA prior to paper I were performed in the absence of an external electron donor that promotes LPMO activity. Even though we could not detect activity on non-crystalline substrates i.e. soluble chito-oligosaccharides in our assays, it is still possible that e.g. mucins contain stretches of oligosaccharides that can be cleaved by GbpA. Indeed, mucin contains a substantial amount of GlcNAc. Preliminary experiments using commercial mucin sources have been conducted, but so far without detecting GbpA activity (Loose et al., unpublished observations). GbpA has been proposed to act as a 'dual role colonization factor' (Vezzulli et al., 2008) since the protein is not only important for colonization of intestinal tissue but also for attachment to marine chitin, as in e.g. the exoskeleton of crustaceans (Stauder et al., 2012, Kirn et al., 2005). While, so far, no obvious role for GbpA in biomass degradation has been described, it is possible that *V. cholerae* attached to crustaceans obtains nutrients from the host's exoskeleton via GbpA activity, presumably in combination with chitinase activity. This scenario would make sense, especially in aquatic environments, since GbpA helps the bacteria to attach to the crustacean and hence brings it to close proximity of a nutrient source.

Paper II

The focus of the work described in paper II was to study the influence of the reductant on LPMO activity. The first step was to provide a proof-of-concept demonstrating that a fungal CDH is able to reduce a bacterial LPMO, i.e. that CDH can act as a universal electron donor for LPMOs. Initial activity tests showed that two AA10s only sharing 23.1% sequence identity, the chitin-active AA10 CBP21 and the cellulose-active AA10 CelS2, could both be activated by *Mt*CDH, a CDH from the fungus *Myriococcum thermophilum*. Activation of LPMOs by CDH had so far only been shown for fungal LPMOs (Langston et al., 2011, Phillips et al., 2011a). Li *et al*. (2012) suggested that a conserved region on the surface of fungal LPMOs, which includes a lysine and an aspartic acid separated by a Proline-Glycine-Proline motif, might act as a recognition site for the binding of CDH. When comparing the two bacterial AA10s with fungal AA9s (Figure 24) it becomes apparent that the proposed recognition site is not present in the AA10s, suggesting that these bacterial LPMOs would not be activated by fungal CDHs, given the hypothesis by Li *et al*. (2012) is correct. However, opposite to this prediction, we found that the bacterial proteins are activated by the fungal CDH. The fact that CDH serves as an electron donor for bacterial LPMOs indicates that the

previously proposed recognition site is not involved and that the electrons are transferred in another way. A similar conclusion was reached by Tan *et al*. (2015) who described a biomolecular docking (HADDOCK) study of *Nc*CDH-*Nc*LPMO9F that indicated docking of the cytochrome domain of the CDH (via its haem propionate group) near the copper site of the LPMO for enzymes that are freely accessible, i.e. not substrate bound. Indeed, a recent NMR study has shown that the cytochrome domain of a CDH interacts directly with the copper active site of an AA9 LPMO (Courtade et al., 2016). Since the copper active site is the most conserved structural element of LPMOs, it is plausible to argue that this is the site where electrons are transferred from CDH to the LPMO.

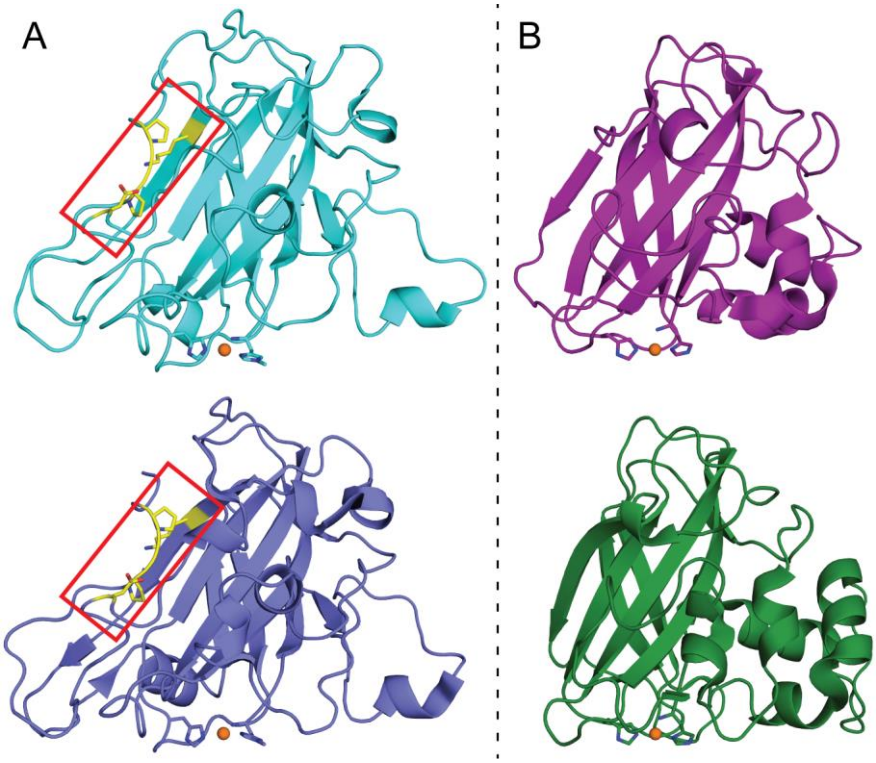

Figure 24. Cartoon representations of LPMO structures depicting the putative CDH recognition site of AA9s. (A) *Nc*LPMO9M (cyan, PDB ID 4EIS) and *Ta*LPMO9A (blue, PDB ID 2YET). The residues involved in the putative binding site for CDH are shown in yellow (red box). (B) CBP21 (magenta, PDB ID 2BEM) and CelS2 (green, PDB ID 4OY7) do not possess this putative CDH recognition site. The figure was made with PyMol (DeLano and Lam, 2005).

Further insight into the effect of reductants was gained by performing dose-response experiments in which the amount of reductant was varied. Interestingly, increasing amounts of electron donor yielded increasing amounts of aldonic acids produced by CBP21,

independent of the reductant. The trends were identical for *Mt*CDH and ascorbic acid (Figures 4 and 5 in paper II). Increasing the concentration of *Mt*CDH showed beneficial effects for product formation in short term incubations and lead to an increased initial LPMO activity. If only considering the product formation after 4 h, it even appears that the dose response is direct proportional to the amount of reductant, except for the highest *Mt*CDH concentration. High amounts of reductants affect the reaction negatively, especially at longer incubation times (see the 24 h time point for both 3 and 5 μM *Mt*CDH; Figure 4 in paper II). For ascorbic acid, a time course experiment revealed that increasing the concentration of ascorbic acid not only increases the initial rate, but also the overall yield of oxidized products. However, at the highest concentration of ascorbate (10 mM) the rate seems to be identical to what is achieved with 5 mM ascorbate, and the end yield of LPMO-generated oxidized products is lower compared to 5 mM ascorbate. The explanation for the dose-response relationship observed by increasing the reductant concentration is not straightforward. For CDH it seems logical that increasing the enzyme concentration will also increase the number of "productive" interactions of the LPMO and the CDH. Since the electron transfer rate from CDH to the LPMO is very fast in solution [(Kracher et al., 2016), papers II and III], it is probably the delivery of the second electron to the substrate-bound LPMO that is rate-limiting.

The loss of LPMO activity observed for high CDH concentrations may be caused by a variety of factors. Firstly, it is well established that *Mt*CDH is able to reduce O_2 [(Pricelius et al., 2009), paper II]. Thus, an excess of *Mt*CDH may exhaust the O_2 concentration at the substrate surface and at the same time produce harmful ROS that may inactivate the LPMO. Since all reactions are vigorously shaken, the first argument is probably not valid since the system will continuously be O_2-saturated. Thus, it is more likely that production of ROS (both H_2O_2, $O_2^{\bullet-}$ and potentially even more harmful species) mediate inactivation of the enzymes in the reaction mixture. Indeed, results described in paper III show that the loss of LPMO activity over time is caused by enzyme inactivation (see below).

For the small molecule reductant the explanation for the dose-response effects are even more complex and uncertain. The increase in LPMO activity with increasing reductant concentration may be related to the redox potential of the system. An increasing concentration of a reducing agent leads to a lowering of reduction potential in the solution, i.e. to a more powerful reducing environment that might facilitate the reduction of the LPMO (before, during and after catalysis) and thereby lead to faster initial rates. Similar to the system that

includes CDH, too high concentrations of ascorbic acid lead to a decreased product yield. This might be related to the formation of ROS due to the instability of ascorbic acid.

As shown before, LPMOs themselves produce H_2O_2 in the presence of a reductant (Kittl et al., 2012) but not when an LPMO substrate is present (Isaksen et al., 2014). Hydrogen peroxide measurements clearly confirmed these previous observations, but also showed that the hydrogen peroxide is present in the very beginning of the reaction and disappears over time.

The issue of enzyme inactivation during LPMO action has been addressed in a recent study. Scott *et al*. (2015) showed that cellulose degradation by an industrial enzyme cocktail (Cellic CTec3) gave higher conversion yields in the presence of an externally added AA9 and a catalase. The yields in the absence of catalase were significantly reduced, an observation which the authors attributed to hydrogen peroxide production by the LPMO (Scott et al., 2015). The experiments by Scott *et al*. clearly show that hydrogen peroxide affects saccharification of the substrate negatively. However, it is not clear whether LPMOs produce hydrogen peroxide directly, or if the hydrogen peroxide that accumulates in the absence of an LPMO-substrate interaction is formed via other ROS, like superoxide. The formation of hydrogen peroxide requires two electrons whereas the formation of a superoxide requires one electron when transferred to molecular oxygen. In solution, superoxide rapidly dismutates to form hydrogen peroxide, hence hydrogen peroxide measurements may reflect the formation of other ROS and hydrogen peroxide may not be the cause of LPMO inactivation. How the proteins are affected by hydrogen peroxide remains unclear, but in the presence of metals like free copper, potentially harmful ROS can be formed.

These results demonstrate that the rate of LPMO activity is strongly influenced by the reductant. A saturated system cannot be reached under these conditions since too high levels of reductant affect the reaction negatively. A 1000-fold excess of a small molecule electron donor compared to the protein amount appears sufficient to reduce the LPMO, but still higher concentrations are needed in order to yield stable reaction kinetics.

The catalytic rates and product yields of LPMOs depend on various factors, including the availability of oxygen and substrate, the pH, the amount and type of reductant, and the formation, presence and potential impact of ROS. The efficiency of small molecule electron donors like ascorbic acid, gallic acid or reduced glutathione is dependent on the pH. Increasing the pH of the system reduces the redox potential which implies increased reducing

power. For the hydroquinone/quinone system, it has been shown that the potential shifts approximately -60 mV/pH unit (Walczak et al., 1997). Considering this, it is very difficult to determine a pH-optimum for LPMO-reactions since this requires control of the reducing potential in the system.

Another factor that affects the LPMO-reaction is the substrate. Most LPMO-activity has been shown on insoluble substrates. The effect of crystallinity on CBP21-activity has been analyzed by Nakagawa *et al*. (2013) who showed that decreased chitin crystallinity (caused by milling) decreased the synergy between chitinases and CBP21. β-chitin substrates with high crystallinity usually have bigger particle sizes that swell upon hydration. These traits make it more difficult to handle the substrate. Interestingly, in the standard reactions described in this thesis, the maximum concentration of produced aldonic acids was approximately 1.6-1.7 mM yielding an estimated total conversion of the chitin substrate of roughly 20%. Since plenty of substrate was still present in the reaction, this leads to the assumption that the substrate *per se* is not depleted. However, it is conceivable that the accessible binding sites on the surface of the chitin particles are depleted. As indicated in paper II and shown in paper III, part of the aldonic acids remains bound to the substrate.

In order to detect if the morphology of the substrate changes due to LPMO activity, scanning electron micrographs were taken. Chitin that had been subject to LPMO reactions (CBP21, *Mt*CDH and lactose) and untreated chitin (i.e. chitin that had not been treated with CBP21 or reductant) were washed with fixing solution (1.25% glutaraldehyde, 2% paraformaldehyde in 0.1 M PIPES pH 7.2) and freeze-dried. Indeed, as shown in Figure 25, LPMO action had a dramatic effect on the chitin surface. The micrographs show that the untreated chitin particles had a rather smooth surface whereas the chitin treated for 6 h with CBP21 exhibited rough patches. After a 24 h treatment most of the CBP21-treated chitin displayed a rough surface. These micrographs clearly show that the enzymatic treatment had a dramatic effect on the surface of the substrate and it is thus conceivable that LPMO action stops because of depletion of accessible binding sites on the substrate surface.

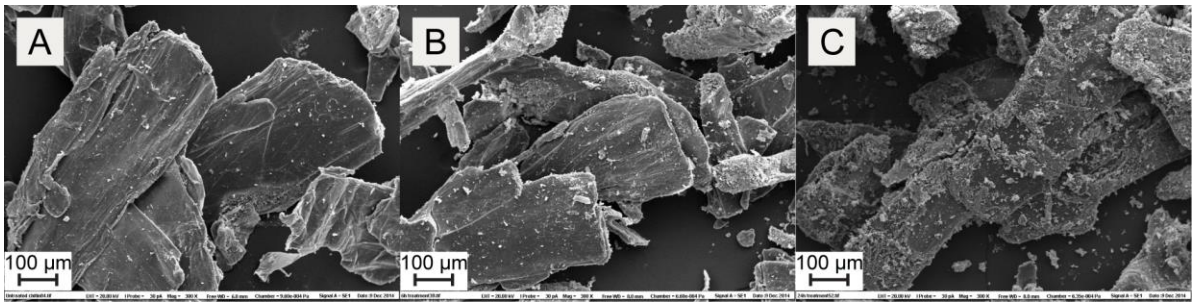

Figure 25. Scanning electron micrographs of β-chitin taken at 300x magnification. The micrographs show untreated β-chitin (A) and β-chitin treated with 1.0 µM CBP21 and 1.5 µM *Mt*CDH/3.0 mM lactose for 6 h (B) or 24 h (C).

In paper II, *Mt*CDH and lactose were used as reducing agent for CBP21 and a linear product formation rate was observed for up to 10 h. In contrast, the reaction containing ascorbic acid as reducing agent showed a faster initial rate for less than 90 min and thereafter a very slow second phase of the reaction. The short lived reaction in the presence of ascorbic acid can be explained by the short half-life of the reductant. In a very recent study, Kracher *et al.* (2016) determined the half-life of 1.0 mM ascorbic acid at pH 6.0 to 33 min. Due to the instability of ascorbic acid, the reducing potential in solution is increased and it is thus conceivable that in this case the reductant becomes rate-limiting. It is also possible that the abrupt decline in enzyme activity is caused by inactivation of the enzyme. Notably, progress curves similar to those obtained with ascorbic acid appear in Paper III, where the stable small molecule reductant gallic acid was used. So, enzyme inactivation seems a more plausible explanation for the decline in activity than depletion of the reductant.

In contrast, when using the enzymatic electron donor and applying a well-balanced system, more stable reaction kinetics were achieved. As described in the introduction, *Mt*CDH possesses a dehydrogenase domain and a cytochrome domain. The DH domain obtains two electrons from oxidation of one lactose molecule. One electron is transferred to the CYT domain via IET. In order to enter the next catalytic cycle, re-oxidation of *Mt*CDH has to occur. The re-oxidation can either take place by transferring the electrons to O_2 and produce hydrogen peroxide or by transferring them to the LPMO (Figure 22). Since O_2 and CBP21 reduction by *Mt*CDH are relatively slow and fast, respectively, it would be expected that the LPMO would be the prefered electron acceptor. Of course, this depends on the time required by CBP21 to complete the catalytic cycle, i.e. to return to its oxidized form. Since we did not observe formation of hydrogen peroxide in the CDH-CBP21-chitin reactions, as discussed

before, presumably all electrons are transferred to the LPMO, at least in the linear part of the reaction. Moreover, the presence of the LPMO stimulates CDH activity which supports the notion that the LPMO is a more efficient electron acceptor than O_2. If we consider that all electrons obtained by *Mt*CDH through lactose oxidation are consumed by CBP21 in chitin oxidation, the number of oxidized lactose molecules should equal the number of oxidized chitin molecules. By inspecting the data in Figure 6A and B in paper II, this seems not to be the case since the concentration of lactobionic acid is around 50% higher than the chitobionic acid (in the linear phase of the reactions). However, not all chitbionic acid has been accounted for. For these reactions, β-chitin particles were used as substrate and only the soluble fraction (i.e. solubilized oxidized chito-oligosaccharides) of the sample was analyzed. When adding a chitinase to such a similar reaction, it becomes apparent that for this kind of experiment, approximately one third of the oxidized chitin remains attached to the insoluble chitin particles, which accounts for most of the "missing" chitobionic acid. Furthermore, since chitin generally is 5-10% deacetylated, and partially deacetylated oxidized chitooligosaccharides are not quantifiable in the UPLC-HILIC method due to altered retention times and lack of standards, a few percent of the oxidized chitin is not quantifiabel. In conclusion, it does indeed seem like almost all electrons generated by *Mt*CDH are consumed by CBP21.

Our experiments provide evidence that LPMO-activity is influenced by many factors. Figure 26 clearly visualizes that LPMOs can be very efficient. Given the right conditions, CBP21 was able to clarify a sample containing 5 g/L chitin nano-fibers.

Due to the many factors that influence an LPMO reaction, and due to a mostly qualitative approach in the literature of characterized LPMOs, little is known about LPMO kinetics. Based on to the complications discussed above, comparison of the few rates that have been reported [(Vaaje-Kolstad et al., 2010, Agger et al., 2014, Borisova et al., 2015, Frandsen et al., 2016, Cannella et al., 2016) and paper I in this thesis] is challenging and published values should be evaluated critically.

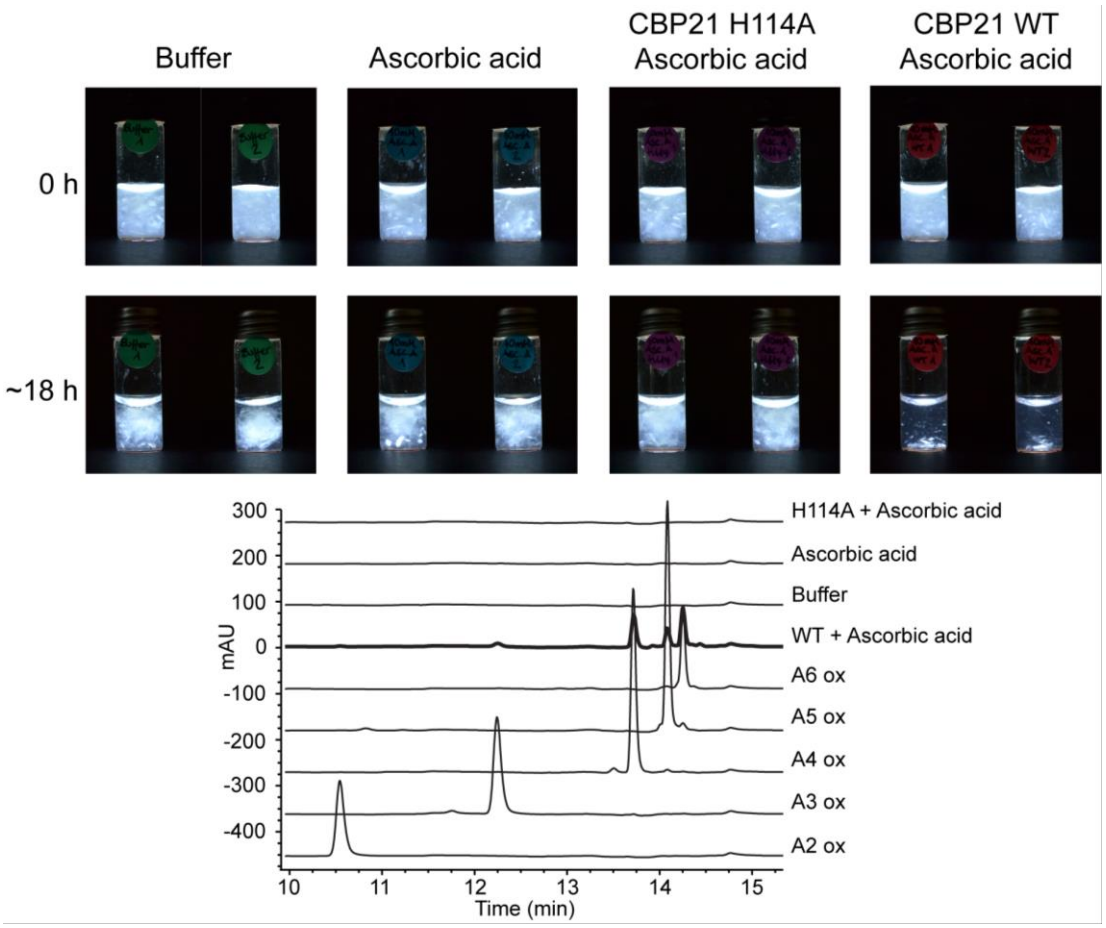

Figure 26. Degradation of chitin nano-fibers by CBP21. The photos show reaction mixtures containing CBP21, chitin and ascorbic acid, as well as control reactions, before and after incubation. The samples containing buffer, buffer and ascorbic acid or buffer, ascorbic acid and the inactive H114A mutant of CBP21 show minor changes after incubation whereas the reaction with the wildtype enzyme yields an almost clear reaction mixture. The HPLC results (lower panel) confirm that chitin degradation only took place in the wildtype reactions. The chromatograms represent the supernatants of the 18 h incubations. Aldonic acids were only detected in the wildtype reaction. The $(GlcNAc)_nGlcNAc1A$ standards A2 ox – A6 ox possess a DP of two to six respectively. The reaction conditions were 5.0 g/L chitin nanofibers (sonicated in 5.0 mM acetic acid), 50 mM Tris-HCl pH 8.0, and, if applicable, 1.0 µM protein and/or 10 mM ascorbic acid. The reactions were set up in duplicate and incubated horizontally at 20°C and 800 rpm.

Paper III

The goal of the study described in paper III was to gain insight into LPMO-activity by site-directed mutagenesis. Residues located on the substrate-binding surface of CBP21 and residues located close to the active site, preferentially highly conserved residues were targeted for mutation. In addition, two amino acids located more distant from the active site were mutated to generate controls. In general, the residues were mutated to an alanine but three residues were mutated to amino acids that are naturally occurring in LPMOs, namely W178F, I180R and F187Y. Figure 27 gives a structural overview of all mutated residues.

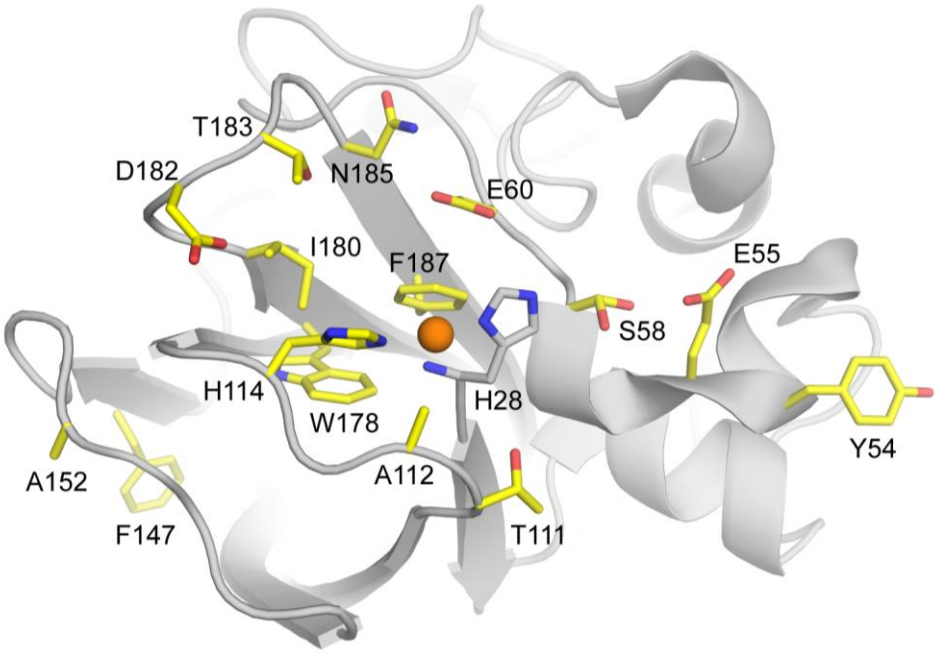

Figure 27. Cartoon representation of CBP21. The side chains of residues selected for mutation are shown as yellow sticks. The side chain of His28, the N-terminal residue, and an essential part of the histidine brace, is shown in grey sticks. The copper is shown as an orange sphere. The figure was made with PyMol (DeLano and Lam, 2005).

As a prelude to this study, an important aspect of the activity assay was evaluated, namely the ratio between LPMO-generated oxidized products remaining attached to the insoluble chitin particles and solubilized oxidized products. It was decided to use chitin particles, and not the more convenient chitin nano-fibers, since the latter substrate does not allow sufficiently high substrate concentrations, due to viscosity issues. Since some mutants were expected to display very low activity, it was essential to be able to quantify all oxidized products generated, since

most of the products were expected to remain associated with the chitin particles for these enzyme variants. This expectation was based on the idea that variants with low activity would not reduce the DP to a level that allowed dissociation of reaction products into solution.

Considering the above, and in contrast to the experiments described in paper II, the total amount of products was measured using samples that, subsequent to the terminated LPMO reaction, had been treated with chitinases and the β-hexosaminidase chitobiase. Comparing the soluble products with the total products after 24 h incubation, it appeared that solubilization of the products is dependent on the activity of the protein. For the CBP21 wildtype and mutants with wildtype-like activity, approximately one third or less of the total products remained on the substrate. Higher relative amounts of products remained on the chitin in reaction with mutants with lower activity, as expected. Product formation over time by the wildtype was linear when measuring total products or solubilized products only. This indicates that CBP21 performs the oxidative cleavages in a regular distance, maybe even similar to a processive manner. As discussed above, the decreased solubilization of products for mutants with low activity may be explained as follows: If the enzyme preferentially introduces chain breaks far apart from each other, and if in total, few chain breaks are introduced, the products will not be soluble and will remain associated with the insoluble chitin particles. It should be noted that the longest fully acetylated, aldonic acid chito-oligosaccharides hitherto observed in solution after a CBP21-β-chitin reaction has a DP of 10-12. In order to avoid product solubilization issues, characterization of the mutants was carried out by quantifying the total amount of oxidized products. Product formation by the CBP21 variants was followed over time using *Mt*CDH/lactose or gallic acid as reducing agent. Gallic acid was used instead of ascorbic acid, since it has been shown to be much more stable over time (Kracher et al., 2016), thus avoiding potential reductant auto-oxidation problems. Interestingly, initial product formation was faster in the presence of 0.5 μM *Mt*CDH and 5.0 mM lactose compared to 1.0 mM gallic acid. However, this difference is most likely reductant concentration dependent, since the dose-response experiments described in paper II clearly show that LPMO activity depends on the concentration of the electron donor. Indeed, when incubating the gallic acid samples up to 48 h, activity profiles similar to the *Mt*CDH samples at 24 h were obtained (some differences were observed and these will be discussed below). What stands out from the mutant activity data is that five residues seem to be crucial for enzyme activity; single amino acid mutants E55A, E60A, H114A, I180R and D182A had only very low or no activity in experiments using either source of electrons (note that of these

mutants, I180R is special since it is rather drastic and likely less "clean" than the other mutations).

In the planning stage of this study we expected to observe that non-detrimental mutations of conserved residues on the substrate binding surface and near the active site would materialize in different catalytic rates, reflecting the impact of the mutation on the overall performance of the enzyme (as commonly observed for enzymes). Clear functional differences between the CBP21 variants were indeed observed, but, most surprisingly, generally not in the form of a decrease in initial rate. Most mutants showed wildtype-like rates early in the reaction, but, relative to the wildtype, their activity disappeared earlier, at time points that varied between the mutants. This loss of activity could be caused by a variety of factors, such as alteration of substrate preferences, loss of substrate binding, reduced affinity to copper, changed coordination and/or redox properties of the copper, increased rate of futile cycling (i.e. quick consumption of reductant and/or O_2), or increased enzyme inactivation by ROS. These options are discussed in more detail below.

Since most mutations were made on the substrate binding surface, and some of the mutants already had been demonstrated to bind less well to chitin (Vaaje-Kolstad et al. 2005b), additional chitin-binding assays were performed using reaction conditions, with gallic acid, similar to those used in the activity assays. The binding data show that chitin-binding was reduced for most mutants, except the two control mutants, W178F (buried residue), T111A and T183A. Some trends stand out. Firstly, mutants shown to be essentially inactive (E55A, E60A, H114A, I180R and D182A) display almost no binding to β-chitin. Based on this observation one might draw the conclusion that binding thus is essential for catalysis. However, surprisingly, this is not correct, since mutants Y54A and S58A show very little affinity to β-chitin, but nevertheless display wildtype-like activity in the first hours of the activity assay. The same applies to F187Y, which, however, only shows initial wild-type-like activity when using gallic acid, while being almost inactive when using *Mt*CDH as electron donor. Thus one may draw the unprecedented conclusion that chitin-binding as measured in our substrate-binding assay is not necessary for successful catalysis by CBP21, suggesting that catalytically productive binding is a transient event that is uncoupled from more "permanent binding" that is measured in the binding assay.

The question of the abrupt loss of activity remains. A highly surprising and potentially very important finding of Paper III is that several of the CBP21 mutants show strongly reduced yields, but almost no change in the initial catalytic rate. Based on the observations described

in paper II, we know that too much reductant is detrimental for CBP21, possibly due to damage caused by elevated levels of ROS. Furthermore, paper II also teaches that at normally used reductant concentrations (i.e. those used in Paper III), almost no ROS (measured as H_2O_2) are formed, presumably because all enzymes are occupied with catalyzing chitin oxidation and not direct reduction of O_2. It is conceivable that mutants with a lower degree of "permanent binding" are more likely to move idle in solution and thereby cause production of ROS that may damage the enzyme.

Building on this line of thought, the question arises how exactly "permanent binding" affects LPMO stability? Does binding protect the LPMOs from themselves, by reducing generation of ROS and/or sensitivity for produced ROS? Could non-productive substrate binding reduce unwanted production of ROS by the LPMO? Interestingly, two recent studies on the role of CBMs in LPMOs (Forsberg et al., 2016, Crouch et al., 2016) show data that may be interpreted to correspond with what is observed for the CBP21 mutants. Both papers report that the LPMOs lacking the CBM bind very weakly to the substrate, compared to the full length enzyme and that the activity of the single LPMO domains ceases abruptly.

For the H114A mutant the loss of activity can be attributed to the disruption of the copper active site since H114 contributes one coordinating nitrogen to the histidine brace. A functional copper coordination in a histidine brace is thus impossible. E55A, E60A and I180R change the copper coordination as discussed below, which might contribute to the drastic reduction of activity. The introduction of a bulky, charged amino acid, arginine, into the active site might also interfere with the architecture of the active site and prevent activity. Even though "permanent binding" is not necessary for activity, the decreased binding ability of the mutants might reflect another reason for the reduced activity. It is possible that some residues like D182A or E55A that are important for binding are also crucial for the proper orientation and positioning of the protein on the substrate and thereby locating the active site in a position where activity can take place.

The "protective binding" hypothesis seems to explain the decline in activity seen for most mutants that bind weakly, but still several observations remain unexplained. For example, T183A and W187F bind almost as well to chitin as the wildtype, but display a substantially shorter time during which they are active (i.e. low yields). It is conceivable that other effects, such as changes in electron transfer rates and/or changes in the coordination of the copper also could affect the generation of damaging ROS species or the sensitivity for such species. To obtain more insight into these aspects of the mutational effects, all variants were analyzed

by stopped-flow spectrometry, to measure the rate of reduction of CBP21 by *Mt*CDH, and by electron paramagnetic resonance spectroscopy (EPR) to assess copper coordination.

In light of the discussed interaction between LPMOs and CDH above and in paper II, the site of interaction and electron transfer between these enzymes is most likely the copper-binding active site of the LPMO and the cytochrome domain of the CDH. The interaction will most likely bring the two redox centers within 14 Å of each other (maximum distance for transferring electrons through a protein, as determined by (Moser et al., 2010)), thereby enabling direct electron transfer. Changes in the environment of the copper-site and the copper coordination itself, may affect the orientation of the interacting proteins and thereby also change the electron transfer (ET) rate. This is indeed what was observed when measuring electron transfer from the *Mt*CDH cytochrome domain to CBP21 variants. However, only a few mutants showed highly reduced transfer rates (H114A, F187Y, E55A and F147A), whereas most variants retained an ET rate that is believed to be more than fast enough for reduction of CBP21, given that the catalytic rate of CBP21 is in the "per minute" range. It should be noted that the ET assay only analyzes the speed of transfer of the first electron in catalysis, i.e. reduction of the LPMO active site copper from Cu(II) to Cu(I). Thus, we cannot rule out that a mutation with no apparent detrimental effect on ET affects the transfer of the second electron needed to complete a catalytic cycle, especially if transfer of this electron occurs via a different interaction site than the site used for the first electron. The issue of the second electron has been briefly discussed in paper II and by Courtade and colleagues, and it was speculated that the LPMO can either store a second electron, or that it is provided by the enzyme itself via oxidation of a tyrosine or tryptophan. To complete the catalytic cycle, two electrons have to be provided by the external electron donor upon release of the LPMO from the substrate (Courtade et al., 2016).

The decreased ET rate observed for the H114A mutant can be explained by the LPMO-CDH interaction. By removing one histidine from the histidine brace, the copper coordination is affected and hence influences the interactions. The F187Y mutant is located at the buried axial position of the copper. This mutation changes the copper-coordination, as discussed later, and seems to be important for the ability to accept electrons from CDH, since also the activity of this mutant is strongly affected. For the two other mutants, E55A and F147A divergent electron transfer data were observed. The ET could not be evaluated as it possessed significantly changed properties, which prevented data-fitting. Nevertheless, it appears that both mutants showed a slower electron transfer than the wildtype. In the E55A mutant the

surface charge was changed, which also affects the copper coordination geometry, probably via a hydrogen bonding network including several water molecules. The change observed for the F147A mutant was unexpected. However, the product formation during the time-course experiment proved that even though the ET took place at a different (slower) pace, it was still fast enough to yield wild-type like rates.

EPR experiments were carried out to identify the residues that influence the copper coordination geometry. As previously shown by Forsberg *et al*. (2014b), the CBP21 wildtype spectrum was rhombic ($g_z > g_y > g_x$) indicating a copper coordination geometry between trigonal bipyramidal and square pyramidal. Mutations having an effect on the copper coordination geometry is illustrated in Figure 28.

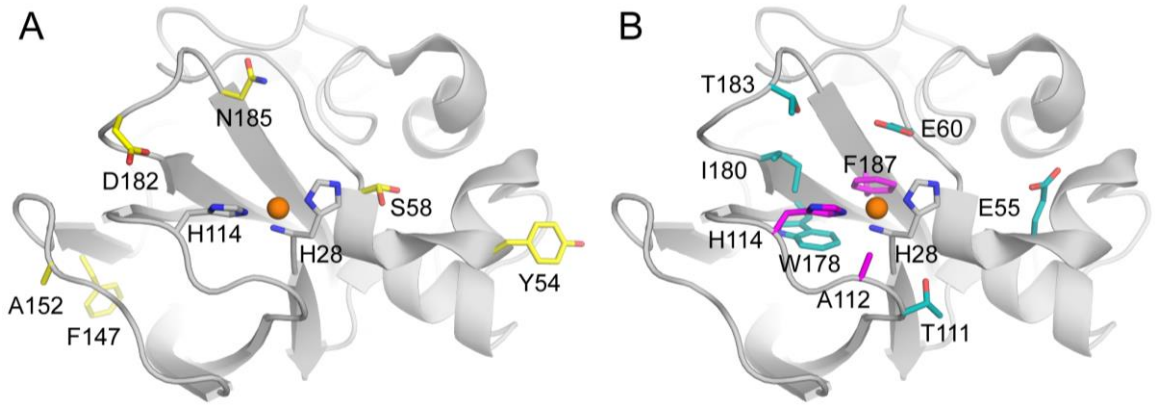

Figure 28. Residues affecting the copper coordination geometry of CBP21. Cartoon representation of CBP21 with the mutated residues shown as colored sticks. Residues whose mutation did not influence the EPR spectrum are shown in yellow, panel A, residues that affect the EPR spectrum are shown in panel (B). In panel B, residues closer than 4 Å to the copper are colored magenta (except H28, which is colored gray) and residues further away than 4 Å from the copper are colored turquoise. The copper is shown as orange sphere. Note that the serine (S58) is shown in two conformations.

Mutations closer than 4 Å to the copper (A112G, H114A and F187Y) showed more axial EPR spectra ($g_z > g_y \sim g_x$) compared to the wildtype. By removing one coordinating nitrogen from the histidine brace the copper is only bound by one histidine, i.e. two nitrogen ligands. The removed nitrogen ligand is probably replaced by a water molecule that is free to adapt its coordination geometry. This rearrangement of the copper coordination results in a more axial spectrum, possibly indicating a shift towards a square pyramidal geometry. A similar observation was made for the A112G mutant. As discussed in the introduction, access to the axial position of LPMOs (assuming a tetragonally distorted octahedral geometry) can be

restricted by an alanine or a tyrosine (Hemsworth et al., 2013b, Forsberg et al., 2014a, Borisova et al., 2015). The mutation of H114 and A112 allow some rearrangement around the copper. The water molecules coordinating the copper encounter less steric hindrance, probably leading to a more square pyramidal geometry that is energetically more favorable. This observation in return suggests that the A112 in CBP21 forces the copper coordination from square pyramidal to an intermediate between trigonal bipyramidal and square pyramidal. The F187Y mutant also leads to a more axial EPR spectrum compared to the wildtype. Instead of removing steric hindrance, an additional OH group that may act as a copper ligand and which is present in AA9s and some AA10s is introduced. Thus the copper coordination may adapt a square pyramidal geometry.

Other mutations that are located further away than 4 Å from the copper showed changes in the g_z and $g_{x,y}$ region of the EPR spectra as well, namely E55A, W178F, I180R, T111A, E60A and T183A. However, these changes were less pronounced than the shifts for the already described mutants. The g_z and $|A_z|$ values determined for W178F, I180R and T111A are different to the values estimated for the wildtype. These mutations affect the second coordination sphere probably leading to changes in amino acid side chain arrangement and hydrogen bonding network that involves residues or waters that directly interact with the copper. E60A possibly influences the copper coordination geometry via a water molecule that interacts with a “first sphere” water molecule or by small structural rearrangements of the protein itself due to the mutation, which is more likely to be the case for T183A and E55A.

4. Concluding remarks and perspectives

Since their discovery in 2010, LPMOs have received a lot of attention. One major research interest concerns the use of these enzymes in industrial conversion of biomass. Although LPMOs today are used industrially, for example in commercial cellulase cocktails for biorefining of lignocellulosic biomass, little is known about their mode of action. This lack of knowledge raises interesting scientific issues and may also harm optimal industrial exploitation of LPMOs. The main objective of the work described in this thesis was to obtain a better understanding of factors determining catalytic activity of chitin-active LPMOs.

In paper I, a fast quantitative assay is described that facilitates measuring the products formed by chitin-active LPMOs. Using this method, the rather complex product profile yielded by LPMOs could be reduced to only one oxidized product, making product quantification fast and convenient. In addition, this publication showed that a protein, which has clearly been identified as virulence factor, GbpA from *V. cholerae*, possesses a catalytic activity. Whether additional substrates that are more relevant for virulence, e.g. mucins, can be degraded by GbpA (or other AA10s involved in virulence) remains to be elucidated. Together with recent work on LPMOs from *E. faecalis* and *L. monocytogenes*, Paper I is likely to spur further studies on the hitherto unknown role of these oxidative enzymes, for example in virulence. As already predicted in 2012 (Horn et al., 2012), novel LPMO substrates are likely to be discovered.

Paper II addresses some of the key issues related to LPMO activity. This paper shows that the source and amount of electrons provided to the LPMO strongly affect catalytic performance. Additionally, the experimental data provide evidence that a fungal protein electron donor, CDH, is able to donate electrons to bacterial AA10s and that, indeed, one LPMO reaction requires the delivery of two external electrons. The plethora of reducing agents that have been shown to activate LPMOs indicate that there is no conserved mechanism for these proteins to acquire electrons and that they are able to utilize almost any source of electrons. The data presented in Paper II and the additional discussion of these issues in section 3 show that the amount and stability of the reducing agent present in an LPMO reaction is especially important to take into account when designing LPMO experiments, and likely, also when applying LPMOs in industry.

Paper III describes the in-depth characterization of a series of mutants of the chitin-active LPMO CBP21. The study showed that substrate binding is not likely to be related to the product formation rate. Interestingly, most mutants showed a similar initial rate as the wildtype, indicating that the overall productivity of the protein is dependent on the life-time of the LPMO. The data in paper III indicate that the conserved site of this protein is a well-balanced, complex system of interacting amino acids, in which most changes have a significant effect on enzyme performance.

Overall, this work provides novel pieces that may be added to the big puzzle of LPMO activity. The present data and discussion also point out several pit-falls that can be encountered when working with LPMOs and also show how these can be avoided. In addition, this thesis contains information that is important for the experimental designs of LPMO assays. The mutant collection described in Paper III should form a valuable resource for further studies on unraveling the structural basis of LPMO activity and hopefully contribute to, eventually, unravelling how LPMO performance could be improved, either by engineering the enzyme or by optimizing process conditions.

5. References

AACHMANN, F. L., SØRLIE, M., SKJÅK-BRÆK, G., EIJSINK, V. G. H. & VAAJE-KOLSTAD, G. 2012. NMR structure of a lytic polysaccharide monooxygenase provides insight into copper binding, protein dynamics, and substrate interactions. *Proc. Natl. Acad. Sci. U.S.A.,* 109**,** 18779-18784.

AGGER, J. W., ISAKSEN, T., VÁRNAI, A., VIDAL-MELGOSA, S., WILLATS, W. G., LUDWIG, R., HORN, S. J., EIJSINK, V. G. H. & WESTERENG, B. 2014. Discovery of LPMO activity on hemicelluloses shows the importance of oxidative processes in plant cell wall degradation. *Proc. Natl. Acad. Sci. U.S.A.,* 111**,** 6287-6292.

AWRAMIK, S. M. 1992. The oldest records of photosynthesis. *Photosynth Res,* 33**,** 75-89.

BAYER, E. A., BELAICH, J. P., SHOHAM, Y. & LAMED, R. 2004. The cellulosomes: multienzyme machines for degradation of plant cell wall polysaccharides. *Annu Rev Microbiol,* 58**,** 521-554.

BEESON, W. T., PHILLIPS, C. M., CATE, J. H. & MARLETTA, M. A. 2012. Oxidative cleavage of cellulose by fungal copper-dependent polysaccharide monooxygenases. *J Am Chem Soc,* 134**,** 890-892.

BEESON, W. T., VU, V. V., SPAN, E. A., PHILLIPS, C. M. & MARLETTA, M. A. 2015. Cellulose degradation by polysaccharide monooxygenases. *Annu. Rev. Biochem.,* 84**,** 923-946.

BEIER, S. & BERTILSSON, S. 2013. Bacterial chitin degradation-mechanisms and ecophysiological strategies. *Front Microbiol,* 4**,** 149.

BELL, E. A., BOEHNKE, P., HARRISON, T. M. & MAO, W. L. 2015. Potentially biogenic carbon preserved in a 4.1 billion-year-old zircon. *Proc Natl Acad Sci U S A,* 112**,** 14518-14521.

BERKA, R. M., GRIGORIEV, I. V., OTILLAR, R., SALAMOV, A., GRIMWOOD, J., REID, I., ISHMAEL, N., JOHN, T., DARMOND, C., MOISAN, M. C., HENRISSAT, B., COUTINHO, P. M., LOMBARD, V., NATVIG, D. O., LINDQUIST, E., SCHMUTZ, J., LUCAS, S., HARRIS, P., POWLOWSKI, J., BELLEMARE, A., TAYLOR, D., BUTLER, G., DE VRIES, R. P., ALLIJN, I. E., VAN DEN BRINK, J., USHINSKY, S., STORMS, R., POWELL, A. J., PAULSEN, I. T., ELBOURNE, L. D. H., BAKER, S. E., MAGNUSON, J., LABOISSIERE, S., CLUTTERBUCK, A. J., MARTINEZ, D., WOGULIS, M., DE LEON, A. L., REY, M. W. & TSANG, A. 2011. Comparative genomic analysis of the thermophilic biomass-degrading fungi *Myceliophthora thermophila* and *Thielavia terrestris*. *Nature Biotechnology,* 29**,** 922-927.

BHOWMICK, R., GHOSAL, A., DAS, B., KOLEY, H., SAHA, D. R., GANGULY, S., NANDY, R. K., BHADRA, R. K. & CHATTERJEE, N. S. 2008. Intestinal Adherence of *Vibrio cholerae* Involves a Coordinated Interaction between Colonization Factor GbpA and Mucin. *Infection and Immunity,* 76**,** 4968-4977.

BISCHOF, R. H., RAMONI, J. & SEIBOTH, B. 2016. Cellulases and beyond: the first 70 years of the enzyme producer *Trichoderma reesei*. *Microbial Cell Factories,* 15.

BISSARO, B., FORSBERG, Z., NI, Y., HOLLMANN, F., VAAJE-KOLSTAD, G. & EIJSINK, V. G. H. 2016. Fueling biomass-degrading oxidative enzymes by light-driven water oxidation. *Green Chemistry*.

BLACKWELL, J. 1988. Physical Methods for the Determination of Chitin Structure and Conformation. *Methods in Enzymology,* 161**,** 435-442.

BOLAM, D. N., CIRUELA, A., MCQUEEN-MASON, S., SIMPSON, P., WILLIAMSON, M. P., RIXON, J. E., BORASTON, A., HAZLEWOOD, G. P. & GILBERT, H. J. 1998. Pseudomonas cellulose-binding domains mediate their effects by increasing enzyme substrate proximity. *Biochemical Journal,* 331**,** 775-781.

BOOK, A. J., LEWIN, G. R., MCDONALD, B. R., TAKASUKA, T. E., WENDT-PIENKOWSKI, E., DOERING, D. T., SUH, S., RAFFA, K. F., FOX, B. G. & CURRIE, C. R. 2016. Evolution of High Cellulolytic Activity in Symbiotic Streptomyces through Selection of Expanded Gene Content and Coordinated Gene Expression. *Plos Biology,* 14.

BOOK, A. J., YENNAMALLI, R. M., TAKASUKA, T. E., CURRIE, C. R., PHILLIPS, G. N. & FOX, B. G. 2014. Evolution of substrate specificity in bacterial AA10 lytic polysaccharide monooxygenases. *Biotechnology for Biofuels,* 7.

BORASTON, A. B., BOLAM, D. N., GILBERT, H. J. & DAVIES, G. J. 2004. Carbohydrate-binding modules: fine-tuning polysaccharide recognition. *Biochemical Journal,* 382**,** 769-781.

BORISOVA, A. S., ISAKSEN, T., DIMAROGONA, M., KOGNOLE, A. A., MATHIESEN, G., VARNAI, A., ROHR, A. K., PAYNE, C. M., SORLIE, M., SANDGREN, M. & EIJSINK, V. G. H. 2015. Structural and Functional Characterization of a Lytic Polysaccharide Monooxygenase with Broad Substrate Specificity. *Journal of Biological Chemistry,* 290**,** 22955-22969.

BRAMELD, K. A. & GODDARD, W. A. 1998a. The role of enzyme distortion in the single displacement mechanism of family 19 chitinases. *Proceedings of the National Academy of Sciences of the United States of America,* 95**,** 4276-4281.

BRAMELD, K. A. & GODDARD, W. A. 1998b. Substrate distortion to a boat conformation at subsite-1 is critical in the mechanism of family 18 chitinases. *Journal of the American Chemical Society,* 120**,** 3571-3580.

BRZEZINSKA, M. S., JANKIEWICZ, U., BURKOWSKA, A. & WALCZAK, M. 2014. Chitinolytic Microorganisms and Their Possible Application in Environmental Protection. *Current Microbiology,* 68**,** 71-81.

BURNUM, K. E., CALLISTER, S. J., NICORA, C. D., PURVINE, S. O., HUGENHOLTZ, P., WARNECKE, F., SCHEFFRAHN, R. H., SMITH, R. D. & LIPTON, M. S. 2011. Proteome insights into the symbiotic relationship between a captive colony of Nasutitermes corniger and its hindgut microbiome. *ISME J,* 5**,** 161-164.

CAMPBELL, L. L. & WILLIAMS, O. B. 1951. A study of chitin-decomposing micro-organisms of marine origin. *J Gen Microbiol,* 5**,** 894-905.

CANNELLA, D., HSIEH, C. W. C., FELBY, C. & JORGENSEN, H. 2012. Production and effect of aldonic acids during enzymatic hydrolysis of lignocellulose at high dry matter content. *Biotechnology for Biofuels,* 5.

CANNELLA, D., MÖLLERS, K. B., FRIGAARD, N. U., JENSEN, P. E., BJERRUM, M. J., JOHANSEN, K. S. & FELBY, C. 2016. Light-driven oxidation of polysaccharides by photosynthetic pigments and a metalloenzyme. *Nat. Commun.,* 7**,** 11134.

CANTAREL, B. L., COUTINHO, P. M., RANCUREL, C., BERNARD, T., LOMBARD, V. & HENRISSAT, B. 2009. The Carbohydrate-Active EnZymes database (CAZy): an expert resource for Glycogenomics. *Nucleic Acids Res,* 37**,** D233-238.

CARROAD, P. A. & TOM, R. A. 1978. Bioconversion of Shellfish Chitin Wastes - Process Conception and Selection of Microorganisms. *Journal of Food Science,* 43**,** 1158-1161.

CHAPLIN, A. K., WILSON, M. T., HOUGH, M. A., SVISTUNENKO, D. A., HEMSWORTH, G. R., WALTON, P. H., VIJGENBOOM, E. & WORRALL, J. A. R. 2016. Heterogeneity in the Histidine-brace Copper Coordination Sphere in

Auxiliary Activity Family 10 (AA10) Lytic Polysaccharide Monooxygenases. *Journal of Biological Chemistry,* 291**,** 12838-12850.

CHAUDHURI, S., BRUNO, J. C., ALONZO, F., 3RD, XAYARATH, B., CIANCIOTTO, N. P. & FREITAG, N. E. 2010. Contribution of chitinases to *Listeria monocytogenes* pathogenesis. *Appl Environ Microbiol,* 76**,** 7302-7305.

CHEN, P. & SOLOMON, E. I. 2004. Oxygen activation by the noncoupled binuclear copper site in peptidylglycine alpha-hydroxylating monooxygenase. Reaction mechanism and role of the noncoupled nature of the active site. *J Am Chem Soc,* 126**,** 4991-5000.

CHIU, E., HIJNEN, M., BUNKER, R. D., BOUDES, M., RAJENDRAN, C., AIZEL, K., OLIERIC, V., SCHULZE-BRIESE, C., MITSUHASHI, W., YOUNG, V., WARD, V. K., BERGOIN, M., METCALF, P. & COULIBALY, F. 2015. Structural basis for the enhancement of virulence by viral spindles and their in vivo crystallization. *Proceedings of the National Academy of Sciences of the United States of America,* 112**,** 3973-3978.

CHU, H. H., HOANG, V., HOFEMEISTER, J. & SCHREMPF, H. 2001. A *Bacillus amyloliquefaciens* ChbB protein binds beta- and alpha-chitin and has homologues in related strains. *Microbiology,* 147**,** 1793-1803.

COCINERO, E. J., GAMBLIN, D. P., DAVIS, B. G. & SIMONS, J. P. 2009. The building blocks of cellulose: the intrinsic conformational structures of cellobiose, its epimer, lactose, and their singly hydrated complexes. *J Am Chem Soc,* 131**,** 11117-11123.

CORRÊA, T. L. R., DOS SANTOS, L. V. & PEREIRA, G. A. G. 2016. AA9 and AA10: from enigmatic to essential enzymes. *Applied Microbiology and Biotechnology,* 100**,** 9-16.

COURTADE, G., WIMMER, R., ROHR, A. K., PREIMS, M., FELICE, A. K., DIMAROGONA, M., VAAJE-KOLSTAD, G., SORLIE, M., SANDGREN, M., LUDWIG, R., EIJSINK, V. G. & AACHMANN, F. L. 2016. Interactions of a fungal lytic polysaccharide monooxygenase with beta-glucan substrates and cellobiose dehydrogenase. *Proc Natl Acad Sci U S A,* 113**,** 5922-5927.

COUTINHO, P. M., DELEURY, E., DAVIES, G. J. & HENRISSAT, B. 2003. An evolving hierarchical family classification for glycosyltransferases. *Journal of Molecular Biology,* 328**,** 307-317.

CRAGG, S. M., BECKHAM, G. T., BRUCE, N. C., BUGG, T. D. H., DISTEL, D. L., DUPREE, P., ETXABE, A. G., GOODELL, B. S., JELLISON, J., MCGEEHAN, J. E., MCQUEEN-MASON, S. J., SCHNORR, K., WALTON, P. H., WATTS, J. E. M. & ZIMMER, M. 2015. Lignocellulose degradation mechanisms across the Tree of Life. *Current Opinion in Chemical Biology,* 29**,** 108-119.

CROISIER, F. & JÉRÔME, C. 2013. Chitosan-based biomaterials for tissue engineering. *European Polymer Journal,* 49**,** 780-792.

CROUCH, L. I., LABOUREL, A., WALTON, P. H., DAVIES, G. J. & GILBERT, H. J. 2016. The Contribution of Non-catalytic Carbohydrate Binding Modules to the Activity of Lytic Polysaccharide Monooxygenases. *J Biol Chem,* 291**,** 7439-49.

CUSKIN, F., LOWE, E. C., TEMPLE, M. J., ZHU, Y. P., CAMERON, E. A., PUDLO, N. A., PORTER, N. T., URS, K., THOMPSON, A. J., CARTMELL, A., ROGOWSKI, A., HAMILTON, B. S., CHEN, R., TOLBERT, T. J., PIENS, K., BRACKE, D., VERVECKEN, W., HAKKI, Z., SPECIALE, G., MUNOZ-MUNOZ, J. L., DAY, A., PENA, M. J., MCLEAN, R., SUITS, M. D., BORASTON, A. B., ATHERLY, T., ZIEMER, C. J., WILLIAMS, S. J., DAVIES, G. J., ABBOTT, D. W., MARTENS, E. C. & GILBERT, H. J. 2015. Human gut Bacteroidetes can utilize yeast mannan through a selfish mechanism. *Nature,* 517**,** 165-U86.

DAVIES, G. & HENRISSAT, B. 1995. Structures and mechanisms of glycosyl hydrolases. *Structure,* 3**,** 853-859.

DEKKER, R. F. & RICHARDS, G. N. 1976. Hemicellulases: their occurrence, purification, properties, and mode of action. *Adv Carbohydr Chem Biochem,* 32**,** 277-352.

DELANO, W. L. & LAM, J. W. 2005. PyMOL: A communications tool for computational models. *Abstracts of Papers of the American Chemical Society,* 230**,** U1371-U1372.

DIMAROGONA, M., TOPAKAS, E., OLSSON, L. & CHRISTAKOPOULOS, P. 2012. Lignin boosts the cellulase performance of a GH-61 enzyme from *Sporotrichum thermophile*. *Bioresour. Technol.,* 110**,** 480-487.

DIXON, R. A., LAMB, C. J., MASOUD, S., SEWALT, V. J. H. & PAIVA, N. L. 1996. Metabolic engineering: Prospects for crop improvement through the genetic manipulation of phenylpropanoid biosynthesis and defense responses - A review. *Gene,* 179**,** 61-71.

DUCHESNE, L. C. & LARSON, D. W. 1989. Cellulose and the Evolution of Plant Life. *Bioscience,* 39**,** 238-241.

EASTWOOD, D. C., FLOUDAS, D., BINDER, M., MAJCHERCZYK, A., SCHNEIDER, P., AERTS, A., ASIEGBU, F. O., BAKER, S. E., BARRY, K., BENDIKSBY, M., BLUMENTRITT, M., COUTINHO, P. M., CULLEN, D., DE VRIES, R. P., GATHMAN, A., GOODELL, B., HENRISSAT, B., IHRMARK, K., KAUSERUD, H., KOHLER, A., LABUTTI, K., LAPIDUS, A., LAVIN, J. L., LEE, Y. H., LINDQUIST, E., LILLY, W., LUCAS, S., MORIN, E., MURAT, C., OGUIZA, J. A., PARK, J., PISABARRO, A. G., RILEY, R., ROSLING, A., SALAMOV, A., SCHMIDT, O., SCHMUTZ, J., SKREDE, I., STENLID, J., WIEBENGA, A., XIE, X. F., KUES, U., HIBBETT, D. S., HOFFMEISTER, D., HOGBERG, N., MARTIN, F., GRIGORIEV, I. V. & WATKINSON, S. C. 2011. The Plant Cell Wall-Decomposing Machinery Underlies the Functional Diversity of Forest Fungi. *Science,* 333**,** 762-765.

EHRLICH, H., RIGBY, J. K., BOTTING, J. P., TSURKAN, M. V., WERNER, C., SCHWILLE, P., PETRASEK, Z., PISERA, A., SIMON, P., SIVKOV, V. N., VYALIKH, D. V., MOLODTSOV, S. L., KUREK, D., KAMMER, M., HUNOLDT, S., BORN, R., STAWSKI, D., STEINHOF, A., BAZHENOV, V. V. & GEISLER, T. 2013. Discovery of 505-million-year old chitin in the basal demosponge *Vauxia gracilenta*. *Sci Rep,* 3**,** 3497.

ERIKSSON, K. E., PETTERSSON, B. & WESTERMARK, U. 1974. Oxidation: an important enzyme reaction in fungal degradation of cellulose. *FEBS Lett,* 49**,** 282-285.

FAN, Y. M., SAITO, T. & ISOGAI, A. 2008. Preparation of chitin nanofibers from squid pen beta-chitin by simple mechanical treatment under acid conditions. *Biomacromolecules,* 9**,** 1919-1923.

FOLEY, M. H., COCKBURN, D. W. & KOROPATKIN, N. M. 2016. The Sus operon: a model system for starch uptake by the human gut Bacteroidetes. *Cell Mol Life Sci,* 73**,** 2603-2617.

FONTES, C. M. & GILBERT, H. J. 2010. Cellulosomes: highly efficient nanomachines designed to deconstruct plant cell wall complex carbohydrates. *Annu Rev Biochem,* 79**,** 655-681.

FORSBERG, Z., MACKENZIE, A. K., SØRLIE, M., RØHR, Å. K., HELLAND, R., ARVAI, A. S., VAAJE-KOLSTAD, G. & EIJSINK, V. G. H. 2014a. Structural and functional characterization of a conserved pair of bacterial cellulose-oxidizing lytic polysaccharide monooxygenases. *Proc. Natl. Acad. Sci. U.S.A.,* 111**,** 8446-8451.

FORSBERG, Z., NELSON, C. E., DALHUS, B., MEKASHA, S., LOOSE, J. S., CROUCH, L. I., RØHR, Å. K., GARDNER, J. G., EIJSINK, V. G. & VAAJE-KOLSTAD, G. 2016. Structural and Functional Analysis of a Lytic Polysaccharide Monooxygenase

Important for Efficient Utilization of Chitin in *Cellvibrio japonicus*. *J Biol Chem,* 291**,** 7300-7312.

FORSBERG, Z., RØHR, Å. K., MEKASHA, S., ANDERSSON, K. K., EIJSINK, V. G. H., VAAJE-KOLSTAD, G. & SØRLIE, M. 2014b. Comparative study of two chitin-active and two cellulose-active AA10-type lytic polysaccharide monooxygenases. *Biochemistry,* 53**,** 1647-1656.

FORSBERG, Z., VAAJE-KOLSTAD, G., WESTERENG, B., BUNÆS, A. C., STENSTRØM, Y., MACKENZIE, A., SØRLIE, M., HORN, S. J. & EIJSINK, V. G. H. 2011. Cleavage of cellulose by a CBM33 protein. *Protein Sci.,* 20**,** 1479-1483.

FRANDSEN, K. E., SIMMONS, T. J., DUPREE, P., POULSEN, J. C., HEMSWORTH, G. R., CIANO, L., JOHNSTON, E. M., TOVBORG, M., JOHANSEN, K. S., VON FREIESLEBEN, P., MARMUSE, L., FORT, S., COTTAZ, S., DRIGUEZ, H., HENRISSAT, B., LENFANT, N., TUNA, F., BALDANSUREN, A., DAVIES, G. J., LO LEGGIO, L. & WALTON, P. H. 2016. The molecular basis of polysaccharide cleavage by lytic polysaccharide monooxygenases. *Nat Chem Biol,* 12**,** 298-303.

FROMMHAGEN, M., SFORZA, S., WESTPHAL, A. H., VISSER, J., HINZ, S. W. A., KOETSIER, M. J., VAN BERKEL, W. J. H., GRUPPEN, H. & KABEL, M. A. 2015. Discovery of the combined oxidative cleavage of plant xylan and cellulose by a new fungal polysaccharide monooxygenase. *Biotechnol. Biofuels,* 8**,** 101.

FUCHS, R. L., MCPHERSON, S. A. & DRAHOS, D. J. 1986. Cloning of a *Serratia marcescens* Gene Encoding Chitinase. *Appl Environ Microbiol,* 51**,** 504-509.

GAILL, F., PERSSON, J., SUGIYAMA, J., VUONG, R. & CHANZY, H. 1992. The Chitin System in the Tubes of Deep-Sea Hydrothermal Vent Worms. *Journal of Structural Biology,* 109**,** 116-128.

GARAJOVA, S., MATHIEU, Y., BECCIA, M. R., BENNATI-GRANIER, C., BIASO, F., FANUEL, M., ROPARTZ, D., GUIGLIARELLI, B., RECORD, E., ROGNIAUX, H., HENRISSAT, B. & BERRIN, J. G. 2016. Single-domain flavoenzymes trigger lytic polysaccharide monooxygenases for oxidative degradation of cellulose. *Scientific Reports,* 6**,** 28276

GARCIA-GONZALEZ, E., POPPINGA, L., FÜNFHAUS, A., HERTLEIN, G., HEDTKE, K., JAKUBOWSKA, A. & GENERSCH, E. 2014. *Paenibacillus larvae* Chitin-Degrading Protein PlCBP49 Is a Key Virulence Factor in American Foulbrood of Honey Bees. *Plos Pathogens,* 10**,** e10044284.

GARDNER, J. G., CROUCH, L., LABOUREL, A., FORSBERG, Z., BUKHMAN, Y. V., VAAJE-KOLSTAD, G., GILBERT, H. J. & KEATING, D. H. 2014. Systems biology defines the biological significance of redox-active proteins during cellulose degradation in an aerobic bacterium. *Mol. Microbiol.,* 94**,** 1121-1133.

GARDNER, K. H. & BLACKWELL, J. 1975. Refinement of the structure of beta-chitin. *Biopolymers,* 14**,** 1581-1595.

GERENTE, C., LEE, V. K. C., LE CLOIREC, P. & MCKAY, G. 2007. Application of chitosan for the removal of metals from wastewaters by adsorption - Mechanisms and models review. *Critical Reviews in Environmental Science and Technology,* 37**,** 41-127.

GILBERT, H. J. 2007. Cellulosomes: microbial nanomachines that display plasticity in quaternary structure. *Mol Microbiol,* 63**,** 1568-1576.

GOODAY, G. W. 1990. The Ecology of Chitin Degradation. *Advances in Microbial Ecology,* 11**,** 387-430.

GRULA, J. W. 2005. Evolution of photosynthesis and biospheric oxygenation contingent upon nitrogen fixation? *International Journal of Astrobiology,* 4**,** 251-257.

GUDMUNDSSON, M., KIM, S., WU, M., ISHIDA, T., MOMENI, M. H., VAAJE-KOLSTAD, G., LUNDBERG, D., ROYANT, A., STÅHLBERG, J., EIJSINK, V. G., BECKHAM, G. T. & SANDGREN, M. 2014. Structural and electronic snapshots during the transition from a Cu(II) to Cu(I) metal center of a lytic polysaccharide monooxygenase by X-ray photoreduction. *J Biol Chem,* 289**,** 18782-18792.

HARRIS, P. V., WELNER, D., MCFARLAND, K. C., RE, E., NAVARRO POULSEN, J. C., BROWN, K., SALBO, R., DING, H., VLASENKO, E., MERINO, S., XU, F., CHERRY, J., LARSEN, S. & LO LEGGIO, L. 2010. Stimulation of lignocellulosic biomass hydrolysis by proteins of glycoside hydrolase family 61: structure and function of a large, enigmatic family. *Biochemistry,* 49**,** 3305-3316.

HASUNUMA, T., OKAZAKI, F., OKAI, N., HARA, K. Y., ISHII, J. & KONDO, A. 2013. A review of enzymes and microbes for lignocellulosic biorefinery and the possibility of their application to consolidated bioprocessing technology. *Bioresource Technology,* 135**,** 513-522.

HEMSWORTH, G. R., DAVIES, G. J. & WALTON, P. H. 2013a. Recent insights into copper-containing lytic polysaccharide mono-oxygenases. *Curr Opin Struct Biol,* 23**,** 660-668.

HEMSWORTH, G. R., HENRISSAT, B., DAVIES, G. J. & WALTON, P. H. 2014. Discovery and characterization of a new family of lytic polysaccharide monooxygenases. *Nat. Chem. Biol.,* 10**,** 122-126.

HEMSWORTH, G. R., TAYLOR, E. J., KIM, R. Q., GREGORY, R. C., LEWIS, S. J., TURKENBURG, J. P., PARKIN, A., DAVIES, G. J. & WALTON, P. H. 2013b. The copper active site of CBM33 polysaccharide oxygenases. *J. Am. Chem. Soc.,* 135**,** 6069-6077.

HENRIKSSON, G., JOHANSSON, G. & PETTERSSON, G. 2000. A critical review of cellobiose dehydrogenases. *J Biotechnol,* 78**,** 93-113.

HENRISSAT, B. 1991. A classification of glycosyl hydrolases based on amino acid sequence similarities. *Biochem J,* 280 (Pt 2)**,** 309-316.

HERVE, C., ROGOWSKI, A., BLAKE, A. W., MARCUS, S. E., GILBERT, H. J. & KNOX, J. P. 2010. Carbohydrate-binding modules promote the enzymatic deconstruction of intact plant cell walls by targeting and proximity effects. *Proceedings of the National Academy of Sciences of the United States of America,* 107**,** 15293-15298.

HEUTS, D. P. H. M., WINTER, R. T., DAMSMA, G. E., JANSSEN, D. B. & FRAAIJE, M. W. 2008. The role of double covalent flavin binding in chito-oligosaccharide oxidase from *Fusarium graminearum*. *Biochem. J.,* 413**,** 175-183.

HOELL, I. A., DALHUS, B., HEGGSET, E. B., ASPMO, S. I. & EIJSINK, V. G. 2006. Crystal structure and enzymatic properties of a bacterial family 19 chitinase reveal differences from plant enzymes. *FEBS J,* 273**,** 4889-4900.

HOLM, L. & ROSENSTROM, P. 2010. Dali server: conservation mapping in 3D. *Nucleic Acids Research,* 38**,** W545-W549.

HON, D. N. S. 1994. Cellulose - a Random-Walk Along Its Historical Path. *Cellulose,* 1**,** 1-25.

HORN, S. J., VAAJE-KOLSTAD, G., WESTERENG, B. & EIJSINK, V. G. H. 2012. Novel enzymes for the degradation of cellulose. *Biotechnol. Biofuels,* 5**,** 45.

HULT, E. L., KATOUNO, F., UCHIYAMA, T., WATANABE, T. & SUGIYAMA, J. 2005. Molecular directionality in crystalline beta-chitin: hydrolysis by chitinases A and B from *Serratia marcescens* 2170. *Biochemical Journal,* 388**,** 851-856.

IGARASHI, K., MOMOHARA, I., NISHINO, T. & SAMEJIMA, M. 2002. Kinetics of inter-domain electron transfer in flavocytochrome cellobiose dehydrogenase from the white-rot fungus *Phanerochaete chrysosporium*. *Biochem. J.,* 365**,** 521-526.

ISAKSEN, T., WESTERENG, B., AACHMANN, F. L., AGGER, J. W., KRACHER, D., KITTL, R., LUDWIG, R., HALTRICH, D., EIJSINK, V. G. H. & HORN, S. J. 2014. A C4-oxidizing lytic polysaccharide monooxygenase cleaving both cellulose and cello-oligosaccharides. *J. Biol. Chem.,* 289**,** 2632-2642.

JACQUIOD, S., FRANQUEVILLE, L., CECILLON, S., VOGEL, T. M. & SIMONET, P. 2013. Soil bacterial community shifts after chitin enrichment: an integrative metagenomic approach. *PLoS One,* 8**,** e79699.

JAYAKUMAR, R., PRABAHARAN, M., SUDHEESH KUMAR, P. T., NAIR, S. V. & TAMURA, H. 2011. Biomaterials based on chitin and chitosan in wound dressing applications. *Biotechnol Adv,* 29**,** 322-337.

KARKEHABADI, S., HANSSON, H., KIM, S., PIENS, K., MITCHINSON, C. & SANDGREN, M. 2008. The first structure of a glycoside hydrolase family 61 member, Cel61B from *Hypocrea jecorina*, at 1.6 A resolution. *J Mol Biol,* 383**,** 144-154.

KARLSSON, J., SALOHEIMO, M., SIIKA-AHO, M., TENKANEN, M., PENTTILA, M. & TJERNELD, F. 2001. Homologous expression and characterization of Cel61A (EG IV) of *Trichoderma reesei*. *Eur J Biochem,* 268**,** 6498-6507.

KAWADA, M., CHEN, C. C., ARIHIRO, A., NAGATANI, K., WATANABE, T. & MIZOGUCHI, E. 2008. Chitinase 3-like-1 enhances bacterial adhesion to colonic epithelial cells through the interaction with bacterial chitin-binding protein. *Laboratory Investigation,* 88**,** 883-895.

KENRICK, P. & CRANE, P. R. 1997. The origin and early evolution of plants on land. *Nature,* 389**,** 33-39.

KEYHANI, N. O., LI, X. B. & ROSEMAN, S. 2000. Chitin catabolism in the marine bacterium *Vibrio furnissii* - Identification and molecular cloning of a chitoporin. *Journal of Biological Chemistry,* 275**,** 33068-33076.

KEYHANI, N. O. & ROSEMAN, S. 1999. Physiological aspects of chitin catabolism in marine bacteria. *Biochimica Et Biophysica Acta-General Subjects,* 1473**,** 108-122.

KIM, S., STÅHLBERG, J., SANDGREN, M., PATON, R. S. & BECKHAM, G. T. 2014. Quantum mechanical calculations suggest that lytic polysaccharide monooxygenases use a copper-oxyl, oxygen-rebound mechanism. *Proc Natl Acad Sci U S A,* 111**,** 149-154.

KIRN, T. J., JUDE, B. A. & TAYLOR, R. K. 2005. A colonization factor links *Vibrio cholerae* environmental survival and human infection. *Nature,* 438**,** 863-866.

KITTL, R., KRACHER, D., BURGSTALLER, D., HALTRICH, D. & LUDWIG, R. 2012. Production of four *Neurospora crassa* lytic polysaccharide monooxygenases in *Pichia pastoris* monitored by a fluorimetric assay. *Biotechnol. Biofuels,* 5**,** 79.

KJAERGAARD, C. H., QAYYUM, M. F., WONG, S. D., XU, F., HEMSWORTH, G. R., WALTON, D. J., YOUNG, N. A., DAVIES, G. J., WALTON, P. H., JOHANSEN, K. S., HODGSON, K. O., HEDMAN, B. & SOLOMON, E. I. 2014. Spectroscopic and computational insight into the activation of O2 by the mononuclear Cu center in polysaccharide monooxygenases. *Proc Natl Acad Sci U S A,* 111**,** 8797-8802.

KLEMM, D., HEUBLEIN, B., FINK, H. P. & BOHN, A. 2005. Cellulose: fascinating biopolymer and sustainable raw material. *Angew Chem Int Ed Engl,* 44**,** 3358-3393.

KOLBE, S., FISCHER, S., BECIREVIC, A., HINZ, P. & SCHREMPF, H. 1998. The *Streptomyces reticuli* alpha-chitin-binding protein CHB2 and its gene. *Microbiology,* 144 (Pt 5)**,** 1291-1297.

KOSHLAND, D. E. 1953. Stereochemistry and the Mechanism of Enzymatic Reactions. *Biological Reviews of the Cambridge Philosophical Society,* 28**,** 416-436.

KRACHER, D., SCHEIBLBRANDNER, S., FELICE, A. K., BRESLMAYR, E., PREIMS, M., LUDWICKA, K., HALTRICH, D., EIJSINK, V. G. & LUDWIG, R. 2016. Extracellular electron transfer systems fuel cellulose oxidative degradation. *Science,* 352**,** 1098-1101.

KUMAR, M. N. V. R. 2000. A review of chitin and chitosan applications. *Reactive & Functional Polymers,* 46**,** 1-27.

KURITA, K. 2006. Chitin and chitosan: functional biopolymers from marine crustaceans. *Mar Biotechnol (NY),* 8**,** 203-226.

LAINE, R. A. 1994. A calculation of all possible oligosaccharide isomers both branched and linear yields 1.05 x 10(12) structures for a reducing hexasaccharide: the Isomer Barrier to development of single-method saccharide sequencing or synthesis systems. *Glycobiology,* 4**,** 759-767.

LAIRSON, L. L., HENRISSAT, B., DAVIES, G. J. & WITHERS, S. G. 2008. Glycosyltransferases: Structures, functions, and mechanisms. *Annual Review of Biochemistry,* 77**,** 521-555.

LANGSTON, J. A., SHAGHASI, T., ABBATE, E., XU, F., VLASENKO, E. & SWEENEY, M. D. 2011. Oxidoreductive cellulose depolymerization by the enzymes cellobiose dehydrogenase and glycoside hydrolase 61. *Appl. Environ. Microbiol.,* 77**,** 7007-7015.

LARSBRINK, J., ROGERS, T. E., HEMSWORTH, G. R., MCKEE, L. S., TAUZIN, A. S., SPADIUT, O., KLINTER, S., PUDLO, N. A., URS, K., KOROPATKIN, N. M., CREAGH, A. L., HAYNES, C. A., KELLY, A. G., CEDERHOLM, S. N., DAVIES, G. J., MARTENS, E. C. & BRUMER, H. 2014. A discrete genetic locus confers xyloglucan metabolism in select human gut Bacteroidetes. *Nature,* 506**,** 498-502.

LEVASSEUR, A., DRULA, E., LOMBARD, V., COUTINHO, P. M. & HENRISSAT, B. 2013. Expansion of the enzymatic repertoire of the CAZy database to integrate auxiliary redox enzymes. *Biotechnol. Biofuels,* 6**,** 41.

LEVI-KALISMAN, Y., FALINI, G., ADDADI, L. & WEINER, S. 2001. Structure of the nacreous organic matrix of a bivalve mollusk shell examined in the hydrated state using cryo-TEM. *J Struct Biol,* 135**,** 8-17.

LI, X., BEESON, W. T., PHILLIPS, C. M., MARLETTA, M. A. & CATE, J. H. D. 2012. Structural basis for substrate targeting and catalysis by fungal polysaccharide monooxygenases. *Structure,* 20**,** 1051-1061.

LI, X. B. & ROSEMAN, S. 2004. The chitinolytic cascade in Vibrios is regulated by chitin oligosaccharides and a two-component chitin catabolic sensor/kinase. *Proceedings of the National Academy of Sciences of the United States of America,* 101**,** 627-631.

LO LEGGIO, L., SIMMONS, T. J., POULSEN, J. C., FRANDSEN, K. E., HEMSWORTH, G. R., STRINGER, M. A., VON FREIESLEBEN, P., TOVBORG, M., JOHANSEN, K. S., DE MARIA, L., HARRIS, P. V., SOONG, C. L., DUPREE, P., TRYFONA, T., LENFANT, N., HENRISSAT, B., DAVIES, G. J. & WALTON, P. H. 2015. Structure and boosting activity of a starch-degrading lytic polysaccharide monooxygenase. *Nat. Commun.,* 6**,** 5961.

LOMBARD, V., BERNARD, T., RANCUREL, C., BRUMER, H., COUTINHO, P. M. & HENRISSAT, B. 2010. A hierarchical classification of polysaccharide lyases for glycogenomics. *Biochemical Journal,* 432**,** 437-444.

LOMBARD, V., GOLACONDA RAMULU, H., DRULA, E., COUTINHO, P. M. & HENRISSAT, B. 2014. The carbohydrate-active enzymes database (CAZy) in 2013. *Nucleic Acids Res,* 42**,** D490-495.

LOOSE, J. S. M., FORSBERG, Z., FRAAIJE, M. W., EIJSINK, V. G. H. & VAAJE-KOLSTAD, G. 2014. A rapid quantitative activity assay shows that the *Vibrio*

cholerae colonization factor GbpA is an active lytic polysaccharide monooxygenase. *FEBS Lett.,* 588**,** 3435-3440.

LU, Y., ZHANG, Y. H. & LYND, L. R. 2006. Enzyme-microbe synergy during cellulose hydrolysis by *Clostridium thermocellum*. *Proc Natl Acad Sci U S A,* 103**,** 16165-16169.

MARTENS, E. C., CHIANG, H. C. & GORDON, J. I. 2008. Mucosal glycan foraging enhances fitness and transmission of a saccharolytic human gut bacterial symbiont. *Cell Host Microbe,* 4**,** 447-457.

MARTENS, E. C., KOROPATKIN, N. M., SMITH, T. J. & GORDON, J. I. 2009. Complex glycan catabolism by the human gut microbiota: the Bacteroidetes Sus-like paradigm. *J Biol Chem,* 284**,** 24673-24677.

MARTINEZ, D., BERKA, R. M., HENRISSAT, B., SALOHEIMO, M., ARVAS, M., BAKER, S. E., CHAPMAN, J., CHERTKOV, O., COUTINHO, P. M., CULLEN, D., DANCHIN, E. G. J., GRIGORIEV, I. V., HARRIS, P., JACKSON, M., KUBICEK, C. P., HAN, C. S., HO, I., LARRONDO, L. F., DE LEON, A. L., MAGNUSON, J. K., MERINO, S., MISRA, M., NELSON, B., PUTNAM, N., ROBBERTSE, B., SALAMOV, A. A., SCHMOLL, M., TERRY, A., THAYER, N., WESTERHOLM-PARVINEN, A., SCHOCH, C. L., YAO, J., BARABOTE, R., NELSON, M. A., DETTER, C., BRUCE, D., KUSKE, C. R., XIE, G., RICHARDSON, P., ROKHSAR, D. S., LUCAS, S. M., RUBIN, E. M., DUNN-COLEMAN, N., WARD, M. & BRETTIN, T. S. 2008. Genome sequencing and analysis of the biomass-degrading fungus *Trichoderma reesei* (syn. *Hypocrea jecorina*) (vol 26, pg 553, 2008). *Nature Biotechnology,* 26**,** 1193-1193.

MEDIE, F. M., DAVIES, G. J., DRANCOURT, M. & HENRISSAT, B. 2012. Genome analyses highlight the different biological roles of cellulases. *Nature Reviews Microbiology,* 10**,** 227-U.

MEKASHA, S., FORSBERG, Z., DALHUS, B., BACIK, J. P., CHOUDHARY, S., SCHMIDT-DANNERT, C., VAAJE-KOLSTAD, G. & EIJSINK, V. G. H. 2016. Structural and functional characterization of a small chitin-active lytic polysaccharide monooxygenase domain of a multi-modular chitinase from *Jonesia denitrificans*. *Febs Letters,* 590**,** 34-42.

MINKE, R. & BLACKWELL, J. 1978. Structure of Alpha-Chitin. *Journal of Molecular Biology,* 120**,** 167-181.

MITSUHASHI, W., KAWAKITA, H., MURAKAMI, R., TAKEMOTO, Y., SAIKI, T., MIYAMOTO, K. & WADA, S. 2007. Spindles of an entomopoxvirus facilitate its infection of the host insect by disrupting the peritrophic membrane. *Journal of Virology,* 81**,** 4235-4243.

MOJZSIS, S. J., ARRHENIUS, G., MCKEEGAN, K. D., HARRISON, T. M., NUTMAN, A. P. & FRIEND, C. R. 1996. Evidence for life on Earth before 3,800 million years ago. *Nature,* 384**,** 55-59.

MONREAL, J. & REESE, E. T. 1969. Chitinase of Serratia Marcescens. *Canadian Journal of Microbiology,* 15**,** 689-696.

MONZINGO, A. F., MARCOTTE, E. M., HART, P. J. & ROBERTUS, J. D. 1996. Chitinases, chitosanases, and lysozymes can be divided into procaryotic and eucaryotic families sharing a conserved core. *Nat Struct Biol,* 3**,** 133-140.

MOSER, C. C., ANDERSON, J. L. R. & DUTTON, P. L. 2010. Guidelines for tunneling in enzymes. *Biochimica Et Biophysica Acta-Bioenergetics,* 1797**,** 1573-1586.

MUZZARELLI, R. A. A., BOUDRANT, J., MEYER, D., MANNO, N., DEMARCHIS, M. & PAOLETTI, M. G. 2012. Current views on fungal chitin/chitosan, human chitinases, food preservation, glucans, pectins and inulin: A tribute to Henri

Braconnot, precursor of the carbohydrate polymers science, on the chitin bicentennial. *Carbohydrate Polymers,* 87**,** 995-1012.

MUZZARELLI, R. A. A., WECKX, M., FILIPPINI, O. & SIGON, F. 1989. Removal of Trace-Metal Ions from Industrial Waters, Nuclear Effluents and Drinking-Water, with the Aid of Cross-Linked Normal-Carboxymethyl Chitosan. *Carbohydrate Polymers,* 11**,** 293-306.

MÜLLER, G., VÁRNAI, A., JOHANSEN, K. S., EIJSINK, V. G. & HORN, S. J. 2015. Harnessing the potential of LPMO-containing cellulase cocktails poses new demands on processing conditions. *Biotechnol Biofuels,* 8**,** 187.

NAAS, A. E., MACKENZIE, A. K., MRAVEC, J., SCHUCKEL, J., WILLATS, W. G. T., EIJSINK, V. G. H. & POPE, P. B. 2014. Do Rumen Bacteroidetes Utilize an Alternative Mechanism for Cellulose Degradation? *Mbio,* 5.

NAKAGAWA, Y. S., EIJSINK, V. G. H., TOTANI, K. & VAAJE-KOSTAD, G. 2013. Conversion of alpha-Chitin Substrates with Varying Particle Size and Crystallinity Reveals Substrate Preferences of the Chitinases and Lytic Polysaccharide Monooxygenase of *Serratia marcescens*. *Journal of Agricultural and Food Chemistry,* 61**,** 11061-11066.

NAKAGAWA, Y. S., KUDO, M., LOOSE, J. S., ISHIKAWA, T., TOTANI, K., EIJSINK, V. G. & VAAJE-KOLSTAD, G. 2015. A small lytic polysaccharide monooxygenase from *Streptomyces griseus* targeting alpha- and beta-chitin. *FEBS J,* 282**,** 1065-1079.

NOWICKA, B. & KRUK, J. 2016. Powered by light: Phototrophy and photosynthesis in prokaryotes and its evolution. *Microbiol Res,* 186-187**,** 99-118.

O'SULLIVAN, A. C. 1997. Cellulose: the structure slowly unravels. *Cellulose,* 4**,** 173-207.

PARK, J. K., KEYHANI, N. O. & ROSEMAN, S. 2000. Chitin catabolism in the marine bacterium *Vibrio furnissii* - Identification, molecular cloning, and characterization of a N-N '-diacetylchitobiose phosphorylase. *Journal of Biological Chemistry,* 275**,** 33077-33083.

PASPALIARI, D. K., LOOSE, J. S., LARSEN, M. H. & VAAJE-KOLSTAD, G. 2015. *Listeria monocytogenes* has a functional chitinolytic system and an active lytic polysaccharide monooxygenase. *FEBS J,* 282**,** 921-936.

PEISACH, J. & BLUMBERG, W. E. 1974. Structural Implications Derived from Analysis of Electron-Paramagnetic Resonance-Spectra of Natural and Artificial Copper Proteins. *Archives of Biochemistry and Biophysics,* 165**,** 691-708.

PETERSON, R. W. & WALTON, J. H. 1943. The Autoxidation of Ascorbic Acid1. *Journal of the American Chemical Society,* 65**,** 1212-1217.

PHILLIPS, C. M., BEESON, W. T., CATE, J. H. & MARLETTA, M. A. 2011a. Cellobiose dehydrogenase and a copper-dependent polysaccharide monooxygenase potentiate cellulose degradation by *Neurospora crassa*. *ACS Chem. Biol.,* 6**,** 1399-1406.

PHILLIPS, C. M., IAVARONE, A. T. & MARLETTA, M. A. 2011b. Quantitative proteomic approach for cellulose degradation by *Neurospora crassa*. *J. Proteome Res.,* 10**,** 4177-4185.

POPE, P. B., MACKENZIE, A. K., GREGOR, I., SMITH, W., SUNDSET, M. A., MCHARDY, A. C., MORRISON, M. & EIJSINK, V. G. 2012. Metagenomics of the Svalbard reindeer rumen microbiome reveals abundance of polysaccharide utilization loci. *PLoS One,* 7**,** e38571.

PRICELIUS, S., LUDWIG, R., LANT, N., HALTRICH, D. & GUEBITZ, G. M. 2009. Substrate specificity of *Myriococcum thermophilum* cellobiose dehydrogenase on mono-, oligo-, and polysaccharides related to in situ production of H2O2. *Appl Microbiol Biotechnol,* 85**,** 75-83.

PRUZZO, C., VEZZULLI, L. & COLWELL, R. R. 2008. Global impact of *Vibrio cholerae* interactions with chitin. *Environ Microbiol,* 10**,** 1400-10.

QUINLAN, R. J., SWEENEY, M. D., LO LEGGIO, L., OTTEN, H., POULSEN, J. C., JOHANSEN, K. S., KROGH, K. B., JØRGENSEN, C. I., TOVBORG, M., ANTHONSEN, A., TRYFONA, T., WALTER, C. P., DUPREE, P., XU, F., DAVIES, G. J. & WALTON, P. H. 2011. Insights into the oxidative degradation of cellulose by a copper metalloenzyme that exploits biomass components. *Proc. Natl. Acad. Sci. U.S.A.,* 108**,** 15079-15084.

REESE, E. T., SIU, R. G. & LEVINSON, H. S. 1950. The biological degradation of soluble cellulose derivatives and its relationship to the mechanism of cellulose hydrolysis. *J Bacteriol,* 59**,** 485-497.

REGUERA, G. & LESCHINE, S. B. 2001. Chitin degradation by cellulolytic anaerobes and facultative aerobes from soils and sediments. *FEMS Microbiol Lett,* 204**,** 367-374.

RINAUDO, M. 2006. Chitin and chitosan: Properties and applications. *Progress in Polymer Science,* 31**,** 603-632.

RUSSELL, J. B., MUCK, R. E. & WEIMER, P. J. 2009. Quantitative analysis of cellulose degradation and growth of cellulolytic bacteria in the rumen. *FEMS Microbiol Ecol,* 67**,** 183-197.

RYE, C. S. & WITHERS, S. G. 2000. Glycosidase mechanisms. *Current Opinion in Chemical Biology,* 4**,** 573-580.

SAITO, A., MIYASHITA, K., BIUKOVIC, G. & SCHREMPF, H. 2001. Characteristics of a *Streptomyces coelicolor* A3(2) extracellular protein targeting chitin and chitosan. *Appl Environ Microbiol,* 67**,** 1268-1273.

SAITO, Y., OKANO, T., GAILL, F., CHANZY, H. & PUTAUX, J. L. 2000. Structural data on the intra-crystalline swelling of beta-chitin. *Int J Biol Macromol,* 28**,** 81-8.

SALOHEIMO, M., NAKARI-SETALA, T., TENKANEN, M. & PENTTILA, M. 1997. cDNA cloning of a *Trichoderma reesei* cellulase and demonstration of endoglucanase activity by expression in yeast. *Eur J Biochem,* 249**,** 584-591.

SCHNELLMANN, J., ZELTINS, A., BLAAK, H. & SCHREMPF, H. 1994. The novel lectin-like protein CHB1 is encoded by a chitin-inducible *Streptomyces olivaceoviridis* gene and binds specifically to crystalline alpha-chitin of fungi and other organisms. *Mol Microbiol,* 13**,** 807-819.

SCHREMPF, H. 2001. Recognition and degradation of chitin by Streptomycetes. *Antonie Van Leeuwenhoek,* 79**,** 285-289.

SCHUSTER, A. & SCHMOLL, M. 2010. Biology and biotechnology of Trichoderma. *Applied Microbiology and Biotechnology,* 87**,** 787-799.

SCOTT, B. R., HUANG, H. Z., FRICKMAN, J., HALVORSEN, R. & JOHANSEN, K. S. 2015. Catalase improves saccharification of lignocellulose by reducing lytic polysaccharide monooxygenase-associated enzyme inactivation. *Biotechnol. Lett.,* 38**,** 425-434.

SHALLOM, D. & SHOHAM, Y. 2003. Microbial hemicellulases. *Current Opinion in Microbiology,* 6**,** 219-228.

SHOHAM, Y., LAMED, R. & BAYER, E. A. 1999. The cellulosome concept as an efficient microbial strategy for the degradation of insoluble polysaccharides. *Trends in Microbiology,* 7**,** 275-281.

SINNOTT, M. L. 1990. Catalytic Mechanisms of Enzymatic Glycosyl Transfer. *Chemical Reviews,* 90**,** 1171-1202.

STAUDER, M., HUQ, A., PEZZATI, E., GRIM, C. J., RAMOINO, P., PANE, L., COLWELL, R. R., PRUZZO, C. & VEZZULLI, L. 2012. Role of GbpA protein, an

important virulence-related colonization factor, for *Vibrio cholerae*'s survival in the aquatic environment. *Environ Microbiol Rep,* 4**,** 439-445.

SUNNA, A., GIBBS, M. D., CHIN, C. W., NELSON, P. J. & BERGQUIST, P. L. 2000. A gene encoding a novel multidomain beta-1,4-mannanase from *Caldibacillus cellulovorans* and action of the recombinant enzyme on kraft pulp. *Appl Environ Microbiol,* 66**,** 664-670.

SUZUKI, K., SUGAWARA, N., SUZUKI, M., UCHIYAMA, T., KATOUNO, F., NIKAIDOU, N. & WATANABE, T. 2002. Chitinases A, B, and C1 of *Serratia marcescens* 2170 produced by recombinant *Escherichia coli*: Enzymatic properties and synergism on chitin degradation. *Bioscience Biotechnology and Biochemistry,* 66**,** 1075-1083.

SUZUKI, K., SUZUKI, M., TAIYOJI, M., NIKAIDOU, N. & WATANABE, T. 1998. Chitin binding protein (CBP21) in the culture supernatant of *Serratia marcescens* 2170. *Biosci Biotechnol Biochem,* 62**,** 128-135.

TAKASUKA, T. E., BOOK, A. J., LEWIN, G. R., CURRIE, C. R. & FOX, B. G. 2013. Aerobic deconstruction of cellulosic biomass by an insect-associated Streptomyces. *Scientific Reports,* 3.

TAKEMOTO, Y., MITSUHASHI, W., MURAKAMI, R., KONISHI, H. & MIYAMOTO, K. 2008. The N-Terminal Region of an Entomopoxvirus Fusolin Is Essential for the Enhancement of Peroral Infection, whereas the C-Terminal Region Is Eliminated in Digestive Juice. *Journal of Virology,* 82**,** 12406-12415.

TAN, T. C., KRACHER, D., GANDINI, R., SYGMUND, C., KITTL, R., HALTRICH, D., HALLBERG, B. M., LUDWIG, R. & DIVNE, C. 2015. Structural basis for cellobiose dehydrogenase action during oxidative cellulose degradation. *Nat. Commun.,* 6**,** 7542.

TEWS, I., PERRAKIS, A., OPPENHEIM, A., DAUTER, Z., WILSON, K. S. & VORGIAS, C. E. 1996. Bacterial chitobiase structure provides insight into catalytic mechanism and the basis of Tay-Sachs disease. *Nature Structural Biology,* 3**,** 638-648.

TEWS, I., TERWISSCHA VAN SCHELTINGA, A. C., PERRAKIS, A., WILSON, K. S. & DIJKSTRA, B. W. 1997. Substrate-assisted catalysis unifies two families of chitinolytic enzymes. *Journal of the American Chemical Society,* 119**,** 7954-7959.

THARANATHAN, R. N. & KITTUR, F. S. 2003. Chitin--the undisputed biomolecule of great potential. *Crit Rev Food Sci Nutr,* 43**,** 61-87.

TICE, M. M. & LOWE, D. R. 2006. Hydrogen-based carbon fixation in the earliest known photosynthetic organisms. *Geology,* 34**,** 37-40.

TORATANI, T., SHOJI, T., IKEHARA, T., SUZUKI, K. & WATANABE, T. 2008. The importance of chitobiase and N-acetylglucosamine (GlcNAc) uptake in N,N '-diacetylchitoblose [(GlcNAC)(2)] utilization by *Serratia marcescens* 2170. *Microbiology-Sgm,* 154**,** 1326-1332.

TUVENG, T. R., ARNTZEN, M. Ø., BENGTSSON, O., GARDNER, J. G., VAAJE-KOLSTAD, G. & EIJSINK, V. G. 2016. Proteomic investigation of the secretome of *Cellvibrio japonicus* during growth on chitin. *Proteomics***,** 1904-1914.

VAAJE-KOLSTAD, G., BØHLE, L. A., GÅSEIDNES, S., DALHUS, B., BJØRÅS, M., MATHIESEN, G. & EIJSINK, V. G. 2012. Characterization of the chitinolytic machinery of *Enterococcus faecalis* V583 and high-resolution structure of its oxidative CBM33 enzyme. *J Mol Biol,* 416**,** 239-254.

VAAJE-KOLSTAD, G., HORN, S. J., SØRLIE, M. & EIJSINK, V. G. 2013. The chitinolytic machinery of *Serratia marcescens*-a model system for enzymatic degradation of recalcitrant polysaccharides. *FEBS J,* 280**,** 3028-3049.

VAAJE-KOLSTAD, G., HORN, S. J., VAN AALTEN, D. M., SYNSTAD, B. & EIJSINK, V. G. 2005a. The non-catalytic chitin-binding protein CBP21 from *Serratia marcescens* is essential for chitin degradation. *J. Biol. Chem.,* 280**,** 28492-28497.

VAAJE-KOLSTAD, G., HOUSTON, D. R., RIEMEN, A. H., EIJSINK, V. G. H. & VAN AALTEN, D. M. 2005b. Crystal structure and binding properties of the *Serratia marcescens* chitin-binding protein CBP21. *J. Biol. Chem.,* 280**,** 11313-11319.

VAAJE-KOLSTAD, G., WESTERENG, B., HORN, S. J., LIU, Z., ZHAI, H., SØRLIE, M. & EIJSINK, V. G. H. 2010. An oxidative enzyme boosting the enzymatic conversion of recalcitrant polysaccharides. *Science,* 330**,** 219-222.

VAN AALTEN, D. M. F., KOMANDER, D., SYNSTAD, B., GASEIDNES, S., PETER, M. G. & EIJSINK, V. G. H. 2001. Structural insights into the catalytic mechanism of a family 18 exo-chitinase. *Proceedings of the National Academy of Sciences of the United States of America,* 98**,** 8979-8984.

VÁRNAI, A., SIIKA-AHO, M. & VIIKARI, L. 2013. Carbohydrate-binding modules (CBMs) revisited: reduced amount of water counterbalances the need for CBMs. *Biotechnol Biofuels,* 6**,** 30.

VEBØ, H. C., SNIPEN, L., NES, I. F. & BREDE, D. A. 2009. The Transcriptome of the Nosocomial Pathogen *Enterococcus faecalis* V583 Reveals Adaptive Responses to Growth in Blood. *Plos One,* 4**,** e7660.

VEBØ, H. C., SOLHEIM, M., SNIPEN, L., NES, I. F. & BREDE, D. A. 2010. Comparative genomic analysis of pathogenic and probiotic Enterococcus faecalis isolates, and their transcriptional responses to growth in human urine. *PLoS One,* 5**,** e12489.

VEZZULLI, L., GUZMAN, C. A., COLWELL, R. R. & PRUZZO, C. 2008. Dual role colonization factors connecting *Vibrio cholerae*'s lifestyles in human and aquatic environments open new perspectives for combating infectious diseases. *Curr Opin Biotechnol,* 19**,** 254-259.

VU, V. V., BEESON, W. T., PHILLIPS, C. M., CATE, J. H. & MARLETTA, M. A. 2014a. Determinants of regioselective hydroxylation in the fungal polysaccharide monooxygenases. *J Am Chem Soc,* 136**,** 562-565.

VU, V. V., BEESON, W. T., SPAN, E. A., FARQUHAR, E. R. & MARLETTA, M. A. 2014b. A family of starch-active polysaccharide monooxygenases. *Proc Natl Acad Sci U S A,* 111**,** 13822-13827.

WALCZAK, M. M., DRYER, D. A., JACOBSON, D. D., FOSS, M. G. & FLYNN, N. T. 1997. pH-dependent redox couple: Illustrating the Nernst equation using cyclic voltammetry. *Journal of Chemical Education,* 74**,** 1195-1197.

WALTON, P. H. & DAVIES, G. J. 2016. On the catalytic mechanisms of lytic polysaccharide monooxygenases. *Curr Opin Chem Biol,* 31**,** 195-207.

WARNECKE, F., LUGINBUHL, P., IVANOVA, N., GHASSEMIAN, M., RICHARDSON, T. H., STEGE, J. T., CAYOUETTE, M., MCHARDY, A. C., DJORDJEVIC, G., ABOUSHADI, N., SOREK, R., TRINGE, S. G., PODAR, M., MARTIN, H. G., KUNIN, V., DALEVI, D., MADEJSKA, J., KIRTON, E., PLATT, D., SZETO, E., SALAMOV, A., BARRY, K., MIKHAILOVA, N., KYRPIDES, N. C., MATSON, E. G., OTTESEN, E. A., ZHANG, X., HERNANDEZ, M., MURILLO, C., ACOSTA, L. G., RIGOUTSOS, I., TAMAYO, G., GREEN, B. D., CHANG, C., RUBIN, E. M., MATHUR, E. J., ROBERTSON, D. E., HUGENHOLTZ, P. & LEADBETTER, J. R. 2007. Metagenomic and functional analysis of hindgut microbiota of a wood-feeding higher termite. *Nature,* 450**,** 560-565.

WEISSBERGER, A., LUVALLE, J. E. & THOMAS, D. S. 1943. Oxidation Processes. XVI.1 The Autoxidation of Ascorbic Acid. *Journal of the American Chemical Society,* 65**,** 1934-1939.

WESTERENG, B., ARNTZEN, M. O., AACHMANN, F. L., VARNAI, A., EIJSINK, V. G. H. & AGGER, J. W. 2016a. Simultaneous analysis of C1 and C4 oxidized oligosaccharides, the products of lytic polysaccharide monooxygenases acting on cellulose. *Journal of Chromatography A,* 1445**,** 46-54.

WESTERENG, B., ARNTZEN, M. Ø., AGGER, J. W., VAAJE-KOLSTAD, G. & EIJSINK, V. G. H. 2016b. Analyzing activities of lytic polysaccharide monooxygenases by liquid chromatography and mass spectrometry. *In press*.

WESTERENG, B., CANNELLA, D., AGGER, J. W., JØRGENSEN, H., ANDERSEN, M. L., EIJSINK, V. G. H. & FELBY, C. 2015. Enzymatic cellulose oxidation is linked to lignin by long-range electron transfer. *Sci. Rep.,* 5**,** 18561.

WESTERENG, B., ISHIDA, T., VAAJE-KOLSTAD, G., WU, M., EIJSINK, V. G. H., IGARASHI, K., SAMEJIMA, M., STAHLBERG, J., HORN, S. J. & SANDGREN, M. 2011. The Putative Endoglucanase PcGH61D from *Phanerochaete chrysosporium* Is a Metal-Dependent Oxidative Enzyme that Cleaves Cellulose. *Plos One,* 6**,** e27807.

WILSON, D. B. 2011. Microbial diversity of cellulose hydrolysis. *Curr Opin Microbiol,* 14**,** 259-263.

WOLFENDEN, R., LU, X. D. & YOUNG, G. 1998. Spontaneous hydrolysis of glycosides. *Journal of the American Chemical Society,* 120**,** 6814-6815.

WONG, E., VAAJE-KOLSTAD, G., GHOSH, A., HURTADO-GUERRERO, R., KONAREV, P. V., IBRAHIM, A. F., SVERGUN, D. I., EIJSINK, V. G., CHATTERJEE, N. S. & VAN AALTEN, D. M. 2012. The *Vibrio cholerae* colonization factor GbpA possesses a modular structure that governs binding to different host surfaces. *PLoS Pathog,* 8**,** e1002373.

WU, M., BECKHAM, G. T., LARSSON, A. M., ISHIDA, T., KIM, S., PAYNE, C. M., HIMMEL, M. E., CROWLEY, M. F., HORN, S. J., WESTERENG, B., IGARASHI, K., SAMEJIMA, M., STÅHLBERG, J., EIJSINK, V. G. H. & SANDGREN, M. 2013. Crystal Structure and Computational Characterization of the Lytic Polysaccharide Monooxygenase GH61D from the Basidiomycota Fungus *Phanerochaete chrysosporium*. *Journal of Biological Chemistry,* 288**,** 12828-12839.

WYMELENBERG, A. V., GASKELL, J., MOZUCH, M., SABAT, G., RALPH, J., SKYBA, O., MANSFIELD, S. D., BLANCHETTE, R. A., MARTINEZ, D., GRIGORIEV, I., KERSTEN, P. J. & CULLEN, D. 2010. Comparative transcriptome and secretome analysis of wood decay fungi *Postia placenta* and *Phanerochaete chrysosporium*. *Appl. Environ. Microbiol.,* 76**,** 3599-3610.

YAKOVLEV, I., VAAJE-KOLSTAD, G., HIETALA, A. M., STEFANCZYK, E., SOLHEIM, H. & FOSSDAL, C. G. 2012. Substrate-specific transcription of the enigmatic GH61 family of the pathogenic white-rot fungus *Heterobasidion irregulare* during growth on lignocellulose. *Appl. Microbiol. Biotechnol.,* 95**,** 979-990.

ZELTINS, A. & SCHREMPF, H. 1997. Specific interaction of the Streptomyces chitin-binding protein CHB1 with alpha-chitin--the role of individual tryptophan residues. *Eur J Biochem,* 246**,** 557-564.

ZHU, L., WU, Q., DAI, J., ZHANG, S. & WEI, F. 2011. Evidence of cellulose metabolism by the giant panda gut microbiome. *Proc Natl Acad Sci U S A,* 108**,** 17714-17719.

ZOBELL, C. E. & RITTENBERG, S. C. 1938. The Occurrence and Characteristics of Chitinoclastic Bacteria in the Sea. *J Bacteriol,* 35**,** 275-287.

Paper I

A rapid quantitative activity assay shows that the *Vibrio cholerae* colonization factor GbpA is an active lytic polysaccharide monooxygenase

Jennifer S.M. Loose, Zarah Forsberg, Marco W. Fraaije, Vincent G.H. Eijsink, Gustav Vaaje-Kolstad, 2014, *FEBS Lett.,* 588**,** 3435-3440.

FEBS Letters 588 (2014) 3435–3440

journal homepage: www.FEBSLetters.org

A rapid quantitative activity assay shows that the *Vibrio cholerae* colonization factor GbpA is an active lytic polysaccharide monooxygenase

Jennifer S.M. Loose [a], Zarah Forsberg [a], Marco W. Fraaije [b], Vincent G.H. Eijsink [a], Gustav Vaaje-Kolstad [a,*]

[a] Department of Chemistry, Biotechnology and Food Science, Norwegian University of Life Sciences, P.O. Box 5003, N-1432 Aas, Norway
[b] Molecular Enzymology Group, Groningen Biomolecular Sciences and Biotechnology Institute, University of Groningen, Nijenborgh 4, Groningen, The Netherlands

ARTICLE INFO

Article history:
Received 27 June 2014
Revised 30 July 2014
Accepted 30 July 2014
Available online 7 August 2014

Edited by Stuart Ferguson

Keywords:
Lytic polysaccharide monooxygenase
AA10
AA9
AA11
GbpA
Colonization factor
Vibrio cholerae

ABSTRACT

The discovery of the copper-dependent lytic polysaccharide monooxygenases (LPMOs) has revealed new territory for chemical and biochemical analysis. These unique mononuclear copper enzymes are abundant, suggesting functional diversity beyond their established roles in the depolymerization of biomass polysaccharides. At the same time basic biochemical methods for characterizing LPMOs, such as activity assays are not well developed. Here we describe a method for quantification of C1-oxidized chitooligosaccharides (aldonic acids), and hence LPMO activity. The method was used to quantify the activity of a four-domain LPMO from *Vibrio cholerae*, GbpA, which is a virulence factor with no obvious role in biomass processing.

1. Introduction

An important development in the field of carbohydrate-active enzymes is the identification of the lytic polysaccharide monooxygenases (LPMOs). These proteins are copper-dependent metalloenzymes that cleave the β-1,4 glycosidic bonds of polysaccharides by an oxidative mechanism. LPMOs are currently classified in families 9, 10 and 11 of the auxiliary activities (AAs) in the Carbohydrate Active Enzyme database (CAZy; [1]). AA9-type and AA11-type LPMOs are found exclusively in fungi. The AA10 family is dominated by bacterial enzymes, but also contains members from eukaryotic organisms and viruses.

The conserved active site property that unifies the three LPMO families is the copper binding site. One copper atom is coordinated by three nitrogen ligands provided by two histidine imidazoles and the N-terminal amino group in a T-shaped histidine brace arrangement [2–5]. The reaction mechanism employed by LPMOs involves reduction of the active site copper by an externally provided electron and subsequent activation of dioxygen. This enables hydrogen abstraction and subsequent hydroxylation of either the C1 or C4 glycosidic carbon, resulting in bond cleavage and a monooxygenated product (Fig. 1; [2,6–9]). Notably, both types of oxidations have been observed for LPMOs acting on cellulose, whereas for chitin-active LPMOs only C1 oxidation has been described. The steps of the catalytic itinerary are yet to be verified experimentally, but have been analyzed for AA9-type LPMOs by density functional theory calculations [10,11].

So far, only LPMOs related to biomass degradative systems have been characterized. Interestingly, several pathogenic bacteria produce AA-10 type LPMO domains, which have been identified as virulence factors [12]. One prominent example is the *Vibrio cholerae* colonization factor GbpA, which is thought to enable *V. cholerae* to attach to both aquatic transfer vectors and the epithelial cell surfaces of the host [13–16]. GbpA is a four-domain protein with an N-terminal LPMO10 domain, two domains putatively involved in bacterial cell surface binding and a C-terminal chitin binding domain [15]. GbpA has been thought to passively mediate

Abbreviations: COAA, chitooligosaccharide aldonic acid; ChitO, chitooligosaccharide oxidase; DP, degree of polymerization; HILIC, hydrophilic interaction chromatography; LPMO, lytic polysaccharide monooxygenase; AA, auxiliary activities; ACN, acetonitrile

* Corresponding author.
E-mail address: gustko@nmbu.no (G. Vaaje-Kolstad).

http://dx.doi.org/10.1016/j.febslet.2014.07.036
0014-5793/

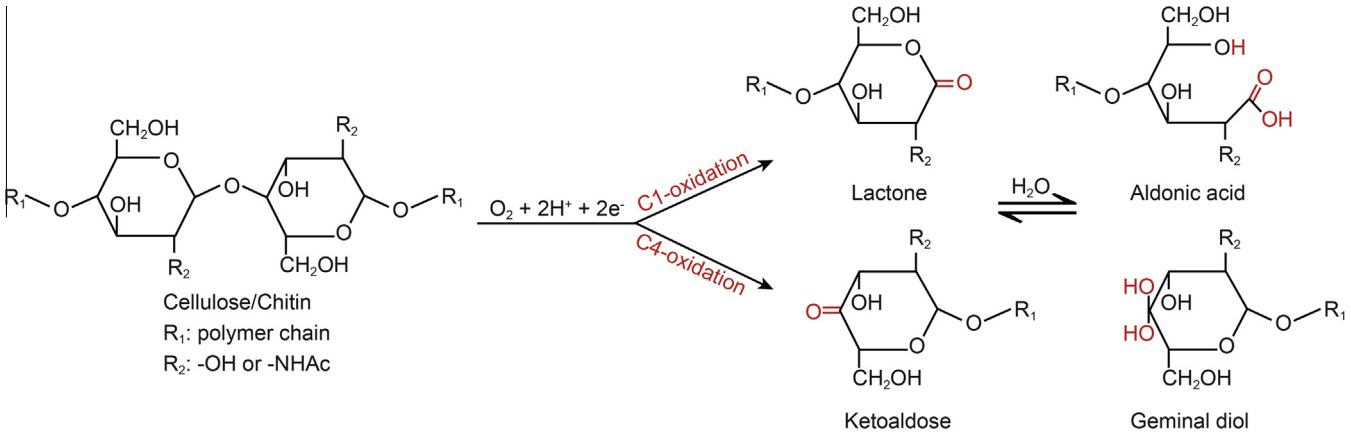

Fig. 1. LPMO reaction scheme. Oxidative cleavage of glycosidic bonds in cellulose or chitin by LPMOs results in oxidation of the C1 or C4 carbon. The products resulting from C1 or C4 oxidation (δ-1,5-lactone or 4-ketoaldose, respectively) are in pH-dependent equilibrium with their respective hydrates (aldonic acid or geminal diol, respectively). It should be noted that oxidation of the C4 carbon has only been observed experimentally for cellulose-cleaving LPMOs.

attachment of *V. cholerae* to chitin and mucin glycans, but the presence of a putatively active LPMO suggests a more active role of this protein in virulence. Notably, GbpA-like proteins occur in several other pathogenic bacteria, such as *Listeria monocytogenes*, *Bacillus cereus* and *Yersinia pestis*.

Analysis of LPMO activity is challenging, even at the qualitative level, due to the complexity of the products, autoxidation of reactants, lack of commercially available standards, the insolubility of the substrate, and complicated analytical methods. Kittl et al. described an appealing fluorimetric method based on quantification of H_2O_2 resulting from futile cycling by the LPMO [17]. However, this method cannot be used to determine substrate cleaving rates of LPMOs. Our own unpublished attempts to develop a reliable assay have yielded several failures and literature is almost devoid of quantitative data for LPMO activity. In this study we have developed a method for rapid and reproducible quantitative analysis of LPMO activity towards chitin, based on careful copper saturation of the enzyme combined with use of a fast chromatographic method. Using this method, we show that GbpA possesses LPMO activity, thus providing evidence of LPMO activity in a virulence factor not obviously involved in conversion of chitin or other biomass polysaccharides.

2. Materials and methods

2.1. Cloning, protein expression and purification

Chromosomal DNA from *Serratia marcescens* BJL200 was extracted and purified from cells using the E.Z.N.A Bacterial DNA kit (Omega Bio-Tek) and subsequently used for cloning the gene encoding the *S. marcescens* GH20 β-*N*-acetylhexosaminidase, chitobiase (*chb*; Genebank ID: L43594). Amplification of the *chb* gene was achieved by PCR, using primers enabling ligation independent cloning (LIC) using the pET30 Xa/LIC vector kit (Merck-Millipore; forward primer: 5′GGTATTGAGGGTCGCGATCAACAGCTGGT3′, reverse primer: 5′AGAGGAGAGTTAGAGCCCTAGACCTTCTCGGC3′). The PCR product was inserted into the pET30-Xa/LIC vector according to the instructions provided by the supplier, yielding a construct named pET-30Xa/LIC-*chb*, which upon expression will yield recombinant chitobiase containing an N-terminal hexa-histidine tag. The vector was propagated in *Escherichia coli* BL21 star (DE3) (LB medium; 100 μg/mL kanamycin). The sequence of the inserted PCR product was verified by DNA sequencing using the Eurofins sequencing service (Eurofins-MWG). For protein production cells were cultured at 37 °C until OD_{600} = 0.5, followed by induction with 0.1 mM IPTG and incubation at 30 °C for 3 h with shaking at 200 rpm. The culture was harvested by centrifugation at 7741*g* and resuspended in lysis/binding buffer (20 mM Tris–HCl pH 8.0, 20 mM imidazole) followed by cell disruption by sonication using a Vibra cell Ultrasonic Processor (Sonics). The disruption procedure was carried out by applying a cycle of 5 s sonication and 5 s pause for 4 min using 30% amplitude. The sample was kept on ice throughout the sonication procedure. Cell debris was removed by centrifugation at 7741*g* and the crude extract was finally passed through a 0.2 μm filter using a syringe. The protein was then purified by immobilized metal ion chromatography using a Bio-Rad Econo column containing 10 mL Ni-NTA Agarose resin (Qiagen) equilibrated with 20 mM Tris-HCl pH 8.0, 20 mM imidazole, operated by a BioLogic low-pressure protein purification system (BioRad). The protein extract was applied at a flow of 1.0 mL/min and unbound protein was discarded. Elution of bound protein (chitobiase) was accomplished by changing the eluent to 20 mM Tris–HCl pH 8.0, 500 mM imidazole. The eluted protein was concentrated and subjected to buffer exchange (to 20 mM Tris–HCl pH 8.0) using Amicon Ultra centrifugal filters (Millipore) with a 10 kDa cutoff.

Chitooligosaccharide oxidase (ChitO) N-terminally fused to maltose binding protein encoded by the pBAD-MBP-*chitO* expression vector was expressed and purified as described previously [18,19], with minor modifications. Briefly, LB medium supplemented with 50 μg/mL ampicillin, 15 μg/mL kanamycin, 12.5 μg/mL tetracyclin and 0.4% (w/v) arabinose was inoculated with BL21 star cells containing pBAD-MBP-*chitO*. After 70 h at 17 °C, the cells were harvested by centrifugation at 7741*g*, resuspended in lysis/binding buffer (50 mM potassium phosphate buffer, pH7.6, 10% glycerol) and disrupted by sonication as described above. The extract was cleared by centrifugation at 7741*g* and sterile filtered through a 0.2 μm filter using a syringe. The fusion protein (henceforth referred to as ChitO) was purified by a two-step procedure involving ion exchange and gel filtration chromatography. Firstly, the protein extract was loaded onto a 5 mL DEAE Sepharose FF anion exchange column (GE Healthcare) with a flow rate of 0.8 mL/min using an Äkta purifier chromatography system (GE Healthcare). Application of a 120 min linear NaCl gradient (0–1.0 M) eluted the protein bound to the column material. Fractions containing ChitO (assessed by SDS–PAGE) were pooled and concentrated using Amicon Ultra centrifugal filters (Millipore) with 10 kDa cutoff. Impurities in the ChitO concentrate were removed by gel filtration using an Äkta purifier chromatography system operating a HiLoad 16/60 Superdex 75 size exclusion column (GE Healthcare). The flow rate was set to 0.7 mL/min and

the eluent used was 20 mM Tris–HCl pH 8.0. Fractions containing pure ChitO (assessed by SDS–PAGE) were pooled and concentrated using Amicon Ultra centrifugal filters (Millipore) with 10 kDa cut-off, adjusted to 10% glycerol (v/v) and stored at −20 °C until use.

GbpA, in its native form, was expressed in BL21 star (DE3) cells containing the pET22b vector encoding *gbpA* as previously reported by Wong et al. [15].

Protein concentrations were determined using the BioRad protein assay for chitobiase and ChitO, using BSA as a standard, and by absorbance at A280 for GbpA, using the theoretical extinction coefficient (http://web.expasy.org/protparam/).

2.2. Cu(II) saturation and desalting of GbpA

GbpA was saturated with copper ($Cu(II)SO_4$) by incubating a 5.0 mg/mL solution of pure GbpA in 20 mM Tris–HCl pH 8.0 with a 3-fold molar excess of $Cu(II)SO_4$ for 30 min at room temperature. Excess copper was removed by passing 1 mL of the enzyme solution through a PD MidiTrap G-25 (GE Healthcare) desalting column pre-equilibrated with 20 mM Tris–HCl pH 8.0. To ensure no free copper was included in the desalted protein, only the first mL eluting from the column was used for further work. The protein solution was stored at 4 °C until further use. If stored for more than 2 weeks, the copper saturation procedure was repeated before use of the enzyme. The procedure was carried out at room temperature using gravity flow.

2.3. Preparation of β-chitin nano-fibers

Beta-chitin was purchased from France Chitin (Orange, France). The β-chitin nanofibers were produced according to the protocol described by Fan et al. [20]. In short, 100 mg β-chitin (France Chitin, Orange, France) was suspended in 10 mL 1.8 mM acetic acid and sonicated at 27% amplitude for 4 min, using a Vibra Cell Ultrasonic Processor (Sonics). The substrate was stored at 4 °C until use.

2.4. LPMO activity assay

LPMO activity was assayed by incubating 5 mg/mL β-chitin nanofibers with 2.0 μM LPMO in 500 μL reactions buffered by 50 mM Bis–Tris–HCl pH 6.8 in the presence of 1.0 mM ascorbate. Reactions were incubated at 37 °C in an Eppendorf Comfort Thermomixer with a thermostated lid, at 800 rpm. 50 μL samples were taken with 5 min intervals and immediately filtered using a 96-well filter plate (Millipore) operated by a Millipore vacuum manifold, to separate insoluble substrate particles from the soluble products and to stop the reaction (activity of GbpA towards soluble chitooligosaccharides could not be detected; results not shown). At this stage, reaction products were either analyzed directly by MALDI-TOF MS and UPLC (see below) or further degraded by chitobiase for minimizing product complexity. The latter procedure was accomplished by adding chitobiase to a final concentration of 2.0 μM, followed by incubation at 37 °C for 2 h. The resulting products were then analyzed and quantified by UPLC.

2.5. Preparation of aldonic acid standards

N-acetyl-chitooligosaccharides (Megazyme; 95% purity) with a degree of polymerization (DP) ranging from 1 to 6 were dissolved to a final concentration of 3.0 mM in 50 mM Tris–HCl pH 8.0 and incubated overnight with 0.12 mg/mL ChitO at 20 °C. The resulting chitooligosaccharide aldonic acids [COAAs; $(GlcNAc)_{1-5}GlcNAc1A$] and GlcNAc1A were verified by UPLC and MALDI-TOF MS as described by Vaaje-Kolstad et al. [9]. The UPLC method used applied a slightly modified gradient in order to enable separation and identification of GlcNAc1A in addition to $(GlcNAc)_{1-5}$GlcNAc1A; 80% ACN (A): 20% 15 mM Tris–HCl pH 8.0 (B) was run for 3.5 min, followed by a 5.5 min gradient to 70% A: 30% B and a 0.5 min gradient to 55% A: 45% B. The latter condition was held for 1 min, followed by column reconditioning obtained by a 1 min gradient back to initial conditions (80% A: 20% B) and subsequent running at these conditions for 4 min.

2.6. Quantitative analysis of GlcNAcGlcNAc1A

Rapid quantitative analysis of GlcNAcGlcNAc1A was carried out using a short hydrophilic interaction chromatography (HILIC) column (Acquity UPLC BEH Amide, 50 mm) and a novel running protocol. The sample injection volume was 7.0 μL and the flow rate 0.4 mL/min. The gradient was as follows: 78% ACN (A): 22% 15 mM Tris–HCl pH 8.0 (B) held for 4 min, followed by a 1 min gradient to 62% A: 38% B. Column reconditioning was obtained by a 1 min gradient back to initial conditions (78% A: 22% B) and subsequently running at these conditions for 1 min. Products were detected by monitoring absorbance at either 195 nm, for qualitative analysis of all products, or 205 nm, for quantitative analysis of GlcNAcGlcNAc1A only. At 205 nm signals generally get smaller, and information is lost, but the signal-to-noise ratio near the GlcNAcGlcNAc1A peak is better and peak integration is more accurate.

3. Results and discussion

So far, analysis of LPMO activity has been limited to qualitative approaches, with a few exceptions. Vaaje-Kolstad et al. determined an initial rate of $\sim 1\ min^{-1}$ for CBP21, a chitin active LPMO10, using a multi-step assay involving several enzymes [9]. Agger et al. reported initial rates ranging from $1.8\ min^{-1}$ to $6.6\ min^{-1}$ for an LPMO9 acting on various plant cell wall polysaccharides, exploiting the ability of this LPMO to act on soluble substrates [21], an ability that has never been observed for chitin-active LPMOs. In both these cases the enzyme was used "as is", meaning that the degree of copper saturation was not controlled. In the present study, we have used a simple approach based on quantifying COAAs, with well controlled copper saturation of the enzyme. The approach used in this study was based on quantifying COAAs. Since COAAs are not commercially available, standards must be generated in-house by either chemical or enzymatic means. Conveniently, Heuts et al. 6 years ago reported characterization of an enzyme (chitooligosaccharide oxidase; ChitO) that regioselectively oxidizes the reducing end C1 carbon of chitooligosaccharides, yielding COAAs [18]. By incubating ChitO with native chitooligosaccharides, COAAs could be generated with near 100% efficiency (Fig. 2). It must be noted that it is critical to perform sample separation and analysis at pH 8.0, since the aldonic acid/lactone equilibrium is driven far towards the aldonic acid form at this pH. Lactones are not observed at pH 8.0, as demonstrated by MALDI-TOF MS (Fig. 3; [9]), and thus do not need to be considered.

The chromatographic method for separating COAAs published by Vaaje-Kolstad et al. is able to provide base line separation of COAAs having up to eight sugar units (DP8), meaning that not all soluble products can be quantified by the existing UPLC method. Furthermore, a search for rapid variants of this method, using a shorter column (see Section 2) showed that the best solution, reducing the run time from 26 min to 7 min, only was able to resolve the chitobionic acid, whereas all other COAAs appeared in a part of the chromatogram that is less well resolved (Fig. 3A). In order to obtain a simpler product mixture only comprising GlcNAc and chitobionic acid, chitobiase, a family 20 *N*-acetylhexosaminidase, was used to

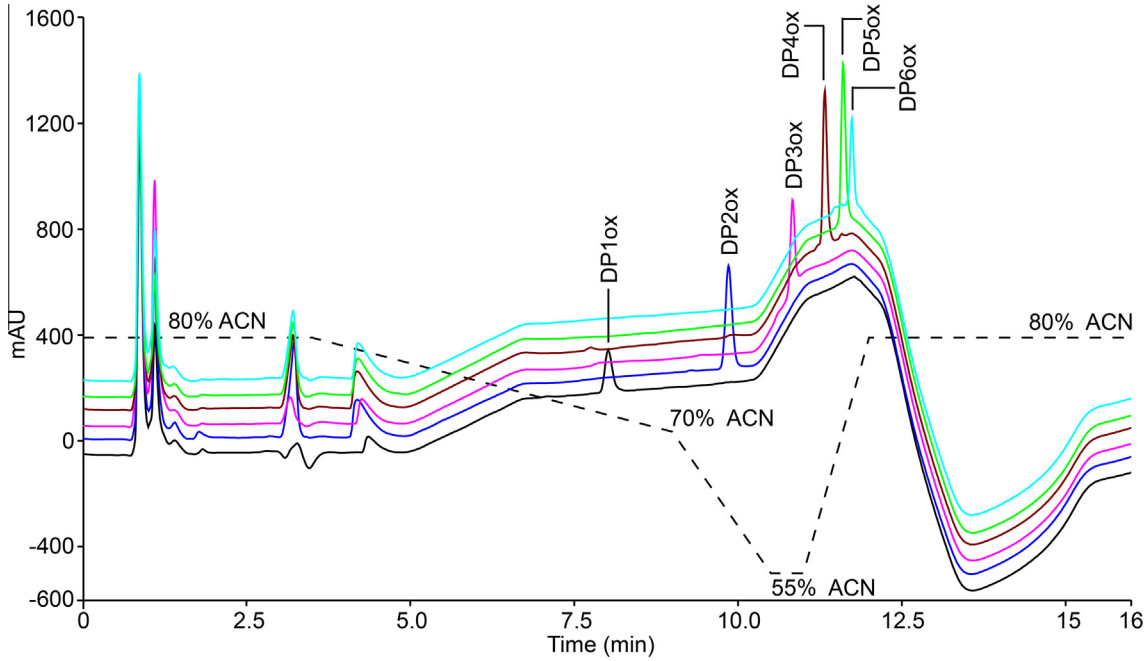

Fig. 2. Analysis of COAAs generated with ChitO using HILIC. Chromatography was conducted as described previously using a 150 mm column [9], but with a slightly altered gradient (dashed line) and run time (16 min). The solid lines show the analysis of ChitO-generated GlcNAc1A (DP1ox, black line), $(GlcNAc)_1GlcNAc1A$ (DP2ox, blue line), $(GlcNAc)_2GlcNAc1A$ (DP3ox, pink line), $(GlcNAc)_3GlcNAc1A$ (DP4ox, red line), $(GlcNAc)_4GlcNAc1A$ (DP5ox, green line) and $(GlcNAc)_5GlcNAc1A$ (DP6ox, light blue line). The *Y*-axis reflects absorbance at 195 nm and the dashed line represents the acetonitrile (ACN) gradient. Peaks in the chromatograms appearing before 5.0 min represent buffer components.

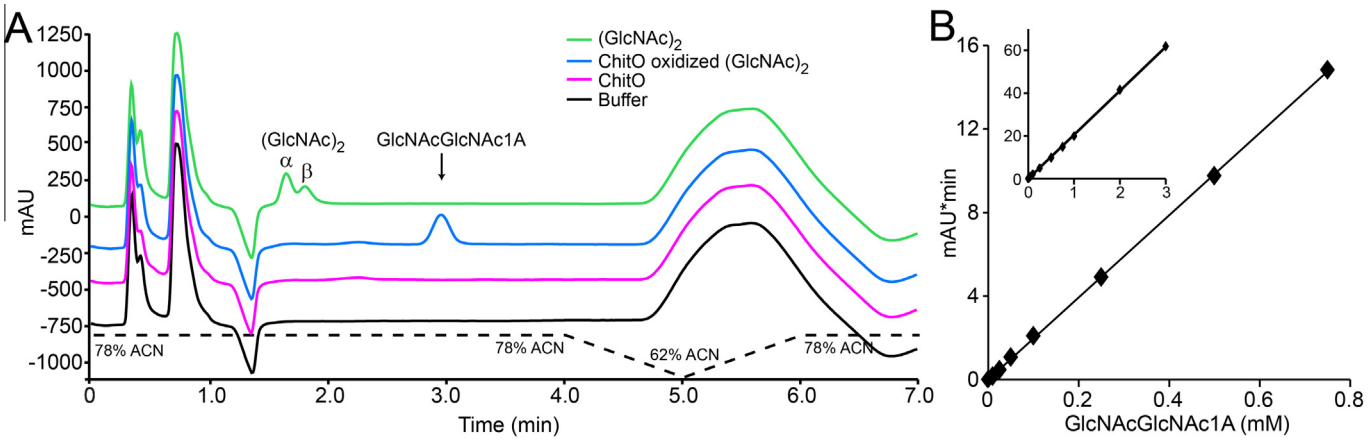

Fig. 3. Enzymatic oxidation of chitobiose to GlcNAcGlcNAc1A (chitobionic acid), analyzed using the shortened HILIC procedure. (A) Chromatograms showing 1.0 mM $(GlcNAc)_2$ in its native form (green line) in 50 mM Bis–Tris pH 6.8 or fully oxidized to chitobionic acid (GlcNAcGlcNAc1A; blue line) with 0.12 mg/mL ChitO in the same buffer. Chromatograms representing 0.12 mg/mL ChitO in 50 mM Bis–Tris pH 6.8 (pink line) and the buffer only (black line) are shown for reference. The *Y*-axis reflects absorbance at 195 nm. The two anomers of $(GlcNAc)_2$ are partially resolved and indicated by "α" and "β". The ACN gradient is indicated by the dashed line. Note that the absorption increase caused by the decrease in ACN is shifted approximately 1 min due to the delay from the mixing chamber to the detector. Peaks in the chromatograms appearing before 1.5 min represent buffer components. (B) Standard curve for chitobionic acid ranging from 0.01 to 0.75 mM. The inset graph (same axis legends as the main graph) shows the standard curve extended up to 3.0 mM chitobionic acid. The *Y*-axis reflects absorbance at 205 nm. The slope of the curve is 19.7 mAU*min/mM GlcNAcGlcNAc1A and $R^2 = 0.99$.

hydrolyze soluble COAAs. The main role of chitobiase in vivo is to hydrolyze chitobiose, the main product of chitin hydrolysis by family 18 chitinases, to GlcNAc [22–24]. Chitobiase operates by an exo-mechanism, releasing sugar moieties from the non-reducing end of the sugar chain and the enzyme is able to efficiently hydrolyze chitooligosaacharides [22]. When incubated with COAAs, chitobiase was able to depolymerize all soluble chitooligosaccharides to two final end products, GlcNAc and GlcNAcGlcNAc1A (chitobionic acid) (Fig. 4). It is not surprising that chitobiase cannot hydrolyze chitobionic acid since the open ring structure of the aldonic acid is likely to prevent productive binding of the substrate. Fig. 3B shows that the newly developed chromatographic method allows accurate quantification of chitobionic acid in concentrations ranging from 0.01 to 3.0 mM.

By using the method described above, the rate of substrate oxidation can be quantified for any LPMO that cleaves chitin chains by hydroxylation of the C1 carbon. However, working with LPMOs is not trivial, and several precautions are needed in order to ensure reliable results. Even though LPMOs show tight binding of copper (with K_d's in the low nM range; [4,25,26]), there will always be

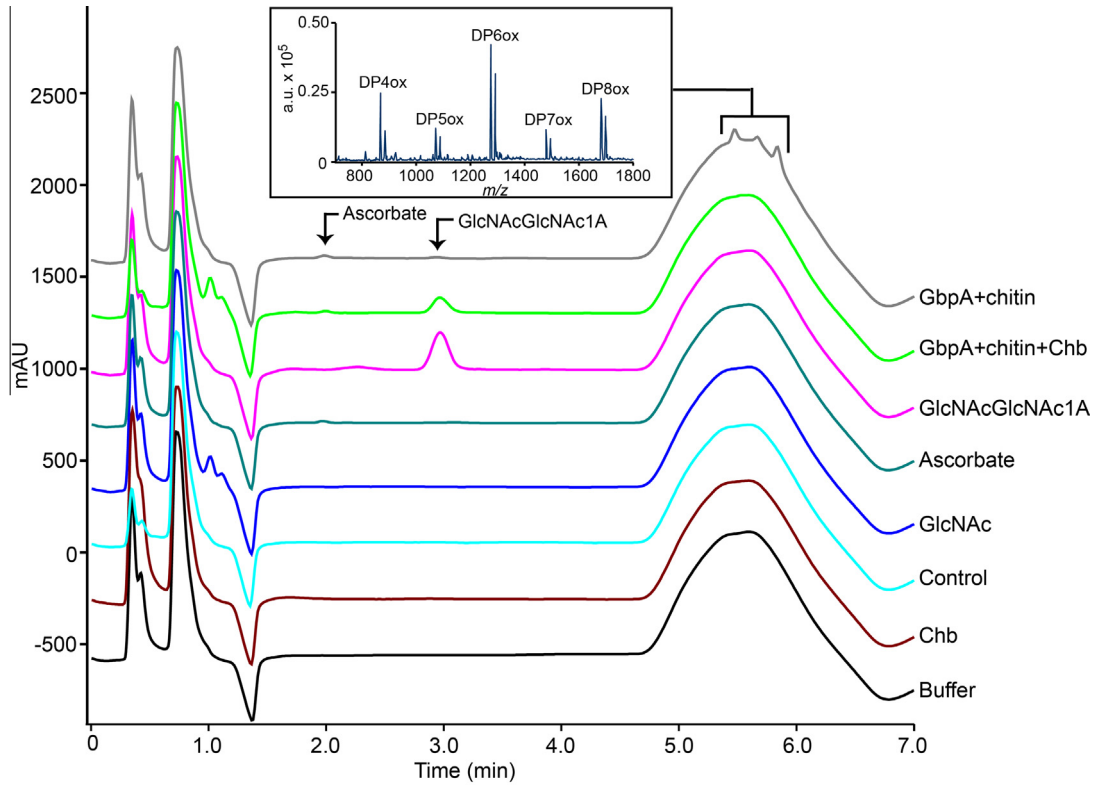

Fig. 4. Analysis of LPMO activity. Reaction products emerging from the activity of 2.0 μM GbpA on 5.0 mg/mL β-chitin nanofibers in 50 mM Bis–Tris pH 6.8 and with 1.0 mM ascorbate as reducing agent, analyzed by MALDI–TOF MS (inset) and HILIC (gray line). In the mass spectrum, each COAA is identified by one major peak that represents the mass of the $[M+Na^+]$ adduct. Peaks of lower intensity representing masses of the $[M+K^+]$, $[M-H^++2Na^+]$, $[M-H^++K^++Na^+]$ and/or $[M-H^++2\,K^+]$ adducts also occur but are not labeled. The masses observed for the $[M+Na^+]$ adducts were 869.1 (DP4ox), 1072.1 (DP5ox), 1275.2 (DP6ox), 1478.3 (DP7ox) and 1681.3 (DP8ox), with DPn_{ox} indicating $(GlcNAc)_{n-1}$-GlcNAcA. All COAAs elute between 5.5 and 6 min. Chitobiase treatment of the product mixture leaves chitobionic acid as the sole aldonic acid (green line), with the α- and β-anomers of GlcNAc eluting at ~1.0 min. Control chromatograms show 1.0 mM chitobionic acid (pink line), 1.0 mM ascorbate (dark green line), 1.0 mM GlcNAc (blue line), 2.0 μM chitobiase ("Chb"; brown line), all in the reaction buffer (50 mM Bis–Tris pH 6.8). Chromatograms representing the reaction buffer and the negative control (all reaction constituents except ascorbate) are shown by the black and cyan line, respectively. All samples were analyzed using the 7-minute HILIC protocol described in Section 2.

some free copper ions in solution, which are prone to precipitation as $Cu(OH)_2$) at the mildly acidic to mildly alkaline pH values commonly used for storage of proteins (the solubility product constant, K_{sp}, is 2.2×10^{-20} for $Cu(OH)_2$). Thus, if copper-saturated LPMOs are stored for a long period of time before use, a certain degree of the LPMOs in solution will be in an apo-form, which will be reflected in loss of activity (result not shown). A solution to the problem is to perform a Cu(II) saturation and desalting step before conducting an experiment as outlined in the Section 2. It should be noted that addition of excess copper in LPMO reaction mixtures, which could be envisioned as an alternative way of copper saturating the LPMOs, is not advisable, since dissolved Cu(II) is a catalyst for the autooxidation of reducing agents, which will lead to electron and oxygen depletion and enzyme damage caused by reactive oxygen species formed. This is especially critical when ascorbate is used as an electron donor [27].

Using the methods for enzyme preparation and quantitative product analysis described above, we were able to detect and quantify LPMO activity for the *V. cholerae* GbpA protein that carries an N-terminal LPMO10 domain. The protein was purified, copper saturated and desalted prior to use. Product formation over time was linear and the initial reaction rate for GbpA acting on β-chitin nanofibers was determined to be 2.7 min^{-1} (Fig. 5). This rate is similar to what was found for CBP21 activity towards β-chitin particles (~1 min^{-1}).

In conclusion, we report on methodological aspects of LPMO enzymology and describe a method for quantifying the oxidation rate of a chitin-targeting LPMO. Notably, the method described here is based on analysis of soluble products, meaning that oxidations not leading to solubilization are not considered and that rates are likely to be underestimated. Furthermore, importantly, we also show that GbpA, a *V. cholerae* virulence/colonization factor,

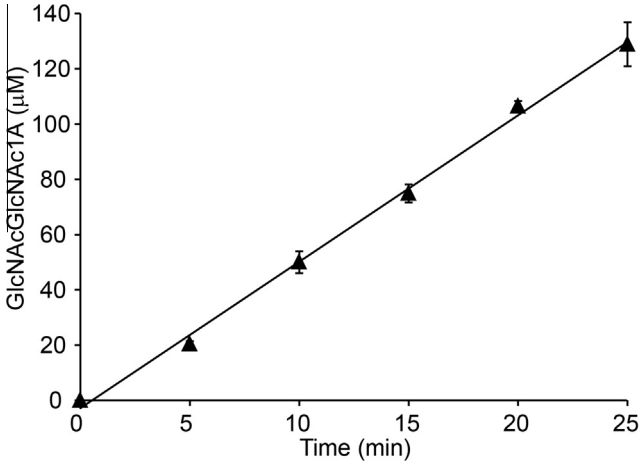

Fig. 5. Generation of COAAs by GbpA over time. The reaction rate was determined for 2.0 μM GbpA acting on 5.0 mg/mL β-chitin nanofibers in 50 mM Bis–Tris pH 6.8 and 1.0 mM ascorbate. Chitobiase was used to degrade resulting COAAs to GlcNAc and GlcNAcGlcNAc1A. The latter product was analyzed by the 7 min HILIC method described (see Methods and Materials and Fig. 4) and quantified using the ChitO generated GlcNAcGlcNAc1A standard. The straight black line represents the curve fitted the data by linear regression yielding a slope of 5.3 μM GlcNAcGlcNAc1A/min and an $R^2 = 0.99$. This gives a rate of 2.7 min^{-1}. All reactions were performed in triplicates and standard deviations are indicated by error bars.

is an active LPMO. Based on this finding the role of GbpA in *V. cholerae* virulence and transfer may need reconsideration.

Ackowledgments

This work was supported by the Norwegian Research Council Grants 214138 (to G.V.-K.) and 214613 & 216162 (to V.G.H.E.). Z.F. was supported by the Vista program of the Norwegian Academy of Science and Letters, Grant No. 6505. We thank Daan M.F. van Aalten for providing the vector encoding the *gbpA* gene and Stine Lislebø for cloning the chitobiase (*chb*) gene.

References

[1] Levasseur, A., Drula, E., Lombard, V., Coutinho, P.M. and Henrissat, B. (2013) Expansion of the enzymatic repertoire of the CAZy database to integrate auxiliary redox enzymes. Biotechnol. Biofuels 6, 41.
[2] Forsberg, Z., Mackenzie, A.K., Sørlie, M., Røhr, A.K., Helland, R., Arvai, A.S., Vaaje-Kolstad, G. and Eijsink, V.G.H. (2014) Structural and functional characterization of a conserved pair of bacterial cellulose-oxidizing lytic polysaccharide monooxygenases. Proc. Natl. Acad. Sci. USA 111, 8446–8451.
[3] Hemsworth, G.R., Davies, G.J. and Walton, P.H. (2013) Recent insights into copper-containing lytic polysaccharide mono-oxygenases. Curr. Opin. Struct. Biol. 23, 660–668.
[4] Hemsworth, G.R., Taylor, E.J., Kim, R.Q., Gregory, R.C., Lewis, S.J., Turkenburg, J.P., Parkin, A., Davies, G.J. and Walton, P.H. (2013) The copper active site of CBM33 polysaccharide oxygenases. J. Am. Chem. Soc. 135, 6069–6077.
[5] Quinlan, R.J., Sweeney, M.D., Lo Leggio, L., Otten, H., Poulsen, J.C., Johansen, K.S., Krogh, K.B., Jorgensen, C.I., Tovborg, M., Anthonsen, A., Tryfona, T., Walter, C.P., Dupree, P., Xu, F., Davies, G.J. and Walton, P.H. (2011) Insights into the oxidative degradation of cellulose by a copper metalloenzyme that exploits biomass components. Proc. Natl. Acad. Sci. USA 108, 15079–15084.
[6] Beeson, W.T., Phillips, C.M., Cate, J.H. and Marletta, M.A. (2012) Oxidative cleavage of cellulose by fungal copper-dependent polysaccharide monooxygenases. J. Am. Chem. Soc. 134, 890–892.
[7] Forsberg, Z., Vaaje-Kolstad, G., Westereng, B., Bunæs, A.C., Stenstrøm, Y., Mackenzie, A., Sørlie, M., Horn, S.J. and Eijsink, V.G.H. (2011) Cleavage of cellulose by a CBM33 protein. Protein Sci. 20, 1479–1483.
[8] Phillips, C.M., Beeson, W.T., Cate, J.H. and Marletta, M.A. (2011) Cellobiose dehydrogenase and a copper-dependent polysaccharide monooxygenase potentiate cellulose degradation by *Neurospora crassa*. ACS Chem. Biol. 6, 1399–1406.
[9] Vaaje-Kolstad, G., Westereng, B., Horn, S.J., Liu, Z.L., Zhai, H., Sørlie, M. and Eijsink, V.G.H. (2010) An oxidative enzyme boosting the enzymatic conversion of recalcitrant polysaccharides. Science 330, 219–222.
[10] Kim, S., Ståhlberg, J., Sandgren, M., Paton, R.S. and Beckham, G.T. (2014) Quantum mechanical calculations suggest that lytic polysaccharide monooxygenases use a copper-oxyl, oxygen-rebound mechanism. Proc. Natl. Acad. Sci. USA 111, 149–154.
[11] Kjaergaard, C.H., Qayyum, M.F., Wong, S.D., Xu, F., Hemsworth, G.R., Walton, D.J., Young, N.A., Davies, G.J., Walton, P.H., Johansen, K.S., Hodgson, K.O., Hedman, B. and Solomon, E.I. (2014) Spectroscopic and computational insight into the activation of O_2 by the mononuclear Cu center in polysaccharide monooxygenases. Proc. Natl. Acad. Sci. USA 111, 8797–8802.
[12] Frederiksen, R.F., Paspaliari, D.K., Larsen, T., Storgaard, B.G., Larsen, M.H., Ingmer, H., Palcic, M.M. and Leisner, J.J. (2013) Bacterial chitinases and chitin-binding proteins as virulence factors. Microbiology 159, 833–847.
[13] Bhowmick, R., Ghosal, A., Das, B., Koley, H., Saha, D.R., Ganguly, S., Nandy, R.K., Bhadra, R.K. and Chatterjee, N.S. (2008) Intestinal adherence of *Vibrio cholerae* involves a coordinated interaction between colonization factor GbpA and mucin. Infect. Immun. 76, 4968–4977.
[14] Kirn, T.J., Jude, B.A. and Taylor, R.K. (2005) A colonization factor links *Vibrio cholerae* environmental survival and human infection. Nature 438, 863–866.
[15] Wong, E., Vaaje-Kolstad, G., Ghosh, A., Hurtado-Guerrero, R., Konarev, P.V., Ibrahim, A.F.M., Svergun, D.I., Eijsink, V.G.H., Chatterjee, N.S. and van Aalten, D.M.F. (2012) The *Vibrio cholerae* colonization factor GbpA possesses a modular structure that governs binding to different host surfaces. PLoS Pathog. 8, 1.
[16] Zampini, M., Pruzzo, C., Bondre, V.P., Tarsi, R., Cosmo, M., Bacciaglia, A., Chhabra, A., Srivastava, R. and Srivastava, B.S. (2005) *Vibrio cholerae* persistence in aquatic environments and colonization of intestinal cells: involvement of a common adhesion mechanism. FEMS Microbiol. Lett. 244, 267–273.
[17] Kittl, R., Kracher, D., Burgstaller, D., Haltrich, D. and Ludwig, R. (2012) Production of four *Neurospora crassa* lytic polysaccharide monooxygenases in *Pichia pastoris* monitored by a fluorimetric assay. Biotechnol. Biofuels 5, 79.
[18] Heuts, D.P., Winter, R.T., Damsma, G.E., Janssen, D.B. and Fraaije, M.W. (2008) The role of double covalent flavin binding in chito-oligosaccharide oxidase from *Fusarium graminearum*. Biochem. J. 413, 175–183.
[19] Ferrari, A.R., Gaber, Y. and Fraaije, M.W. (2014) A fast, sensitive and easy colorimetric assay for chitinase and cellulase activity detection. Biotechnol. Biofuels 7, 37.
[20] Fan, Y., Saito, T. and Isogai, A. (2008) Preparation of chitin nanofibers from squid pen beta-chitin by simple mechanical treatment under acid conditions. Biomacromolecules 9, 1919–1923.
[21] Agger, J.W., Isaksen, T., Varnai, A., Vidal-Melgosa, S., Willats, W.G., Ludwig, R., Horn, S.J., Eijsink, V.G.H. and Westereng, B. (2014) Discovery of LPMO activity on hemicelluloses shows the importance of oxidative processes in plant cell wall degradation. Proc. Natl. Acad. Sci. USA 111, 6287–6292.
[22] Drouillard, S., Armand, S., Davies, G.J., Vorgias, C.E. and Henrissat, B. (1997) *Serratia marcescens* chitobiase is a retaining glycosidase utilizing substrate acetamido group participation. Biochem. J. 328, 945–949.
[23] Tews, I., Perrakis, A., Oppenheim, A., Dauter, Z., Wilson, K.S. and Vorgias, C.E. (1996) Bacterial chitobiase structure provides insight into catalytic mechanism and the basis of Tay-Sachs disease. Nat. Struct. Biol. 3, 638–648.
[24] Vaaje-Kolstad, G., Horn, S.J., Sørlie, M. and Eijsink, V.G.H. (2013) The chitinolytic machinery of *Serratia marcescens* – a model system for enzymatic degradation of recalcitrant polysaccharides. FEBS J. 280, 3028–3049.
[25] Aachmann, F.L., Sørlie, M., Skjåk-Bræk, G., Eijsink, V.G.H. and Vaaje-Kolstad, G. (2012) NMR structure of a lytic polysaccharide monooxygenase provides insight into copper binding, protein dynamics, and substrate interactions. Proc. Natl. Acad. Sci. USA 109, 18779–18784.
[26] Forsberg, Z., Røhr, A.K., Mekasha, S., Andersson, K.K., Eijsink, V.G.H., Vaaje-Kolstad, G. and Sørlie, M. (2014) Comparative study of two chitin-active and two cellulose-active AA10-type lytic polysaccharide monooxygenases. Biochemistry 53, 1647–1656.
[27] Buettner, G.R. (1986) Ascorbate autoxidation in the presence of iron and copper chelates. Free Radic. Res. Commun. 1, 349–353.

Paper II

Activation of bacterial lytic polysaccharide monooxygenases with cellobiose dehydrogenase

Jennifer S.M. Loose, Zarah Forsberg, Daniel Kracher, Stefan Scheiblbrandner, Roland Ludwig, Vincent G.H. Eijsink, Gustav Vaaje-Kolstad, 2016

Manuscript submitted to *Biochemistry*, under revision

Activation of Bacterial Lytic Polysaccharide Monooxygenases with Cellobiose Dehydrogenase

*Jennifer S.M. Loose[1], Zarah Forsberg[1], Daniel Kracher[2], Stefan Scheiblbrandner[2], Roland Ludwig[2], Vincent G.H. Eijsink[1] and Gustav Vaaje-Kolstad[1]**

Department of Chemistry, Biotechnology and Food Science, Norwegian University of Life Sciences, Ås, Norway.

University of Natural Resources and Life Sciences, Department of Food Sciences and Technology, Food Biotechnology Laboratory, Vienna, Austria.

*To whom correspondence should be addressed: Gustav Vaaje-Kolstad, Department of Chemistry, Biotechnology, and Food Science, The Norwegian University of Life Sciences, 1432 Ås, Norway, Tel.: +47 67232573; E-mail: gustav.vaaje-kolstad@nmbu.no

Funding Sources

This work was supported by the Research Council of Norway Grants 214138 (JSML and GV-K) and 214613 (VGHE), The Norwegian Academy of Science and Letters Vista Program Grant 6510 (ZF), the European Commission (project INDOX FP7-KBBE-2013-7-613549) (RL), the Austrian Science Fund (project BioToP; FWF W1224) (DK) and the Austrian-Singaporean graduate school program (IGS BioNano Tech) (SS).

KEYWORDS: Lytic polysaccharide monooxygenase (LPMO), cellobiose dehydrogenase (CDH), electron transfer, electron donor, hydrogen peroxide, chitin, cellulose, enzyme kinetics.

ABSTRACT

Lytic polysaccharide monooxygenases (LPMOs) represent a recent addition to the carbohydrate-active enzymes and are classified as auxiliary activity (AA) families 9, 10, 11 and 13. LPMOs are crucial for effective degradation of recalcitrant polysaccharides like cellulose or chitin. These enzymes are copper-dependent and utilize a redox mechanism to cleave glycosidic bonds that is dependent on molecular oxygen and an external electron donor. The electrons can be provided by various sources, such as chemical compounds (e.g. ascorbate) or by enzymes (e.g. cellobiose dehydrogenases, CDHs, from fungi). Here, we demonstrate that a fungal CDH from *Myriococcum thermophilum* (*Mt*CDH), can act as an electron donor for bacterial family AA10 LPMOs. We show that employing an enzyme as electron donor is advantageous since this enables a kinetically controlled supply of electrons to the LPMO. The rate of chitin oxidation by CBP21 was essentially identical to that of co-substrate (lactose) oxidation by *Mt*CDH, indicating that the majority of electrons generated by *Mt*CDH were consumed by the CBP21 reaction. Finally, the one electron reduction of the CBP21 active site copper by *Mt*CDH was determined to be substantially faster that chitin oxidation by the LPMO. Overall, *Mt*CDH seems to be a universal electron donor for both bacterial and fungal LPMOs, indicating that their electron transfer mechanisms are similar.

Lytic polysaccharide monooxygenases (LPMOs) are copper-dependent enzymes that employ an oxidative mechanism to cleave the glycosidic bonds of polysaccharides [1-5]. The main substrates for LPMOs are insoluble polysaccharides such as chitin or cellulose [1-3], but LPMO activity has also been demonstrated for xyloglucan [6], xylan [7] soluble cello-oligosaccharides [8] and starch [9]. LPMOs are currently classified as family 9, 10, 11 and 13 of the auxiliary activities (AAs) in the CAZy database [10]. So far, AA9, AA11 and AA13-type LPMOs (LPMO9s, LPMO11s and LPMO13s) have only been identified in fungi, whereas AA10-type LPMOs (LPMO10s) have been found in eukaryotes, prokaryotes and viruses. The active site of these enzymes contains a solvent exposed copper-ion that is coordinated by two conserved histidines in a histidine brace [3, 11, 12]. The role of the copper ion is to activate a dioxygen molecule that lead to hydroxylation of either the C1 or C4 carbon of the substrate [4, 13, 14]. The hydroxylation event yields an unstable hemiketal intermediate that results in spontaneous cleavage of the glycosidic bond through an elimination reaction [4, 15]. For catalysis by LPMOs to occur, the copper ion must be reduced by an external electron donor prior to the activation of dioxygen. It is known from laboratory experiments that functional electrons include small-molecule reductants like ascorbic acid [1] or gallic acid [3], lignin present in plant cell walls [16-18], certain redox-active proteins, such as cellobiose dehydrogenase (CDH) [4, 19, 20] and combinations of plant-derived phenolic compounds and a glucose-methanol-choline oxidase/dehydrogenase [21]. CDH has only been found in fungi. Several studies have reported that LPMOs and CDHs are co-transcribed and co-expressed during fungal growth on plant cell wall material [22-24], which has led to the notion that CDH may be the primary natural electron donor for (fungal) LPMOs [25].

CDHs are two-domain proteins comprising a flavin adenine dinucleotide (FAD)-binding dehydrogenase (DH) domain coupled to a heme-binding cytochrome (CYT) domain [26-28]. CDH oxidizes di- or oligosaccharides to their corresponding aldonic acids. In this process, the two

electrons obtained from the substrate are stored in the DH domain by reduction of the FAD. By internal electron transfer, one electron can be transferred from the DH domain to the CYT domain (by reduction of the heme group). CDHs can thereby perform two-electron reduction reactions (via the DH domain) or one-electron reductions (via the CYT domain). CDHs are capable of efficient transfer of electrons to both small chemical compounds and proteins [29-31]. In the absence of a good electron acceptor, O_2 can also be reduced to yield H_2O_2 (or O_2^- in some in cases) [32].

Since the discovery of CDHs, their *in vivo* role has been uncertain. The widespread occurrence of these enzymes has generated several hypotheses on their functions, especially linked to their ability to produce H_2O_2. Hydrogen peroxide can act as an antimicrobial agent [33, 34] or together with Fe(II), create hydroxyl radicals, one of the strongest oxidizing agents in aqueous systems [35], in a Fenton-reaction. It has been suggested that such hydroxyl radicals can degrade or modify cellulose, indicating a role of CDHs in unspecific plant cell wall degradation [36-38]. The discovery of LPMOs and the notion that these enzymes are good electron acceptors for one-electron transfer from the CYT domain of CDH [25] has shed new light on these issues. Notably, reduced LPMOs are also able to produce H_2O_2 in the absence of a substrate [8, 39]. A simplified scheme illustrating the CDH-LPMO system is shown in Fig. 1.

The specificity of the electron transfer reaction between CDHs and LPMOs has hitherto not been investigated in detail, one key question being if there is any specificity at all or if an enzyme such as CDH can reduce any LPMO. In the present study we report on the ability of a fungal CDH to activate bacterial LPMO10s, including an analysis of the rate of electron transfer between the proteins. We show that both chitin and cellulose-active LPMO10s can utilize CDH as a source of electrons and we compare the functionality of the LPMO10-CDH interaction with previously studied LPMO9-CDH interactions. Importantly, so far, the LPMO literature is almost devoid of kinetic data, which is likely due to the difficulty of obtaining

linear progress curves, which again is likely due to the use of unstable small molecule reductants. We show here that careful experimental design based on using CDH/lactose for the generation of reducing equivalents gives superior control of the reaction kinetics.

EXPERIMENTAL PROCEDURES

Protein expression and purification

Cellobiose dehydrogenase from the thermophilic ascomycetous fungus *Myriococcum thermophilum* (*Mt*CDH) was expressed in *Pichia pastoris* and purified as previously reported [40]. The production of *Mt*CDH was performed at 4 L-scale in a laboratory bioreactor (MBR, Switzerland) according to the *Pichia* Fermentation Process guidelines (Invitrogen). In short, the cultivation was initiated by adding 0.4 L of a pre-culture grown over night at 30°C and 120 rpm. Expression of recombinant protein was induced with methanol. The cultivation temperature was 30°C, the airflow rate was kept constant at 6 liter min^{-1}, and the stirrer speed was 800 rpm. Samples were taken regularly and checked for CDH activity. Purification of *Mt*CDH was done by a two-step chromatographic procedure (all equipment from GE Healthcare) using hydrophobic interaction chromatography (PHE-Sepharose FF resin) and anion exchange chromatography (Source 15Q resin). The purest CDH fractions were pooled, concentrated using Amicon Ultra centrifugal filters (Millipore) with a molecular weight cut-off of 10 kDa and sterile filtered (0.2 µm). The purity of *Mt*CDH was confirmed by SDS-PAGE.

Streptomyces coelicolor LPMO10C, *Sc*LPMO10C (also known as CelS2), was expressed in *E. coli* as previously described [41]. In brief, a fresh transformant containing the *Sc*LPMO10C encoding plasmid was inoculated and grown in LB medium supplemented with ampicillin (100 µg/mL) at 37°C for approximately 16 h without induction. The protein was harvested from the periplasmic space using a cold osmotic shock method [42]. Purification was carried out by anion exchange chromatography using a 5 mL HiTrap DEAE FF column (GE Healthcare) in 50 mM Tris-HCl pH 7.5 and the protein was eluted by applying a linear salt gradient (0-500 mM NaCl over 60 column volumes). Subsequently the partially purified protein was loaded onto a HiLoad 16/60 Superdex 75 size exclusion chromatography column (GE Healthcare) operated

with a running buffer consisting of 50 mM Tris-HCl pH 7.5 and 200 mM NaCl. Fractions containing pure LPMO were pooled and concentrated using an Amicon Ultra centrifugal filter (Millipore) with a molecular weight cut-off of 10 kDa, before the enzyme concentration was determined using the Bradford assay (Bio-Rad).

Chitobiase from *Serratia marcescens* (*Sm*GH20A) was expressed and purified as previously described by Loose *et al.* [43] with minor changes. In short, BL21 star cells containing the pET30 Xa/LIC vector with the *chb* gene were grown in LB medium supplemented with 100 µg/mL kanamycin at 37°C to an OD_{600} = 0.5 after which protein production was induced by addition of IPTG to a final concentration of 0.3 mM, followed by incubation at 30°C for 5 h with shaking at 160 rpm. The culture was harvested and resuspended in lysis/binding buffer (20 mM Tris-HCL pH 8.0, 5 mM imidazole). The cells were disrupted by incubating 30 min with 0.1 mg/mL lysozyme followed by sonication using a Vibra cell sonicator (Sonics) using 27 % amplitude and a repeated cycle of 5 s on and 1 s off for a total duration of 3 min. The extract was loaded onto 5 mL Ni-NTA Agarose resin (Protino, Macherey-Nagel) using 20 mM Tris-HCl, pH 8.0, 5 mM imidazole as running buffer. The protein was eluted with 20 mM Tris-HCl, pH 8.0, 500 mM imidazole. The eluted chitobiase was concentrated and the imidazole was removed using an Amicon Ultra centrifugal filter (Millipore) with 10 kDa cut-off. The enzyme concentration was determined using the Bradford assay (Bio-Rad).

CBP21 from *Serratia marcescens* (*Sm*LPMO10A) was expressed and purified as previously described by Vaaje-Kolstad *et al.* [44]. In short, *E. coli* BL21 DE3 cells harboring a pRSETB vector containing the *cbp21* gene were grown in TB-medium supplemented with ampicillin (100 µg/mL) overnight in a Harbinger LEX bioreactor (Harbinger Biotech, Toronto, Canada) at 37°C. The cells were harvested by centrifugation and the periplasmic content was extracted using the cold osmotic shock method. The extract was adjusted to 20 mM Tris-HCl, pH 8.0, 1.0 M $(NH_4)_2SO_4$ and applied to 10 mL chitin beads (NEB) using a BioLogic chromatographic

system from BioRad. After non-bound protein had passed through the column, CBP21 was eluted with 20 mM acetic acid. The protein was concentrated using an Amicon Ultra centrifugal filter with a 10 kDa cut-off (Millipore) and the buffer was exchanged to 20 mM Tris-HCl, pH 8.0. The protein concentration was determined using A_{280} and the theoretical extinction coefficient.

Chitinase 18C (ChiC) from *S. marcescens* was produced and purified as described previously by Vaaje-Kolstad *et al.* [44]. In short, this was accomplished by expression of the enzyme in *E. coli*, followed by extraction of periplasmic proteins by cold osmotic shock and one-step purification by standard ion exchange chromatography, using Q-Sepharose Fast Flow at pH 9.4 and a 0 – 100 mM NaCl linear gradient for elution of the chitinase. The protein concentration was determined using A_{280} and the theoretical extinction coefficient.

Chitooligosaccharide oxidase (m-ChitO) from *Fusarium graminearum* N-terminally fused to maltose binding protein encoded by the pBAD-MBP-*chitO* expression vector was expressed as previously described [45] with minor changes. The culture was harvested and the pellet was resuspended in 20 mM Tris-HCl, pH 8.0, containing 10 % glycerol. The cells were disrupted by sonication for 2.5 min (5 sec on, 1 sec off) at an amplitude of 30 %. The crude extract was loaded on a 5 mL DEAE FF column (GE Healthcare) and m-ChitO was eluted using a stepwise gradient from 15 mM NaCl to 250 mM NaCl in 20 mM Tris-HCl, pH 8.0. Fractions containing m-ChitO were pooled and concentrated using Amicon Ultra centrifugal filters (Millipore) with 10 kDa cut- off. The concentrated protein sample was then subjected to a size exclusion chromatography step using a HiLoad 16/60 Superdex 75 size exclusion column (GE Healthcare), operated in 20 mM Tris-HCl, pH 8.0. Fractions containing m-ChitO that was at least 85 % pure were pooled and concentrated. The enzyme concentration was determined using the Bradford assay (Bio-Rad).

Cu(II) saturation and desalting of LPMOs.

CBP21 and *Sc*LPMO10C were saturated with Cu(II) according to the protocol described by Loose *et al.* [43]. Briefly, the LPMOs were saturated by incubating them with $Cu(II)SO_4$ in a 1:3 molar ratio (enzyme:copper) at room temperature for 30 min. After saturation, excess $Cu(II)SO_4$ was removed by passing the proteins through a PD MidiTrap G-25 (GE Healthcare) desalting column using 25 mM Bis-Tris, pH 6.0, as running buffer.

Stopped-flow spectroscopy.

Pre-steady state kinetic studies measured the re-oxidation of CDH`s heme *b* cofactor by CPB21 and were performed with a SX-20 stopped-flow apparatus (Applied Photophysics, Leatherhead, UK) equipped with a flow cell with a path length of 10 mm and a diode array detector. Using the sequential mixing mode, 20 μM *Mt*CDH and a 3-fold molar excess of cellobiose were initially mixed (1:1) and held in an ageing loop until re-oxidation of the FAD cofactor by ambient oxygen and hence full depletion of cellobiose was observed. After 95 s, full re-oxidation of the FAD cofactor after observed, while about ~80 % of the heme *b* was still reduced and was subsequently mixed (1:1) with the CPB21 solution. The re-oxidation rate of the heme *b* cofactor was measured at 563 nm and was used to determine the electron transfer rate from *Mt*CDH to CPB21 (k_{obs}, s^{-1}). The FAD re-oxidation was measured at 449 nm and was used to determine the rate of the oxidative half-reaction in the presence of oxygen (air saturated buffer ~ 250 μM). Observed traces were fitted to an exponential function using the Pro-Data software suite (Applied Photophysics). All species were prepared in 50 mM sodium phosphate buffer, pH 6.0, and final concentrations of the enzymes in the measurement cell were 5.0 μM *Mt*CDH and 15, 25 or 50 μM of CPB21. All measurements were carried out at 30°C in triplicates.

LPMO activity assays.

Reactions containing 1.0 μM CBP21 or *Sc*LPMO10C, with 10 mg/mL β-chitin or Avicel, respectively, in the presence of 1.5 μM *Mt*CDH and 3.0 mM lactose buffered in 25 mM or 50 mM BisTris pH 6.0 were incubated at 40°C in an Eppendorf Comfort Thermomixer with a temperature-controlled lid, shaking at 1000 rpm. Samples were taken at various time points and immediately filtered using a 96-well filter plate (Millipore) operated by a Millipore vacuum manifold to stop chitin oxidation. Samples used to monitor lactose oxidation over time were adjusted to 100 mM NaOH in order to stop *Mt*CDH activity. For all CBP21 reactions, except reactions used to analyze the product profile, the soluble products were treated with 2.0 μM chitobiase for 2 h at 37°C to convert the chitooligosaccharides to chitobionic acid and GlcNAc. The resulting products were analyzed and quantified by UPLC as previously described by Loose *et al.* [43]. The analysis of products generated by *Sc*LPMO10C is described below.

Product analysis by HPAEC-PAD.

Oxidized cello-oligosaccharides generated by *Sc*LPMO10C were analyzed by high performance anion exchange chromatography (HPAEC) using a Dionex Bio-LC connected to a CarboPac PA1 column operated with a flow rate of 0.25 mL/min in 0.1 M NaOH (Eluent A) and a column temperature of 30°C. Products were separated as previously described [46] using a stepwise gradient with increasing amount of eluent B (0.1 M NaOH and 1 M NaOAc) as follows: 0-10 % B over 10 min, 10-30 % B over 25 min, 30-100 % B over 5 min, 100-0 % B over 1 min, 0 % B over 9 min. Oxidation of lactose over time by *Mt*CDH was analyzed by separating lactose and lactobionic acid by HPAEC-PAD, using a steeper gradient, as follows: 0-10 % B over 10 min, 10-18 % B over 10 min, 18-30 % B over 1 min, 30-100 % B over 1 min, 100-0 % B over 0.1 min and 0 % B over 13.9 min. Eluted oligosaccharides were monitored using a pulsed amperometric detector (PAD) and chromatograms were recorded using

Chromeleon 7.0 software. In-house made standards (see below) were run at regular intervals to allow quantification.

Product analysis by UPLC – Oxidized chitooligosaccharides (aldonic acids) were analyzed and quantified using an Aquity UPLC® BEH Amide 1.7 µm column run in HILIC (hydrophilic interaction) mode. To quantify chitobionic acid, a 2.1 x 50 mm column was utilized with the following gradient: 22% eluent A (15 mM Tris–HCl pH 8.0), 78% eluent B (100% acetonitrile): for 4 min, followed by a 1 min gradient to 62% B. The column was reconditioned by a 1 min gradient to initial conditions (22% A, 78% B) and additional running at these conditions for 1 min. To obtain a full product profile, a 2.1 x 150 mm column was used, applying the following gradient: 26% A and 74% B for 5 min, followed by a 2 min gradient to 62% B. These conditions were held for 1 min. The column was reconditioned by a 2 min gradient to 26% A and 74% B and additional running for 2 min. The flow rate was 0.4 mL/min and eluted chitooligosaccharides were monitored at 205 nm and 195 nm.

Production of chitobionic acid and lactobionic acid standards.

Chitobionic acid standards were produced as previously described by Loose *et al*. [43]. In short, 2.0 mM chitobiose (95 % pure, Megazyme) in 25 mM Bis-Tris pH 6.0 were incubated with 0.1 mg/mL m-ChitO over night at 22°C. The oxidized products were analyzed by UPLC. At least 97% of the chitobiose was oxidized.

Lactobionic acid standards were produced by incubating 3.0 mM lactose with 1.5 µM *Mt*CDH in 25 mM Bis-Tris pH 6.0. In order to speed up the reaction and obtain complete oxidation of all lactose added, 1.0 µM CBP21 and 10 mg/mL β-chitin were added to the reaction (*Mt*CDH will oxidize lactose substantially faster when an efficient electron acceptor like CBP21 is present in the reaction mixture). The samples were incubated in an Eppendorf Comfort Thermomixer with a temperature-controlled lid, at 40°C and 1000 rpm. After 48 – 72 h samples were taken to assure complete oxidation of lactose to lactobionic acid. When full

oxidation was reached, the sample was filtered (0.45 μm) and stored at -20°C until further use. Lactobionic acid could be base line separated from the oxidized chitooligosaccharides produced by CBP21 in the reaction using the HPAEC method described for analysis of oxidized cellooligosaccharides (see above).

Hydrogen Peroxide assays.

Hydrogen peroxide (H_2O_2) was quantified by using the Amplex® Red Hydrogen Peroxide/Peroxidase Assay Kit (Molecular Probes) according to the instructions provided by the manufacturer. In short, the concentration of hydrogen peroxide was determined by mixing 5 μL of sample with 45 μL of 1 × reaction buffer (50 mM sodium phosphate, pH 7.4), followed by addition of 50 μL of the Amplex® Red working solution (100 μM Amplex® Red reagent and 0.2 U/mL horseradish peroxidase in 1 × reaction buffer) and incubation for 30 min at room temperature in 96-well plates. The amount of the colorimetrically detectable product of the assay, resorufin, was quantified by measuring absorbance at 540 nm using a Multiskan FC spectrophotometer (Thermo Scientific). The standard curve, ranging from 0.5 to 17 μM, was made by diluting the H_2O_2 standard stock solution supplied with the kit in 1 × reaction buffer. Before addition of the Amplex® Red working solution, all standard samples were adjusted to 2.5 mM Bis-Tris, pH 6.0, to generate conditions identical to those of the experimental samples.

RESULTS

Electron transfer from MtCDH to CBP21.

Stopped-flow experiments with reduced *Mt*CDH and copper-saturated CBP21-Cu(II) showed fast electron transfer between the proteins. During the interaction between the enzymes, a monophasic reaction was observed and the electron transfer rates were obtained from a single exponential fit. The electron transfer rate increased proportionally with the concentration of CBP21 (Fig. 2), which indicates a fast, bimolecular reaction. At 50 µM CBP21, the observed electron transfer rate reached 32 s^{-1}. The observed re-oxidation rate of the heme *b* cofactor by oxygen (in an air saturated buffer) in absence of CBP21 was 0.013 s^{-1}, which is very low. The observed FAD re-oxidation rate of the oxidative half-reaction was k_{obs} = 3.2 min^{-1} (data not shown).

Activation of bacterial LPMOs by MtCDH.

Qualitative enzyme activity assays showed that *Mt*CDH can act as an electron donor for CBP21 and *Sc*LPMO10C from *Streptomyces coelicolor*, which target chitin and cellulose as substrates, respectively (Fig. 3). Analysis of reaction products by UPLC, HPAEC-PAD and by MALDI-TOF MS showed that the products were aldonic acids giving double sodium adducts that are characteristic for the presence of a carboxylic group [1, 41]; MS results not shown.

Dose response experiments.

In order to determine a suitable lactose concentration for the *Mt*CDH-CBP21 experiments, the effect of lactose concentrations ranging from 0.5-10 mM was investigated. The quantity of LPMO-generated products (which were all converted to chitobionic acid by chitobiase treatment) increased with increasing lactose concentrations, plateauing at 3.0 mM (Fig. 4A). Using 3.0 mM lactose as substrate for *Mt*CDH, the effect of varying the concentration of *Mt*CDH was investigated. These experiments showed that faster initial rates (i.e. higher product levels after 4 h) were obtained by increasing the *Mt*CDH concentration up to 3 µM, whereas

the yield after 24 h showed a maximum at 1.5 μM *Mt*CDH (Fig. 4B). Thus, increasing the *Mt*CDH concentration seems to be beneficial for the short term activity of CBP21, but reduces LPMO activity during longer incubation times. For comparison, the dose-response relationship between CBP21 and ascorbate as electron donor was also investigated (Fig. 5). Increasing concentrations of ascorbate resulted in both higher initial rates of chitin oxidation and final yields of oxidized products, except for the highest ascorbate concentration (10 mM), which resulted in a progress curve with an initial phase similar to that of 5 mM ascorbate, but had a lower final yield. It is notable that the progress curves with ascorbate showed linearity during the first 1.5 h of the reaction only, after which LPMO activity declined substantially. This is different when using *Mt*CDH, as shown below.

LPMO kinetics.

Using the optimum conditions obtained from the dose-response experiments (Fig. 4) the reaction kinetics of CBP21 with the *Mt*CDH/lactose system as electron-donor was monitored (Fig. 6A). The product formation curve was essentially linear and enzyme activity remained stable for up to 10 hours. The linear part of the curve has a slope of 2.2 μM min^{-1} indicating an apparent rate of 2.2 min^{-1} for CBP21 (note that in this experiment only solubilized oxidized products are monitored; see below for further details). An identical experiment where *Mt*CDH+lactose was substituted by 1.0 mM ascorbate, showed a bi-phasic product formation curve, where the rate of product formation dropped substantially after approximately 1.5 h of incubation (Fig. 6A), as was also observed in the CBP21-ascorbate dose-response experiment depicted in Fig. 5.

The influence of CBP21 on the activity of *Mt*CDH was quantified by monitoring lactose oxidation in the presence of chitin and in the presence or absence of the LPMO (Fig. 6B). In the presence of CBP21 a linear progress curve was observed (slope = 3.23 μM min^{-1}), whereas

the CBP21 deficient reaction shows an initial burst, followed by linear progress (slope = 1.67 μM min^{-1}).

Soluble products formed by CBP21 represent only a part of the LPMO activity and in order to quantify the total amount of oxidized products formed during catalysis, an endo-chitinase (ChiC from *S. marcescens*) was added to CBP21/*Mt*CDH/lactose/chitin reaction mixtures. In the presence of 0.02 μM or 0.2 μM ChiC, the formation of oxidized products over time was still linear (Fig. 6C; i.e. chitinase activity does not reduce substrate availability). The chitinase containing reactions yielded 1.3 times (0.02 μM ChiC) and 1.5 times (0.2 μM ChiC) more oxidized products compared to reactions only containing CBP21 and *Mt*CDH/lactose (Fig. 6C). So, the actual product formation rate for *Mt*CDH/lactose fueled CBP21 is approximately 3.3 μM min^{-1}, corresponding to an apparent rate constant of 3.3 min^{-1}. It is noteworthy that the apparent rates of chitin oxidation (3.3 μM min^{-1}) and lactose oxidation (3.23 μM min^{-1}) are very similar. The reduction in product formation rate after 10 h is likely due to substrate depletion, since at that point, i.e. at 1.4 mM oxidized products, approximately 6 % of the disaccharides in the substrate is oxidized, which is similar to previously observed maximum values [1].

Generation of H_2O_2 by MtCDH and CBP21.

The generation of H_2O_2 in enzyme reactions containing *Mt*CDH and/or CBP21 was quantified at various time points during a 90-min incubation period (Fig. 7). Reactions containing *Mt*CDH and lactose showed production of H_2O_2 that increased over time to ~150 μM after 90 mins. CBP21 alone did not generate H_2O_2 (Fig. 7B) but, expectedly, generated H_2O_2 when also ascorbate was added to the reaction (Fig. 7A). When CBP21 and its substrate, β-chitin were both present in the reaction containing either *Mt*CDH + lactose or ascorbate as electron donors, formation of H_2O_2 was very low and decreased over time. In fact, for the reaction with *Mt*CDH + lactose as electron donor, H_2O_2 could only be detected immediately

after mixing the reaction mixture constituents (~10 μM) and was below the detection limit of the assay in subsequent measurements. A similar trend was observed for ascorbate, but the initial level of H_2O_2 was slightly higher (~20 μM) and the decrease was slower, reaching ~5 μM after 90 minutes. In a control reaction, it was shown that the presence of chitohexaose, which is a soluble chitin fragment that is not cleaved by CPB21, had no effect on H_2O_2-production by the CDH-lactose-CBP21 system (Fig. 7B). Taken together, these observations show that reducing equivalents are channeled towards oxidative polysaccharide cleavage rather than direct oxygen reduction and that the presence of LPMO substrate prevents the formation of H_2O_2 by both CDH and the LPMO.

DISCUSSION

CDHs are universal electron donors for LPMOs. CDHs have been shown to act as an electron donor for several fungal family AA9 LPMOs (LPMO9s; [4, 19]). In the present study, we show that *Mt*CDH can efficiently transfer electrons from lactose to two bacterial LPMOs that only share 23% sequence identity, target different substrates and share less than 15 % sequence identity with their fungal counterparts (Fig. 2 & 3). Observed electron transfer rates up to 32 s^{-1} were reached, meaning that electron transfer from CDH to the bacterial LPMOs is as efficient as transfer to LPMO9s [25] or to other protein electron acceptors like cytochrome *c* [47]. This indicates that CDHs can act as a general electron donor for LPMOs, independent on LPMO origin and seemingly independent of LPMO sequence. It has been suggested that LPMO9s share a conserved region located distantly from the active site, which may have evolved to interact with the CDH cytochrome domain for electron transfer [48, 49]. This region is not conserved in the bacterial LPMO10s. A conserved site for potential protein-protein interactions was neither found on the surface of the cytochrome domain of CDH [25]. All in all, available data indicate that electron transfer between CDH and LPMOs does not depend on protein-protein interactions and conserved docking sites. Electron transfer is more likely to only involve the actual sites of oxidation and reduction, which, for LPMOs, is the copper site and its conserved histidine brace.

Putative protein electron donors in bacterial LPMO-containing chitinolytic/cellulolytic enzyme systems have not yet been identified, but the redox active protein "cbp2D" from *Cellvibrio japonicus* has been shown to be crucial for degradation of crystalline cellulose by the bacterium and has been proposed to represent a bacterial counterpart to CDH [50]. Clearly, fungal CDHs cannot be considered a natural electron donor for bacterial LPMOs, but, importantly, the present data add support to the emerging notion that LPMOs may receive electrons from many sources. The combination of a chitin-active LPMO (CBP21) with CDH

offered unprecedented possibilities for in-depth studies of the CDH-LPMO interplay, since CDH does not act on the LPMO substrate (which is chitin, not cellulose).

Use of MtCDH provides linear kinetics for CBP21. Despite intense research on LPMOs in recent years, kinetic data are scarce. It has been difficult to obtain linear progress curves which is likely due to the common use of small molecule electron donors such as ascorbate, reduced glutathinone, and L-cysteine. Such reducing agents are prone to autooxidation, which not only depletes the concentration of reductant, but also generates reactive oxygen species that can affect the stability of the proteins in the reaction. Indeed, a recent study reported that H_2O_2 generated by futile LPMO activity reduced the activity of the glycoside hydrolases present in the enzyme cocktail [51]. We show here that, when using an optimal LPMO:CDH ratio, the progress curves are linear until substrate depletion comes into play (Fig. 6A). Catalysis by LPMOs is slow (in the "per minute" range), whereas reduction of the LPMO active site copper can be substantially faster (in the "second range"; Fig. 2). With this in mind, it is not surprising that the data in Fig. 4 and Fig. 5 show that dosing of electrons is important. When feeding electrons too fast to the LPMOs, side reactions are likely to occur. While an initial faster product formation rate is obtained, LPMO activity ceases more rapidly, which not only may preclude kinetic analysis, but which also is disadvantageous in an applied setting. Comparison of Fig. 4 (CDH/lactose) with Fig. 5 (ascorbic acid) clearly shows that, when dosing the CDH optimally, CDH comprises a stable electron-donating system for the LPMO, in contrast to unstable ascorbic acid (Fig. 6A). Notably, the CDH/lactose system allows tuning of LPMO activity in chitin degradation reactions by simply regulating the concentration of lactose.

It is likely that ascorbate is depleted at the time point where the slope of the progress curves becomes drastically reduced (Figs. 4 & 6A). Interestingly, CBP21 activity does not completely cease after this time point (Fig. 6A), which means that CBP21 obtains electrons from elsewhere, possibly from the chitin itself. Indeed, the original discovery that CBP21 boosts

chitin degradation by chitinases was based on experiments that did not involve an externally added electron donor [44].

The electron donor is rate limiting for CBP21. While the data in Fig. 4 and Fig. 5 show that too high electron supply may be detrimental for overall process efficiency, they also clearly show that the availability of electrons is a rate limiting factor in the reaction. Looking only at initial CPB21 rates, there are clear dose-response effects. For ascorbate it seems that 5 mM is the optimal concentration, yielding an apparent initial rate of 13 min^{-1} (0.22 sec^{-1}) for CBP21 (Fig. 5). Interestingly, this is in the same range as the observed rates for a cellulose-active fungal LPMO using the highly efficient light-induced electron transfer system [52]. The increase to 10 mM ascorbate gives a similar initial rate, but a lower yield, indicating either enzyme inactivation or O_2 depletion through ascorbate autooxidation (O_2 depletion being less likely due to the rigorous shaking of the reaction mixture). The same trend (faster initial rate, but lower final yield) is observed when increasing the concentration of *Mt*CDH. *Mt*CDH is able to generate substantial amounts of H_2O_2 in the absence of an electron acceptor (Fig. 7) and one could thus expect production of H_2O_2 if there is a shortage of electron acceptor. It should be noted that H_2O_2 generated by either ascorbate or *Mt*CDH likely is the downstream product of other ROS generated, like $O_2^{\cdot -}$, which is more reactive than H_2O_2 and which may damage the enzymes.

Oxidation rates of lactose and chitin are equal. Under the conditions used here *Mt*CDH oxidized lactose at a steady-state turnover rate of appr. 1.1 min^{-1}. This is in agreement with the observed FAD re-oxidation rate of the oxidative half-reaction (k_{obs} = 3.2 min^{-1}), which represents the theoretical upper limit of CDH's oxygen reactivity. Fig. 2 shows that CBP21 is a much better electron acceptor for *Mt*CDH than oxygen with observed rates in the order of tenths per second. Consequently, in the presence of an LPMO and its substrate, lactose oxidation by *Mt*CDH did not lead to the formation of H_2O_2 (Fig. 7) indicating that *Mt*CDH

transfers the majority of its electrons to CBP21 and that CBP21 becomes re-oxidized by acting on its polysaccharide substrate. The slow steady-state turnover rate of chitin oxidation, compared to the fast electron transfer rate observed from *Mt*CDH to CBP21 in solution, indicates that the transfer of the first electron is not the rate-limiting step of the reaction. Furthermore, in order to perform successful catalysis, CBP21 must bind to the insoluble substrate, meaning that successful catalysis by the LPMO also depends on the substrate binding equilibrium (CBP21 has a binding dissociation constant of ~1 μM; [44]). Moreover, the monooxygenase reaction requires two electrons, thus requiring interaction with two reduced *Mt*CDH molecules (or the same molecule twice) to complete the catalytic cycle. The mechanism of LPMO reduction by *Mt*CDH is not known, but is thought to occur in part through direct reduction of the active site copper by *Mt*CDH's cytochrome domain [25]. While it is highly likely that transfer of the first electron [i.e. reduction of Cu(II) to Cu(I)] occurs in solution, the nature of the second electron transfer step is not clear. Several scenarios are thinkable, the discussion of which is beyond the scope of this paper. All these scenarios have possible rate-limiting steps, such as recruitment of the second electron and dissociation of the LPMO from the substrate, which may be the reason for the low overall catalytic rate.

Interestingly, our experimental approach, with quantification of chitobionic acid (product resulting from CBP21 catalysis), lactobionic acid (product resulting from *Mt*CDH catalysis) and reduction of O_2 to H_2O_2, allowed us to monitor the total flow of electrons in the reaction system. Thus we were able to show that under conditions where the carbohydrate substrates were not limiting and where the CBP21:*Mt*CDH ratio used yielded a linear progress curve, chitin and lactose were oxidized at an identical speed amounting to approximately ~3 μM min^{-1}. Since CDH-driven oxidation of one lactose molecule yields two electrons and the LPMO-driven oxidation of chitin is thought to require two electrons, our results indicate that the majority electrons generated by *Mt*CDH are consumed by CBP21 in the reaction. This is in

agreement with the low concentration of H_2O_2 in reactions containing CBP21, *Mt*CDH and the respective enzyme substrates (Fig. 7), i.e. little futile O_2 reduction takes place by either of the enzymes. These data thus support the proposed catalytic mechanism for LPMO mediated chitin oxidation [1, 49, 53].

In conclusion, the present data provide the first detailed insight into the activation of a bacterial LPMO by a protein electron donor and show how linear kinetics may be obtained by using such a donor. Clearly, LPMOs are good electron acceptors and it is conceivable that all natural LPMO containing enzyme systems depend on a carefully balanced cascade of enzymatic redox reactions that are optimized for biomass conversion (or other, yet to be discovered LPMO functionalities; [49]), while preventing non-desirable generation of reactive oxygen species.

FIGURE 1

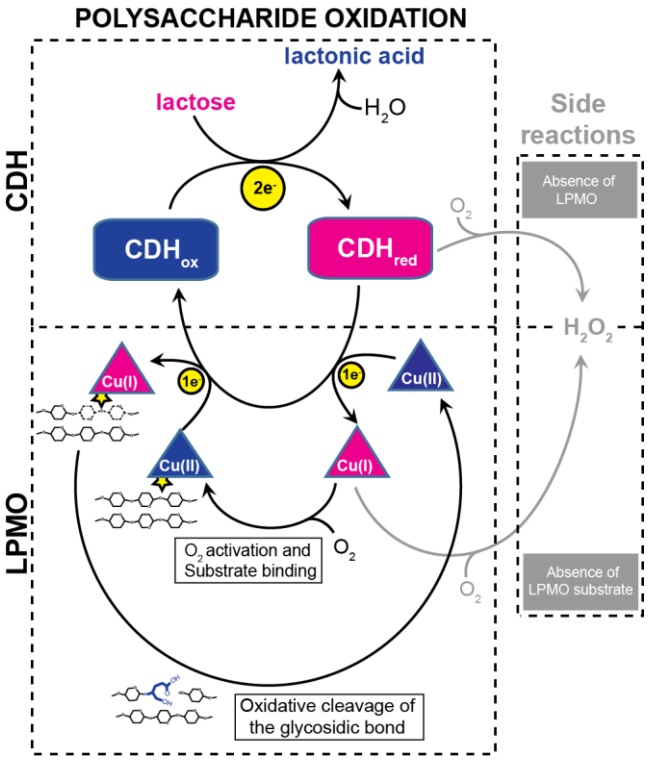

Figure 1. Lytic polysaccharide oxidation by the CDH-LPMO system. The LPMO is illustrated by a triangular cartoon, CDH in a square cartoon with rounded corners. Electrons are shown by yellow circles. Enzymes are colored blue in their oxidized form and pink in their reduced form. The LPMO substrate is indicated by two tethered chains representing a polysaccharide crystal.

FIGURE 2

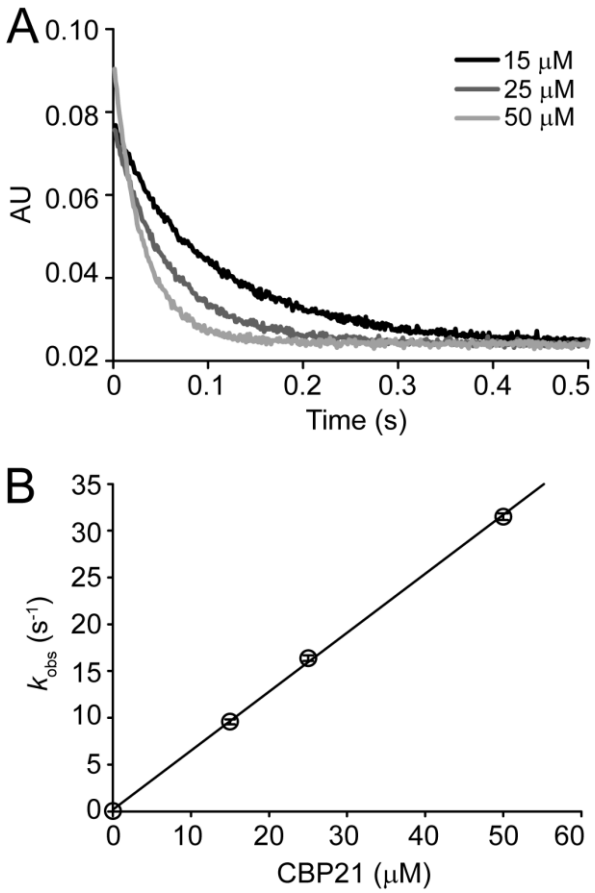

Figure 2. Reaction of reduced *Mt*CDH-heme with CBP21-Cu(II). (A) Oxidation of 5 μM *Mt*CDH by CBP21 (15, 25 and 50 μM) was followed in a stopped-flow spectrometer at 563nm. Observed electron transfer rates are plotted in (B). Partially reduced *Mt*CDH was obtained by reduction with cellobiose, in 50 mM sodium phosphate buffer, pH 6.0. Error bars show the standard deviation of 3 replicates. Concentrations are those after mixing.

FIGURE 3

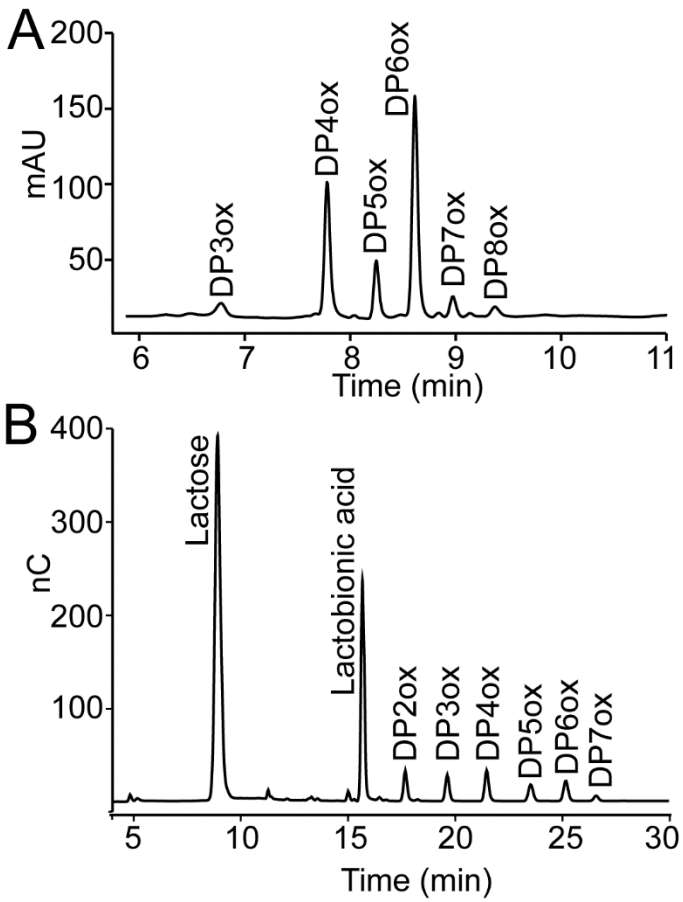

Figure 3. Product profiles from LPMO-CDH reactions. Chromatographic analysis of reaction products arising from incubation of 1.5 μM *Mt*CDH and 3.0 mM lactose with (A) 1.0 μM CBP21 and 10 mg/mL β-chitin or (B) 1.0 μM *Sc*LPMO10C and 10 mg/mL Avicel for 4 h. Both reactions were buffered in 25 mM Bis-Tris pH 6.0. Peaks are labeled as follows: DP, degree of polymerization; ox, oxidized at C1 (aldonic acids). In-house made standards were used to verify product identities and product distributions were also verified by MALDI-TOF MS (not shown). Some (small) peaks in both chromatograms were not possible to identify (unlabeled peaks in the chromatograms) and most likely represent background noise.

FIGURE 4

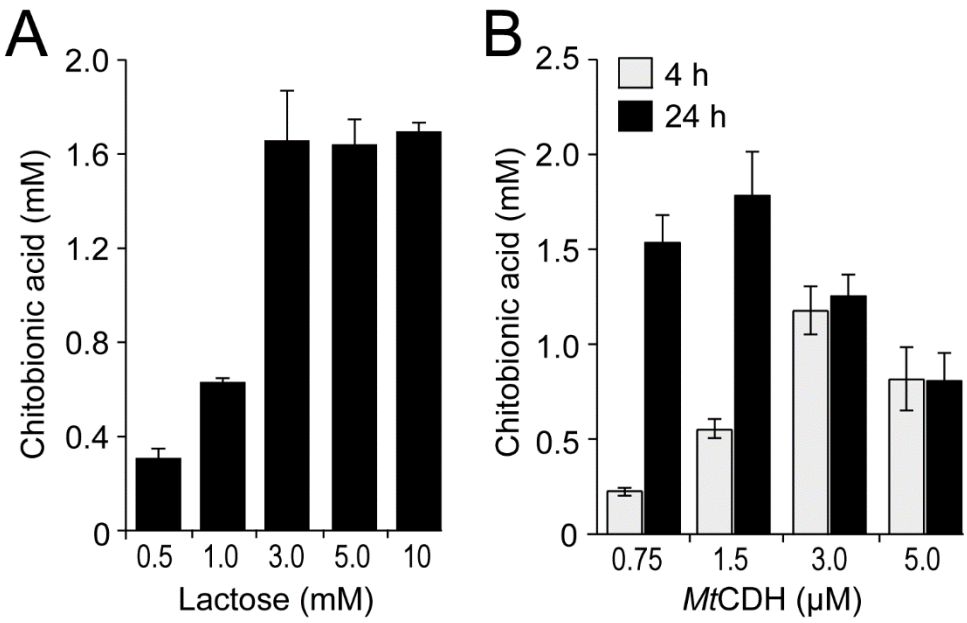

Figure 4. Dose-response experiments. Accumulation of oxidized products was measured after 4 h (grey bars, panel B only) and 24 h (black bars). (A) Degradation of 10 mg/mL β-chitin by 1.0 μM CBP21, 1.5 μM *Mt*CDH at varying concentrations of lactose. (B) Degradation of 10 mg/mL β-chitin by 1.0 μM CBP21 in the presence of 3.0 mM lactose and varying concentrations of *Mt*CDH. The standard deviations for all experiments are shown by error bars (n=3). All reactions (panels A and B) were buffered in 25 mM Bis-Tris, pH 6.0.

FIGURE 5

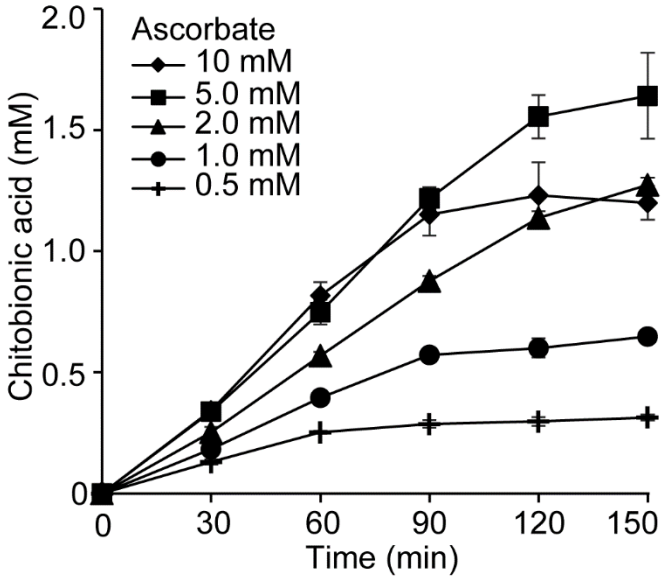

Figure 5. CBP21 activity at varying concentrations of ascorbic acid. Time course reactions were monitored for the degradation of 10 mg/mL β-chitin by 1.0 μM CBP21 in the presence of ascorbate concentrations ranging from 0.5 to 10 mM as indicated in the graph inset. Standard deviations are shown by error bars (n=3). All reactions were conducted in 50 mM Bis-Tris, pH 6.0.

FIGURE 6

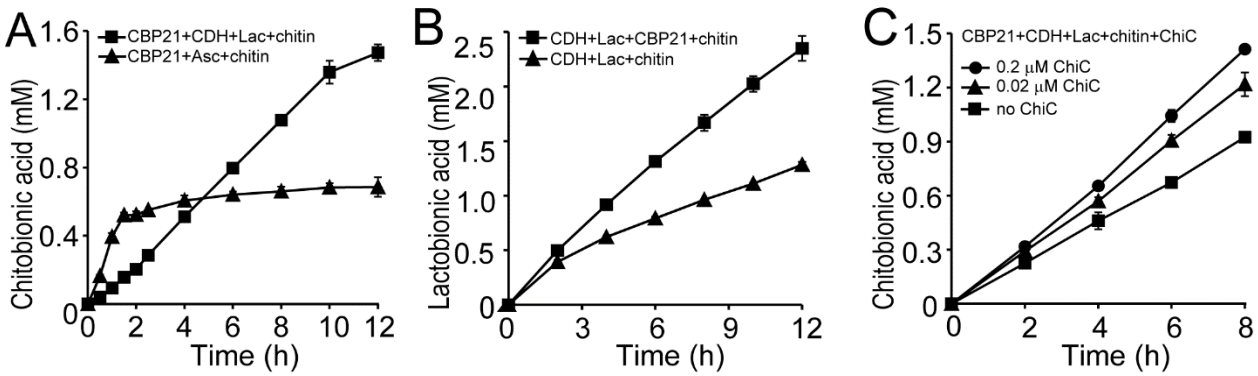

Figure 6. Degradation of β-chitin by CBP21 and oxidation of lactose by *Mt*CDH. (A) Time course analysis of degradation of 10 mg/ml β-chitin (equivalent to 24.6 mM chitobiose) by 1.0 μM CBP21 using either 1.5 μM *Mt*CDH and 3.0 mM lactose (squares) or 1.0 mM ascorbate (triangles) as reducing agents. (B) Oxidation of lactose by 1.5 μM *Mt*CDH in the presence (squares) or absence (triangles) of 1.0 μM CBP21. (C) Degradation of β-chitin by 1.0 μM CBP21 in the presence of 1.5 μM *Mt*CDH, 3.0 mM lactose and 0, 0.02 or 0.2 μM ChiC. All reactions contained 10 mg/ml β-chitin. The standard deviations for all experiments are shown by error bars (n=3). All reactions (panels A, B and C) were buffered in 25 mM Bis-Tris, pH 6.0.

FIGURE 7

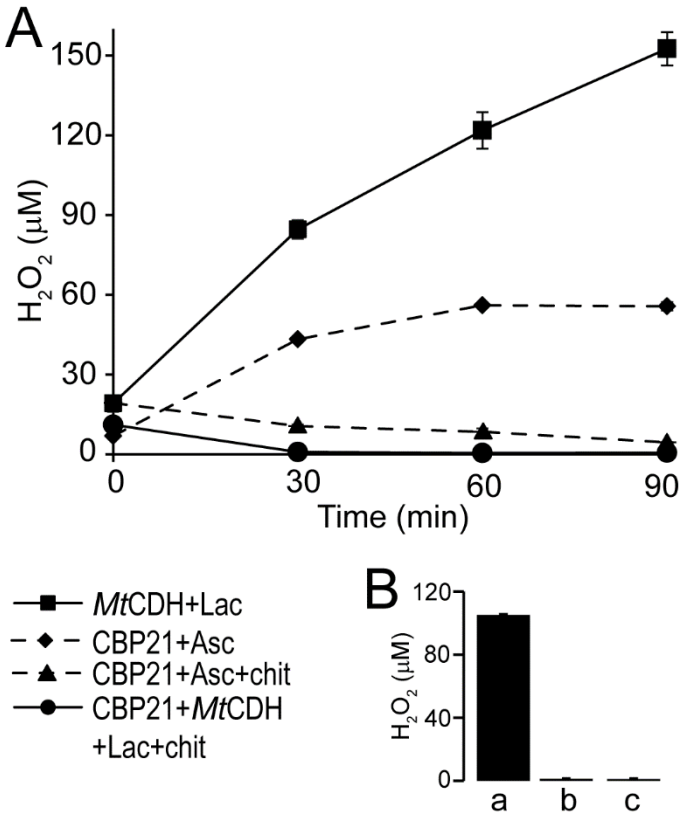

Figure 7. Analysis of H_2O_2 generated in reactions containing CBP21 and *Mt*CDH. (A) Time course analysis of H_2O_2 generated in reactions containing 1.0 μM CBP21 and 1.0 mM ascorbate (diamonds), 1.0 μM CBP21, 1.0 mM ascorbate and 10 mg/mL β-chitin (triangles), 1.5 μM *Mt*CDH and 3.0 mM lactose (squares) and 1.5 μM *Mt*CDH, 3.0 mM lactose, 1.0 μM CBP21 and 10 mg/mL β-chitin (circles). (B) Control experiments showing generation of H_2O_2 in reactions containing 0.9 mM $(GlcNAc)_6$, 1.0 μM CBP21, 1.5 μM *Mt*CDH and 3.0 mM lactose (a), 1.0 μM CBP21 in buffer (b) and 1.5 μM *Mt*CDH in buffer (c). Reactions were analyzed after 90 min incubation at 40°C and 1000 rpm. All reactions (panels A and B) were buffered in 25 mM Bis-Tris, pH 6.0. Standard deviations for all experiments are shown by error bars (n=3).

AUTHOR INFORMATION

Corresponding Author

*To whom correspondence should be addressed: Gustav Vaaje-Kolstad, Department of Chemistry, Biotechnology, and Food Science, The Norwegian University of Life Sciences, 1432 Ås, Norway, Tel.: +47 67232573; E-mail: gustav.vaaje-kolstad@nmbu.no

Author Contributions

J.S.M.L. designed, performed and analyzed the experiments, and wrote the paper. Z.F. designed, performed and analyzed the experiments and contributed to writing the paper. D.K. designed and supervised stopped-flow experiments and wrote parts of the paper. S.S. analyzed stopped-flow experiments and drew graphs for the paper. R.L. analyzed fast kinetic data and wrote parts of the paper. V.G.H.E. proposed experiments, analyzed data and wrote parts of the paper. G.V-K. initiated and supervised the project, proposed experiments, analyzed data and wrote parts of the paper.

Conflict of interest

The authors declare that they have no conflicts of interest with the contents of this article.

ABBREVIATIONS

AA, auxiliary activity; LPMO, lytic polysaccharide monooxygenase; CDH, cellobiose dehydrogenase; FAD, flavin adenine dinucleotide; CYT, cytochrome; DH, dehydrogenase; CAZy, carbohydrate-active enzyme database; CAZymes, carbohydrate-active enzymes; DP, degree of polymerization; ox, oxidized.

REFERENCES

(1) Vaaje-Kolstad, G., Westereng, B., Horn, S. J., Liu, Z., Zhai, H., Sørlie, M., and Eijsink, V. G. H. (2010) An oxidative enzyme boosting the enzymatic conversion of recalcitrant polysaccharides, *Science 330*, 219-222.

(2) Forsberg, Z., Vaaje-Kolstad, G., Westereng, B., Bunæs, A. C., Stenstrøm, Y., MacKenzie, A., Sørlie, M., Horn, S. J., and Eijsink, V. G. H. (2011) Cleavage of cellulose by a CBM33 protein, *Protein Sci. 20*, 1479-1483.

(3) Quinlan, R. J., Sweeney, M. D., Lo Leggio, L., Otten, H., Poulsen, J. C., Johansen, K. S., Krogh, K. B., Jørgensen, C. I., Tovborg, M., Anthonsen, A., Tryfona, T., Walter, C. P., Dupree, P., Xu, F., Davies, G. J., and Walton, P. H. (2011) Insights into the oxidative degradation of cellulose by a copper metalloenzyme that exploits biomass components, *Proc. Natl. Acad. Sci. U.S.A. 108*, 15079-15084.

(4) Phillips, C. M., Beeson, W. T., Cate, J. H., and Marletta, M. A. (2011) Cellobiose dehydrogenase and a copper-dependent polysaccharide monooxygenase potentiate cellulose degradation by *Neurospora crassa*, *ACS Chem. Biol. 6*, 1399-1406.

(5) Horn, S. J., Vaaje-Kolstad, G., Westereng, B., and Eijsink, V. G. H. (2012) Novel enzymes for the degradation of cellulose, *Biotechnol. Biofuels 5*, 45.

(6) Agger, J. W., Isaksen, T., Várnai, A., Vidal-Melgosa, S., Willats, W. G., Ludwig, R., Horn, S. J., Eijsink, V. G. H., and Westereng, B. (2014) Discovery of LPMO activity on hemicelluloses shows the importance of oxidative processes in plant cell wall degradation, *Proc. Natl. Acad. Sci. U.S.A. 111*, 6287-6292.

(7) Frommhagen, M., Sforza, S., Westphal, A. H., Visser, J., Hinz, S. W. A., Koetsier, M. J., van Berkel, W. J. H., Gruppen, H., and Kabel, M. A. (2015) Discovery of the combined oxidative cleavage of plant xylan and cellulose by a new fungal polysaccharide monooxygenase, *Biotechnol. Biofuels 8*, 101.

(8) Isaksen, T., Westereng, B., Aachmann, F. L., Agger, J. W., Kracher, D., Kittl, R., Ludwig, R., Haltrich, D., Eijsink, V. G. H., and Horn, S. J. (2014) A C4-oxidizing lytic polysaccharide monooxygenase cleaving both cellulose and cello-oligosaccharides, *J. Biol. Chem. 289*, 2632-2642.

(9) Lo Leggio, L., Simmons, T. J., Poulsen, J. C., Frandsen, K. E., Hemsworth, G. R., Stringer, M. A., von Freiesleben, P., Tovborg, M., Johansen, K. S., De Maria, L., Harris, P. V., Soong, C. L., Dupree, P., Tryfona, T., Lenfant, N., Henrissat, B., Davies, G. J., and Walton, P. H. (2015) Structure and boosting activity of a starch-degrading lytic polysaccharide monooxygenase, *Nat. Commun. 6*, 5961.

(10) Levasseur, A., Drula, E., Lombard, V., Coutinho, P. M., and Henrissat, B. (2013) Expansion of the enzymatic repertoire of the CAZy database to integrate auxiliary redox enzymes, *Biotechnol. Biofuels 6*, 41.

(11) Aachmann, F. L., Sørlie, M., Skjåk-Bræk, G., Eijsink, V. G. H., and Vaaje-Kolstad, G. (2012) NMR structure of a lytic polysaccharide monooxygenase provides insight into copper binding, protein dynamics, and substrate interactions, *Proc. Natl. Acad. Sci. U.S.A. 109*, 18779-18784.

(12) Hemsworth, G. R., Taylor, E. J., Kim, R. Q., Gregory, R. C., Lewis, S. J., Turkenburg, J. P., Parkin, A., Davies, G. J., and Walton, P. H. (2013) The copper active site of CBM33 polysaccharide oxygenases, *J. Am. Chem. Soc. 135*, 6069-6077.

(13) Kim, S., Ståhlberg, J., Sandgren, M., Paton, R. S., and Beckham, G. T. (2014) Quantum mechanical calculations suggest that lytic polysaccharide monooxygenases use a copper-oxyl, oxygen-rebound mechanism, *Proceedings of the National Academy of Sciences of the United States of America 111*, 149-154.

(14) Walton, P. H., and Davies, G. J. (2016) On the catalytic mechanisms of lytic polysaccharide monooxygenases, *Curr Opin Chem Biol 31*, 195-207.

(15) Beeson, W. T., Phillips, C. M., Cate, J. H., and Marletta, M. A. (2012) Oxidative cleavage of cellulose by fungal copper-dependent polysaccharide monooxygenases, *Journal of the American Chemical Society 134*, 890-892.

(16) Dimarogona, M., Topakas, E., and Christakopoulos, P. (2013) Recalcitrant polysaccharide degradation by novel oxidative biocatalysts, *Appl. Microbiol. Biotechnol. 97*, 8455-8465.

(17) Dimarogona, M., Topakas, E., Olsson, L., and Christakopoulos, P. (2012) Lignin boosts the cellulase performance of a GH-61 enzyme from *Sporotrichum thermophile*, *Bioresour. Technol. 110*, 480-487.

(18) Westereng, B., Cannella, D., Agger, J. W., Jørgensen, H., Andersen, M. L., Eijsink, V. G. H., and Felby, C. (2015) Enzymatic cellulose oxidation is linked to lignin by long-range electron transfer, *Sci. Rep. 5*, 18561.

(19) Langston, J. A., Shaghasi, T., Abbate, E., Xu, F., Vlasenko, E., and Sweeney, M. D. (2011) Oxidoreductive cellulose depolymerization by the enzymes cellobiose dehydrogenase and glycoside hydrolase 61, *Appl. Environ. Microbiol. 77*, 7007-7015.

(20) Sygmund, C., Kracher, D., Scheiblbrandner, S., Zahma, K., Felice, A. K., Harreither, W., Kittl, R., and Ludwig, R. (2012) Characterization of the two *Neurospora crassa* cellobiose dehydrogenases and their connection to oxidative cellulose degradation, *Appl. Environ. Microbiol. 78*, 6161-6171.

(21) Kracher, D., Scheiblbrandner, S., Felice, A. K., Breslmayr, E., Preims, M., Ludwicka, K., Haltrich, D., Eijsink, V. G., and Ludwig, R. (2016) Extracellular electron transfer systems fuel cellulose oxidative degradation, *Science*.

(22) Yakovlev, I., Vaaje-Kolstad, G., Hietala, A. M., Stefanczyk, E., Solheim, H., and Fossdal, C. G. (2012) Substrate-specific transcription of the enigmatic GH61 family of the pathogenic white-rot fungus *Heterobasidion irregulare* during growth on lignocellulose, *Appl. Microbiol. Biotechnol. 95*, 979-990.

(23) Wymelenberg, A. V., Gaskell, J., Mozuch, M., Sabat, G., Ralph, J., Skyba, O., Mansfield, S. D., Blanchette, R. A., Martinez, D., Grigoriev, I., Kersten, P. J., and Cullen, D. (2010) Comparative transcriptome and secretome analysis of wood decay fungi *Postia placenta* and *Phanerochaete chrysosporium*, *Appl. Environ. Microbiol. 76*, 3599-3610.

(24) Phillips, C. M., Iavarone, A. T., and Marletta, M. A. (2011) Quantitative proteomic approach for cellulose degradation by *Neurospora crassa*, *J. Proteome Res. 10*, 4177-4185.

(25) Tan, T. C., Kracher, D., Gandini, R., Sygmund, C., Kittl, R., Haltrich, D., Hallberg, B. M., Ludwig, R., and Divne, C. (2015) Structural basis for cellobiose dehydrogenase action during oxidative cellulose degradation, *Nat. Commun. 6*, 7542.

(26) Cameron, M. D., and Aust, S. D. (2001) Cellobiose dehydrogenase-an extracellular fungal flavocytochrome, *Enzyme Microb. Technol. 28*, 129-138.

(27) Igarashi, K., Momohara, I., Nishino, T., and Samejima, M. (2002) Kinetics of inter-domain electron transfer in flavocytochrome cellobiose dehydrogenase from the white-rot fungus *Phanerochaete chrysosporium*, *Biochem. J. 365*, 521-526.

(28) Zamocky, M., Ludwig, R., Peterbauer, C., Hallberg, B. M., Divne, C., Nicholls, P., and Haltrich, D. (2006) Cellobiose dehydrogenase-a flavocytochrome from wood-degrading, phytopathogenic and saprotropic fungi, *Curr. Protein Pept. Sci. 7*, 255-280.

(29) Samejima, M., and Eriksson, K. E. L. (1992) A Comparison of the catalytic properties of cellobiose - quinone oxidoreductase and cellobiose oxidase from *Phanerochaete chrysosporium*, *Eur. J. Biochem. 207*, 103-107.

(30) Schou, C., Christensen, M. H., and Schülein, M. (1998) Characterization of a cellobiose dehydrogenase from *Humicola insolens*, *Biochem. J. 330*, 565-571.

(31) Baminger, U., Subramaniam, S. S., Renganathan, V., and Haltrich, D. (2001) Purification and characterization of cellobiose dehydrogenase from the plant pathogen *Sclerotium* (*Athelia*) *rolfsii*, *Appl. Environ. Microbiol. 67*, 1766-1774.

(32) Mason, M. G., Nicholls, P., Divne, C., Hallberg, B. M., Henriksson, G., and Wilson, M. T. (2003) The heme domain of cellobiose oxidoreductase: a one-electron reducing system, *Biochim. Biophys. Acta 1604*, 47-54.

(33) Thallinger, B., Argirova, M., Lesseva, M., Ludwig, R., Sygmund, C., Schlick, A., Nyanhongo, G. S., and Guebitz, G. M. (2014) Preventing microbial colonisation of catheters: Antimicrobial and antibiofilm activities of cellobiose dehydrogenase, *Int. J. Antimicrob. Agents 44*, 402-408.

(34) McDonnell, G., and Russell, A. D. (1999) Antiseptics and disinfectants: Activity, action, and resistance, *Clin. Microbiol. Rev. 12*, 147-179.

(35) Wood, P. M. (1988) The potential diagram for oxygen at pH 7, *Biochem. J. 253*, 287-289.

(36) Kirk, T. K., Ibach, R., Mozuch, M. D., Conner, A. H., and Highley, T. L. (1991) Characteristics of cotton cellulose depolymerized by a brown-rot fungus, by acid, or by chemical oxidants, *Holzforschung 45*, 239-244.

(37) Hyde, S. M., and Wood, P. M. (1997) A mechanism for production of hydroxyl radicals by the brown-rot fungus *Coniophora puteana*: Fe(III) reduction by cellobiose dehydrogenase and Fe(II) oxidation at a distance from the hyphae, *Microbiol-Uk 143*, 259-266.

(38) Kremer, S. M., and Wood, P. M. (1992) Production of fenton reagent by cellobiose oxidase from cellulolytic cultures of *Phanerochaete chrysosporium*, *Eur. J. Biochem. 208*, 807-814.

(39) Kittl, R., Kracher, D., Burgstaller, D., Haltrich, D., and Ludwig, R. (2012) Production of four *Neurospora crassa* lytic polysaccharide monooxygenases in *Pichia pastoris* monitored by a fluorimetric assay, *Biotechnol. Biofuels 5*, 79.

(40) Zamocky, M., Schümann, C., Sygmund, C., O'Callaghan, J., Dobson, A. D. W., Ludwig, R., Haltrich, D., and Peterbauer, C. K. (2008) Cloning, sequence analysis and heterologous expression in *Pichia pastoris* of a gene encoding a thermostable cellobiose dehydrogenase from *Myriococcum thermophilum*, *Protein Expr. Purif. 59*, 258-265.

(41) Forsberg, Z., Mackenzie, A. K., Sørlie, M., Røhr, Å. K., Helland, R., Arvai, A. S., Vaaje-Kolstad, G., and Eijsink, V. G. H. (2014) Structural and functional characterization of a conserved pair of bacterial cellulose-oxidizing lytic polysaccharide monooxygenases, *Proc. Natl. Acad. Sci. U.S.A. 111*, 8446-8451.

(42) Manoil, C., and Beckwith, J. (1986) A Genetic approach to analyzing membrane-protein topology, *Science 233*, 1403-1408.

(43) Loose, J. S. M., Forsberg, Z., Fraaije, M. W., Eijsink, V. G. H., and Vaaje-Kolstad, G. (2014) A rapid quantitative activity assay shows that the *Vibrio cholerae* colonization factor GbpA is an active lytic polysaccharide monooxygenase, *FEBS Lett. 588*, 3435-3440.

(44) Vaaje-Kolstad, G., Houston, D. R., Riemen, A. H., Eijsink, V. G. H., and van Aalten, D. M. (2005) Crystal structure and binding properties of the *Serratia marcescens* chitin-binding protein CBP21, *J. Biol. Chem. 280*, 11313-11319.

(45) Heuts, D. P. H. M., Winter, R. T., Damsma, G. E., Janssen, D. B., and Fraaije, M. W. (2008) The role of double covalent flavin binding in chito-oligosaccharide oxidase from *Fusarium graminearum*, *Biochem. J. 413*, 175-183.

(46) Westereng, B., Agger, J. W., Horn, S. J., Vaaje-Kolstad, G., Aachmann, F. L., Stenstrøm, Y. H., and Eijsink, V. G. H. (2013) Efficient separation of oxidized cello-oligosaccharides generated by cellulose degrading lytic polysaccharide monooxygenases, *J. Chromatogr. A 1271*, 144-152.

(47) Rogers, M. S., Jones, G. D., Antonini, G., Wilson, M. T., and Brunori, M. (1994) Electron-transfer from *Phanerochaete chrysosporium* cellobiose oxidase to equine cytochrome c and *Pseudomonas aeruginosa* cytochrome c-551, *Biochem. J. 298*, 329-334.

(48) Li, X., Beeson, W. T., Phillips, C. M., Marletta, M. A., and Cate, J. H. D. (2012) Structural basis for substrate targeting and catalysis by fungal polysaccharide monooxygenases, *Structure 20*, 1051-1061.

(49) Beeson, W. T., Vu, V. V., Span, E. A., Phillips, C. M., and Marletta, M. A. (2015) Cellulose degradation by polysaccharide monooxygenases, *Annu. Rev. Biochem. 84*, 923-946.

(50) Gardner, J. G., Crouch, L., Labourel, A., Forsberg, Z., Bukhman, Y. V., Vaaje-Kolstad, G., Gilbert, H. J., and Keating, D. H. (2014) Systems biology defines the biological significance of redox-active proteins during cellulose degradation in an aerobic bacterium, *Mol. Microbiol. 94*, 1121-1133.

(51) Scott, B. R., Huang, H. Z., Frickman, J., Halvorsen, R., and Johansen, K. S. (2015) Catalase improves saccharification of lignocellulose by reducing lytic polysaccharide monooxygenase-associated enzyme inactivation, *Biotechnol. Lett. 38*, 425-434.

(52) Cannella, D., Möllers, K. B., Frigaard, N. U., Jensen, P. E., Bjerrum, M. J., Johansen, K. S., and Felby, C. (2016) Light-driven oxidation of polysaccharides by photosynthetic pigments and a metalloenzyme, *Nat. Commun. 7*, 11134.

(53) Hemsworth, G. R., Henrissat, B., Davies, G. J., and Walton, P. H. (2014) Discovery and characterization of a new family of lytic polysaccharide monooxygenases, *Nat. Chem. Biol. 10*, 122-126.

GRAPHIC FOR THE TABLE OF CONTENTS

For Table of Contents Use Only

Activation of Bacterial Lytic Polysaccharide Monooxygenases with Cellobiose Dehydrogenase

*Jennifer S.M. Loose[1], Zarah Forsberg[1], Daniel Kracher[2], Stefan Scheiblbrandner[2], Roland Ludwig[2], Vincent G.H. Eijsink[1] and Gustav Vaaje-Kolstad[1]**

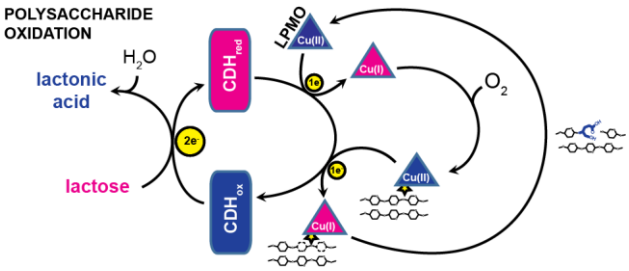

Paper III

Insights into catalysis by lytic polysaccharide monooxygenases through site-directed mutagenesis of CBP21 from *Serratia marcescens*

Jennifer S.M. Loose, Åsmund K. Røhr, Bastien Bissaro, Daniel Kracher, Roland Ludwig, Morten Sørlie, Vincent G.H. Eijsink, Gustav Vaaje-Kolstad, 2016

Manuscript in preparation

Insights into catalysis by lytic polysaccharide monooxygenases through site-directed mutagenesis of CBP21 from *Serratia marcescens*

Jennifer S.M. Loose , Åsmund K. Røhr , Bastien Bissaro , Daniel Kracher , Roland Ludwig , Morten Sørlie , Vincent G.H. Eijsink and Gustav Vaaje-Kolstad *

Department of Chemistry, Biotechnology and Food Science, Norwegian University of Life Sciences, Ås, Norway.

University of Natural Resources and Life Sciences, Department of Food Sciences and Technology, Food Biotechnology Laboratory, Vienna, Austria.

*To whom correspondence should be addressed: Gustav Vaaje-Kolstad, Department of Chemistry, Biotechnology, and Food Science, The Norwegian University of Life Sciences (NMBU), 1432 Ås, Norway, Tel.: +47 67232573; E-mail: gustav.vaaje-kolstad@nmbu.no

Abstract

Lytic polysaccharide monooxygenases (LPMOs) catalyze the oxidative cleavage of glycosidic bonds in the presence of dioxygen and an external electron donor. LPMOs act in synergy with glycoside hydrolases and play an important role in the conversion of biomass. Even though these enzymes have been intensely studied in the past few years, several aspects of their catalytic mechanism and their mode of action remain unclear. In the present study, we present a comprehensive, in-depth study of the enzymatic properties of a chitin-active family AA10 LPMO, CBP21, from the soil bacterium *Serratia marcescens*. The roles of 13 amino acids putatively involved in substrate binding and/or catalysis were investigated. Activity data revealed several residues that are essential for activity. Interestingly, several mutations that reduced overall enzyme performance did not affect the catalytic rate of the enzyme, but rather its lifetime. Most mutations leading to reduced enzyme performance also had a negative effect on the enzyme's affinity for chitin, suggesting that substrate binding prevents premature enzyme inactivation. Several mutants showed a change in the rate of electron transfer from a cellobiose dehydrogenase to CBP21 in solution, but these changes did not correlate with changes of catalytic performance, indicating that this process is not rate limiting for the LPMO reaction. Finally, electron paramagnetic resonance spectroscopy revealed mutations that altered copper coordination geometry in the active site. These mutations included residues distant from the copper ion, which possibly explains why these residues are important for catalytic performance.

INTRODUCTION

Lytic polysaccharide monooxygenases (LPMOs) are copper-dependent redox enzymes that cleave glycosidic bonds of polysaccharides by an oxidative mechanism (Vaaje-Kolstad et al., 2010, Forsberg et al., 2011, Quinlan et al., 2011, Phillips et al., 2011, Horn et al., 2012). Based on sequence similarity, these enzymes are divided into four different families of the auxiliary activities (AA) in the CAZy database, AA9, AA10, AA11 and AA13 (Lombard et al., 2014, Levasseur et al., 2013). Genes encoding LPMOs are found in the genomes of organisms representing all three domains of life, namely eukaryota, bacteria and archaea, and are especially abundant amongst fungi and bacteria. So far, the AA9 and AA13 families only contain fungal enzymes, whereas AA11s occur in fungi and bacteria and AA10s can be found in fungi, bacteria, archaea and viruses.

The ubiquitous occurrence of LPMOs indicates that these enzymes are of major importance. Indeed, it has been shown that LPMOs act synergistically with biomass degrading glycoside hydrolases (Harris et al., 2010, Vaaje-Kolstad et al., 2010, Forsberg et al., 2011, Nakagawa et al., 2015, Müller et al., 2015, Vaaje-Kolstad et al., 2012), and hence play a crucial role in the conversion of recalcitrant biomass and the global carbon cycle. LPMOs commonly act on insoluble, recalcitrant substrates such as chitin and cellulose (Vaaje-Kolstad et al., 2010, Forsberg et al., 2011, Quinlan et al., 2011), but cleavage of xyloglucan (Agger et al., 2014), xylan (Frommhagen et al., 2015), starch (Vu et al., 2014, Lo Leggio et al., 2015) and soluble cello-oligosaccharides (Isaksen et al., 2014) has also been observed. Interestingly, some LPMOs have been identified as virulence factors in bacteria (Kirn et al., 2005, Chaudhuri et al., 2010), indicating that LPMOs may have additional biological roles. The biologically relevant substrates for these latter LPMOs have yet to be found but activity on chitin has been demonstrated for some of them (Loose et al., 2014, Paspaliari et al., 2015).

Since their discovery in 2010, a substantial effort has been made to shed light on LPMO-activity and the underlying reaction mechanism. All LPMOs structurally analyzed to date possess a core structure consisting of two β-sheets that resemble a fibronectin or immunoglobin-fold (Beeson et al., 2015). Loops connecting the β-strands form parts of the active site and the substrate binding surface and show large variation. Most LPMOs possess a relatively flat substrate binding surface (Vaaje-Kolstad et al., 2005b, Karkehabadi et al., 2008), that most likely enables the enzymes to interact with crystalline substrates. Interactions with

substrate seem to involve several polar interactions, whereas aromatic side chains contribute via aromatic-carbohydrate π interactions, especially for cellulose-active LPMOs (Li et al., 2012, Beeson et al., 2015, Wu et al., 2013, Vaaje-Kolstad et al., 2005a, Vaaje-Kolstad et al., 2005b, Aachmann et al., 2012, Courtade et al., 2016, Frandsen et al., 2016). Recent structural investigations of an LPMO9 with bound cello-oligomers have revealed that a hydrogen bonding network between the oligosaccharide and the protein holds the ligand in place (Frandsen et al., 2016). The chitin active AA10-type LPMO CBP21 (or *Sm*LPMO10A) has been studied thoroughly when it comes to substrate binding. Site-directed mutagenesis studies showed that, next to a solvent exposed tyrosine and one of the histidines involved in copper coordination, at least four polar amino acids are important for substrate binding (Vaaje-Kolstad et al., 2005b). The importance of polar residues in chitin binding by CBP21 was later confirmed by NMR studies (Aachmann et al., 2012).

The central catalytic feature of LPMOs is the so-called histidine brace that coordinates the copper (Quinlan et al., 2011, Aachmann et al., 2012, Hemsworth et al., 2013a). EPR studies on a fungal cellulose-active LPMO9 revealed the presence of a type 2 copper center. The ligands were identified by X-ray crystallography, showing a T-shaped histidine brace comprising the N-terminal histidine, its (N-terminal) amino group, and another histidine. Additional coordination sites for the copper are usually occupied by water in the remaining equatorial position, a conserved tyrosine in the proximal (i.e. towards the protein center) axial position and an additional water molecule in the distal (solvent-exposed) axial position (Quinlan et al., 2011). The T-shaped histidine brace also occurs in AA10-type LPMOs, but in most AA10s the axial tyrosine is replaced by a phenylalanine. Notably, the presence of water ligands depends on the oxidation state of the copper (Hemsworth et al., 2013b, Gudmundsson et al., 2014). Furthermore, LPMOs seem to vary as to the accessibility of the distal axial copper coordination site due to structural variation (Hemsworth et al., 2013b, Forsberg et al., 2014a, Borisova et al., 2015). In EPR studies on a chitin-binding AA10, the copper active site could not clearly be assigned to site to type 1 or 2 in the Peisach-Blumberg classification (Peisach and Blumberg, 1974). Even though the overall axial envelope suggests a type 2 copper center, the spin Hamiltonian tensors fall between the classifications (Hemsworth et al., 2013b). The copper sites of other chitin-active AA10s also fall between type 1 and 2, whereas the copper sites of two cellulose-active AA10s, CelS2 and E8, can clearly be assigned to type 2 copper (Forsberg et al., 2014b). These observations suggested a correlation between the type of copper center

and substrate specificity (Forsberg et al., 2014b), but recently, chitin-active *Cj*LPMO10A was shown to possess a type 2 copper center (Forsberg et al., 2016).

For reactivity, LPMOs require molecular oxygen and an external reductant (Vaaje-Kolstad et al., 2010). A wide array of reductants has been used in experiments, including small-molecule electron donors such as ascorbic acid (Vaaje-Kolstad et al., 2010) and gallic acid (Quinlan et al., 2011), lignin (Dimarogona et al., 2012, Westereng et al., 2015, Hu et al., 2014), and redox active enzymes including cellobiose dehydrogenase (Phillips et al., 2011, Langston et al., 2011, Sygmund et al., 2012) or other family AA3_2 flavoenzymes (Garajova et al., 2016) that may use phenolic compounds as electron shuttles (Kracher et al., 2016).

Although details of catalysis by LPMOs remain unknown, several reaction mechanisms have been proposed. Common for all is that the initial step of catalysis involves activation of O_2 by a reduced active-site copper (Cu(I)), forming a Cu(II)-superoxide intermediate. The species that performs the hydrogen abstraction from the substrate can either be this intermediate (Phillips et al., 2011, Beeson et al., 2012) or an oxidatively more powerful species such as an oxyl radical (Kim et al., 2014). It has been noted that catalysis may involve formation of Cu(III) species, such as a Cu(III)-oxyl radical, which could perhaps be stabilized by the conserved tyrosine/ate residue in those LPMOs that contain this residue (Beeson et al., 2015).

Proton abstraction and subsequent hydroxylation of the substrate can take place at two positions, leading to oxidation of either the C1 carbon or the C4 carbon in the scissile β-1,4-glycosidic bond. The products formed by the reaction are a δ-1,5-lactone (C1 oxidation) or a 4-ketoaldose (C4 oxidation) which are in a pH-dependent equilibrium with their hydrated forms, an aldonic acid and a geminal diol respectively. The oxidative region-selectivity is not absolute and some LPMOs produce both C1 and C4 oxidized products. So far, C4 oxidation or combined C1/C4 oxidation has only been observed for LPMOs acting on β-glucans.

Current ideas about catalysis by LPMOs are derived from structural and computational studies, as well as studies of model-complexes (Beeson et al., 2015, Walton and Davies, 2016). Other experimental data on LPMO functionality are scarce. For example, only a very few studies have probed the contributions of various LPMO surface-residues to substrate-binding and catalysis using site-directed mutagenesis and the mutants that have been made have not been characterized in detail (Harris et al., 2010; Vaaje-Kolstad et al., 2005a,b). In order to gain more insight into the contributions of various residues to LPMO activity, we have carried out site-

directed mutagenesis using the chitin-active LPMO10 from *Serratia marcescens* called CBP21 or *Sm*LPMO10A. Mutational effects were characterized by analyzing substrate affinity and by measuring catalytic activity using a small molecule reductant or an enzymatic electron donor. Differences between the two reduction modes were detected. Additionally, electron transfer rates from the protein electron donor to the LPMO were measured for all variants. We also assessed mutational effects on the copper site by EPR, a method that is very sensitive to conformational changes around the paramagnetic ion. Thus, we have generated a unique experimental data set of in-depth characterized LPMO variants that takes us closer to understanding the LPMO reaction mechanism.

EXPERIMENTAL PROCEDURES

Cloning, Site-directed Mutagenesis, Protein Expression and Purification

Cellobiose Dehydrogenase from *Myriococcum thermophilum* with a C-terminal His_6-tag was expressed in *Pichia pastoris* and purified as previously described by Zamocky et al. (2008) with an additional immobilized metal affinity step (all equipment from GE Healthcare, Little Chalfont, United Kingdom). The purification was carried out first by hydrophobic interaction chromatography (PHE-Sepharose FF resin) then by immobilized metal affinity chromatography (HisTrap FF resin) and as a last step by anion exchange chromatography (Q-source). The protein concentration was determined using the Bradford method (Biorad, Hercules, USA)

CBP21 from *Serratia marcescens* (also known as *Sm*LPMO10A) and all its variants were expressed and purified as previously reported by Vaaje-Kolstad et al. (Vaaje-Kolstad et al., 2005b). Briefly, *E. coli* BL21 star (DE3) cells containing the pRSETB vector with the *cbp21* gene were grown at 37°C overnight in two times 500 mL TB-medium containing 8.5 mM KH_2PO_4 and 36 mM K_2HPO_4, and 100 µg/mL ampicillin using a Harbinger LEX bioreactor (Harbinger Biotech, Toronto, Canada). The cells were collected by centrifugation and the protein was isolated from the periplasmic space using a cold osmotic shock method (Manoil and Beckwith, 1986) as described previously (Brurberg et al., 1996). The periplasmic extract was sterilized by filtration over a 0.45 µm filter. For purification of the LPMO, the periplasmic extract (approximately 200 mL) was adjusted to the binding buffer [1.0 M $(NH_4)_2SO_4$, 25 mM Tris-HCl pH 8.0) and loaded onto 10 mL chitin beads (NEB, Ipswich, USA). After the non-binding protein had passed the enzyme was eluted using 20 mM acetic acid. The eluted protein was immediately adjusted to 20 mM Tris-HCl pH 8.0. Subsequently, the enzyme solution was concentrated and the acetic acid was removed by ultrafiltration using an Amicon Ultra centrifugal filter with a 10 kDa cut off (Millipore Merck KGaA, Darmstadt, Germany).The protein concentration was determined using the absorbance at 280 nm and the theoretical extinction coefficient.

Mutations were generated using the QuickChange II site-directed mutagenesis kit (Agilent Technologies, Santa Clara, USA). After DNA sequencing, the mutated expression vectors were transformed into chemically competent *E. coli* BL21 star (DE3) cells by heat shock. All mutants were produced in soluble form and could be purified using standard methods.

Chitobiase from *Serratia marcescens* (*Sm*GH20A) was expressed and purified as reported by Loose *et al*. (2014). Briefly, BL21 star (DE3) cells harbouring the pET30 Xa/LIC vector with the *chb* gene were grown at 37°C to an OD_{600} = 0.5 in TB-medium supplemented with 100 µg/mL kanamycin using a Harbinger LEX bioreactor (Harbinger Biotech, Toronto, Canada). Protein production was induced by adding 0.3 mM IPTG (final concentration) and the culture was further incubated at 30°C for 5h. The cells were harvested by centrifugation and kept at -20°C until use. For protein purification, the cell pellet (from approximately 300 mL culture) was thawed on ice and resuspended in 25 mL binding buffer (20 mM Tris-HCl pH 8.0, 5.0 mM imidazole) supplemented with 0.1 g/L lysozyme followed by 30 min incubation on ice. The cells were disrupted by sonication (Vibra cell sonicator, Sonics, Newtown, USA) at 27% amplitude in a repeated cycle of 5 sec on, 2 sec off, for 3 min in total. After removing cell debris by centrifugation, the protein extract was loaded onto 3.0 mL Ni-NTA Agarose resin (Protino, Machrey-Nagel, Düren, Germany). After the non-bound protein had passed the column, chitobiase was eluted in 20 mM Tris-HCl pH 8.0, 500 mM imidazole. The sample was concentrated and the imidazole was removed using an Amicon Ultra centrifugal filter with a 10 kDa cut off (Millipore Merck KGaA, Darmstadt, Germany). The protein concentration was determined using the Bradford assay (Biorad, Hercules, USA)

Chitinase A (ChiA, or *Sm*Chi18A) (Brurberg et al., 1994) and Chitinase C (ChiC, or *Sm*Chi18C) (Synstad et al., 2008) from *Serratia marcescens* were expressed, harvested and the periplasmic extract was prepared like for CBP21. The periplasmic extract was sterile filtered (0.45 µm), adjusted to 50 mM Tris-HCl pH 8.0 and loaded onto 10 mL chitin beads (NEB, Ipswich, USA). Non-bound protein was discarded and the respective protein was eluted in 20 mM acetic acid. The sample was adjusted to 20 mM Tris-HCl, concentrated and the acetic acid was removed using an Amicon Ultra centrifugal filter with a 10 kDa cut off (Millipore Merck KGaA, Darmstadt, Germany). The protein concentration was determined using the absorbance at 280 nm and the theoretical extinction coefficient.

Cu(II)-saturation and Desalting

All CBP21 variants were copper-saturated prior to activity assays. The procedure was carried out as described by Loose *et al*. (2014). In brief, the enzyme solution was incubated with 3 fold molar excess of $Cu(II)SO_4$ for 30 min at RT. The excess copper was removed by desalting the protein in 25 mM MES pH 6.0 using a PD Midi-Trap G-25 desalting column (GE healthcare, Little Chalfont, United Kingdom).

Stopped-flow Spectroscopy

The electron transfer from *Mt*CDH to the LPMO was followed by measuring re-oxidation of the heme *b* domain of *Mt*CDH at 563 nm, using a SX-20 stopped-flow apparatus (Applied Photophysics, Leatherhead, United Kingdom). All enzymes used were adjusted to 50 mM potassium phosphate/NaOH pH 6.0. Applying the sequential mixing mode, a 10 µM *Mt*CDH solution in 50 mM potassium phosphate/NaOH pH 6.0 was mixed with a 30 µM cellobiose solution in a 1:1 ratio to reduce the protein. Depletion of cellobiose was detected via complete re-oxidation of the FAD co-factor at 449 nm after 115 sec, while, at this point, approximately 70 % of the heme *b* remained reduced. Subsequently, the solution containing partially reduced *Mt*CDH (5 µM, of which appr. 70 % was reduced) was mixed in a 1:1 ratio with an LPMO solution containing 10, 15 or 25 µM of enzyme, and the re-oxidation of the heme *b* domain was measured at 563 nm. The final protein concentrations during the ET measurements were 2.5 µM *Mt*CDH and 5, 7.5 or 12.5 µM LPMO. All measurements were carried out at least in triplicates at 30°C in 50 mM potassium phosphate buffer pH 6.0. The observed traces were fitted to an exponential function using the Pro-Data software suite (Applied Photophysics, Leatherhead, United Kingdom).

LPMO Activity Assay

LPMO reactions, containing 10 g/L β-chitin (France Chitine, Orange, France) and 1.0 µM LPMO, were buffered with 25 mM MES pH 6.0. As reductant, either 0.5 µM *Mt*CDH and 5.0 mM lactose or 1.0 mM gallic acid (stock solution: 100 mM gallic acid dissolved in 100 % EtOH) were used. The samples were incubated at 40°C with shaking at 800 rpm in an Eppendorf Comfort Thermomixer with a temperature-controlled lid. Reactions were stopped by boiling for 20 min when the total amount of oxidized product was analyzed, or by removing

the substrate by filtration using a 96-well filter plate operated by a vacuum manifold (Millipore) when the solubilized products only were analyzed. To be able to quantify the total amount of oxidized products, the boiled samples were further degraded by incubation with a mixture of 3.0 µM ChiA, 3.0 µM ChiB and 4.0 µM Chb (all final concentrations) for 7 h at 40°C, with shaking at 800 rpm. The samples obtained by filtration were degraded by incubation with 4.0 µM Chb for 2 h, under the same conditions. These treatments degrade the stopped reaction to GlcNAc and chitobionic acid.

Production of Chitobionic Acid Standards

Chitobionic acid was produced as previously described by Loose *et al*. (2014) with minor modifications. In short, 2.0 mM chitobiose in 25 mM MES pH 8.0 was incubated with 0.1 g/L m-chitO (Heuts et al., 2008) overnight at 22°C. The complete conversion of chitobiose to chitobionic acid was verified by UPLC.

Product Analysis by UPLC

Chitobionic acid was quantified using an Infinity 1290 UPLC (Agilent Technologies, Santa Clara, USA) equipped with an Aquity BEH Amide 1.7 µm column (Waters, Milford, USA), and operated in HILIC (hydrophilic interaction) mode. To separate the oligosaccharides in the sample, a 2.1 × 150 mm column was operated at 0.4 mL/min using 15 mM Tris HCl pH 8.0 (eluent A) and 100 % acetonitrile (eluent B) as eluents in the following gradient: 0 – 3.5 min, 80 % B : 20 % A; 3.5 – 12 min, gradient to 70 % B : 30 % A; 12 – 13 min, gradient to 55 % B : 45 % A; 13 – 14 min 55 % B : 45 % A; 14 – 15 min, gradient to 80 % B : 20 % A, followed by reconditioning for 3 min. The elution of oligosaccharides was followed at 205 nm.

The analysis of reaction supernatants, i.e. solubilized products was carried out as follows: 0 – 5 min 74 % (B) : 26 % (A), 5 – 7 min gradient to 62 % (B) : 38 % (A), 7 – 8 min 62 % (B) : 38 % (A), 8 – 10 min gradient to 74 % (B) : 26 % (A), and reconditioning for 2 min. The elution of oligosaccharides was followed at 205 nm.

Electron Paramagnetic Resonance Spectroscopy

The EPR samples were prepared from copper saturated enzyme solutions where excess copper had been removed by desalting (described above). Typically, the samples contained 200 µL, 150-300 µM LPMO in 25 mM MES buffer pH 6.0. EPR spectra were recorded using a

BRUKER EleXsys 560 SuperX instrument equipped with an ER 4122 SHQE SuperX high sensitivity cavity and a cold finger. The spectra were recorded using 1 mW microwave power and 10 G modulation amplitude at a temperature of 77 K. All spectra were baseline corrected before the g_z and $|A_z|$ values were determined by numerical simulation using Easyspin 5.0 (Stoll and Schweiger, 2006).

Substrate Binding

Binding experiments were carried out in the same conditions as the LPMO activity assays. Reaction mixtures containing10 g/L β-chitin and 1.0 μM LPMO in 25 mM MES pH 6.0, with or without 1.0 mM gallic acid, were incubated at 40° with shaking at 800 rpm and samples were taken after 1, 2 and 6 h. The samples were filtered using a 96-well filter plate (Millipore) and the concentration of unbound protein was measured using the Bradford assay (BioRad, Hercules, USA). As control for determination of the total amount of protein, for each CBP21 variant, 1.0 μM LPMO was incubated in 25 mM MES pH 6.0 at 40°C and 800 rpm. The quantities of unbound protein in the reactions with chitin were calculated relative to the respective control reactions.

RESULTS

Sequence analysis and mutant design

Residues targeted for mutation were selected by consulting existing literature describing sequence, structural and functional analysis of CBP21 (Vaaje-Kolstad et al., 2005a, Vaaje-Kolstad et al., 2005b, Aachmann et al., 2012) and AA10 LPMOs in general (Forsberg et al., 2014a, Forsberg et al., 2016, Hemsworth et al., 2013a). Additional analysis of conserved residues was performed using ConSurf (Ashkenazy et al., 2010) to map sequence conservation on the CBP21 3D-structure and by creating a multiple sequence alignment of family AA10 LPMOs (Fig. S1). Residues on the substrate binding surface and near the active site showing high conservation and potentially important functional roles were selected, resulting in the generation of 15 single amino acid mutants that include two control mutations (Fig. 1). As default, residues were mutated to alanine or, if the WT had an alanine, glycine. There are four exceptions (W178F, A152R, I180R and F187Y), three of which are mutations that reflect naturally occurring variation in AA10 type LPMOs, whereas the fourth (A152R) is a control mutation thought not to affect the substrate-binding surface. The dataset contains one more such “control mutation”, namely F147A.

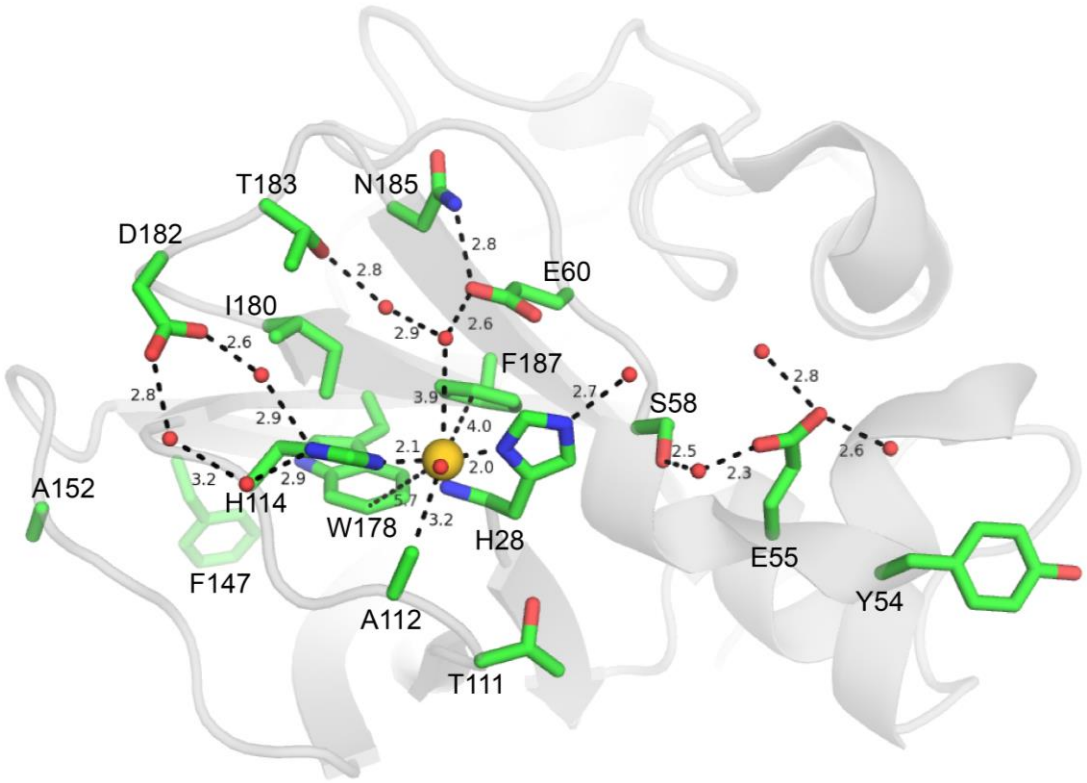

Figure 1. Structure of CBP21. The side chains of residues selected for mutation, as well as the side chain of the N-terminal histidine (H28) are shown as sticks and colored green. Water molecules are shown as red spheres. The copper ion is shown as a gold-colored sphere. Hydrogen-bonds are illustrated with black dashes and the distances are indicated in Å. The distances from W178 and F187 from the copper ion are indicated with dashes and the distances are shown in Å. The distance between the copper ion and the water molecule positioned above (showing as the red sphere on top of the golden sphere) is 2.6 Å.

Analysis of LPMO-generated products

CBP21 is thought to act on the crystalline surfaces of chitin particles. Only products with a low degree of polymerization (DP) are likely to dissociate into solution (~DP8 and lower), meaning that proper analysis of LPMO activity requires solubilization of remaining substrate particles. The latter can be achieved by incubating the reaction mixtures with a large amount of chitinases and chitobiase after stopping the CBP21 reaction. This procedure yields a simple mixture of products to analyze: GlcNAc and GlcNAcGlcNAc1A (chitobionic acid), where the amount of chitobionic acid reflects LPMO activity.

To get an impression of the product distribution and to aid experimental design of the many activity assays needed for comparing CBP21 variants, we compared the amount of soluble

products with the total amount of oxidations in standard activity assays. As expected, for all CBP21 variants, the total amount of oxidations was higher than the amount of solubilized oxidized products (Fig. 2). The ratio of solubilized products versus total oxidized products was dependent on the activity of the LPMO: In reactions with WT CBP21 and CBP21 mutants with WT-like activity (discussed below), the amount of products remaining associated to the chitin particles was in the range of 25-35 % of the total amount of products. For CBP21 variants with lower activities than the WT, the amount of oxidized products remaining associated with the chitin particles was generally larger, ranging approximately from 50-85%. Thus, to obtain a correct comparison of WT and mutant activities, the total amount of oxidized products must be quantified at each time point of the reaction. It may be noted that despite the underestimation of activity when only analyzing soluble products, both total and soluble product accumulation was linear over time for the wildtype (Fig. 2, inset).

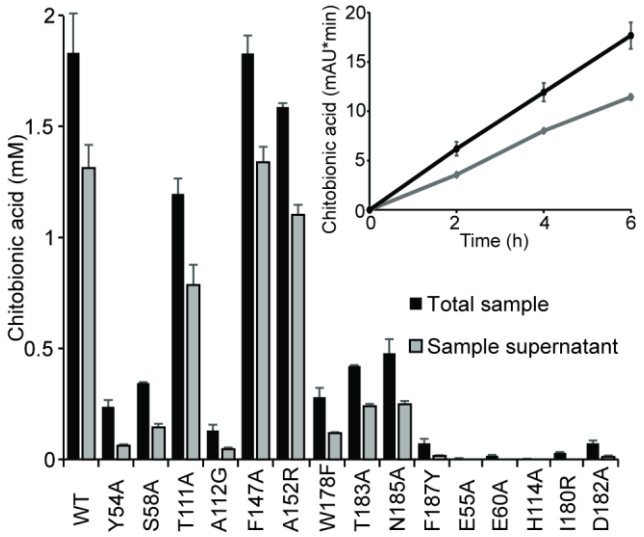

Figure 2: Comparison of total (black) and solubilized (grey) products generated by CBP21 variants in the presence of *Mt*CDH after 24 h incubation. Note that the ratio between total and solubilized product differs between the variants (see text for details). The inset shows that the rate of both total product formation and the formation of soluble products stay constant over time for WT CBP21 (inset). The error bars indicate standard deviations (n=3).

Catalytic activity of CBP21 WT and mutants

The activity of all CBP21 variants over a time period ranging up to 48 hours was analyzed using a small organic acid (gallic acid) or a redox-active protein (*Mt*CDH) as electron donor (Fig. 3). The outcome of the reactions depended to some extend on the reductant used (see below), but overall, the differences in activity between the LPMO variants were similar for both electron donors. The most notable exceptions were A112G and F187Y, which were considerably more active with gallic acid compared to *Mt*CDH. The mutants E55A, E60A, H114A, I180R and D182A were almost inactive compared to the WT (for the sake of simplicity, hereafter referred to as "inactive"), whereas the two "control mutants" (F147A, A152G) showed activities similar to the WT. All other mutants showed reduced activity, at least in terms of final product yields.

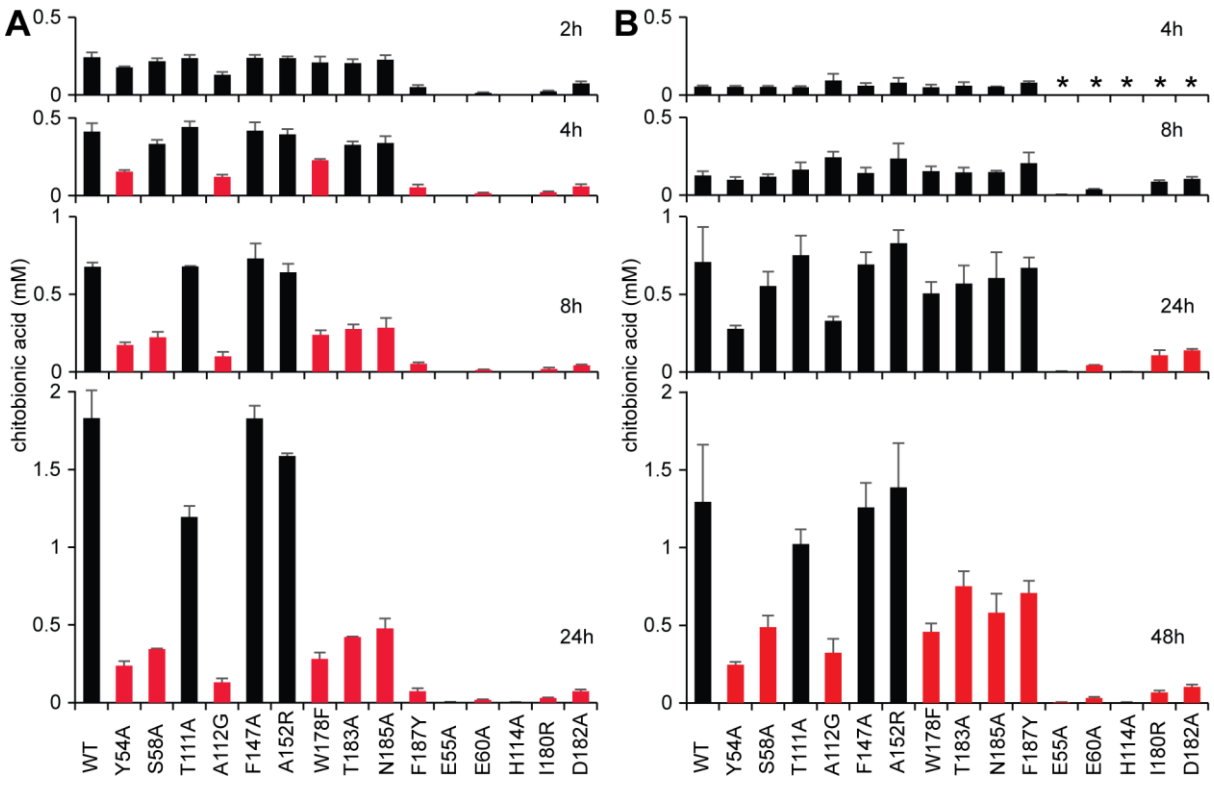

Figure 3. Activity of CBP21 variants. The graphs show total levels of oxidized products after varying incubation times for reactions with *Mt*CDH/lactose (A) or gallic acid (B) as electron donor. Note that the maximum reaction times in panel A and B differ (24 h and 48 h, respectively). Bars are colored red in cases where the product level is not signficantly higher than the product level detected at the preceding time point, meaning that LPMO activity has ceased. The asterisks indicates that no sample was taken at that time point. The error bars indicate standard deviations (n=3).

315 Strikingly, initial rates of almost all active CBP21 variants were similar to the WT (Fig. 3).
316 Over time, clear differences in product yield became apparent, which must be caused by the
317 LPMO variants loosing activity at a rate that depends on the mutation. Notably, some of the
318 mutants classified as "inactive" yielded small amounts of products and these were generated
319 very early in the reaction, suggesting that also in this case rapid inactivation is at least in part
320 causing reduced enzyme performance. All variants, except the most active ones (WT, the two
321 control mutants, and T111A), reached reaction end points, and the incubation time needed to
322 do so depended on the mutation. Clear differences between the reductants were apparent: with
323 *Mt*CDH/lactose, initial rates were higher, but the activities of many mutants ceased earlier
324 (after 2-4 h) compared to gallic acid (after 24 h). For the most active variants, final product
325 yields were higher when using *Mt*CDH/lactose, whereas gallic acid gave slightly higher yields
326 for several of the less active mutants. A112G and, even more so, F187Y stand out as being
327 substantially more active with gallic acid. With *Mt*CDH/lactose the activity of these mutants
328 seems to have ceased at the first measuring point (2h) and final product yields were very low
329 compared to wild-type (7% and 4% of WT for A112G and F187Y, respectively). With gallic
330 acid, the initial rates of these variants were at least as high as the WT; product formation
331 continued over time and the final yields amounted 25 % and 55 % of WT levels for A112G
332 and F187Y, respectively.

333 **Electron Paramagnetic Resonance Spectroscopy**

334 In order to assess changes in the copper coordination geometry, all CBP21 variants were
335 analyzed by electron paramagnetic resonance spectroscopy (EPR) (Table 1 and Figs. 4 and 5).
336 The WT spectrum is rhombic ($g_z > g_y > g_x$) in agreement with a mixed trigonal
337 bipyramidal/square pyramidal geometry as observed in the crystal structures of oxidized chitin-
338 active AA10-type LPMOs (Hemsworth et al., 2013b, Gudmundsson et al., 2014). Mutations in
339 the first coordination sphere or closer than 4 Å to the copper, A112G, H114A and F187Y,
340 resulted in more axial EPR spectra ($g_z > g_y \sim g_x$) compared to the WT. For these three mutants
341 there are also a large shifts in the g_z and/or $|A_z|$ values compared to the WT enzyme (Table 1).

342 Of the other mutations, E55A, W178F, I180R, T111A, E60A and T183A also led to shifts in
343 the g_z and $g_{x,y}$ region of the EPR spectra (Figure 5), however less pronounced than for the inner
344 sphere mutants. Changes were most pronounced in the $g_{x,y}$ regions and could not be quantified
345 because reliable simulation of these g-values and hyperfine splitting values was not possible.
346 The mutants W178F, I180R and T111A had g_z and $|A_z|$ values different from the WT, and the

estimated values are listed in Table 1. These mutations affect the second coordination sphere and may perturb the copper site geometry by several subtle effects, e.g. on hydrogen bonding networks involving residues or waters in the first coordination sphere. No changes in EPR spectra, relative to the WT, were observed for the Y54A, S58A, D182A, N185A, F147A and A152R mutants and data for these mutants are not shown.

Table 1. Spin Hamiltonian Parameters of CBP21 mutants. It should be noted that the EPR spectra for Y54A, S58A, D182A, N185A, F147A and A152R were very similar to the WT spectrum, yielding almost identical g_z and $|A_z|$ values, and are thus not displayed in the table.

	WT [1)]	**A112G**	**H114A**	**F187Y**	**W178F**	**I180R**	**T111A**
G_Z	2.260	2.258	2.290	2.258	2.265	2.266	2.255
$\|A_Z\|$ [3)]	116	155	158	165	122	130	145

[1)] Forsberg *et al*. (2014b)

[2)] Units of 10^{-4} cm^{-1}

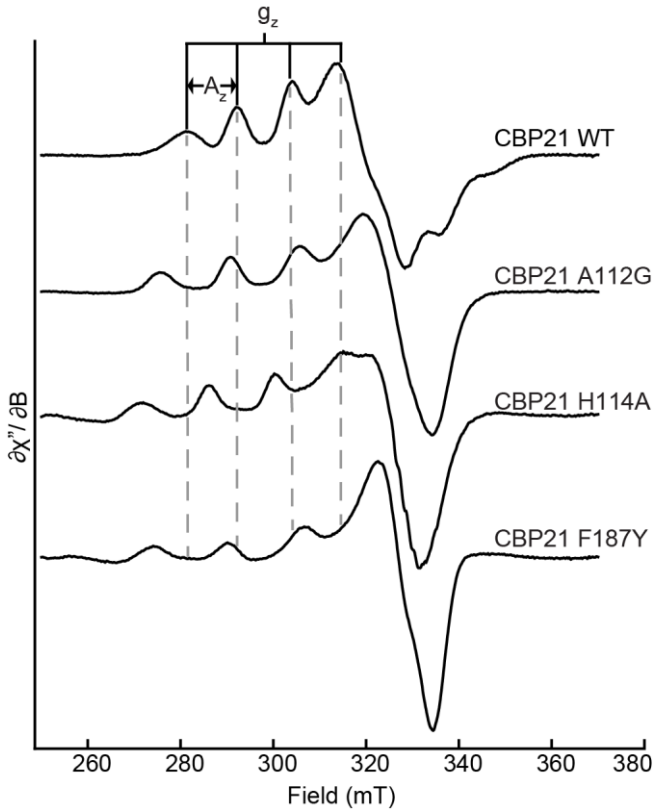

Figure 4. Changes in the EPR spectrum of CBP21 caused by mutation of residues in the first coordination sphere or closer than 4 Å to the copper. The mutants A112G, H114A and F187Y yield more axial EPR spectra compared to the WT indicating that the copper geometry has been altered substantially, allowing water molecules to bind differently in A112G and H114A and potentially adding a coordination bond from the introduced hydroxyl group in F187Y.

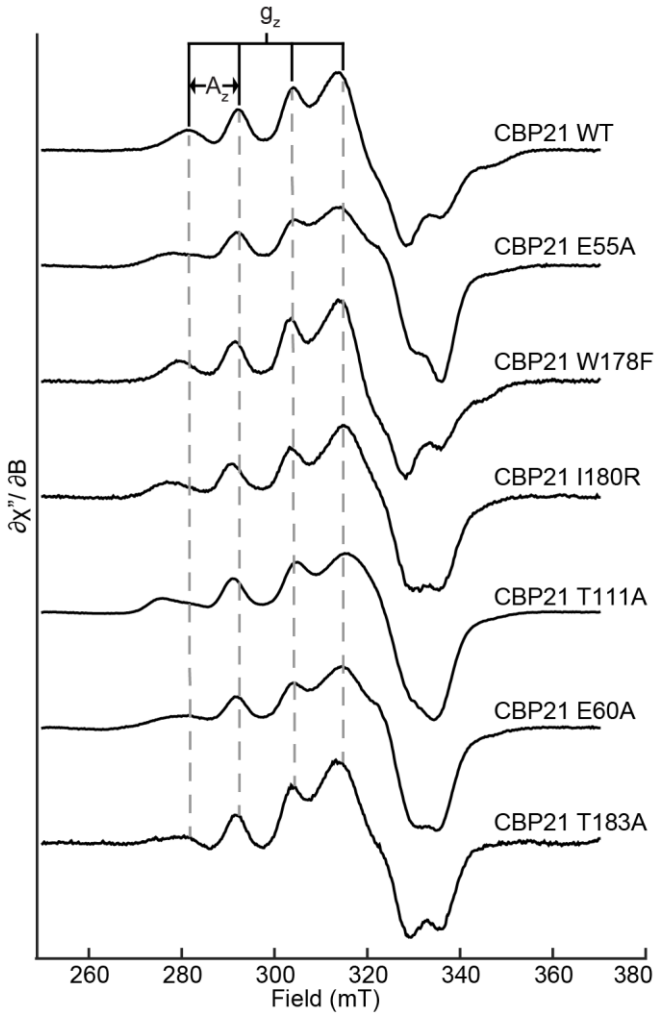

Figure 5. Changes in the EPR spectrum of CBP21 caused by modifications in the second coordination sphere (residues more than 4 Å away from the copper). It is apparent that these mutations alter the copper coordination geometry differently, some altering the EPR envelope predominantly in the g_z region, others the g_x-g_y region (~320 – 350 mT).

Binding of CBP21 WT and mutants to β-chitin

To determine the influence of the various mutations on the binding properties of the enzyme during catalysis, binding assays with β-chitin were performed using activity assay conditions, and binding was assessed at three time points. Although some variation between time points was observed, the general picture is that a stable binding equilibrium was obtained after one hour for all CBP21 variants (Fig.6). Binding properties similar to the WT were observed upon mutation of some of the polar residues surrounding the active site (T111A, T183A and N185A), the Trp buried beneath the active site (W178F), as well as for the control mutants (F147A and

A152R). Mutation of the only solvent exposed aromatic amino acid on the substrate binding surface to Ala (Y54A) almost abolished substrate binding. Similar reductions of binding were observed upon mutation of the negatively charged residues of the substrate binding surface (E55A, E60A and D182A) and mutation of residues in the copper site or very close to the copper site (H114A, S58A, F187Y and I180R). The A112 mutant showed moderately reduced binding, whereas the T183A mutant seemed to bind slightly better than the WT.

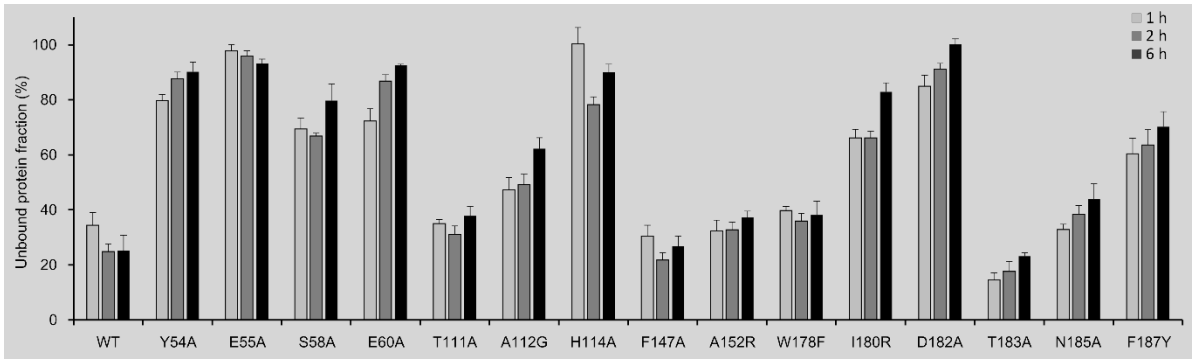

Figure 6. Binding of CBP21 WT and mutants to β-chitin. Binding experiments were performed in identical conditions as used for activity assays with gallic acid, i.e. containing 1.0 μM CBP21 WT or mutant, 1.0 mM gallic acid, 10 mg/ml β-chitin and 25 mM MES pH 6.0. Reactions were shaken at 800 rpm at 40°C. The bars represent the protein in the supernatant of the reaction (i.e. the unbound fraction). The error bars indicate standard deviations (n=3).

Electron transfer (ET) from *Mt*CDH to CBP21 variants

The rates of electron transfer from the heme b domain of *Mt*CDH to CBP21 variants in solution revealed considerable mutational effects (Figure 7 and Table 2). Several mutants showed increased rates, and the largest increases, 6- to 8-fold were observed for two inactive mutants, I180R and E60A. The clearest decreases in ET were observed upon mutation of Y54 and, in particular, upon mutation of two residues coordinating (H114A) the copper or shaping the copper site (F187Y). The ET from *Mt*CDH to the CBP21 variants E55A and F147A could not be assessed due to changed curve shapes that prevented reliable data-fitting. However, both these mutants show a decreased ET. It is interesting to note that the three mutants that by all other assessments resemble the WT all showed changed ET rates.

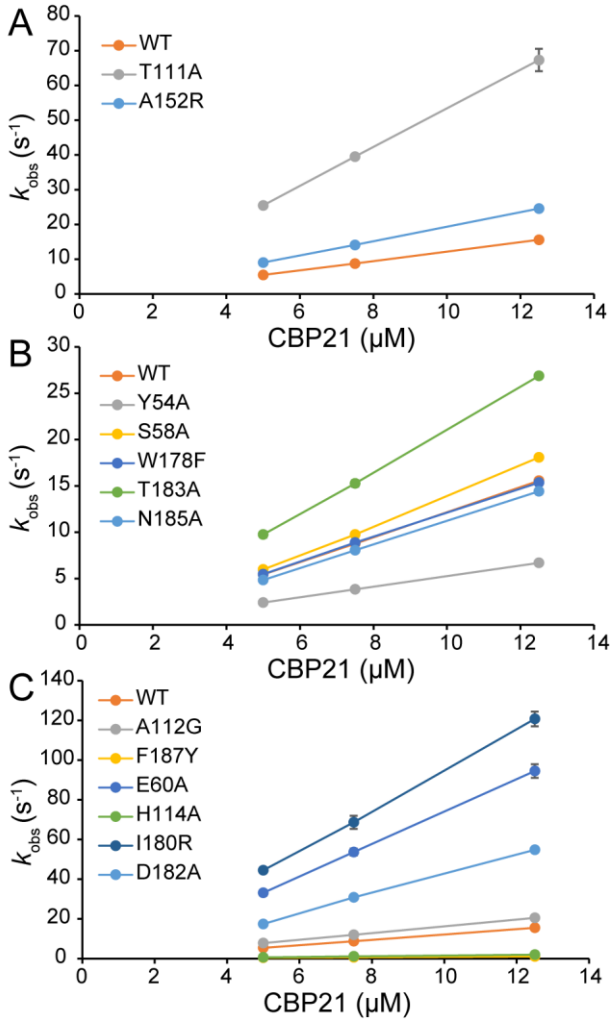

403

404 **Figure 7. Electron transfer from the *Mt*CDH to CBP21 WT and mutants in solution.** Electron
405 transfer was measured by monitoring the re-oxidation 2.5 μM of the *Mt*CDH cytochrome domain at pH
406 6.0 (50 mM potassium phosphate/NaOH). The data are shown in three panels for the sake of clarity.
407 The panels are categorized by the lifetime observed for the variants in the activity assay; (A) WT-like
408 lifetime (B) reduced lifetime and (C) inactive. Note that A112G and F187Y were categorized as
409 "inactive" due to their low reactivity in the presence of *Mt*CDH. The error bars indicate standard
410 deviations (n≥3).

411

DISCUSSION

Despite the importance of LPMOs in biomass conversion processes (Beeson et al., 2015, Cragg et al., 2015, Vermaas et al., 2015, Hemsworth et al., 2015, Corrêa et al., 2016) and great scientific interest in the unique catalytic mechanism of these enzymes (Beeson et al., 2015, Walton and Davies, 2016, Kjaergaard et al., 2014, Frandsen et al., 2016), site-directed mutagenesis data for probing the roles of individual amino acids in catalysis are scarce (Vaaje-Kolstad et al., 2005a, Harris et al., 2010). One factor limiting this type of studies may be the complexity of thoroughly characterizing LPMO activity and kinetics. We have mapped the contribution of individual amino acids on the substrate-binding surface and in the active site of the chitin-active family AA10 LPMO CBP21. To aid in the interpretation of mutational effects on catalytic activity, we have also characterized effects on substrate binding, electron transfer rates and the coordination geometry of the active site copper. The key experimental findings of this study are summarized in Table 2. In addition to providing novel insights into the roles of individual LPMO residues and revealing novel aspects of LPMO functionality, as discussed below, the data in Table 2 are a valuable resource for further studies aimed at unravelling how LPMOs really work.

Table 2. Summary of CBP21 mutant properties.

Variant	Activity CDH[a] 2 h	Activity CDH[a] 24 h	Stop CDH[b]	Activity GA[c] 4 h	Activity GA[c] 48 h	Stop GA[b]	Binding[d] after 2 h	ET[e] (× 10^6 $M^{-1}s^{-1}$)	EPR[f]
WT	100	100	24	100	100	48	75	1.35	-
F147A	99	100	24	109	97	48	78	-	nc
A152R	98	87	24	146	107	48	67	2.08	nc
T111A	98	65	24	92	79	48	69	5.57	ax
N185A	94	26	4	100	45	24	62	1.28	nc
T183A	85	23	4	110	58	24	82	2.29	xy
S58A	90	19	4	95	38	24	33	1.62	nc
W178F	87	15	2	91	35	24	64	1.32	ax
Y54A	74	13	2	95	19	24	12	0.57	nc
A112G	54	7	2	173	25	24	51	1.69	ax
D182A	31	4	2	-	8	8	9	4.96	nc
F187Y	21	4	2	146	55	24	36	0.09	ax
I180R	10	2	2	-	5	8	34	10.19	ax
E60A	6	1	2	-	3	8	13	8.18	xy
E55A	-	-	-	-	-	-	4	-	xy
H114A	-	-	-	-	-	-	22	0.18	ax

[a] data from time point of analyses (2 h or 24 h), WT activity equaling 100% activity.
[b] time point in enzyme assay where the enzyme is observed to no longer be active
[c] data from time point of analyses (4 h or 48 h), WT activity equaling 100% activity.
[d] % CBP21 bound to the substrate 2 h into the enzyme assay.
[e] electron transfer
[f] no change (nc), more axial envelope (ax), changes in g_x-g_y region (xy)

435 Several of the mutants analyzed here have previously been characterized by Vaaje-Kolstad *et*
436 *al.* (2005a, b), before it was known that CBP21 was an enzyme and using conditions (not
437 copper saturated and no added reductant) different from the ones used here. In these early
438 studies, mutants Y54A, D182A, E60A, E55A and H114A showed reduced binding to β-chitin
439 and strongly reduced or no ability to boost chitinase activity, whereas WT behavior was
440 observed for F147A (the activity of this mutant was not assessed) and A152R. All these
441 observations are in accordance with the present data. The only (minor) deviation between these
442 early data and the present data concerns N185A, which in the early work was found to be fully
443 capable of boosting chitinase activity while binding slightly less well to β-chitin, compared to
444 the WT.

445 It is not easy to detect clear trends in Table 2. However, several important general observations
446 can be made. Firstly, there is no correlation between the rate of electron transfer measured in
447 the stopped-flow experiments and LPMO performance. This must imply that the transfer of the
448 first electron to the LPMO, i.e. the reduction of LPMO-Cu(II) to LPMO-Cu(I) measured in the
449 stopped-flow experiments, is not rate-limiting. In line with this, experimentally determined
450 catalytic rates of LPMOs (Vaaje-Kolstad et al., 2010, Loose et al., 2014, Borisova et al., 2015)
451 are lower than the LPMO reduction rate. During the course of the reaction, the LPMO needs
452 to be supplied with a second electron (Vaaje-Kolstad et al., 2010, Loose et al., submitted),
453 meaning that ET processes very well may be rate-limiting, despite the "easy" first reduction of
454 copper. In support of ET processes being of importance, a second observation is that the
455 character of the reductant has considerable effects on the performance of the mutants
456 (summarized in the Results section). Thirdly, the data in Table 2 show that substrate binding
457 and enzyme activity in terms of yields and/or rates are not correlated. For example, Y54A and
458 S58A show greatly reduced binding but show the same initial activity as the WT. Furthermore,
459 several mutants with strongly reduced final product yields show almost WT-like binding (e.g.
460 T183A, N185A). A fourth and potentially very important observation is that several of the
461 mutations do not necessarily affect the catalytic rate of the enzyme, but rather the rate by which
462 the enzyme becomes inactivated.

463

464

465

Discussion of individual CBP21 mutants

All mutated residues discussed below are highly conserved amongst chitin-active family AA10 LPMOs (Fig. S1), unless otherwise indicated. Compared to AA10s that are cellulose active or display activity towards both cellulose and chitin, only the histidine residues of the histidine brace (H28 and H114 in CBP21) and the alanine close to the distal axial copper coordination position (A112 in CBP21) remain 100% structurally conserved (Fig. 1 & S1). The active site glutamate (E60 in CBP21) is also highly conserved in AA10 LPMOs, except for mixed chitin/cellulose active AA10s which display a glutamine at the equivalent spatial location, a feature that is shared with AA9s. The amino acid positioned in the proximal axial copper coordination position (F187 in CBP21) is either Phe or Tyr, a trait seen for all LPMO families. Outside the active site, LPMOs generally show large sequence variation.

H114A. This residue is directly involved in copper coordination and its mutation to alanine renders the enzyme totally inactive. H114A is still able to bind copper, albeit with a quite different EPR spectrum, and shows reduced ability to receive electrons from *Mt*CDH (~10-fold reduction compared to WT) and reduced substrate binding. The latter observation is intriguing since recent data indicate that only the N-terminal histidine of the copper site of LPMOs interact directly with the substrate (Frandsen et al., 2016). However, it is conceivable that conformational changes due to changed copper binding, possibly displacement of the N-terminal histidine, could affect binding to the substrate. Frandsen *et al.* (2016) also suggested that dioxygen binding by the copper ion increases the affinity of the LPMO to the substrate. Thus, it may also be the inability to bind (and activate) dioxygen that decreases substrate binding by the mutant, since the copper site is substantially changed.

E55A. This glutamate is positioned relatively far from the active site (~10.2 Å from the copper; Fig.1) and its mutation abolished enzyme activity. This residue was expected to be involved in substrate binding, which also is evident from our data. However, as observed for the Y54A mutant (Fig. 1 and text further below), substrate binding is not necessary for (initial) activity, so the loss of activity cannot only be related to this fact. Interestingly, the electron transfer rate of this mutant could not be measured since the curve could not be fitted to the mathematical model used for the other variants, but seems to be slower compared to the WT (data not shown). Also, the EPR spectrum deviates from that of the WT, showing changes in the g_x, g_y part (~320-360 mT) of the spectrum. Thus, it may be that the ability to receive electrons and activate dioxygen is compromised for this variant due to a distortion of the active site.

E60A. As previously noted, the amino acid in this position (either Glu or Gln) is conserved in almost all LPMOs and the mutant enzyme shows only marginal activity in the enzyme activity assay. Glu60 is positioned close to the copper and the histidines and interacts with the active site through H-bonded water molecules (Fig. 1; other AA10 structures show similar water clusters in the active site partly coordinated by this glutamate, e.g. *Ef*LPMO10A). Thus, the change in EPR signature for this mutant is not unexpected. Interestingly, this inactive mutant showed an increased ET rate. Data obtained for mutation of the residue in the corresponding position in an AA9 LPMO (Gln) to Glu, Asp or Leu, substantially decreased and even abolished (the Gln to Leu mutation) the ability of this enzyme to stimulate cellulose degradation by cellulases (Harris *et al.* 2010). The network of H-bonded water molecules in the active site thus seems to be delicately designed to fulfil a role in catalysis.

I180R. Most chitin-active LPMO10s have a cavity next to the active site that has been suggested to accommodate dioxygen (Hemsworth et al., 2013b) or the *N*-acetyl moiety of the chitin chain (Forsberg et al., 2014a). In cellulose- active LPMO10s (and most LPMOs in other AA families) this cavity is filled by the side chain of a bulky amino acid, usually arginine. A study of two LPMO10s from *S. coelicolor* showed that one of the enzymes had an arginine-filled cavity and was nevertheless able to cleave chitin chains, suggesting a different role for the cavity than accommodating the chitin *N*-acetyl group. Despite this latter result and the common presence of an arginine at the I180 position of CBP21, mutation of Ile to Arg almost completely abolished catalysis. It is likely that the introduction of a positive charge and/or structural rearrangements caused by the mutation are responsible for the loss of activity. The EPR spectrum of this mutant showed that the mutation changed the coordination of the copper.

F187Y. All LPMO9s, LPMO11s and LPMO13s and a minor fraction of LPMO10s have a Tyr at the position of F187. In these LPMOs, the tyrosine contributes to shaping the copper site as the proximal axial ligand and perhaps even to contributing to parts of the catalytic cycle (Beeson et al., 2015). Indeed, EPR showed that the F187Y mutation affects the copper site, yielding a more axial spectrum, more similar to that seen for LPMO9s. At the same time, electron transfer from CDH was impaired (15-fold compared to WT), perhaps reaching a level that could be rate limiting for CBP21 catalysis and which could explain the low activity of this mutant. In support of this hypothesis, the F187Y mutant performed clearly better when using gallic acid as electron donor (as opposed to *Mt*CDH). This makes sense since the reduction of LPMOs by small molecule reductants is extremely fast, to the extent that it cannot be detected

by the stopped-flow setup used in this study (results not shown). Furthermore, reduction by gallic acid does not depend on a protein-protein interaction as is the case for the CDH-LPMO system (see below for further discussion). Interestingly, a study on LPMO9s showed that mutation of the Tyr in this position to Phe, only resulted in a ~60% decrease in a cellulase stimulation assay (Harris et al. 2010). Thus, this residue does not seem to be essential for catalysis by LPMOs.

A112G. The possible importance of this highly conserved Ala, which restricts access to the copper in its distal axial coordination sphere, was originally pointed out by Hemsworth *et al*. (2013a). Interestingly, this residue is not present in AA9s that display distorted octahedral copper geometry and where a water occupies this axial position. As proposed by Li *et al*., this water could be replaced either by oxygen or by the substrate during catalysis (Li et al., 2012); Frandsen *et al.* (2016) have recently shown that this water is displaced by substrate. Interestingly, the one available structure of an LPMO10 with Tyr in the proximal axial position (i.e. analogous to Phe187 in CBP21) shows that, while this alanine is conserved, it is displaced, making the axial coordination sphere much more accessible (Forsberg et al. 2014). Interestingly, the A112G mutant showed characteristics similar to the F187Y mutant: slightly impaired substrate-binding, reduced activity, which was higher with gallic acid relative to CDH, and a more axial EPR spectrum. The only difference between the mutants is that A112G showed WT-like ET rates, whereas these rates were strongly reduced for F187Y.

D182A. The Asp in this position is located around 9 Å from the copper site on the surface of CBP21. The residue H-bonds a network of water molecules that H-bond to H114 (Fig. 1). Its mutation to Ala reduced enzymatic performance as well as affinity for chitin, whereas the EPR spectrum was not affected. D182A is one of several examples showing less activity and a higher ET rate.

Y54A. The only aromatic residue on the flat binding surface of CBP21 is Y54, which is positioned 15.4 Å away from the copper site (distance measured from the copper to Y54 Cβ atom). Mutation of this residue led to impaired substrate binding and reaction yields and a modest decrease in ET rate, but did not affect initial activity nor the EPR spectrum. It should be noted that this residue often is substituted with a Trp in other LPMO10s.

N185A. The Asn at this position is solvent exposed and located approximately 8.4 Å from the copper and maintains a strong H-bond with the side chain of E60 (Fig. 1). Mutation of this

residue resulted in moderately decreased chitin binding. Catalytic activity in the presence of gallic acid was similar to the WT activity for up to 24 h confirming earlier results. As for most other mutants, activity ceases earlier, for this mutant after 4 h using *Mt*CDH.

S58A. Ser58 is located between E55 and the active site of CBP21. Interestingly, this Ser is substituted by Ala in the two cellulose active LPMOs *Tf*AA10B and *Sc*AA10C (Forsberg et al., 2014b). As for many other amino acids, S58 is important for substrate binding, as already observed by NMR (Aachmann et al., 2012) and also in this study binding is strongly affected. Nevertheless, as for the Y54A mutant, activity persists. Even though the residue is located close to the copper, a change in its coordination could not be observed. This is surprising, since E55A causes a change, probably by interactions with several water molecules.

W178F. Trp178 is part of the aromatic cluster in CBP21, which is positioned "below" the active site. Such a cluster of aromatic amino acids is common for most LPMOs and has been suggested to be involved in electron transfer (Beeson et al., 2015). The side chain of W178 neighbors F187 and is positioned only 5.7 Å from the copper ion. Mutation of this Trp to another aromatic amino acid, Phe, changed copper coordination geometry in the rhombic area and led to a modest effect on substrate binding. In terms of activity, this mutant was similar to many others, in the sense that the initial activity was not changed, whereas the activity ceased earlier compared to the WT, leading to lower product yields.

T183A. Exchanging this polar residue to an Ala does not affect the binding abilities negatively. In addition, this residue appears not to be essential for activity since it overlaps with the WT activity for at least 8 h, only showing an insignificantly decreased product formation after 24 h using gallic acid as an electron donor. Thereafter activity stops. It appears that activity in the presence of *Mt*CDH already ceases before 4h. Nonetheless, T183 influences the copper coordination in the rhombic area. As shown in Figure 1, the change can probably be attributed to altered water coordination by the copper, caused by disruption of the water mediated H-bond between T183 and E60.

T111A. Cellulose-active LPMO10s tend to have a Phe or Trp at this position. Despite of being highly conserved, the exchange from Thr to Ala affected chitin-binding and catalytic activity only marginally. Since the hydroxyl group of T111 interacts with the main chain oxygen of His28, it was anticipated that T111 could contribute to shaping and "preforming" (Hemsworth et al., 2013b) the copper-binding site. Indeed, EPR analysis of the T111A mutant showed a

592 change relative to the WT, but this change was hardly reflected in the enzyme's functional
593 properties.

594 **F147A and A152R (control mutants).** Phe147 and A152 are located in the interface of a
595 crystallographically observed CBP21 dimer and were originally mutated to verify whether
596 CBP21 was dimeric. These two mutations, which are quite rigorous in nature, did not change
597 the overall performance of the enzyme. Slightly decreased binding was observed for the A152R
598 mutant, which can probably be attributed to the introduction of a bulky residue relatively close
599 to the substrate binding surface. The electron transfer from *Mt*CDH to the F147A variant was
600 hampered, exhibiting reduced electron transfer (the raw data was not possible to fit the
601 mathematical model used, but re-oxidation of the *Mt*CDH cytochrome domain was slower
602 compared to the WT). One possible reason is that the protein-protein interaction is altered,
603 which seems less likely as electron transfer most likely occurs right at the copper active site
604 (Courtade et al., 2016). The location of F147 is on the surface of CBP21, at the end of an
605 aromatic cluster spanning through the protein to the copper active site.

606

607 **Effects of mutations on copper coordination geometry**

608 In order to interpret the mutational effects on copper coordination, it is helpful to aid analysis
609 by inspection of the X-ray crystallographic structure of the copper enzyme in its Cu(II) form.
610 Unfortunately, there is presently no structure available of CBP21 with Cu(II) bound, but such
611 a structure conveniently exist for the similar chitin-active LPMO10 from *E. faecalis*
612 (*Ef*LPMO10A; 49% sequence identity; (Gudmundsson et al., 2014)). The copper-active site of
613 CBP21 and *Ef*LPMO10A are essentially identical. In the *Ef*LPMO10A-Cu(II) structure, two
614 water molecules, illustrated in a plane perpendicular to the histidine brace (Fig. 8), bind to the
615 Cu(II) ion revealing an apparent trigonal bipyramidal geometry. In contrast, the EPR spectrum
616 of CBP21 does not display a $d(z^2)$ ground state that would reflect a pure trigonal bipyramidal
617 geometry and an inversed EPR spectrum. The observed rhombic envelope for CBP21 WT with
618 estimated g-values being $g_x = 2.039$, $g_y = 2.116$, and $g_z = 2.260$ (Fig. 4, Table 1 and (Forsberg
619 et al., 2014b)) rather indicate an intermediate between trigonal bipyramidal and square
620 pyramidal geometry with a predominant $d(x^2\text{-}y^2)$ ground state. While the histidine brace is
621 highly conserved among all LPMOs, the geometry of the copper site varies, likely as a result
622 of sequence differences that affect access to the copper coordination sphere. In CBP21, Ala112

seems to affect binding of the water molecules, forcing what appears to be an intermediate between trigonal bipyramidal and square pyramidal geometry. In C4-oxidizing LPMO9s, which lack an amino acid side chain analogous to Ala112, a more axial EPR spectrum is observed, indicative of a distorted octahedral geometry of their copper sites (Borisova et al., 2015).

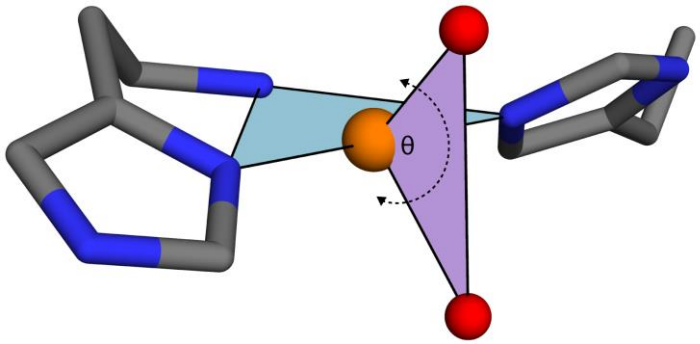

Figure 8. Cooper coordination by *Ef*LPMO10 in the Cu(II) form. The crystal structure of *E. faecalis* (*Ef*LPMO10A; PDB ID 4ALC) with Cu(II) in the active site shows two water molecules coordinating to the metal ion, resulting in an apparent trigonal bipyramidal geometry. Two perpendicular planes, one defined by the histidine brace nitrogen atoms, the other by Cu(II) and the water molecules, can be used to explain the transition between trigonal bipyramidal and square pyramidal geometry. Rotating the indicated Cu(II)-water plane angle Θ ~45° in either direction results in a square pyramidal geometry. Smaller changes in Θ will typically lead to intermediate states of trigonal bipyramidal and square pyramidal geometries.

The three mutations in the immediate environment of the copper, A112G, H114A and F187Y, all led to more axial EPR spectra (narrow $g_{x,y}$ region) compared to the WT. In the mutants A112G and H114A, the more axial EPR spectra can be explained by the fact that water molecules coordinating to the copper ion will experience less steric hindrance, which again can alter the geometry of the complex. This can be exemplified considering Fig. 8, where a change in the angle Θ, rotating the water molecules towards a square pyramidal geometry would result in more axial EPR spectra. Also the angle between the water molecules and the copper may change and alter the geometry of the copper site. The F187Y mutant, which partly mimics the AA9 enzymes that all have a Tyr at this position (also some cellulose active LPMO10s have a

Tyr at this position), may introduce the tyrosine hydroxyl group as a new copper ligand. This modification, along with the A112G and H114A mutants, can shift the geometry towards a tetragonally distorted octahedral geometry with a $d(x^2-y^2)$ ground state, yielding more axial EPR spectra. It is likely that both the mutations A112G and H114A result in reorganization of the active site, and that water molecules occupy free coordination sites that appear due to these changes in geometry.

The mutants introduced > 4 Å away from the copper site also introduce shifts in the estimated g_z and $|A_z|$ values and in the $g_{x,y}$ region of their corresponding EPR spectra, however less pronounced than for the inner sphere mutants. Mutating these amino acid residues may alter their capability to orientate and bind water molecules close to the copper site or alter their role as supporting scaffold of the active site.

Several mutations, including the two "negative controls", F147A and A152R, did not lead to a changed EPR spectrum. The mutants Y54A, S58A, D182A and N185A, are typically thought to be involved in substrate binding and did all show practically identical EPR spectra compared to the WT (results not shown). Thus these residues do not appear to influence the local environment of the copper ion.

Effects of mutations on electron transfer between CDH and CBP21

Rates for transfer of electrons from the CDH cytochrome domain to an LPMO has so far only been analyzed for family AA9 LPMOs (Kracher *et al.* 2016) and for CBP21 WT (Loose et al., submitted). The current study and Loose *et al*. (submitted) show that the CBP21 WT enzyme has a very efficient ET rate constant (1.35×10^6 $M^{-1}s^{-1}$), which is close to interaction rates between different CDHs and cytochrome *c*. For AA9 LPMOs, where the LPMOs and the CDH is produced in concert by the same organism, transfer rates of $0.1\text{-}1.0 \times 10^6$ $M^{-1}s^{-1}$ were observed (Kracher *et al.* 2016). Thus, it is somewhat surprising that such an efficient ET rate is found for two physiologically unrelated enzymes. A possible explanation is that the specificity is restricted to the active site, which indeed is solvent exposed and conserved in all LPMO families. This explanation agrees with the finding of Courtade *et al*. (2016), who showed that the CDH cytochrome domain interacts exclusively with the copper-bound active site of the LPMO.

Some of the CBP21 variants (Y54A, F187Y, H114A) show a lower ET rate than the WT, which indicates that these mutations interfere with either the CDH-CBP21 protein-protein interaction (changing orientation or distance of the cofactor in the ET competent state), or with the electron transfer itself (by changing redox potentials of the cofactors or disrupting an ET pathway). Such decrease of ET is not unexpected since it depends on a transient interaction between the CBP21 active site and the cytochrome domain of CDH. More surprising are the results found for variants I180R, E60A, T111A, D182A, and T183A. These mutations increase the bimolecular rate constant from two-fold to 7.5-fold, probably by a mechanism similar to what causes decrease of the ET transfer rate (see above), but more experiments are needed to understand these changes.

When comparing the stopped-flow data with the steady-state conversion data of *Mt*CDH and CBP21 after 24 h, it is obvious that a high ET rate does only correlate with a high substrate turnover of the WT CBP21 and two other variants (T111A, A152R). A152R shows no big change in the ET rates and substrate turnover rates – this is a mutation without influence on both reactions. T111A has still a fair substrate turnover, but also an increased ET rate. This shows that the mutation is reducing the substrate turnover slightly and that an increased ET rate does not recover it. Therefore, it is safe to conclude that the substrate turnover is the rate limiting step and not the ET. Variants I180R, E60A, D182A, S58A, and A112G demonstrate the same: the substrate turnover is decreased while ET is increased. From these observations we can draw the conclusion that ET and substrate turnover are two separate, uncoupled steps. The CBP21 surface area first interacts with CDH, then with the substrate. Of course, this conclusion is only valid for the transfer of the first electron to the LPMO. How the second needed electron is obtained still remains an open question. A recent study (Loose et al., submitted) showed that both electrons needed for catalysis by CBP21 can be provided by CDH, indicating that transfer of the second electron indeed occurs via CDH. In a general perspective, it is likely that LPMOs are able to pick up electrons from any convenient reducing source located in vicinity of the enzyme.

Mutation of conserved residues reduces CBP21 lifetime

A striking observation that can be made from the activity data (Fig. 3) is the non-classical kinetic behavior of the mutants that show reduced product yields. For most enzymes, a detrimental modification of the active site usually materializes in reduced catalytic activity over the whole period of analysis. For the CBP21 mutants, the initial phase of the reaction is quantitatively similar for all CBP21 variants (except the inactive mutants), followed by an abrupt loss of activity, indicating enzyme inactivation or substrate depletion. CBP21 requires three substrates: dissolved dioxygen, electrons and crystalline chitin. Depletion of dissolved dioxygen is highly unlikely since the reactions are vigorously shaken and contain an equal or larger headspace volume than occupied by the reaction liquid. Depletion of the electron donor is also unlikely. For gallic acid, oxidation of this compound is highly visual as the oxidized form precipitates as a dark green material. Such precipitation was indeed observed for the WT and mutants with WT-like activity, but to a lesser extent for the mutants with reduced or no activity. Depletion of chitin also seems unlikely since the WT and mutants with WT-like activity show linear product formation for the whole reaction period (Fig. 3 and Table 2). It could be argued that modification of the substrate-binding surface or active site could alter the specificity of the enzyme, thus limiting the amount of sites on the substrate that give productive binding. However, this would also reduce the initial activity, which is not observed. In conclusion, this reasoning leaves enzyme inactivation as the most plausible explanation for the abrupt activity losses observed. It is well known that LPMOs generate reactive oxygen species (ROS) when provided with an electron donor (Kittl et al., 2012, Kjaergaard et al., 2014, Loose et al., submitted) and that the presence of the LPMO substrate in addition prevents such futile dioxygen activation (Isaksen et al., 2014, Loose et al., submitted). Also, Scott *et al.* (2015) showed that the presence of catalase, which converts hydrogen peroxide to dioxygen and water, in an enzyme cocktail containing a substantial amount of LPMOs, enhances the activity of the cocktail, presumably due to the removal of harmful ROS produced by the LPMOs. Thus, it is possible that the LPMOs are inactivated by themselves through futile cycling/production of ROS.

When analyzing Table 2, and especially the binding data, most mutants that show reduced or no activity also bind less well to the substrate (the W178A mutant is an exception, but this mutation is special; see discussion of individual mutants). A plausible explanation of the loss of activity may therefore be that binding of the enzyme to the substrate not only positions the

enzyme for catalysis, but also protects it from futile cycling and the subsequent production of harmful ROS that may inactivate itself or other enzymes. Indeed, Li *et al.* (2014) observed hydroxylation of a solvent exposed Tyr in the X-ray reduced structure of the *Neurospora crassa* LPMO9M, indicating protein oxidation (the same authors also claimed to observe a peroxide molecule near the active site). Also, the almost abolished production of hydrogen peroxide of LPMOs bound to their substrates (Isaksen et al., 2014, Loose et al., submitted), supports this hypothesis. Furthermore, if carefully reviewing the literature, the abrupt activity loss in LPMOs reactions have also been observed in other studies: Forsberg *et al*. (2016) showed that by removing the chitin-binding module of the *Cellvibrio japonicus* LPMO *Cj*LPMO10A, activity was reduced, but primarily as a result of an abrupt activity loss early in the reaction. Interestingly, the truncated variant of *Cj*LPMO10A was not able bind to chitin, whereas the CBM bound chitin strongly. In a similar study, Crouch *et al*. (2016) observed the same abrupt enzyme activity reduction phenomenon when studying the significance of cellulose binding modules for the cellulose active LPMOs from *Thermobispora bispora* and *Cellulomonas fimi*. Binding of the truncated variants (LPMO domain only) were, as also observed by Forsberg and colleagues, not capable of binding to the insoluble substrate. All in all it seems that binding of the LPMO to the substrate is beneficial for activity, possibly due to protection or prevention from oxidative damage or causing oxidative damage. It should be noted that a third study on the CBM influence on catalysis by a family AA9 LPMO (Borisova et al 2015), shows no difference in activity of the WT and the truncated variant. However, here the reactions were only monitored for 2 h, thus it is possible that the activity decline phase had not been reached, as is also observed in this study.

Substrate binding by CBP21 seems uncoupled from catalysis

The substrate binding and catalytic activity characteristics of the Y54A and S58A mutants, and especially the former, show an unexpected trend. As already noted, the initial reaction rate of the Y54A mutant is identical to the WT. The phenomenon is especially clear in experiments where gallic acid was used as electron donor. This observation is unprecedented, since it is expected, or at least biochemically sound reasoning, that binding to the substrate is important for activity. The inability of the Y54A mutant to bind chitin is documented both here and in the study of Vaaje-Kolstad in 2005 (Vaaje-Kolstad et al., 2005b), but despite this dramatic difference in binding, initial activity is identical to the WT (Fig. 3). Since neither copper

coordination nor electron transfer is compromised in the Y54A mutant, it is tempting to speculate that the enzyme-substrate interaction that causes oxidative cleavage of the chitin chain is uncoupled from the binding observed in the binding assay. As suggested previously in the discussion, the latter type of binding may be designed to prevent premature inactivation, while catalytically productive binding is a more transient event. More experiments are required to investigate this hypothesis.

Concluding remarks

The discovery of the unique activity represented by the LPMOs has spurred research on these fascinating enzymes. Still, our understanding of how these copper-enzymes work is still limited, one reason being that, since the discovery that LPMOs actually are enzymes, no in-depth mutational studies have been carried out. The objective of the present study was to provide a large dataset, not only to increase our understanding of how CBP21 works, but also to provide a basis for future studies on LPMOs.

It is not trivial to draw conclusions from the present dataset since LPMO activity is controlled by so many variables. However, some trends are clear. Firstly, initial catalytic rates are surprisingly similar for most mutants, whereas enzyme lifetime is dramatically different. Since LPMOs perform powerful oxidative chemistry through a solvent exposed active site, it is conceivable that the active site is constructed and fine-tuned in a way that limits self-destruction by harmful ROS formed near the active site. The EPR spectra collected for the mutants confirm that copper-coordination geometry is easily altered by changing the surroundings of the active site and that these changes may involve both direct side chain-mediated and more indirect water-mediated interactions. Changes in the copper site and its surroundings may affect the generation and perhaps even spatial position of ROS and/or affect the enzyme's ability to handle these ROS in a non self-destructive manner. Several mutants with shortened lifetimes also displayed a reduced ability to bind chitin, suggesting that substrate binding may protect the enzyme by shielding the active site from the solvent.

A second trend in the data concerns the lack of correlation between the mutational effect on catalytic performance and the change in the rate of ET between the LPMO and *Mt*CDH. It thus seems that the one-electron reduction of CBP21 in solution is not rate-limiting for catalysis. A

802 limitation of the ET analysis is that only the transfer of one (the first) electron is analyzed. The
803 site of transfer and the timing of delivery of the second electron needed to complete the catalytic
804 cycle are still unknown, and this second reduction may represent the rate limiting step of the
805 reaction mechanism.

806 The present data reveal residues that are important for catalysis by AA10 LPMOs and the in-
807 depth analysis of mutational effects points towards LPMO properties, such as oxidative
808 stability, that may be important for enzyme performance. If one thing is to be learned from the
809 present study, it is that LPMOs display complex, and to some extent counter-intuitive,
810 relationships between substrate-binding, copper coordination geometry, enzyme stability and
811 catalytic performance. Digging deeper into these relationships will hopefully increase our
812 understanding of these intriguing enzymes and perhaps also improve their potential as
813 industrial biocatalysts.

814 ACKNOWLEDGEMENTS

815 This work was supported by the Research Council of Norway Grants 214138 (JSML and GV-
816 K), 214613 (VGHE), and 240967 (MS, ÅKR), The Norwegian Academy of Science and Letters
817 Vista Program Grant 6510 (ZF), the European Commission (project INDOX FP7-KBBE-2013-
818 7-613549) (RL), the Austrian Science Fund (project BioToP; FWF W1224) (DK), Marie-Curie
819 FP7 COFUND People Programme (AgreenSkills fellowship under grant agreement n° 267196)
820 (BB). We would like to thank the metalloprotein group (K.K. Andersson *et al*.) at Faculty of
821 Mathematics and Natural Sciences, University of Oslo for help with collecting EPR data. We
822 would also like to thank Anne Cathrine Bunæs for assisting with protein expression and
823 purification.

824 REFERENCES

825 AACHMANN, F. L., SØRLIE, M., SKJÅK-BRÆK, G., EIJSINK, V. G. H. & VAAJE-
826 KOLSTAD, G. 2012. NMR structure of a lytic polysaccharide monooxygenase
827 provides insight into copper binding, protein dynamics, and substrate interactions.
828 *Proc. Natl. Acad. Sci. U.S.A.,* 109**,** 18779-18784.

829 AGGER, J. W., ISAKSEN, T., VÁRNAI, A., VIDAL-MELGOSA, S., WILLATS, W. G.,
830 LUDWIG, R., HORN, S. J., EIJSINK, V. G. H. & WESTERENG, B. 2014. Discovery
831 of LPMO activity on hemicelluloses shows the importance of oxidative processes in
832 plant cell wall degradation. *Proc. Natl. Acad. Sci. U.S.A.,* 111**,** 6287-6292.

833 ASHKENAZY, H., EREZ, E., MARTZ, E., PUPKO, T. & BEN-TAL, N. 2010. ConSurf 2010:
834 calculating evolutionary conservation in sequence and structure of proteins and nucleic
835 acids. *Nucleic Acids Res,* 38**,** W529-33.

836 BEESON, W. T., PHILLIPS, C. M., CATE, J. H. & MARLETTA, M. A. 2012. Oxidative
837 cleavage of cellulose by fungal copper-dependent polysaccharide monooxygenases. *J*
838 *Am Chem Soc,* 134**,** 890-892.

839 BEESON, W. T., VU, V. V., SPAN, E. A., PHILLIPS, C. M. & MARLETTA, M. A. 2015.
840 Cellulose degradation by polysaccharide monooxygenases. *Annu. Rev. Biochem.,* 84**,**
841 923-946.

842 BORISOVA, A. S., ISAKSEN, T., DIMAROGONA, M., KOGNOLE, A. A., MATHIESEN,
843 G., VARNAI, A., ROHR, A. K., PAYNE, C. M., SORLIE, M., SANDGREN, M. &
844 EIJSINK, V. G. H. 2015. Structural and Functional Characterization of a Lytic
845 Polysaccharide Monooxygenase with Broad Substrate Specificity. *Journal of*
846 *Biological Chemistry,* 290**,** 22955-22969.

847 BRURBERG, M. B., EIJSINK, V. G. H. & NES, I. F. 1994. Characterization of a Chitinase
848 Gene (Chia) from Serratia-Marcescens Bjl200 and One-Step Purification of the Gene-
849 Product. *Fems Microbiology Letters,* 124**,** 399-404.

850 CHAUDHURI, S., BRUNO, J. C., ALONZO, F., 3RD, XAYARATH, B., CIANCIOTTO, N.
851 P. & FREITAG, N. E. 2010. Contribution of chitinases to *Listeria monocytogenes*
852 pathogenesis. *Appl Environ Microbiol,* 76**,** 7302-7305.

853 CORRÊA, T. L. R., DOS SANTOS, L. V. & PEREIRA, G. A. G. 2016. AA9 and AA10: from
854 enigmatic to essential enzymes. *Applied Microbiology and Biotechnology,* 100**,** 9-16.

855 COURTADE, G., WIMMER, R., ROHR, A. K., PREIMS, M., FELICE, A. K.,
856 DIMAROGONA, M., VAAJE-KOLSTAD, G., SORLIE, M., SANDGREN, M.,
857 LUDWIG, R., EIJSINK, V. G. & AACHMANN, F. L. 2016. Interactions of a fungal
858 lytic polysaccharide monooxygenase with beta-glucan substrates and cellobiose
859 dehydrogenase. *Proc Natl Acad Sci U S A,* 113**,** 5922-5927.

860 CRAGG, S. M., BECKHAM, G. T., BRUCE, N. C., BUGG, T. D. H., DISTEL, D. L.,
861 DUPREE, P., ETXABE, A. G., GOODELL, B. S., JELLISON, J., MCGEEHAN, J. E.,
862 MCQUEEN-MASON, S. J., SCHNORR, K., WALTON, P. H., WATTS, J. E. M. &

ZIMMER, M. 2015. Lignocellulose degradation mechanisms across the Tree of Life. *Current Opinion in Chemical Biology,* 29**,** 108-119.

CROUCH, L. I., LABOUREL, A., WALTON, P. H., DAVIES, G. J. & GILBERT, H. J. 2016. The Contribution of Non-catalytic Carbohydrate Binding Modules to the Activity of Lytic Polysaccharide Monooxygenases. *J Biol Chem,* 291**,** 7439-49.

DI TOMMASO, P., MORETTI, S., XENARIOS, I., OROBITG, M., MONTANYOLA, A., CHANG, J. M., TALY, J. F. & NOTREDAME, C. 2011. T-Coffee: a web server for the multiple sequence alignment of protein and RNA sequences using structural information and homology extension. *Nucleic Acids Res,* 39**,** W13-7.

DIMAROGONA, M., TOPAKAS, E., OLSSON, L. & CHRISTAKOPOULOS, P. 2012. Lignin boosts the cellulase performance of a GH-61 enzyme from *Sporotrichum thermophile*. *Bioresour. Technol.,* 110**,** 480-487.

FORSBERG, Z., MACKENZIE, A. K., SØRLIE, M., RØHR, Å. K., HELLAND, R., ARVAI, A. S., VAAJE-KOLSTAD, G. & EIJSINK, V. G. H. 2014a. Structural and functional characterization of a conserved pair of bacterial cellulose-oxidizing lytic polysaccharide monooxygenases. *Proc. Natl. Acad. Sci. U.S.A.,* 111**,** 8446-8451.

FORSBERG, Z., NELSON, C. E., DALHUS, B., MEKASHA, S., LOOSE, J. S., CROUCH, L. I., RØHR, Å. K., GARDNER, J. G., EIJSINK, V. G. & VAAJE-KOLSTAD, G. 2016. Structural and Functional Analysis of a Lytic Polysaccharide Monooxygenase Important for Efficient Utilization of Chitin in *Cellvibrio japonicus*. *J Biol Chem,* 291**,** 7300-7312.

FORSBERG, Z., RØHR, Å. K., MEKASHA, S., ANDERSSON, K. K., EIJSINK, V. G. H., VAAJE-KOLSTAD, G. & SØRLIE, M. 2014b. Comparative study of two chitin-active and two cellulose-active AA10-type lytic polysaccharide monooxygenases. *Biochemistry,* 53**,** 1647-1656.

FORSBERG, Z., VAAJE-KOLSTAD, G., WESTERENG, B., BUNÆS, A. C., STENSTRØM, Y., MACKENZIE, A., SØRLIE, M., HORN, S. J. & EIJSINK, V. G. H. 2011. Cleavage of cellulose by a CBM33 protein. *Protein Sci.,* 20**,** 1479-1483.

FRANDSEN, K. E., SIMMONS, T. J., DUPREE, P., POULSEN, J. C., HEMSWORTH, G. R., CIANO, L., JOHNSTON, E. M., TOVBORG, M., JOHANSEN, K. S., VON FREIESLEBEN, P., MARMUSE, L., FORT, S., COTTAZ, S., DRIGUEZ, H., HENRISSAT, B., LENFANT, N., TUNA, F., BALDANSUREN, A., DAVIES, G. J., LO LEGGIO, L. & WALTON, P. H. 2016. The molecular basis of polysaccharide cleavage by lytic polysaccharide monooxygenases. *Nat Chem Biol,* 12**,** 298-303.

FROMMHAGEN, M., SFORZA, S., WESTPHAL, A. H., VISSER, J., HINZ, S. W. A., KOETSIER, M. J., VAN BERKEL, W. J. H., GRUPPEN, H. & KABEL, M. A. 2015. Discovery of the combined oxidative cleavage of plant xylan and cellulose by a new fungal polysaccharide monooxygenase. *Biotechnol. Biofuels,* 8**,** 101.

GARAJOVA, S., MATHIEU, Y., BECCIA, M. R., BENNATI-GRANIER, C., BIASO, F., FANUEL, M., ROPARTZ, D., GUIGLIARELLI, B., RECORD, E., ROGNIAUX, H., HENRISSAT, B. & BERRIN, J. G. 2016. Single-domain flavoenzymes trigger lytic

polysaccharide monooxygenases for oxidative degradation of cellulose. *Scientific Reports,* 6**,** 28276

GUDMUNDSSON, M., KIM, S., WU, M., ISHIDA, T., MOMENI, M. H., VAAJE-KOLSTAD, G., LUNDBERG, D., ROYANT, A., STÅHLBERG, J., EIJSINK, V. G., BECKHAM, G. T. & SANDGREN, M. 2014. Structural and electronic snapshots during the transition from a Cu(II) to Cu(I) metal center of a lytic polysaccharide monooxygenase by X-ray photoreduction. *J Biol Chem,* 289**,** 18782-18792.

HARRIS, P. V., WELNER, D., MCFARLAND, K. C., RE, E., NAVARRO POULSEN, J. C., BROWN, K., SALBO, R., DING, H., VLASENKO, E., MERINO, S., XU, F., CHERRY, J., LARSEN, S. & LO LEGGIO, L. 2010. Stimulation of lignocellulosic biomass hydrolysis by proteins of glycoside hydrolase family 61: structure and function of a large, enigmatic family. *Biochemistry,* 49**,** 3305-3316.

HEMSWORTH, G. R., DAVIES, G. J. & WALTON, P. H. 2013a. Recent insights into copper-containing lytic polysaccharide mono-oxygenases. *Curr Opin Struct Biol,* 23**,** 660-668.

HEMSWORTH, G. R., JOHNSTON, E. M., DAVIES, G. J. & WALTON, P. H. 2015. Lytic Polysaccharide Monooxygenases in Biomass Conversion. *Trends in Biotechnology,* 33**,** 747-761.

HEMSWORTH, G. R., TAYLOR, E. J., KIM, R. Q., GREGORY, R. C., LEWIS, S. J., TURKENBURG, J. P., PARKIN, A., DAVIES, G. J. & WALTON, P. H. 2013b. The copper active site of CBM33 polysaccharide oxygenases. *J. Am. Chem. Soc.,* 135**,** 6069-6077.

HEUTS, D. P. H. M., WINTER, R. T., DAMSMA, G. E., JANSSEN, D. B. & FRAAIJE, M. W. 2008. The role of double covalent flavin binding in chito-oligosaccharide oxidase from *Fusarium graminearum*. *Biochem. J.,* 413**,** 175-183.

HORN, S. J., VAAJE-KOLSTAD, G., WESTERENG, B. & EIJSINK, V. G. H. 2012. Novel enzymes for the degradation of cellulose. *Biotechnol. Biofuels,* 5**,** 45.

HU, J. G., ARANTES, V., PRIBOWO, A., GOURLAY, K. & SADDLER, J. N. 2014. Substrate factors that influence the synergistic interaction of AA9 and cellulases during the enzymatic hydrolysis of biomass. *Energy & Environmental Science,* 7**,** 2308-2315.

ISAKSEN, T., WESTERENG, B., AACHMANN, F. L., AGGER, J. W., KRACHER, D., KITTL, R., LUDWIG, R., HALTRICH, D., EIJSINK, V. G. H. & HORN, S. J. 2014. A C4-oxidizing lytic polysaccharide monooxygenase cleaving both cellulose and cello-oligosaccharides. *J. Biol. Chem.,* 289**,** 2632-2642.

KARKEHABADI, S., HANSSON, H., KIM, S., PIENS, K., MITCHINSON, C. & SANDGREN, M. 2008. The first structure of a glycoside hydrolase family 61 member, Cel61B from *Hypocrea jecorina*, at 1.6 A resolution. *J Mol Biol,* 383**,** 144-154.

KIM, S., STÅHLBERG, J., SANDGREN, M., PATON, R. S. & BECKHAM, G. T. 2014. Quantum mechanical calculations suggest that lytic polysaccharide monooxygenases use a copper-oxyl, oxygen-rebound mechanism. *Proc Natl Acad Sci U S A,* 111**,** 149-154.

944 KIRN, T. J., JUDE, B. A. & TAYLOR, R. K. 2005. A colonization factor links *Vibrio cholerae*
945 environmental survival and human infection. *Nature,* 438**,** 863-866.

946 KITTL, R., KRACHER, D., BURGSTALLER, D., HALTRICH, D. & LUDWIG, R. 2012.
947 Production of four *Neurospora crassa* lytic polysaccharide monooxygenases in *Pichia*
948 *pastoris* monitored by a fluorimetric assay. *Biotechnol. Biofuels,* 5**,** 79.

949 KJAERGAARD, C. H., QAYYUM, M. F., WONG, S. D., XU, F., HEMSWORTH, G. R.,
950 WALTON, D. J., YOUNG, N. A., DAVIES, G. J., WALTON, P. H., JOHANSEN, K.
951 S., HODGSON, K. O., HEDMAN, B. & SOLOMON, E. I. 2014. Spectroscopic and
952 computational insight into the activation of O2 by the mononuclear Cu center in
953 polysaccharide monooxygenases. *Proc Natl Acad Sci U S A,* 111**,** 8797-8802.

954 KRACHER, D., SCHEIBLBRANDNER, S., FELICE, A. K., BRESLMAYR, E., PREIMS,
955 M., LUDWICKA, K., HALTRICH, D., EIJSINK, V. G. & LUDWIG, R. 2016.
956 Extracellular electron transfer systems fuel cellulose oxidative degradation. *Science,*
957 352**,** 1098-1101.

958 LANGSTON, J. A., SHAGHASI, T., ABBATE, E., XU, F., VLASENKO, E. & SWEENEY,
959 M. D. 2011. Oxidoreductive cellulose depolymerization by the enzymes cellobiose
960 dehydrogenase and glycoside hydrolase 61. *Appl. Environ. Microbiol.,* 77**,** 7007-7015.

961 LEVASSEUR, A., DRULA, E., LOMBARD, V., COUTINHO, P. M. & HENRISSAT, B.
962 2013. Expansion of the enzymatic repertoire of the CAZy database to integrate auxiliary
963 redox enzymes. *Biotechnol. Biofuels,* 6**,** 41.

964 LI, X., BEESON, W. T., PHILLIPS, C. M., MARLETTA, M. A. & CATE, J. H. D. 2012.
965 Structural basis for substrate targeting and catalysis by fungal polysaccharide
966 monooxygenases. *Structure,* 20**,** 1051-1061.

967 LO LEGGIO, L., SIMMONS, T. J., POULSEN, J. C., FRANDSEN, K. E., HEMSWORTH,
968 G. R., STRINGER, M. A., VON FREIESLEBEN, P., TOVBORG, M., JOHANSEN,
969 K. S., DE MARIA, L., HARRIS, P. V., SOONG, C. L., DUPREE, P., TRYFONA, T.,
970 LENFANT, N., HENRISSAT, B., DAVIES, G. J. & WALTON, P. H. 2015. Structure
971 and boosting activity of a starch-degrading lytic polysaccharide monooxygenase. *Nat.*
972 *Commun.,* 6**,** 5961.

973 LOMBARD, V., GOLACONDA RAMULU, H., DRULA, E., COUTINHO, P. M. &
974 HENRISSAT, B. 2014. The carbohydrate-active enzymes database (CAZy) in 2013.
975 *Nucleic Acids Res,* 42**,** D490-495.

976 LOOSE, J. S. M., FORSBERG, Z., FRAAIJE, M. W., EIJSINK, V. G. H. & VAAJE-
977 KOLSTAD, G. 2014. A rapid quantitative activity assay shows that the *Vibrio cholerae*
978 colonization factor GbpA is an active lytic polysaccharide monooxygenase. *FEBS Lett.,*
979 588**,** 3435-3440.

980 LOOSE, J. S. M., FORSBERG, Z., KRACHER, D., SCHEIBLBRANDNER, S., LUDWIG,
981 R., EIJSINK, V. G. H. & VAAJE-KOLSTAD, G. submitted. Activation of bacterial
982 lytic polysaccharide monooxygenases with cellobiose dehydrogenase.

983 MANOIL, C. & BECKWITH, J. 1986. A Genetic approach to analyzing membrane-protein
984 topology. *Science,* 233**,** 1403-1408.

MÜLLER, G., VÁRNAI, A., JOHANSEN, K. S., EIJSINK, V. G. & HORN, S. J. 2015. Harnessing the potential of LPMO-containing cellulase cocktails poses new demands on processing conditions. *Biotechnol Biofuels,* 8**,** 187.

NAKAGAWA, Y. S., KUDO, M., LOOSE, J. S., ISHIKAWA, T., TOTANI, K., EIJSINK, V. G. & VAAJE-KOLSTAD, G. 2015. A small lytic polysaccharide monooxygenase from *Streptomyces griseus* targeting alpha- and beta-chitin. *FEBS J,* 282**,** 1065-1079.

PASPALIARI, D. K., LOOSE, J. S., LARSEN, M. H. & VAAJE-KOLSTAD, G. 2015. *Listeria monocytogenes* has a functional chitinolytic system and an active lytic polysaccharide monooxygenase. *FEBS J,* 282**,** 921-936.

PEISACH, J. & BLUMBERG, W. E. 1974. Structural Implications Derived from Analysis of Electron-Paramagnetic Resonance-Spectra of Natural and Artificial Copper Proteins. *Archives of Biochemistry and Biophysics,* 165**,** 691-708.

PHILLIPS, C. M., BEESON, W. T., CATE, J. H. & MARLETTA, M. A. 2011. Cellobiose dehydrogenase and a copper-dependent polysaccharide monooxygenase potentiate cellulose degradation by *Neurospora crassa*. *ACS Chem. Biol.,* 6**,** 1399-1406.

QUINLAN, R. J., SWEENEY, M. D., LO LEGGIO, L., OTTEN, H., POULSEN, J. C., JOHANSEN, K. S., KROGH, K. B., JØRGENSEN, C. I., TOVBORG, M., ANTHONSEN, A., TRYFONA, T., WALTER, C. P., DUPREE, P., XU, F., DAVIES, G. J. & WALTON, P. H. 2011. Insights into the oxidative degradation of cellulose by a copper metalloenzyme that exploits biomass components. *Proc. Natl. Acad. Sci. U.S.A.,* 108**,** 15079-15084.

SCOTT, B. R., HUANG, H. Z., FRICKMAN, J., HALVORSEN, R. & JOHANSEN, K. S. 2015. Catalase improves saccharification of lignocellulose by reducing lytic polysaccharide monooxygenase-associated enzyme inactivation. *Biotechnol. Lett.,* 38**,** 425-434.

STOLL, S. & SCHWEIGER, A. 2006. EasySpin, a comprehensive software package for spectral simulation and analysis in EPR. *J Magn Reson,* 178**,** 42-55.

SYGMUND, C., KRACHER, D., SCHEIBLBRANDNER, S., ZAHMA, K., FELICE, A. K., HARREITHER, W., KITTL, R. & LUDWIG, R. 2012. Characterization of the two *Neurospora crassa* cellobiose dehydrogenases and their connection to oxidative cellulose degradation. *Appl. Environ. Microbiol.,* 78**,** 6161-1671.

SYNSTAD, B., VAAJE-KOLSTAD, G., CEDERKVIST, H., SAUA, S. F., HORN, S. J., EIJSINK, V. G. H. & SORLIE, M. 2008. Expression and characterization of endochitinase C from Serratia marcescens BJL200 and its purification by a one-step general chitinase purification method. *Bioscience Biotechnology and Biochemistry,* 72**,** 715-723.

VAAJE-KOLSTAD, G., BOHLE, L. A., GASEIDNES, S., DALHUS, B., BJORAS, M., MATHIESEN, G. & EIJSINK, V. G. H. 2012. Characterization of the Chitinolytic Machinery of Enterococcus faecalis V583 and High-Resolution Structure of Its Oxidative CBM33 Enzyme. *J Mol Biol,* 416**,** 239-254.

VAAJE-KOLSTAD, G., HORN, S. J., VAN AALTEN, D. M., SYNSTAD, B. & EIJSINK, V. G. 2005a. The non-catalytic chitin-binding protein CBP21 from *Serratia marcescens* is essential for chitin degradation. *J. Biol. Chem.,* 280**,** 28492-28497.

VAAJE-KOLSTAD, G., HOUSTON, D. R., RIEMEN, A. H., EIJSINK, V. G. H. & VAN AALTEN, D. M. 2005b. Crystal structure and binding properties of the *Serratia marcescens* chitin-binding protein CBP21. *J. Biol. Chem.,* 280**,** 11313-11319.

VAAJE-KOLSTAD, G., WESTERENG, B., HORN, S. J., LIU, Z., ZHAI, H., SØRLIE, M. & EIJSINK, V. G. H. 2010. An oxidative enzyme boosting the enzymatic conversion of recalcitrant polysaccharides. *Science,* 330**,** 219-222.

VERMAAS, J. V., CROWLEY, M. F., BECKHAM, G. T. & PAYNE, C. M. 2015. Effects of Lytic Polysaccharide Monooxygenase Oxidation on Cellulose Structure and Binding of Oxidized Cellulose Oligomers to Cellulases. *Journal of Physical Chemistry B,* 119**,** 6129-6143.

VU, V. V., BEESON, W. T., SPAN, E. A., FARQUHAR, E. R. & MARLETTA, M. A. 2014. A family of starch-active polysaccharide monooxygenases. *Proc Natl Acad Sci U S A,* 111**,** 13822-13827.

WALTON, P. H. & DAVIES, G. J. 2016. On the catalytic mechanisms of lytic polysaccharide monooxygenases. *Curr Opin Chem Biol,* 31**,** 195-207.

WESTERENG, B., CANNELLA, D., AGGER, J. W., JØRGENSEN, H., ANDERSEN, M. L., EIJSINK, V. G. H. & FELBY, C. 2015. Enzymatic cellulose oxidation is linked to lignin by long-range electron transfer. *Sci. Rep.,* 5**,** 18561.

WU, M., BECKHAM, G. T., LARSSON, A. M., ISHIDA, T., KIM, S., PAYNE, C. M., HIMMEL, M. E., CROWLEY, M. F., HORN, S. J., WESTERENG, B., IGARASHI, K., SAMEJIMA, M., STÅHLBERG, J., EIJSINK, V. G. H. & SANDGREN, M. 2013. Crystal Structure and Computational Characterization of the Lytic Polysaccharide Monooxygenase GH61D from the Basidiomycota Fungus *Phanerochaete chrysosporium*. *Journal of Biological Chemistry,* 288**,** 12828-12839.

ZAMOCKY, M., SCHÜMANN, C., SYGMUND, C., O'CALLAGHAN, J., DOBSON, A. D. W., LUDWIG, R., HALTRICH, D. & PETERBAUER, C. K. 2008. Cloning, sequence analysis and heterologous expression in *Pichia pastoris* of a gene encoding a thermostable cellobiose dehydrogenase from *Myriococcum thermophilum*. *Protein Expr. Purif.,* 59**,** 258-265.

SUPPLEMENTARY MATERIAL

Insights into catalysis by lytic polysaccharide monooxygenases through site-directed mutagenesis of CBP21 from *Serratia marcescens*

Jennifer S.M. Loose , Åsmund K. Røhr , Bastien Bissaro , Daniel Kracher , Roland Ludwig , Morten Sørlie , Vincent G.H. Eijsink and Gustav Vaaje-Kolstad *

Supplementary figures

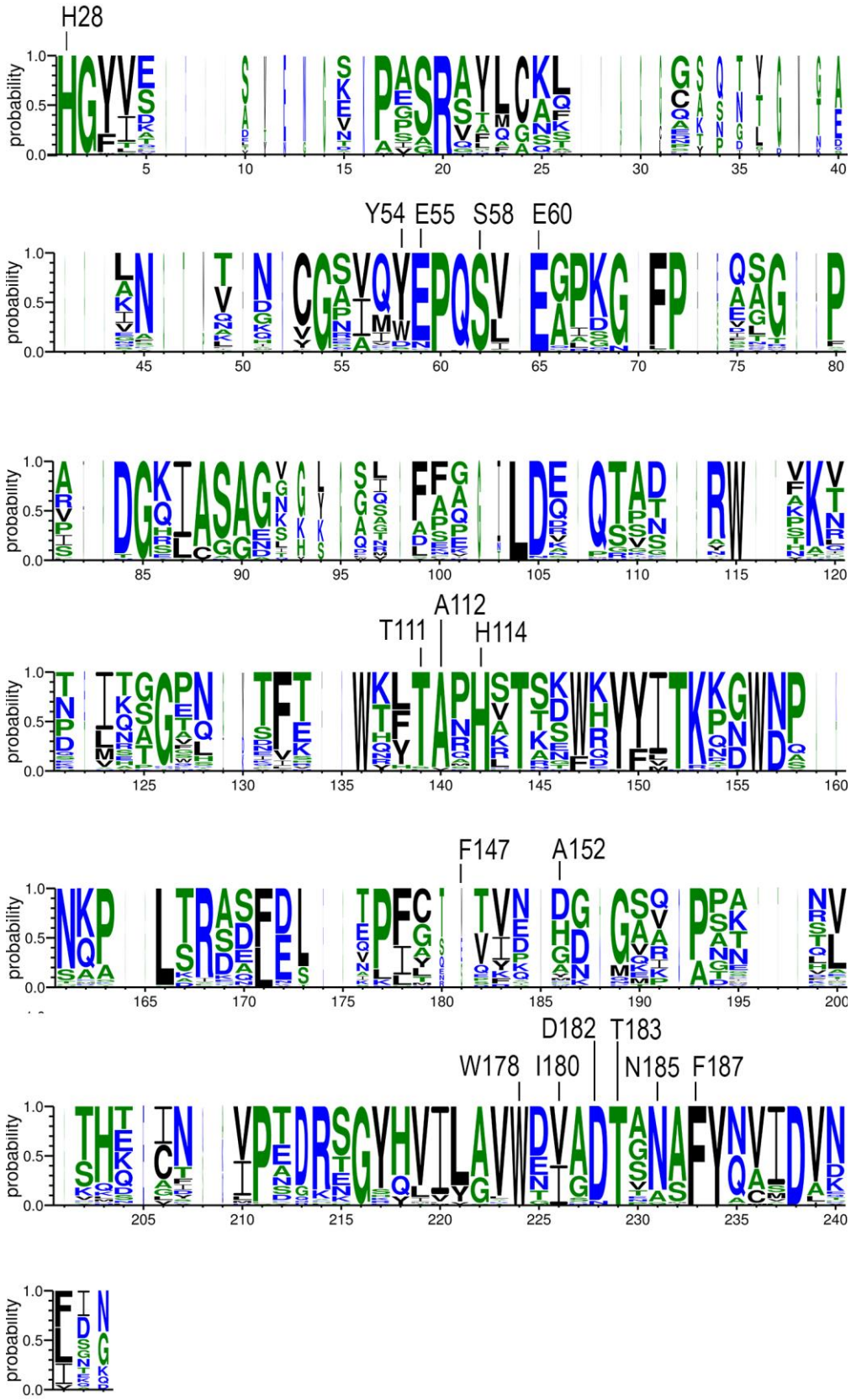

Figure S1. Residue conservation in chitin-active family AA10 LPMOs. The sequence conservation of chitin-active family AA10 LPMOs is illustrated as a sequence logo. The logo is based on a multiple sequence alignment of 73 sequences selected from a cluster of chitin active AA10 LPMOs (derived from in-house phylogenetic analysis). The alignment was made using the T-Coffee Expresso on line tool (Di Tommaso et al., 2011) with PDB 2bem, 5aa7 and 2xwx as structural input. Each position in the sequence logo indicates position variability vertically (most common amino acid at the specific position) and insertions/ deletions horizontally (the more insertions/ deletions, the thinner the amino acid letter). The amino acids of CBP21 mutated in the present study are indicated by labels.